Analysis of the expression of circulating microRNAs in an animal model of Alzheimer's disease

Ruth Elizabeth Aquino Ordinola

ÉCOLE DOCTORALE *SANTE, SCIENCES BIOLOGIQUES ET CHIMIE DU VIVANT*

CENTRE DE BIOPHISIQUE MOLECULAIRE (CBM, UPR 4301) / LABORATORIO DE PROLIFERACIÓN CELULAR Y REGENERACIÓN

THÈSE EN COTUTELLE INTERNATIONALE présentée par :

Ruth Elizabeth AQUINO ORDINOLA

soutenue le : 22 décembre 2021

pour obtenir le grade de :
Docteur de Université d'Orléans
et de la Universidad Peruana Cayetano Heredia

Discipline/ Spécialité : Biologie Moléculaire et Cellulaire/Aspects moléculaires et cellulaires de la biologie

Analysis of the expression of circulating microRNAs in an animal model of Alzheimer's disease

THÈSE dirigée par :

Mme. PICHON Chantal	Professeur, Université d'Orléans
M. BARIL Patrick	Maître de Conférences HDR, Université d'Orléans
Mme. GUERRA GIRALDEZ Cristina	Professeur, Universidad Peruana Cayetano Heredia

RAPPORTEURS :

M. DENOYELLE Christophe	Maître de Conférences HDR, Université de Caen Normandie
Mme. PEREIRA DE SOUSA Fani	Maître de Conférences HDR, University of Beira Interior, Covilhã, Portugal

---

JURY :

M. THANY Steeve	Professeur, Université d'Orléans, Président du jury
M. DENOYELLE Christophe	Maître de Conférences HDR, Université de Caen Normandie
Mme. PEREIRA DE SOUSA Fani	Maitre de Conférences HDR, University of Beira Interior, Covilhã, Portugal
Mme. PICHON Chantal	Professeur, Université d'Orléans
M. BARIL Patrick	Maître de Conférences HDR, Université d'Orléans
Mme. GUERRA GIRALDEZ Cristina	Professeur, Universidad Peruana Cayetano Heredia
Mme. HERRERA VELIT Rosa	Professeur, Universidad Peruana Cayetano Heredia
Mme. TUERO OCHOA Iskra	Professeur, Universidad Peruana Cayetano Heredia

Acknowledgments

I am infinitely grateful to all the people who in one way or another have contributed to achieve my Ph. D project.

At the first I would like to thank all members of the jury: Dr. Christophe Denoyelle, Dr. Steeve Thany, Dr. Patricia Herrera and Dr. Iskra Tuero for their time, effort and for agreeing to be part of the evaluation committee in the defense of my thesis work.

I would like to sincerely thank Prof. Chantal Pichon for agreeing to direct my thesis, infinite thanks also to Dr. Patrick Baril, for having accepted the co-direction of my thesis. Please note, Prof Pichon, that without your positive response and support, it would not have been possible to search and obtain the scholarship to carry out this doctorate. I am particularly grateful to you for this. Likewise, I am also grateful for the financial support that I received from the Franco-Peruvian scholarship to Consejo Nacional de Ciencia, Tecnología e Innovación Tecnológica (CONCYTEC). On the other hand, I thank Dr. Cristina Guerra, for assuming the co-supervision of the thesis from the Peru part, thanks for the trust and support you provided to me. I would like to thanks Dr. Eric Mialhe and Dr. Virna Cedeño, my teachers in the master's degree in Peru who helped me to find this doctorate position in France.

I express my deep gratitude to Prof. Chantal, for hosting me in her laboratory, conducting my thesis project, for the time, the advice and for all the support provided during this Ph.D project and also for the human adventure spent together. Likewise, I also infinitely thank Dr. Patrick Baril for his constant scientific supervision, for his time and patience for his advices both academically and personally and the great support that he gave me in difficult moments. I will never forget that. I express my gratitude and give proof of how fortunate I was to be closed to you two during these two years spent in France, in CBM.

My gratitude comes also to Dr. Arnaud Menuet for allowing me to work in his laboratory "INEM", «Immunologie et Neurogénétique Expérimentales et Moléculaires», thank you for your advice, your time and your support when I was doing the primary culture of Astrocytes. Thanks also to Vidian de Concini for his availability, positive attitude and his support in the execution of experiments specially with the ELISA and Immohistochemitry.

Thanks to Dr. Marc Dhenain, (Group Leader, Molecular Imaging Research Center, Fontenay-aux-Roses, Paris) for accepting to collect and provide the transgenic animal samples for our study. Your impact in this project was important to compare the relevancy of the two-animal models of AD used in this study. I do not forget Suzanne Lam, your Ph. D Student, who spent significant time when collecting the samples with you.

Thanks to Dr. Manuel Forero and his team from the University of Colombia for sharing with me your knowledge and for the bioinformatic engineering of the plugin "Rast track" used to fellow in real time the swimming of rats in the pool.

I also thank David Gosset, for his support in the immunohistochemical analysis, through the handling of the platform "P@CIFIC" – CBM.

I thank Rebeca Caldas for her support in the Peruvian administrative part, thank you for her kindness, patience and for the special way you used to explain me how to deal with the administrative works between France and Peru. You were always pleasant, happy and send me a bit of Peru every time when I was calling you. A lot of thanks for that.

Thanks to all the members of the French team: Dr. Patrick Midoux, Dr. Federico Perche, Dr. Cristine Gonçalves, Dr. Anthony Delalande, Dr. Jean-Marc Malinge, Dr. Philippe Germain Virginie Malard, Alexia Perrin, Laëtitia Cobret, Vinodini Vijayarangan, Christophe Delehedde. Yoan Laurent, Amnadine Suet, Aghate Leloux, Delphine Mazhe, Rudy Clémençon and Cyril Gimpied. All of you in one way or another have helped with this goal. Thanks also to Albert Ngalle-Loth, although we met each other only in the last few months, I appreciate your positive attitude and words of encouragement. I also thank Martial Bruno for his kindness and moral support. Also, to Christine Gabant, and Marie-Christine Perdereau.

Thanks to the Peruvian team of the Neuroscience and Behavior laboratory, especially Laura Baquedano, Javier Vasquez, Edson Bernal and Francisco Quispealaya. Thanks, Laura, for the support with animal handling, Morris, etc. Thank you also for your friendship and to be closed to me. Thanks, Javier, for the infinite and unconditional support in the execution of experiments in Lima. Thanks, Edson and thanks to Mr. Francisco, it was very pleasant to meet you. Thanks also to Nazareth Carigga and Vanessa Minaya.

Thanks to the French Peruvian group with Spanish roots: Eric Eveno, Karla Arbulu and Justo Torres. I will never forget your warm welcome. Thank for your support and for all the good times shared with you. Sincerely thanks. Thanks to the Peruvian friends still located in France: Beatriz and David Arbulu, Gloria Yepez, Darinkha Malki and Elena Santa Cruz. Thanks for the good time spent together. Thanks to my best friends; Cinthya Cueva and Bernabe Ayala, “Friendship without borders”, thankfor taking care of me although being geographically far from me and specially during the difficult moments that I have experienced. Our friendship began from the master's degree and will never ended. I promise.

I would also like to thank and dedicate this thesis to my family.

Specially to my father José Aquino, thank you, Daddy, for giving me so much, for these 29 years spent with me. Thank you for filling me with learning and courage. I would have wanted to express my deep, extreme, gratitude to you and express as well my deep love to you in a situation different to this time. It is however no longer possible. In this dark period, where you left me and our family, I have survived, because you teach me to stand, even wanting to fall every time. Life has separated us, but my heart is with you, every day, in every step, at every moment. I have so much to tell you and so much to thank you dad

... I love you, forever and to infinity.

My thanks also come to my mother Petronila Ordinola, thank you Mom for taking me in your arms and defying the distance and healing my soul with words full of love, hope, and faith. Thank you, Mom, for teaching me to see life in colors, to smile and help me through these difficult times. Every night, every call, every laugh, your joy, has filled me with faith and stronghold. Thanks for being so strong Mom and for showing me that there are always reasons to be happy.

To Erika Aquino, thank you for being the best sister, thank you for trying to paint my life in colors at any time. Thank you for your support in all several aspects. Thank you for being very supportive and helping us all, you are great person. You have given me the best signs of brotherhood, solidarity and love. Thanks to my brother Frank Aquino, it has been a difficult period for us, but every day knowing that you continue, that you are looking for opportunities, and knowing that you are well fills me with light. Thanks for your support and your love.

I leave proof of my deep love for all of you.

TABLE OF CONTENTS

List of Figures and Tables

Figures in Chapter 1. Bibliographic study

Figures and Tables in Chapter 2. Material and Methods

Figures in Chapter 3. Results

Figures in Chapter 4. Discussion and Conclusions

Figure 1. Overview of the injection of OAβ and FAβ in the hippocampus of rats and the role of miR-146a in mild and chronic inflammation.

List of Abbreviatons

AD: Alzheimer's disease

ADAD: Autosomal dominant Alzheimer disease

AICD: Amyloid precursor protein intracellular domain

APP: Amyloid precursor protein

APOE: Apolipoprotein E

Arg1: Arginase 1

AMO: anti-miRNA oligonucleotide

Aβ1-40,1-42/Aβ40, Aβ42: Amyloid β-peptide

Aβ: 40/42 residues length Amyloid β-peptide

BACE1: β-site amyloid precursor protein cleaving enzyme 1

BBB: blood-brain barrier

BDNF: Brain-derived neurotrophic factor

CFH: Complement factor H

CNS: Central nervous system

CSF: Cerebrospinal fluid

CTF: C-terminal fragment

DMEM: Dulbecco's Modified Eagle's Medium

ECF: Extracellular fluid

ECM: Extracellular matrix

ELISA: Enzyme-Linked Immunosorbent Assay

EOAD: Early onset Alzheimer's disease

FBS: Fetal bovine serum

HAG: Human astroglial

HDL: high-density lipoprotein

HMG: Human microglial

HNG: Human neuron-glial

h-tau: Hyperphosphorylated tau

IFN-γ: Interferon γ

IL: Interleukin

iNOS: Inducible nitric oxide synthase

IRAK1/2: Interleukin-1 receptor-associated kinase 1/2

L-glu: L-glutamine

LPS: Lipopolysaccharide

LOAD: Late onset Alzheimer's disease

MAPK: Mitogen-activated protein kinase

miRNA/miR: MicroRNA

MWM: Morris Water Maze

NFTs: Neurofibrillary tangles

NF-κB: Nuclear factor κB

NO: Nitric oxide

qRT-PCR: quantitative Real Time Polymerase Chain Reaction

ROS: Reactive oxygen species

PDGF: Platelet-derived growth factor

PDGF-β: Platelet-derived growth factor subunit β

Pre-miRNA: Precursor microRNA

pri-miRNA: Primary microRNA

PrP: Prion protein

PRR: Pattern Recognition Receptors

PSEN1 and PSEN-2: Presenilinas 1 and 2

PNS: Peripheral Central Nervous

RISC: RNA-Induced Silencing Complex

RNA: Ribonucleic acid

ROS: Reactive Oxygen Species

rRNA: Ribosomal RNA

sAPP: Soluble amyloid precursor protein

TGF-β Transforming growth factor β

TLR Toll-like receptor

TNF-α Tumor necrosis factor α

TRAF6 Tumor necrosis factor receptor-associated factor 6

TREM2 Triggering receptor expressed on myeloid cells 2

Résumé

La maladie d'Alzheimer (MA) est une maladie neurodégénérative progressive, affectant 36 millions de personnes dans le monde. Plusieurs enquêtes épidémiologiques ont estimé que le nombre de patients atteints de MA passera à plus de 66 millions dans le monde en 2030. Cette maladie est donc devenue l'un des plus grands défis du 21e siècle en termes de santé.

Deux formes de MA ont été identifiées. La forme sporadique de la MA est la forme la plus courante. Elle représente, en effet, plus de 99% des cas et affecte principalement les personnes âgées de plus de 65 ans. Les facteurs associés à cette forme ne sont pas bien connus et impliquent majoritairement le vieillissement, des facteurs environnementaux et des troubles du sommeil. La forme familiale, à l'inverse, est moins courante et représente moins de 1 % des cas. Sous cette forme, les symptômes cliniques se déclarent beaucoup plus tôt, dès l'âge de 45 ans. Des mutations autosomiques dominantes ont été identifiées dans les séquences des gènes codant pour l'apolipoprotéine E 4 (Apoe4), la protéine précurseur amyloïde (APP) et les protéines préséniles 1 et 2 (PS1 &2). Ces protéines sont directement impliquées dans la production de formes tronquées de la β-Amyloïde (βA) dans le cerveau. Dans les deux cas, la MA se caractérise par un déclin cognitif progressif et une perte de mémoire due à des lésions neuronales dans des régions cérébrales particulières notamment dans l'hippocampe. Les deux principales caractéristiques de l'apparition de la MA comprennent l'accumulation d'enchevêtrements neurofibrillaires intraneuronaux (ENF) et l'apparition de dépôts extracellulaires de la βA. D'autres caractéristiques comprennent la gliose, l'inflammation chronique, l'excitotoxicité, le stress oxydatif et l'homéostasie calcique altérée, qui illustrent la complexité de la maladie.

L'un des enjeux majeurs dans la prise en charge de cette pathologie neurodégénérative est la détection des signes cliniques suffisamment précoce pour pouvoir intervenir efficacement. De nos jours, les lésions neuronales associées à MA sont détectées trop tardivement ce qui explique l'échec des traitements pharmacologiques. Des traitements palliatifs sont mis en place pour essayer de ralentir la progression de cette maladie et permettent, à défaut de guérir la pathologie, d'améliorer le confort des patients qui présentent d'importants troubles de la mémoire et d'orientation spatiale. L'enjeu est donc de détecter des marqueurs précoces bien avant que les signes cliniques ne se manifestent et que les lésions neuronales deviennent incurables. C'est dans ce contexte précis que la détection des microARNs circulant trouve un intérêt particulier pour le dépistage précoce de la MA. Les microARNs sont des acides nucléiques de petites tailles qui contrôlent des réseaux entiers de gènes impliquées dans de nombreuses réponses biologiques aussi essentielles que le développement embryonnaire, la morphogénèse et le contrôle de l'homéostasie. Des dérèglements de leurs niveaux expression ont été rapportés dans la plupart des pathologies si ce n'est toutes. Un fait remarquable associé au microARN est leur grande stabilité dans les fluides corporels tel que le sang, les urines, la salive ou encore dans nombreux liquides interstitielles. Des défauts d'expression de certains microARNs ont été rapportés dans le sang périphérique de patients atteints de cancer ou de maladies cardiovasculaires ainsi que chez des patients atteints de la MA. Ces microARNs représentent par conséquent des cibles diagnostiques intéressantes pour le dépistage non invasif de pathologies.

C'est dans ce contexte précis que s'inscrit ce travail de doctorat. L'objectif majeur de notre étude visait à évaluer la valeur diagnostique de microARNs circulants dans un modèle animal de la MA. Pour cela, la première partie de ce doctorat a été consisté à la mise en place d'un modèle animal de MA par injection intra-hippocampique de peptide βA 1-42 à

différentes concentrations chez rats adultes. L'étude comportementale de nos animaux d'expérience a permis de révéler que de façon similaire à ce qu'on observe en clinique humaine, les animaux traités avec βA 1-42 présentaient des défauts d'apprentissage et d'orientation spatiale liés à une perte de mémoire. La caractérisation histologique et immunohistochimique des tissus neuronaux a permis de révéler la présence en nombre d'important d'astrogliose dans l'hipoccampe qui pourrait expliquer les défauts cognitifs observés. Ce premier travail expérimental a été réalisé au Laboratoire de Neurosciences et du Comportement à Lima au Pérou (Laboratoire de cotutelle de Doctorat). Dans un deuxième temps, nous avons évalué le niveau d'expression des microARNs circulants dans le sérum de ces animaux de laboratoire par qRT-PCR et ceci en fonction du temps. Ce travail a été réalisé dans le deuxième laboratoire de cotutelle de thèse, au Centre de Biophysique Moléculaire du CNRS localisé à Orléans en France. Pour cela, nous avons sélectionné une liste de plusieurs microARNs (miR-9a-5p, miR-146a-5p, miR-29a-3p, miR-29c-3p, miR-125b-5p, miR-181c-5p, miR-191-5p, miR-106b-5p et miR-135a-5p) sur la base des données bibliographiques qui indiquaient leur présence quasi systématique dans les échantillons cliniques des patients diagnostiqués avec cette pathologie. Les résultats de ces analyses moléculaires a permis de révéler que parmi l'ensemble de ces microARNs, 4 d'entre eux, les miR-9a, miR-29a, miR-29c, miR-146a, présentaient des défauts d'expression important dans le sérum des animaux infusés avec le peptide βA 1-42 par rapport aux animaux contrôles, non infusés. Nous avons alors établi la cinétique d'expression précise de ces 4 microARNs en fonction du temps post-infusion des peptides βA 1-42. Nous rapportons des différences notables d'expression chronologique de ces 4 microARNs notamment dès le $7^{ième}$ jour pour les miR-29a et miR-29c et au $14^{ième}$ jour pour le miR-146a. Nous avons alors comparé ces profils d'expression avec ceux détectés dans le sérum d'animaux transgéniques de la MA exprimant la forme mutée APP et de PS1. Ces animaux de laboratoire ont été

obtenus sous la forme de collaboration avec le Centre de Recherche en Imagerie Moléculaire, Fontenay-aux-Roses à Paris. Cette étude comparative a permis de révéler des différences d'expression de ces 4 microARNs qui tend à montrer que ces 2 modèles ; l'un transgénique et l'autre généré sur tissus adulte, ne mettent pas en jeu les mêmes mécanismes physiopathologiques à l'origine de la formation de plaque amyloïde. Nous avons alors focalisé la suite de nos travaux sur le miR-146a. D'une part parce que ce microARN présentait un profil d'expression atypique au cours du temps dans notre modèle animal et d'autre part parce qu'il n'était pas dérégulé dans le modèle de transgène animal représentatif de la forme héréditaire de la pathologie d'Alzheimer.

Dans la troisième partie de ce travail de doctorat, nous avons étudié le profil d'expression de ce microARN dans le liquide céphalorachidien (LCR) de notre modèle animal infusé avec les peptides βA. De façon surprenante nous avons constaté que ce microARN était surexprimé dans ce liquide corporel neuronal alors qu'il était sous-exprimé dans le sérum. Des hypothèses permettant d'expliquer ces résultats ont été proposées. Nous avons ensuite réalisé des études fonctionnelles pour tenter de mieux comprendre le rôle de ce microARN dans l'initiation de la pathologie. Pour cela, nous avons prélevé puis cultivé des cellules d'astrocytes de rat que nous avons ensuite traitées avec le peptide βA 1-42 à différentes concentrations. Deux formes d'agrégation βA ont été évaluées ; oligomère (OβA) et fibrillaire (FβA) en présence ou en l'absence d'un inhibiteur pharmacologique BMS-345541 de la voie NF-κB, suspectée comme étant une des voies de régulation du miR-146a. Nos résultats ont montré que les deux espèces de βA conduisent à une expression positive de ce microARN et à l'activation de la voie de signalisation NF-κB. Également, la régulation à la baisse d'IRAK-1 et de TRAF-6, principales cibles transcriptomiques de miR-146a, a été démontrée. En revanche, nous avons trouvé une régulation positive inattendue pour la cible

IRAK-2. De la même façon, nous n'avons pas détecté de production de cytokines inflammatoires dans ces cultures primaires suite à leur traitement avec les peptides OβA ou FβA. Ceci nous amène à penser que l'induction du miR-146a aurait pour fonction de contrecarrer l'activation de la voie de signalisation NF-κB activées dans les cellules astrocytaires suite au traitement avec OβA et FβA. Ce microARN jouerait par conséquent un rôle anti-inflammatoire par une régulation retro négative de la voie de signalisation NF-κB en contrôlant l'expression d'IRAK-1 et TRAF-6 conjointement à un mécanisme compensatoire sur la cible IRAK-2. Cette hypothèse a été confirmée plus tardivement à l'aide d'inhibiteur moléculaire du miR-146a. Le traitement avec cet antagoniste permet de restaurer l'expression d'IRAK 1 et TRAF-6 dans les cultures d'astrocyte et conduit à l'expression transcriptionnelle de cytokines inflammatoires tel qu'IL-6, IL-1β et CXCL1.

En conclusion, ce travail de doctorat a permis pour la première fois, à notre connaissance, d'établir des profils d'expression anormaux de microARNs circulants dans un modèle animal de la MA obtenu par injection intra-hippocampique de peptide βA 1-42 dans le cerveau d'animaux de laboratoire. Ces données sont d'autant plus intéressantes qu'elles permettent de corréler directement l'expression de microARNs sanguins avec la présence de βA dans un tissu neurologique au stade adulte qui représente, à l'inverse des modèles de souris transgéniques, 95 % des formes sporadiques de la MA. Ces microARNs pourraient par conséquent représenter des biomarqueurs précoces de cette pathologie. De plus, nous fournissons des informations complémentaires à la littérature sur le mode d'action moléculaire joué par le miR-146a dans les réponses inflammatoires du système nerveux central. Ces résultats sont par conséquent prometteurs et mériteraient d'être explorés plus en détail pour leurs applications potentielles dans le diagnostic précoce et la prise en charge thérapeutique de cette pathologie.

Overview of the PhD project and objectives

Among all dementia disorders, Alzheimer's disease (AD) is the most common in the elderly. Pathologically, the hallmarks of AD are the deposition of amyloid-β (Aβ) peptides in the form of plaques in the extracellular environment and neurofibrillary tangles composed of hyperphosphorylated Tau proteins within neuronal cells, which are associated with cognitive impairment and dementia.

Several evidences suggest that the generation of Aβ peptides plays a central role in the initiation of the pathological cascade in AD, which is generated through the sequential proteolytic cleavage of the amyloid precursor protein (APP) by β-secretase (BACE1) and γ-secretase ((namely, presenilin 1/2 (PSEN1 / 2)). Therefore, the regulation of the expression of these proteins (BACE1, PSEN and APP) can be critical for the establishment of new AD treatment options.

The production of Aβ 1-42 peptides and phosphorylated Tau (P-Tau) have been used in clinical practice to differentiate cases of AD from normal aging with a sensitivity and specificity of more than 85% (Anoop, Singh, Jacob, & Maji, 2010). But, sample collection, transportation, storage, inconsistency of data analysis, and high cost of evaluations result in a real need to discover new classes of biomarkers (Humpel, 2011).

Today, there is still no cure for AD even though there are therapies that can delay the progress of the disease and/or treat the symptoms. For this reason, early diagnosis is essential, since it allows the patient to be given the required care before the advanced stage

is reached (Grela, Turek, & Piekoszewski, 2012). Biomarkers are diagnostic solutions that make it possible to measure changes in the patient's health status, as well as the response to treatment (Humpel, 2011). Regarding AD, different studies were performed to search for biomarkers in cerebrospinal fluid (CSF) and blood, which is more accessible and less invasive (Grela et al., 2012; Wu et al., 2017). Circulating microRNAs (miRNAs) have been proposed as good biomarkers. MiRNAs are small non-coding RNAs, 18-30 nucleotides (nt) in length that regulate gene expression, important biological processes and play an important role in the appearance and development of diseases by affecting the stability or translation of mRNAs, or suppress the translation of certain proteins (S. Kumar & Reddy, 2016). These small molecules are found to be stable in the circulation, resistant to RNAase digestion and to many extreme conditions including extreme pH, high temperature, extended storage, and multiple freeze- thaw cycles (Baldassarre, Felli, Prantera, & Masotti, 2017). More importantly, miRNAs could be detected in different body fluids (Weber et al., 2010) and their expression levels are closely correlated in various pathological stages of disease (X. Chen et al., 2008).

Knowing the regulatory role of miRNAs, numerous studies have been carried out to evaluate the alterations in the specific miRNA levels involved in the regulation of key AD genes (Cogswell et al., 2008; Herrera-Espejo, Santos-Zorrozua, Álvarez-González, Lopez- Lopez, & Garcia-Orad, 2019; P. Kumar et al., 2013). Current evidence on AD findings suggests that dysregulation of miRNAs could contribute to disease risk and that these can be used as potential biomarkers (Delay, Mandemakers, & Hébert, 2012), to diagnose AD in early stages, track the disease progression and predict response to treatment (Henriksen et al., 2014).

There are different experimental models that have been developed to study AD. They are important for understanding and acquiring knowledge about the pathogenesis of AD. They are also essential for identifying biomarkers and evaluating the efficacy of potential therapeutic approaches. Transgenic mice that overexpress human genes associated with familial AD (FAD) leading to amyloid plaque formation are the most widely used animal models. In most experimental models, it is quite rare to find the presence of both amyloid plaques and neurofibrillary tangles.

Today, it is admitted that each model has its own advantages and limitations and none of the available models replicate all features of human AD. Nevertheless, the different animal models are interesting to address some issues of AD pathophysiology, as long as we recognize their intrinsic limitations, to ensure the interpretation of the experimental results with respect to their translation to human AD.

In this Ph. D project co-supervised between the Universidad Peruana Cayetano Heredia and University of Orléans, we aimed to assess the early events triggered by aggregated forms of Aβ 1-42 and to investigate the impact on cognitive performance and to look at the correlation of these events with circulating miRNAs in serum and CSF samples as early biomarkers of AD. In addition, we conducted *in cellulo* studies with primary astrocytes treated with different forms of Aβ peptides.

More specifically, we aimed to address this general scientific question: what will be the expression profile of circulating microRNAs in an animal model of Alzheimer's disease infused intrahippocampally with Aβ peptides? In order to answer to this question, we developed a project in 3 main parts consisting in:

1) Establishment of an animal model of AD generated by intrahippocampal injection of the Aβ 1-42 peptide.
2) Evaluation of the expression of circulating microRNAs associated with the presence of Aβ 1-42 as early biomarkers of AD
3) Molecular and cellular investigation of the biological role of miRNA-146a in development to AD using a simplified in vitro model of this pathology.

To investigate *in vivo* early events, we injected Aβ peptides in the lateral ventricles of the rat brain. Although the synthetic form of Aβ may be less potent than Aβ naturally secreted from cells or human-derived Aβ, studies have shown similar neurotoxic effects. Furthermore, synthetic Aβ peptides are commercially available and can be easily reproduced in the laboratory following established protocols.

We assessed changes in spatial learning and memory using the Morris water maze. Moreover, we determined the presence of miRNAs known to be involved in the regulation of AD key genes in blood serum and CSF samples. Interestingly, we made a comparison of circulating miRNAs expression of our model with an APP/PS1 transgenic mouse model. Finally, we choose to investigate more deeply the impact of Aβ peptides on miR-146a-5p expression, a well-known marker of inflammation. These studies have been conducted on primary rat astrocyte cultures.

The manuscript comprises 4 complementary chapters:

Chapter 1 describes the bibliographic aspects of AD, including the description of the key proteins involved in AD, the progression of AD, and the currently used transgenic and non-

transgenic animal models. Moreover, a bibliographic review of circulating miRNAs in patients and animal models is presented.

Chapter 2 describes all the protocols and techniques used for the development of the project.

In chapter 3, we describe the results consisting of two parts. In part 1 it is shown from the establishment of the in vivo animal model generated by intrahippocampal injection of Aβ 1-42, to the identification of circulating miRNAs. The second part shows the results of mechanistic studies related to miR-146a in a primary culture of astrocytes.

In chapter 4, the results obtained are discussed and the final considerations of this project are shown.

Two manuscripts obtained from this thesis are under submission process:

"Preclinical animal models of Alzheimer disease and relationship with identification of circulating microRNAs as early diagnosis biomarker"

Aquino Ruth, de Concini Vidian, Menuet Arnaud, Guerra Cristina, Baril Patrick, Pichon Chantal Submission in Current Neuropharmacology

"Identification of circulating microRNAs in rat model produced by intrahippocampal injection of Aβ 1-42"

Aquino Ruth, de Concini Vidian, Menuet Arnaud, Gosset David, Baril Patrick, Pichon Chantal. Submission in Cells.

Chapter I Bibliographic study

1. Summary

Alzheimer disease (AD) is a neurocognitive disease characterized by aberrant expressions & functions of Tau, APP, PSEN1, PSEN2 and/or APOE4 proteins. Such dysregulation has been used as basis for the development of in vivo animal models of Alzheimer's disease. To date, there are more than 190 animal models of AD that have contributed to a better understanding of the molecular basis of AD progression. These models have been also extensively used to evaluate therapeutic approaches to treat this neurodegenerative disease. However, there is still some debates about the relevancy of these animal models of AD as none of therapeutic drugs selected in those models have reached the clinic. The vast majority of these AD models are transgenics, based on aspects of the amyloid aggregation and the genetic mutations encountered in the familial form of AD (FAD) that account for only 5 % of AD patient. As a result, the late-onset sporadic form of AD (LOAD) that accounts for more than 90 % of AD patients have been mostly ignored. In this review, we recapitulate the main molecular basis of AD pathogenesis and discuss the latest generation of AD animal models that we found relevant in term of FAD and LOAD forms of AD. Advantages and drawbacks of recent animal models are given and we report the main advances made using them. An important question in the field of AD regarding the identification of relevant early diagnosis molecular markers is addressed with a focus on miRNAs. We provide an overview of significant literature in the field of detection of circulating miRNAs in body fluids of AD patient. We also provide a short list of miRNAs detected both in animal models and in patients that could be considered as promising diagnosis and therapeutic markers for this pathology and they deserve further investigation before possible translation to the clinic.

2. Introduction

Alzheimer's disease (AD) is a chronic and devastating condition in which senile people have abnormal and progressive brain disorders (Domingues, da Cruz, & Henriques, 2017). Dementia is the main clinical syndrome observed in AD patients. The majority of severe cognitive impairments occur after age 65 constituting the late-onset AD (LOAD). Cases of AD that appear early or commonly termed as early-onset AD (EOAD) can be detected in patients younger than 65, but only corresponds to 5% of AD patients. AD is not considered as genetic disease. Although genetic mutations in apolipoprotein E(APOE), presenilin (PSEN) and Amyloid Beta Precursor Protein (APP) genes have been reported, their occurrence is low and concerns only to 1 to 2 % form of AD. These rare forms of inherited Alzheimer disease, referred as Autosomal dominant Alzheimer disease (ADAD), occur at very early age of onset and are characterized by distinctive neurologic symptoms and a rapid disease progression.

AD is a complex and multifactorial pathology in which the appearance of amyloid plaques and the hyperphosphorylation of the Tau protein are the two main characteristics (Figure 1) responsible for the gradual decline of cognitive functions such as loss of memory, language and thinking abilities.

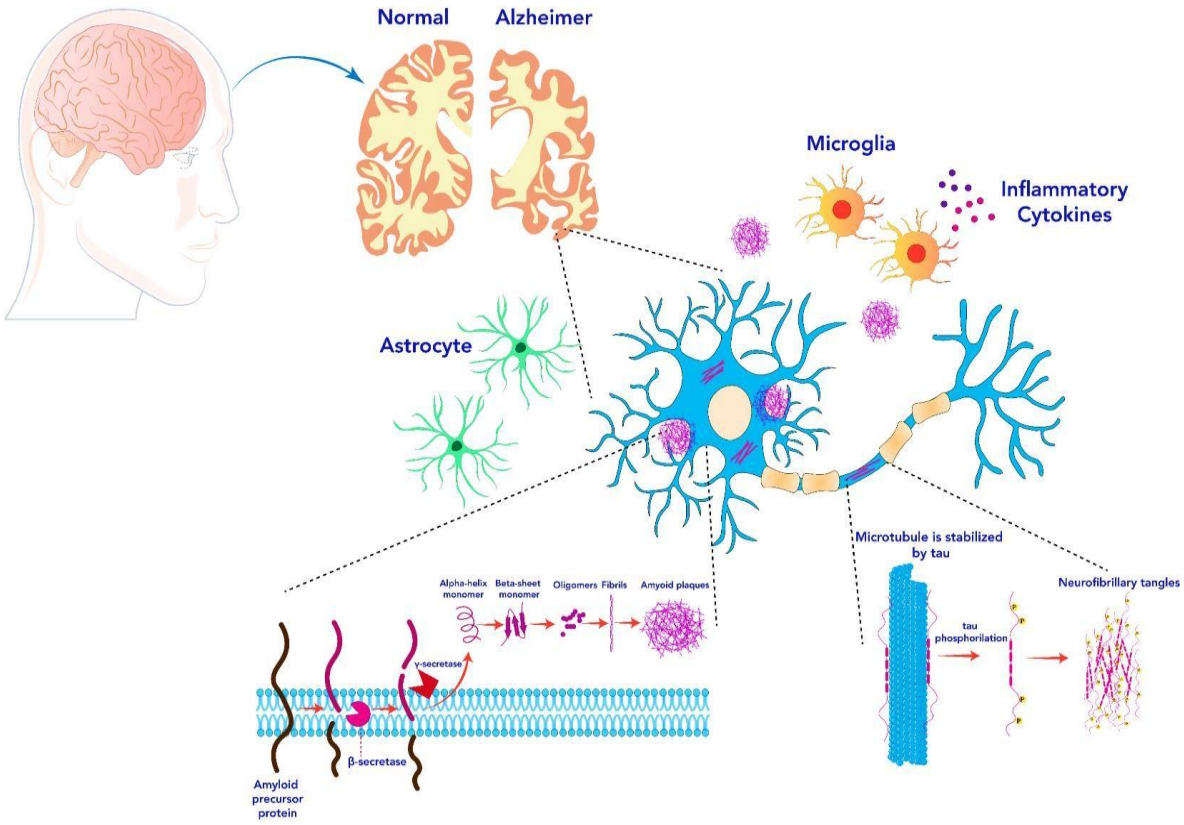

Figure 1. Overview of Alzheimer's disease. AD is a multifactorial neurodegenerative pathology whose main characteristics are the accumulation of extracellular amyloid plaques and intracellular Tau aggregates that form neurofibrillary tangles. Proteolysis of Amyloid Beta Precursor Protein (APP) results in the production of Aβ and amyloid plaques (detailed in the lower left part) as well as the process of hyperphosphorylation of Tau and formation of neurofibrillary tangles (lower right part). The inflammatory context, a feature of AD brains is shown by the presence of reactive astrocytes, activated microglia, and inflammatory cytokines.

Amyloid plaques are deposits of Aβ peptide that accumulate in the extracellular matrix between nerve cells preventing a correct communication (Mullard, 2016). Aβ peptide accumulation arises from cleavage of the APP membrane protein. This type 1 transmembrane integral glycoprotein (Roberts et al., 1994) is encoded by a gene located on chromosome 21, spanning over 290 kilobases, that generates a 695 amino acids protein transported to the cell surface through the Golgi / trans- Golgi network (TGN) network (Agostinho, Pliássova, Oliveira, & Cunha, 2015). During transcription, differential splicing of APP mRNA can give rise to several isoforms. The major isoforms of APP have770, 751, or 695 amino acid residues (Figure 2). The APP751 and APP695 isoforms are produced as a result of exons 7 and / or 8 splicing (Weidemann et al., 1989). There are also other less common isoforms such as L-APP, which lacks exon 15 (Pangalos, Shioi, Efthimiopoulos, Wu, & Robakis, 1996) and APP639 devoid of exons 2, 7 and 8 (Tang et al., 2003). These isoforms are expressed in different amounts and in different cell types; for example, APP695 is the predominant neuronal isoform (Dawkins & Small, 2014), but non-neuronal cells mainly express APP770 and APP751 (Dawkins & Small, 2014; Rohan de Silva et al., 1997). L-APP is expressed in leukocytes, microglia, and astrocytes (König et al., 1992) and APP639 is widely expressed in fetal tissue and only in adult liver (Tang et al., 2003). APP is one of the most abundant proteins in the central nervous system (CNS). Its expression is required for adequate neuronal migration during early embryogenesis (Young-Pearse et al., 2007), the formation of neuromuscular synapses through heterooligomeric interaction with low-density lipoprotein (LDL) receptor-related protein 4 and agrin (a regulator of synaptogenesis) in adult CNS tissues.

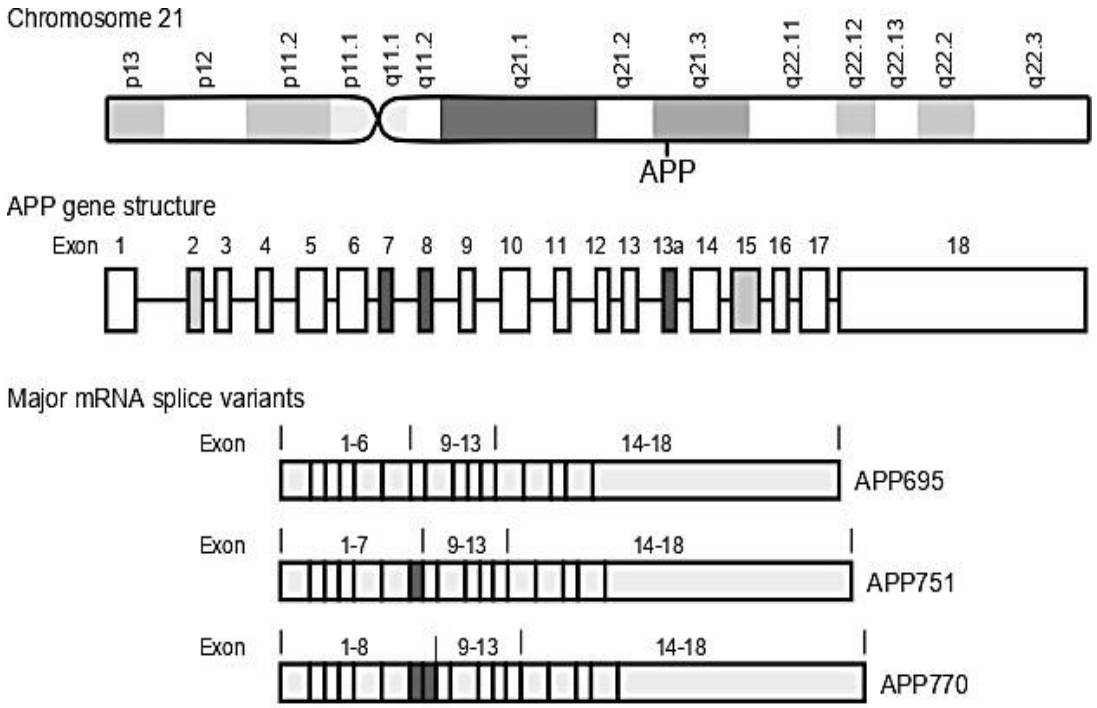

Figure 2. Structure of APP gene, mRNA and protein. The APP gene is located on chromosome 21q21.3. The gene has 18 exons. Differential mRNA splicing of exons 7,8 (dark gray) leads to the expression of isoforms of 695, 751 and 770 amino acids. Exons 2 and 15 (light gray) are spliced into APP639 and L-APP, respectively. The most abundant form in brain is APP695. From (Dawkins & Small, 2014)

The proteolytic cleavage of APP operates through two main pathways: **amyloidogenic and non- amyloidogenic**. The amyloidogenic pathway is responsible for the release of pathologic Aβ peptide outside of the cells. In this pathway, APP is cleaved by a ß- secretase 1 also called BACE1, ASP2 or memapsin 2 to release a small N-terminal ß fragment of APP (sAPPß) and a still-membrane anchored β-carboxyl terminal fragment (CTFβ or C99). This transmembrane CTFβ terminal fragment contains the full length amyloidogenic sequence (Aβ peptide) which is further cleaved by a γ-secretase to generate a Aβ cleavage

product of 43–51 amino acids (Figure 3). The cleavage of γ- secretase is not very precise, which leads to the production of different peptides having different C- terminal. Amongst the different Aβ species, those ending at position 40(Aβ40) are the most abundant (~80-90%), followed by those ending at position 42 (Aβ42, ~5-10%) (Olsson et al., 2014; Takami et al., 2009) (Figure 4). Aβ42 peptides are more hydrophobic and fibrillogenic, and are the principal main species deposited in the brain (Selkoe, 2001). Both Aβ monomers are progressively aggregate in dimers, trimers, oligomers, protofibrils and fibrils to finally form insoluble amyloid plaques (G. F. Chen et al., 2017) (Figure 5). Despite their similarities, Aβ42 monomers are more prone to aggregation and fibrillation than that of Aβ40 peptide and therefore, they are considered more pathogenic (Recuero, Serrano, Bullido, & Valdivieso, 2004).

.

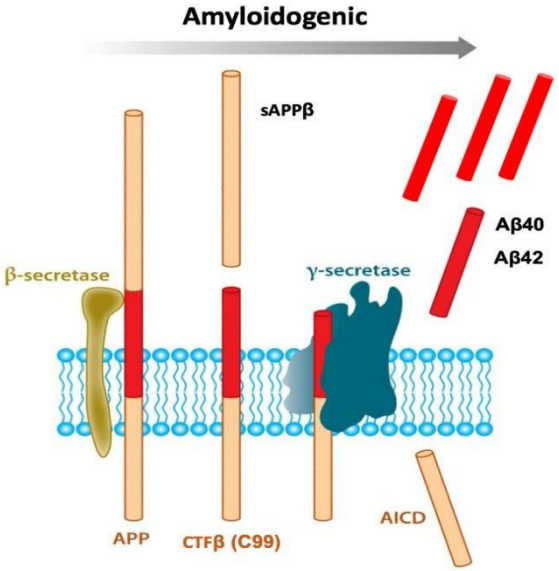

Figure 3. APP proteolysis through the amyloidogenic pathway. Amyloidogenic processing of APP is carried out by the sequential action of membrane bound β- and γ-secretases. β-Secretase cleaves APP into the membrane-tethered C-terminal fragments β (CTFβ or C99) and N-terminal sAPPβ. CTFβ is subsequently cleaved by γ-secretases into

the extracellular Aβ and APP intracellular domain (AICD). From (O'Brien & Wong, 2011) with minor modifications.

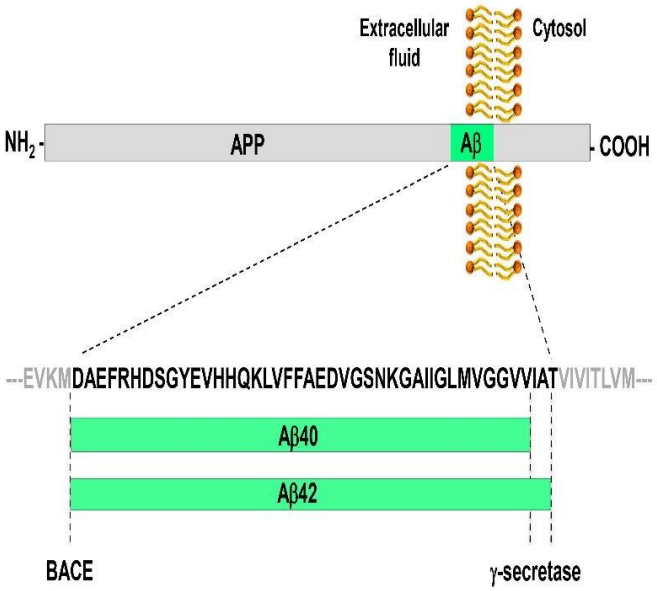

Figure 4. Generation of different Aβ peptide species from the processing of APP by BACE and γ-secretase. One of APP domains is displayed; the Aβ domain is cleaved by β- and γ -secretases. The β-secretase BACE has a single cleavage site on APP and generates the N-terminus of Aβ peptides. The γ-secretase has multiple cleavage sites on APP, which leads to the generation of Aβ peptides of variable length that differ from their C-terminus. The most abundant peptides are Aβ40 and Aβ42. Aβ42 is particularly prone to aggregation. From (Mantile & Prisco, 2020).

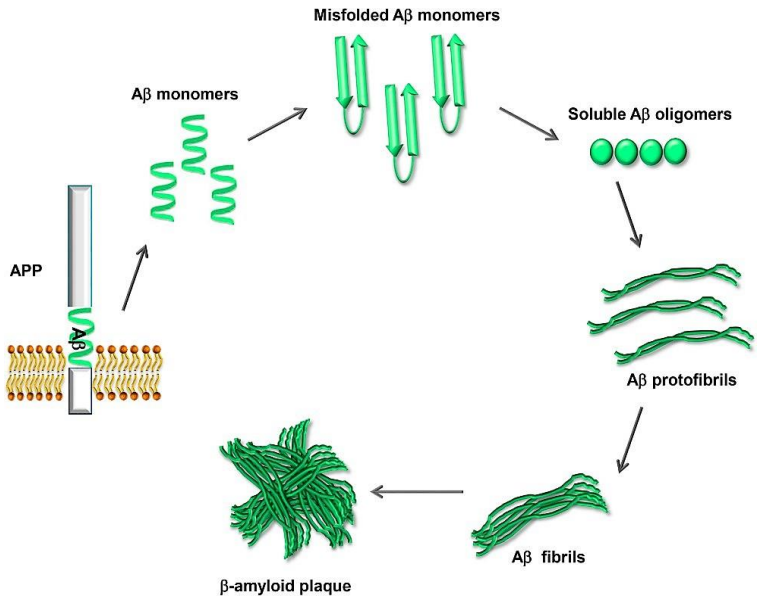

Figure 5. Process of Aβ aggregation and amyloid plaque formation. The Aβ peptide, once excised from APP, is prone to misfolding and self-aggregation. Misfolded Aβ monomers aggregate in dimmers, trimers or small soluble oligomers. The oligomers interact to form protofibrils, which grow to form mature fibrils. Eventually the fibrils aggregate, forming the amyloid plaques that appear in brains with AD. From (Mantile & Prisco, 2020).

In the non-amyloidogenic pathway, APP processing is cleaved by α-secretase at the cellular membrane (Figure 6). This endopeptidase cleaves the APP protein within another site of amyloidogenic sequence (Aβ peptide) preventing the formation of full length Aβ40 and Aβ42 peptides. A soluble APP fragment (sAPPα) and a CTF transmembrane domain (α-CTF) are generated upon cleavage. The soluble APP fragment (sAPPα), shorter than Aβ40 and Aβ42 peptides, are released into the extracellular spaces of neurons cells but cannot aggregate to form fibrils amyloid plaques. These extracellular monomers and even

oligomers are not toxic to the CNS.

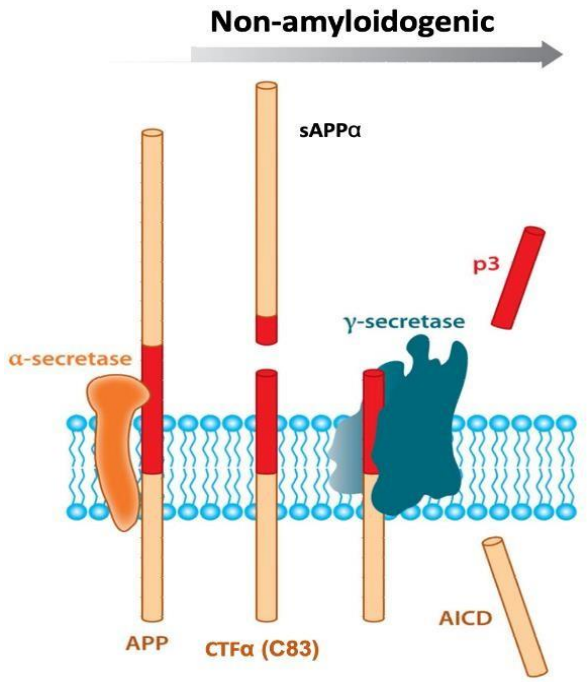

Figure 6. APP proteolysis through the non-amyloidogenic pathway. Non-amyloidogenic processing of APP refers to the sequential processing of APP by membrane bound α-secretases, which cleave within the Aβ domain to generate the membrane-tethered α-C terminal fragment CTFα (C83) and the N-terminal fragment sAPPα. CTFα is then cleaved by γ-secretases to generate extracellular P3 and the APP intracellular domain (AICD). From (O'Brien & Wong, 2011) with minor modifications.

Like the APP, Tau protein is also highly expressed in the CNS but also in several other tissues (De- Paula, Radanovic, Diniz, & Forlenza, 2012). The coding sequence for the Tau protein (MAPT) is located on chromosome 17 and span over 16 exons. The alternative splicing of exons 2, 3 and 10 leads to six possible Tau isoforms (De-Paula et al., 2012; Shahani & Brandt, 2002) highly enriched in axons of neurons (Buée, Bussière, Buée-

Scherrer, Delacourte, & Hof, 2000) (Figure 7). Tau protein is a member of the Microtubules Associated Proteins (MAP) family, its main function in neurons is to coordinate the assembly and stabilization of microtubules (Kolarova, García-Sierra, Bartos, Ricny, & Ripova, 2012; Naseri, Wang, Guo, Sharma, & Luo, 2019) for maintenance of neuronal projections (Naseri et al., 2019) axonal elongation, maturation and transport (De-Paula et al., 2012; Ittner, Ke, & Götz, 2009; Yuan, Kumar, Peterhoff, Duff, & Nixon, 2008). Therefore, Tau is important for synaptic plasticity (Frandemiche et al., 2014; Qu et al., 2017). Tau protein is highly soluble (Jouanne, Rault, & Voisin-Chiret, 2017), very flexible and has a low tendency to aggregate. These properties have contributed to consider this protein as "natively deployed protein" (Mukrasch et al., 2009). Under pathological conditions, tau undergoes different post-translational modifications, such as glycosylation, nitration, ubiquitination, glycation and aberrant phosphorylation (Figure 8). Studies in patients with AD have reported three to four times more phosphorylated form of Tau than in healthy subjects (Cohen et al., 2011; Iqbal, Liu, & Gong, 2016; Jouanne et al., 2017) and many Tau phosphorylation sites have been identified (Figure 9). The degree of phosphorylation of Tau depends on the balance between the activity of kinases such as GSK-3β and CDK5, and phosphatases such as phosphatase 2A (PP2A), which represents 70% of the total activity of phosphatases found in the human brain. (F. Liu, Grundke-Iqbal, Iqbal, & Gong, 2005).

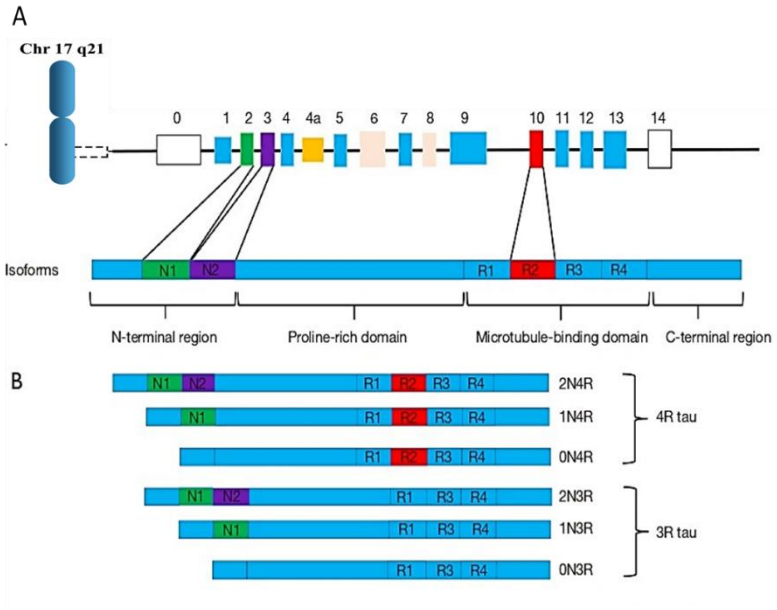

Figure 7. Structure of MAPT gene, mRNA and Tau protein. Tau is encoded by the MAPT gene (16 exons) located on chromosome 17. N1 and N2 domains are encoded by E2 (green) and E3 (purple), respectively. The R2 repeat is encoded by E10 (red box). E1, E4, E5, E7, E9, E11, E12 and E13 constitute the basic component of the Tau protein. E0 and E14 do not encode (blank). E4a (yellow) is transcribed only in peripheral tissue. E6 and E8 (pink) are not expressed in the human brain. Tau isoform is composed of four regions: N-terminal region, a proline-rich domain, a microtubule-binding domain (MBD), and a C-terminal projection region. (B) A total of six isoforms of Tau protein are generated by alternative splicing of exons 2, 3, and 10 (E2, E3, E10). There is the same amount of 3R and 4R Tau in the normal human brain. In Alzheimer's disease the proportion of Tau is altered. From (Y. L. Gao et al., 2018) with minor modifications.

Both GSK-3β and CDK5 kinases are overexpressed in AD, which favour the production of hyperphosphorylated form of Tau protein and thus prevent its binding to tubulin. As a result, disorganized microtubules accumulate in cells that later aggregate in paired helical

filaments (PHF) (Mandelkow, von Bergen, Biernat, & Mandelkow, 2007) and then in neurofibrillary tangles (NFT) (Y. Gao, Tan, Yu, & Tan, 2018; Medeiros, Baglietto-Vargas, & LaFerla, 2011; Querfurth & LaFerla, 2010). Aberrant NFT impairs axonal transport, synaptic metabolism and ultimately loss of cell viability and cell-death (De-Paula et al., 2012; Drechsel, Hyman, Cobb, & Kirschner, 1992). Another consequence of Tau hyperphosphorylation are changes in the conformational state of the protein that make it more prone to self-aggregation (Mukrasch et al., 2009; Smith, 2002; von Bergen et al., 2000).

Clinical findings suggest that Tau aggregation is a hierarchical process that undergoes through different gradual phases; from monomers, dimers, oligomers and finally pre-tangles and neurofibrillary tangles (Patterson et al., 2011). Recently, some studies have brought to light the fibrillogenesis mechanism. It is assumed that, dimers form oligomers, which then elongated to form fibrils (Jouanne et al., 2017), There is an increase of Tau oligomer levels before NFTs are formed and this is present prior the manifestation of clinical symptoms of AD. Fá et al., reported that acute exposure of Tau oligomers in the brain, is detrimental to long-term potentiation (LTP) and memory (Fá et al., 2016). This suggests that the formation of Tau oligomer may represent a sign very early brain aging and AD (Maeda et al., 2006). Note that oligomeric forms of Tau have also been found in other Tauopathies (Gerson et al., 2016; Sengupta et al., 2017; Vuonoet al., 2015).

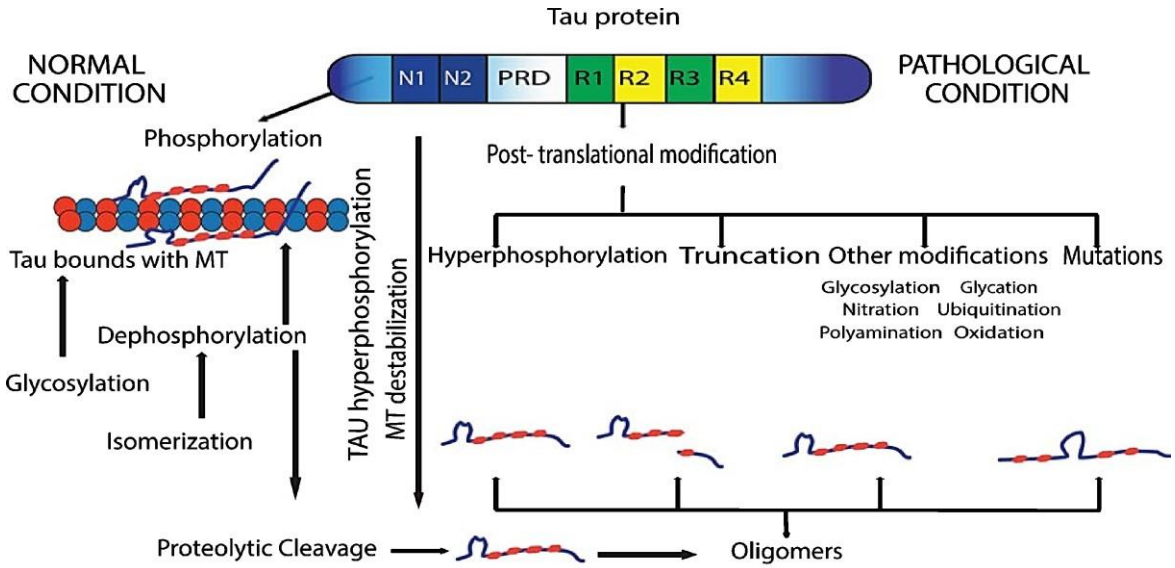

Figure 8. Schematic representation of the mechanism of the post-translational modifications of Tau under normal and pathological conditions. Under pathological conditions, Tau undergoes different post-transcriptional modifications, such as hyperphosphorylation, acetylation, ubiquitination leading to detachment of Tau from microtubules, resulting in destabilization of microtubules in axons. From (Almansoub et al., 2019).

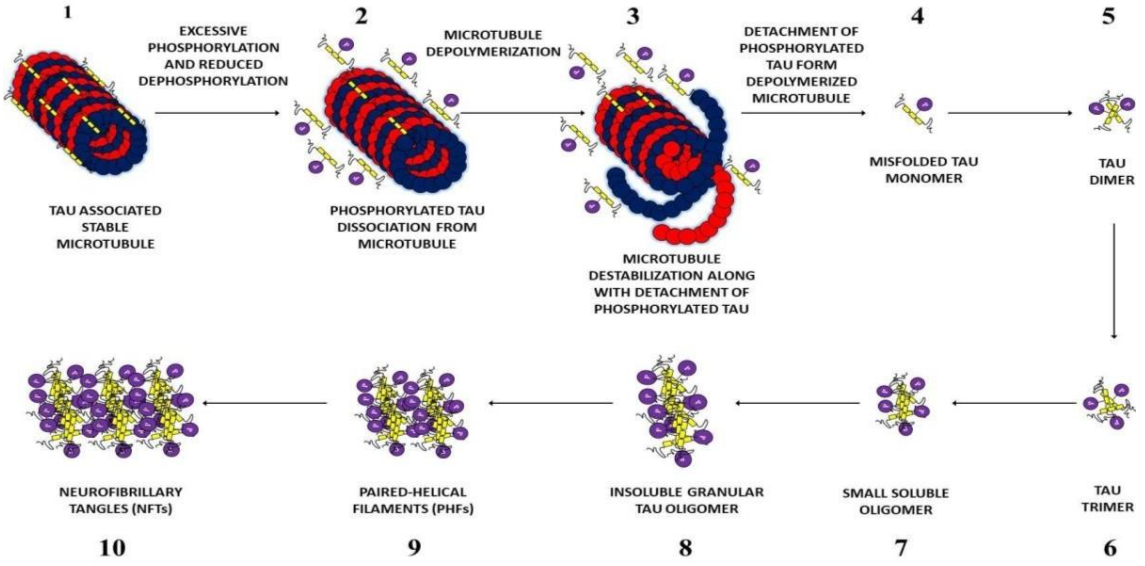

Figure 9. The sequential steps of NFTs formation. Phosphorylated Tau monomers can assemble to form dimers, trimers, oligomers, filaments (both straight and paired helical), and eventually tangles. From (Muralidar, Ambi, Sekaran, Thirumalai, & Palaniappan, 2020).

Another key mediator of AD development is the apolipoprotein E (apoE) gene which is localized on chromosome 19 and contains four exons and three introns (Figure 10A), generating the three main protein isoforms, APOE2, APOE3 and APOE4 (Giau, Bagyinszky, An, & Kim, 2015). APOE is a 35 kDa glycoprotein expressed in the brain and throughout the human body. In peripheral tissues, APOE is produced primarily by the liver and macrophages. Among the general functions of APOE are; the contribution to the homeostasis of cholesterol and other lipids to regulate the transport of lipids from one tissue to another (Mahley & Rall, 2000) and thus facilitating the cellular uptake of lipids (Mahley, 1988). In the CNS, APOE is produced mainly by astrocytes, although it can also be produced by microglia (Elliott, Kim, Jans, & Garner, 2007; LaDu et al., 1998). Cholesterol transport by APOE provides neurons the cholesterol necessary for synapse formation,

plasticity and repair (Poirier, 2008) and is ensured by APOE receptors, which belong to the low- density lipoprotein receptor (LDLR) protein family (Bu, 2009). The human apoE genes has three polymorphic alleles; ε2, ε3, and ε4, with frequencies of 6.4, 78.3, and 14.5 %, respectively (Eisenberg, Kuzawa, & Hayes, 2010). While apoE3 is the most common allele in the world population, apoE2 allele is associated with reduce risk of dementia (C. Liu & Götz, 2013). ApoE4 allele is the most representative risk factor for late-onset Alzheimer's disease (LOAD) (Bu, 2009; Huang & Mucke, 2012) and cerebral amyloid angiopathy (CAA) (Biffi et al., 2010; C. Liu & Götz, 2013). The differences between the three isoforms of APOE depend on presence of cysteine or arginine in amino acids 112 and 158 (Muñoz, Garner, & Ooi, 2019) generating APOE2 (Cys112, Cys158), APOE3 (Cys112, Arg158) and APOE4 (Arg112, Arg158) (J. Chen, Li, & Wang, 2011; Mahley & Rall, 2000) (Figure 10B). According to homozygous or heterozygous status of mutated alleles, six different genotypes can be generated, homozygous ε2 / 2, ε3 / 3 and ε4 / 4, and heterozygous ε2 / 3, ε2 / 4 and ε3 / 4. It is known that the frequency of the APOE4 allele increases dramatically in ~ 40% in AD patients (Farrer et al., 1997), and that homozygous patients for apoE4 isoform are approximately 10 times more likely to develop AD than heterozygous carrier (Corder et al., 1993; Muñoz et al., 2019). The exact mechanism by which apoE4 participates in the progression of AD is not totally clear. However, a direct correlation between APOE4 carrier and detection of senile plaques of Aβ has been reported, suggesting a direct impact of APOE4 in modulation of Aβ plaque clearance. It has been proposed that APOE proteins, especially those from astrocytes, are essential for the degradation and elimination of deposited Aβ, and this process is altered in AD (Koistinaho et al., 2004). Based on studies that reported the presence of apoE4 fragments (14-20 kDa) in the brain with AD (Harris et al., 2003; Rohn, Catlin, Coonse, & Habig, 2012), It has been suggested that the intraneuronal proteolytic cleavage of APOE4 could

promote neuropathology and neurodegeneration in AD. Unlike the other isoforms, APOE4 is more susceptible to proteolysis and its hinge region has multiple protease-sensitive sites, such as cathepsin D (Zhou, Scott, Shelton, & Crutcher, 2006), a protease similar to chymotrypsin (Harris et al., 2003), and aspartic proteases (Marques, Owens, & Crutcher, 2004). Furthermore, other regions are also susceptible to being cleaved such as the N- and C-terminal domains (Elliott et al., 2011) (Figure 11).

The N- and C-terminal fragments are neurotoxic in nature (Andrews-Zwilling et al., 2010), and it has been reported that after APOE4 cleavage, each domain appears to localize to specific lesions in the AD brain. For example, the C-terminal domain has been implicated in Aβ binding and is located in the plaques (Marques et al., 2004; Rohn et al., 2012). Some studies performed in mice expressing C-terminal truncated APOE4 has a lower affinity for Aβ and a reduced ability to eliminate Aβ resulting to behavioral deficits (Bien-Ly et al., 2011). Therefore, APOE4 cleavage leads to the accumulation and aggregation of toxic beta-amyloid species (Figure 12). Other authors have suggested that APOE4 more strongly stimulate Aβ aggregation compared to APOE3 and that the increase in the level of Aβ oligomers is isoform-dependent (i.e., APOE4> APOE3> APOE2) (Hashimoto et al., 2012). Furthermore, APOE4 stabilizes Aβ oligomers more than APOE3 (Cerf, Gustot, Goormaghtigh, Ruysschaert, & Raussens, 2011). Thus, APOE4 detrimentally triggers Aβ aggregation in AD (Uddin et al., 2019). On the other hand, the N-terminal domain is preferentially located within the NFTs (Harris et al., 2003), this has been confirmed with an antibody directed to a putative cleavage site within APOE4 at position D172 (Rohn et al., 2012). Therefore, APOE4 is also associated with increased phosphorylation of Tau and the formation of entangled inclusions (Andrews-Zwilling et al., 2010; Brecht et al., 2004; S. Chang et al., 2005). Among other functions, APOE4 has also been reported induce a

mitochondrial dysfunction (H. K. Chen et al., 2011) (Figure 12). The specific N- terminal fragment has been shown to bind to mitochondrial proteins associated with oxidative phosphorylation (Nakamura, Watanabe, Fujino, Hosono, & Michikawa, 2009). Furthermore, APOE is one of the main lipid acceptors in the CNS and functions to transport cholesterol from cells generating high-density lipoprotein (HDL) particles. Loss of this function due to APOE4 cleavage susceptibility could reduce HDL cholesterol, which is essential for synaptogenesis and neurite outgrowth, and this is consistent with neurodegeneration seen in AD. Furthermore, APOE4 fragments have been shown to cause learning and memory deficits in transgenic mice. Together, these evidences could explain the risk of developing AD associated with the ApoE4 allele (Rohn, 2013).

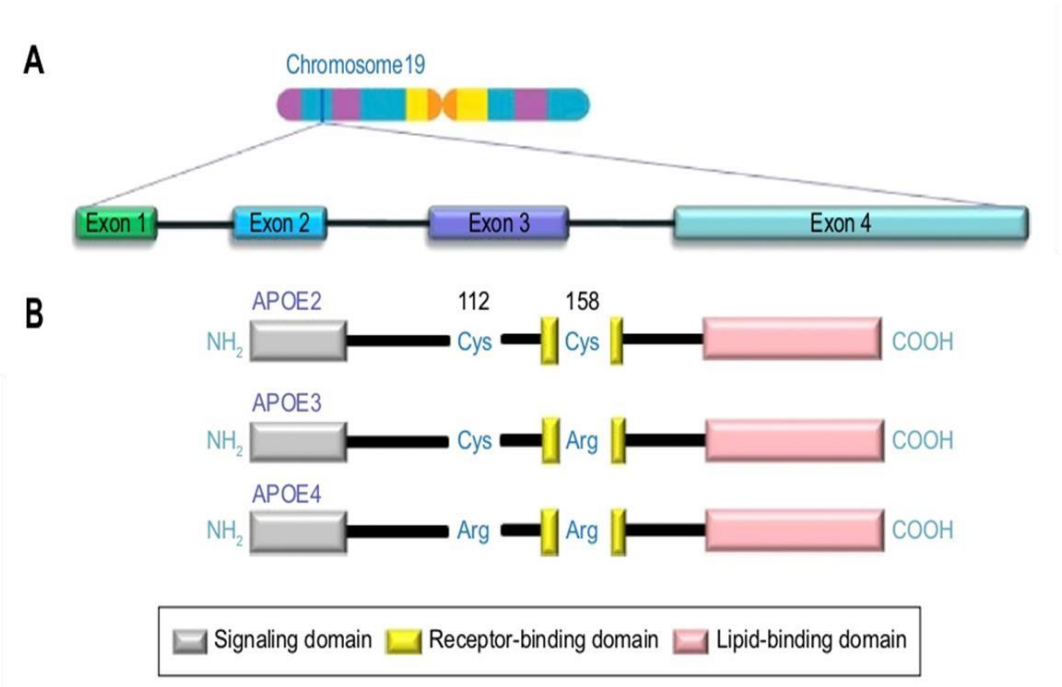

Figure 10. Structure of apoE gene and protein. (A) Location and structure of the apoE gene on chromosome 19. (B) The three major isoforms of APOE are shown, which are located at residues 112 and 158. APOE2 has Cys residues at both positions, APOE3 has a Cys residue at 112 and an Arg residue at 158, and APOE4 has Arg residues at both positions. From (Giau et al., 2015).

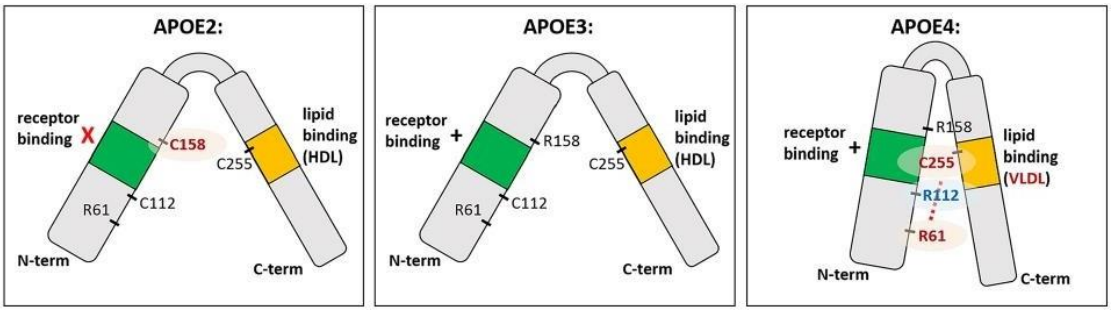

Figure 11. Differences between the structure of APOE isoforms. APOE is a soluble secreted protein, with N-terminal and C-terminal domains joined by a central hinge region. The N-terminal domain contains the receptor-binding domain (green) and the C-terminal domain contains the lipid-binding region (orange). The difference between each isoform is in the position of the amino acids. In APOE2, cysteine is located at position 158 (C158) causing poor receptor binding. In contrast, in APOE4, arginine is positioned at 112 (R112), thus changing the conformation of the entire domain. Therefore, R61 connects to C255 in the terminal c domain (red dotted line). This is the basis of the differences between the functions of APOE4 with respect to other isoforms. One difference is, for example, APOE4's preference for VLDL over HDL. Likewise, it is known that in APOE3 and APOE2, which have C112 instead of R112, there is no interaction of R61 with the domain. From (Fernandez, Hamby, McReynolds, & Ray, 2019).

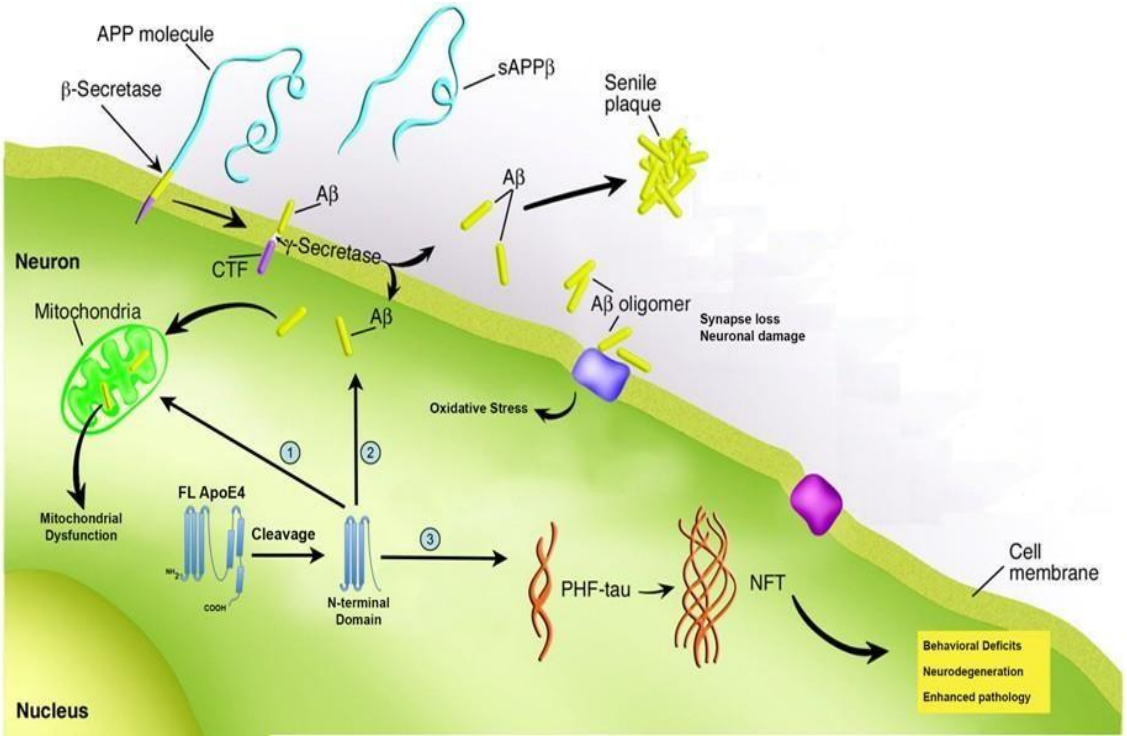

Figure 12. Proteolysis of ApoE4 leads and its implication in AD pathology. It is known that APOE4 promotes the pathogenesis of AD, this occurs after cleavage and the generation of an N-terminal fragment. In turn, the N-terminal fragment leads to a gain in APOE4 toxicity. This can occur through these ways: (1) Altered mitochondrial function caused by the deterioration of the enzymes involved in the respiratory chain complex; (2) Promotes the intracellular accumulation of beta-amyloid by stimulating cell uptake; (3) Induction of tangle-shaped inclusions that resemble neurofibrillary tangles. These results together, generate an enhanced pathology, as well as neuronal deficits at the level of memory and learning and therefore neurodegeneration. From (Rohn, 2013).

Among the genetic factors favoring accumulation of amyloid plaques, mutations of Presenilin 1 and 2 (PSEN1, PSEN2) and APP genes are the main responsible for the appearance of the autosomal dominant Alzheimer's disease form. PSEN1 and PSEN2 are involved in the processing of Aβ by the γ-secretase of the amyloidogenic pathway,

mentioned above. PSEN-1 and PSEN-2 are the main components of the catalytic core of γ-secretase while Nicastrin (NCT), presenilin enhancer (PEN), anterior pharynx defective (APH-1a or APH-1b) are the other components (R. Francis et al., 2002; G. Yu et al., 2000). These four components are essential for full γ -secretase activity (Edbauer et al., 2003) (Figure 13).

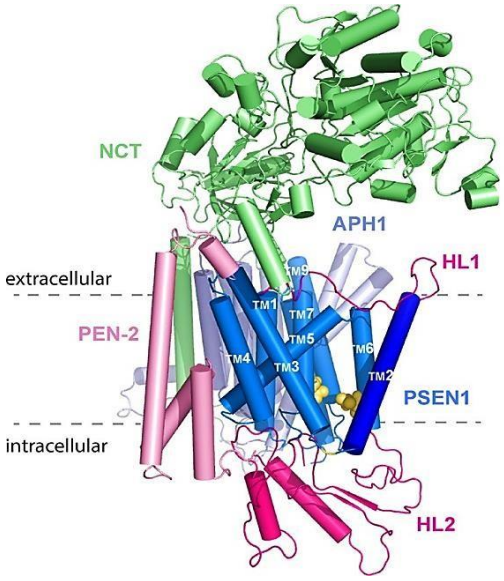

Figure 13. γ-Secretase structure. Lateral view of the γ-secretase complex. NCT (green), APH-1 (silver), PSEN1 (blue) and PSEN-2 (pink). Catalytic aspartates are also shown which are highlighted in yellow. Hydrophilic loop domains 1 and 2 (HL1 and HL2) that bind PSEN1, TMD1-TMD2, and TMD6-TMD7, respectively, are highlighted (hot pink). From (Escamilla-Ayala, Wouters, Sannerud, & Annaert, 2020). TMD (transmembrane domain).

Many pathogenic mutations into the PSEN1 and PSEN2 genes have been respectively reported in AD patients (www.alzhforum.org/mutations; (De-Paula et al., 2012; A. Kumar & Thakur, 2012)). PSEN1 gene is located on chromosome 14 (De-Paula et al., 2012) and has around 221 potentially pathogenic mutations affecting more than 100 amino acids

(www.alzforum.org/mutations; Escamilla-Ayala, Wouters, Sannerud, & Annaert, 2020). PSEN2 gene is located on chromosome 1 (De-Paula et al., 2012) and has only about 19 pathogenic mutations (Lanoiselée et al., 2017) affecting 11 amino acids (www.alzforum.org / mutations) (Figure 14). Mutations in PSEN1, PSEN2 and APP genes are responsible for the appearance of early-onset AD (EOAD) which is autosomal dominant type (Larner, 2011). PSEN1 and PSEN2 genes share a 66% sequence homology, and are ubiquitously expressed (A. Kumar & Thakur, 2012). The transcription rates of both PSENs are affected differently by brain injury or signaling (Nadler et al., 2008; Pluta et al., 2016). Likewise, the existence of a compensatory mechanism among PSENs has been reported, for example PSEN1 deficiency generates a positive regulation of PSEN2 expression (Watanabe, Iqbal, Zheng, Wines-Samuelson, & Shen, 2014).

PSEN1 and PSEN2 have different biological functions. Some studies performed in PSEN1 knockout mice suggest that PSEN1 plays a role in cognitive memory (H. Yu et al., 2001). (Mineur, McLoughlin, Crusio, & Sluyter, 2005). On the other hand, PSEN2 has been evidenced as a less efficient producer of Aβ compared to PSEN1 (Bentahir et al., 2006). PSEN2 has been related to epidermal differentiation (Escamilla-Ayala et al., 2020), and is involved in innate immunity, for example, Agrawal et al., showed that macrophages lacking PSEN2 have a reduced response to lipopolysaccharide (Agrawal, Sawhney, Hickey, & McCarthy, 2016). Also, Jayadey et al., showed that primary murine microglia with loss of PSEN2 gene leads to a greater response to lipopolysaccharide that has been evidenced through measurements of pro-inflammatory cytokines released (Jayadev et al., 2010). PSEN2 deficiency has also been reported to affect the normal functioning of mitochondria (Contino et al., 2017).

Concerning PSEN1 and PSEN2 mutations, it has been mentioned that mutations in the PSEN1 gene are the most important causes of EOAD (Escamilla-Ayala et al., 2020). In

addition, it causes the most severe forms of AD with a very early onset that occurs between approximately 30 to 58 years of age. It has also been reported that some AD patients carrying specific PSEN1 mutations develop some atypical AD symptoms, for example; spastic paraparesis, seizures, degeneration of the corticospinal tract, among others. The clinical atypical phenotypic is dependent on the type of mutation in PSEN1. In contrast to PSEN1, mutations in the PSEN2 gene are a rare cause of EOAD, at least in Caucasian populations. The appearance of AD in these PSEN2 carriers generally appears between 45 to 88 years of age. Likewise, it has been stated mutations in PSEN2 are of lower penetrance, reviewed in (Bekris, Yu, Bird, & Tsuang, 2010).

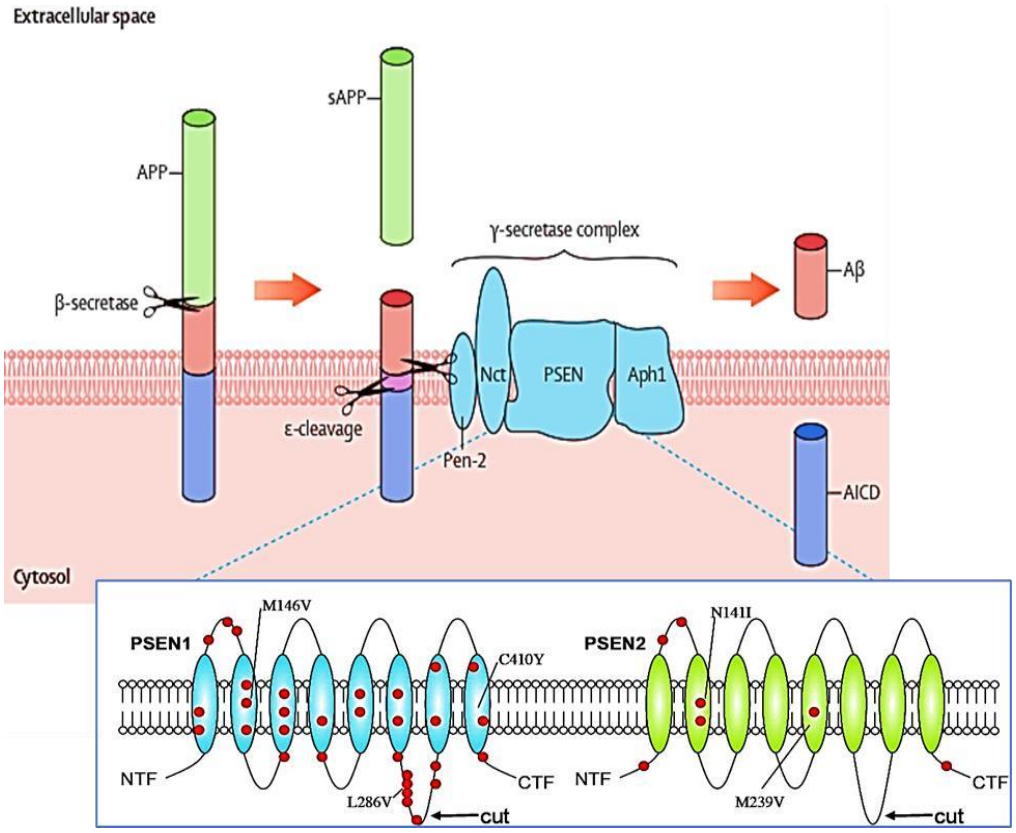

Figure 14. Structure and functions PSEN1 and PSEN2. PSEN1 and PSEN2 are shown as part of the complete y-secretase in the APP processing. The magnified area shows PSEN

1 and PSEN 2, which were schematically represented with mutations (red dots). Autocatalytic cleavage of PSENs (arrow) into N- and C-terminal fragments is required for the activation of the γ-secretase. Adapted from (Chiba, 2013).

3. AD progression

The brain of a healthy adult contains about 100 trillion neurons. They have a body (known as the soma), in which are the nucleus, the smooth and rough endoplasmic reticulum, the mitochondria and the Golgi apparatus, among other cellular organelles and large branched extensions, which make possible the formation of connections with other neurons that allow signal flow throughout the central (CNS) and peripheral (PNS) nervous systems. The main functions of the CNS are to create memories, thoughts, sensations, emotions and motor responses; to achieve this goal, it has two specialized cells: nerve cells (neurons) and glial cells (Uehara, 2020). The latter play a fundamental role, since they are able to guide neurons in development to their destinations, provide myelin sheaths around axons, provide nutrients and protection to the entire nervous system.

Of all the cells in the nervous system, the glial cells play an important role, including; a) astrocytes, which provide nutrients to neurons, regulate the concentrations of ions and chemical compounds in the extracellular fluid, provide structural support in the synaptic process and block toxic substances that could enter the brain; b) the microglia, responsible for degrading dead cells and protecting the brain against invading pathogens in the CNS; c) oligodendrocytes and Schwann cells, which cover axons of neurons in the CNS and PNS with myelin, respectively; d) glial satellites, which cover the body of neurons in the PNS and provide nutrients and structural support; and, e) ependymal cells, which line the ventricles of the brain and the central canal of the spinal cord and which protect the brain thanks to the production and flow of CSF (Uehara, 2020). It is also known that the cerebral cortex has five parts: the primary, the secondary, the tertiary or heteromodal cortex (within

which it is considered a quaternary or supra-modal that belongs to the prefrontal sector of the frontal lobe), the paralimbic and limbic. It is in the tertiary and quaternary heteromodal and limbic areas where AD will present its main initial symptoms. Later, this pathology will affect secondary areas. At first, the anomaly, will appear from the posterior mesial-temporal sectors of the brain (damage and neuronal death in the hippocampus) to the anterior sectors in the prefrontal areas (progressive and irreversible general atrophy) (Uehara, 2020).

The brain is one of the organs with the greatest immunological ability, since it has a blood-lymphatic barrier and lacks conventional lymphatic drainage, it has been observed by histochemical and molecular biology that it has a very active endogenous immune system. Due to this, in cases of brain pathologies, chronic inflammation can damage the healthy tissue progressively generating neuronal death, since neurons such as postmitotic cells cannot be easily replaced (Angosto & González, 2009).

Likewise, neurons are responsible for metabolizing large amounts of glucose for energy; however, as will be seen later, in people with AD there will be a suppression in synaptic function. As a consequence of this, due to the lower amount of glucose that is metabolized, various regions of the brain will be reduced, such as the precuneus area, the lateral parietal lobe and the temporal lobe (Uehara, 2020).

Braak and Braak described the stages in the neuropathology of AD (Figure 15). The progression of AD has been divided into three stages (A-C). In stage A, amyloid is found in the base layer of the frontal, temporal, and occipital lobes. In stage B, amyloid progresses to almost all areas of isocortex and in stage C, amyloid is densely packed (Braak & Braak,

1991).

On the other hand, the Tau modification has been divided into six stages (I-VI). It is believed that from stage I to stage III, 30 years may pass and during this time the disease is not symptomatic. It is also estimated that there are 48 years from stage I to stage V of Braak, in which the symptoms are already evident.

Stage I is considered clinically silent. In Braak stages I and II, the neurofibrillary tangles are centered around the trans entorhinal region. However, stage II differs from stage I, because it is more densely populated with Tau pathology, the appearance of numerous neurofibrillary tangles and neuropil threads has been described in the trans entorhinal region, and some additional ones in the entorhinal region (Guimerà, Gironès & Cruz-Sánchez, 2002).

In stage III, the pathology moves towards the entorhinal region with low levels of Tau in CA1 of the hippocampus and little or no changes in isocortex (Braak & Braak, 1991). The hippocampus is responsible for episodic memory, which is the memory of autobiographical events (Tulving & Markowitsch, 1998). This corresponds to the first symptoms observed in AD and is defined as mild cognitive impairment (MCI). Patients who fit this definition arethree to five times more likely to develop dementia within three to five years (Borroni, Di Luca, & Padovani, 2006). In stage IV, there is an increase in pathology from the entorhinal region towards the amygdala, and the CA1 hippocampus, and towards the association areas of the basal temporal neocortex. At this stage, there is no detectable brain atrophy and the pathology does not meet the criteria for the neuropathological diagnosis of AD. However, in this phase, some individuals have impaired cognitive functions and subtle personality changes.

In Stage V, Tau is found in almost all areas of the hippocampus and isocortex. Another characteristic is the extremely severe destruction of the neocortical associative areas. In Stage VI, the areas are severely affected, the pathological process spreads to the primary areas. Isocortex involvement corresponds to late AD and can be clinically diagnosed (Braak & Braak, 1991). These last two stages correspond to fully developed AD (Guimerà,Gironès & Cruz-Sánchez, 2002).

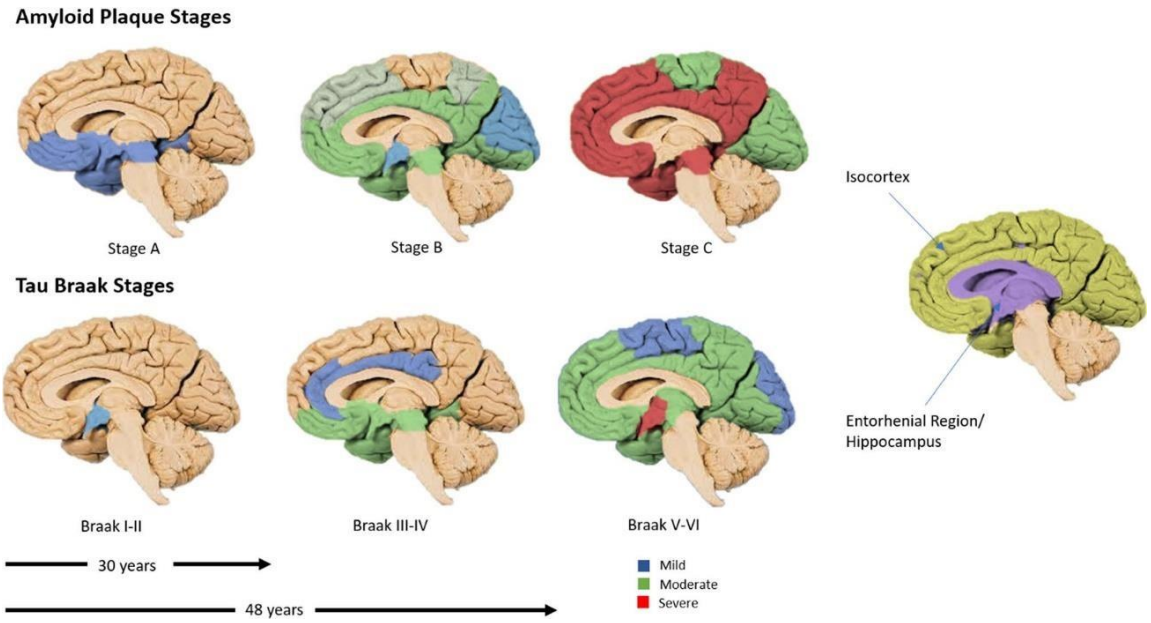

Figure 15. Schematic representation of the amyloid and Tau stages during the progression of Alzheimer's disease, proposed by Braak and Braak. Mild, moderate, and severe correspond to the density of amyloid / tau protein. From (Swarbrick, Wragg, Ghosh, & Stolzing, 2019).

3.1. Phases of Alzheimer's disease

In this section, we describe four phases of Alzheimer's disease: preclinical phase, prodromal phase, mild-moderate phase and advanced phase. Subsequently, the progression of AD will be explained from a molecular point of view.

3.1.1. Preclinical phase

The concept of the preclinical phase arises due to the evidence that the pathological process of AD begins years before the clinical manifestations of the disease. There are data from pathological anatomy studies of patients who had some type of neuronal damage typical of AD, but that they had not clinically manifested the disease until the moment of death (Valls-Pedret, Molinuevo, & Rami, 2010).

In this phase, the individual does not show any type of symptoms. However, it is known that the first molecular alterations occur, which lead to the beginning of a process of neuronal degeneration, but are insufficient to generate the first symptoms, because the brain compensates those changes allowing the person to have a normal life (Bhute et al., 2020; Sperling et al., 2011). This asymptomatic period offers the opportunity to begin to modify treatments of the evolutionary course of the disease, before there is extensive and irreversible brain damage (Valls-Pedret et al., 2010).

3.1.2 Prodromal phase or Mild Cognitive Impairment (MCI)

The prodromal stage is the first symptomatic phase of Alzheimer's disease characterized by the presence of very mild symptoms related to memory (Valls-Pedret et al., 2010). At the biological level, an abnormal amount of Aβ is present and the brain can no longer counteract the damage and death of neuronal cells. Therefore, the patient begins to have a deficiency in cognitive abilities (Uehara, 2020). These mild cognitive problems are perceived only by the individual's closest environment, such as family or friends. Likewise, this type of symptomatology does not interfere with the normal activities carried out by the person (Albert et al., 2014).

It is known that the pathological sequence begins preferentially in the structures of the middle temporal lobe and then spreads to other areas. Alterations in the structure and functioning of the brain have been observed such as the decrease of Aβ42 in CSF, the presence of Aβ42 in the brain, inflammation, oxidative stress, microgliosis, regional hypometabolism, brain atrophy, increased tau and phosphorylated tau in CSF (Uehara, 2020).

In some cases, during this phase, the first “mild” symptoms may appear, as a result of the proliferation of senile plaques, which alters the synapse and destroys neurons. These manifestations are related to information retention and learning difficulties commonly called “hippocampal-type amnesic syndrome”, gradual loss of temporal orientation and contextual references, autobiographical memory disturbances, and episodic memory loss (Lanfranco, Manríquez- Navarro, Avello, & Canales-Johnson, 2012; Valls-Pedret et al., 2010). Finally, the transition from a prodromal to a mild phase involves a reduction in the

frontotemporal region and the hippocampus of the brain, known as atrophy, which are involved in memory processes (Uehara, 2020).

3.1.3. Medium phase (mild-moderate)

In this stage, the pathological alterations progress towards lateral temporal cortical regions (Lanfranco et al., 2012). The memory loss and confusion increase. According to the National Institute on Aging (2010), the first symptoms will be associated with a decrease in memory, difficulty to orient oneself temporally and spatially, sudden mood swings, affective disturbances and apathy. Also, they are likely to hallucinate, delusions, paranoia, and impulsive behaviors (Albert et al., 2014; Calderón & Rodríguez, 2014; Lanfranco et al., 2012).

At the macroscopic level, a generally symmetric and diffuse atrophy is triggered in the brain turns. In the brain, the thickness of the convolutions begins to decrease, the depth of the sulci increases, the ventricular system dilates and the weight and volume of the brain decrease (the more advanced AD is, the less the brain weighs). However, it could also happen, although less frequent, that an asymmetric atrophy is triggered, which affects, more frequently, the temporal lobes, the frontal, parietal or occipital lobes.

Figure 16: Superior view of the brain of an AD patient. In the left hemisphere, the arachnoid and a large part of the vessels that occupy the subarachnoid space have been removed. Note the marked diffuse cerebral atrophy that characterizes AD, the widening of the fissures and the thinning of the circumvolutions. From (Guimerà, Gironès & Cruz-Sánchez, 2002).

At the microscopic level, more serious alterations have been revealed in the hippocampus, subiculum, amygdala, and areas of neocortical association. Likewise, in nucleus basalis of Meynert a predilection for neuronal loss, tangles formation (neurofibrillary degeneration) and absence of senile plaques is revealed (Guimerà, Gironès & Cruz-Sánchez, 2002; Valls-Pedret et al., 2010).

In summary, during this phase, the appearance of plaques appears poorly demarcated and they are called as "diffuse senile plaques" formed by a delicate network of fine fibrils of amyloid filaments, without degenerated neurites or a central zone of condensed amyloid. In the same way, the appearance of "primitive senile plaques" can be evidenced, composed of extracellular deposits of non-fibrillar that makes it insoluble. Plaques begin to appear in an apparently normal neuropil and precede the development of other components, such as

dystrophic neurites or reactive glial cells, as will be mentioned later (Guimerà, Gironès & Cruz-Sánchez, 2002).

3.1.4. Advanced phase (late or severe):

In this stage, the disease progresses towards subcortical deterioration, reaching temporoparietal regions (Lanfranco et al., 2012). In this phase, the brain tissues are completely atrophied, which generates language problems (alterations in literacy), lack of recognition by family members, agnosia, apraxia, gait disturbances, swallowing disturbances, lack of control sphincters, and complete dependence (Lanfranco et al., 2012; Calderón & Rodríguez, 2014). During this phase, neuronal damage involves the individual's motor capacity, which is why it becomes prone to the appearance of blood clots, skin infections and sepsis that, eventually, can cause organ failure. The fact that they cannot swallow causes the patient, instead of using the esophagus in the digestive process, to suck food through the trachea, generating a condition called aspiration pneumonia, which is one of the main causes of death from AD (Uehara, 2020).

At this time, diffuse plaques have become classic senile plaques (neuritic), as a product of neuropil degeneration that contains a central region of amyloid surrounded by reactive astrocytes, microglia and dystrophic neurites corresponding to dendrites and degenerated axons (Guimerà, Gironès & Cruz-Sánchez, 2002, Angosto & González, 2009). Likewise, these evolve until the cellular component disappears (they do not contain associated abnormal neurites) randomly a central zone of condensed amyloid is formed. These are known as burnt plaques. Similarly, during this stage, there is atrophy in the medial temporal

lobe, abnormal concentrations of Tau protein or Aβ in CSF and temporoparietal hypometabolism (Valls-Pedret et al., 2010).

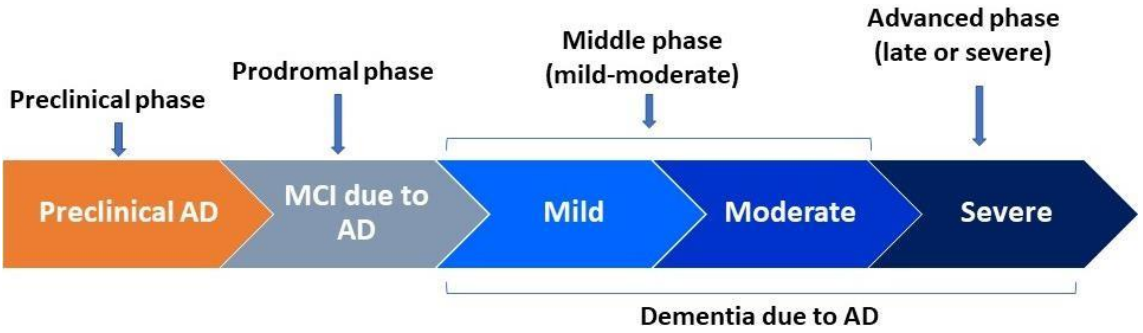

Figure 17. Phases of Alzheimer's disease. Adapted from doi: 10.1002/alz.12068

3.2. AD progression: From a Molecular Point of View

As previously mentioned, AD is a very complex pathology that triggers several intrinsically related phenomena. Therefore, in the next section we explain its progression, considering four most important stages in AD.

3.2.1. First stage: Initiation of the amyloid cascade

At this stage, it has been described that the entorhinal cortex and the hippocampus begin to present various alterations (Lanfranco et al., 2012). Mainly, AD is characterized by an abnormal increase in proteins (Valls-Pedret et al., 2010). Thus, at the histological level, extracellular deposits of Aβ peptide, termed amyloid plaques, are observed in this phase (Lanfranco et al., 2012; Valls-Pedret et al., 2010).

The accumulation in the brain of senile plaques, especially formed by Aβ42 peptide, would be the trigger for AD. This leads to the formation of neurofibrillary tangles, the interruption of synaptic connections, the activation of microglial cells and astrocytes that would generate neuroinflammation and, eventually, a neuronal loss that would induce the development of AD. As previously stated, the literature indicates that the initiation of AD is related to the aggregation of the Aβ, formed by 39-43 amino acids, generated from a proteolytic cleavage of the amyloid precursor protein (APP), for more details see the section **"amyloidogenic pathway".**

Senile plaques produce an inflammatory reaction around Aβ and produce neurotoxic fibrillar aggregations. In addition, there are other very important mutations that are related to AD. For example, mutations related to chromosome 14q, encoding presenilin 1 (PS1); chromosome 1, which encodes presenilin 2 (PS2); chromosome 19q, which encodes apolipoprotein E and, although no mutations have been found in the gene that encodes it, one of its three genetic variants, apoE4, increases the risk of AD (Angosto & González, 2009).

Of these, it has been confirmed that PS (PS1 or PS2) are, at least in part, essential for aspartyl protease γ-secretase to act on APP in the process of releasing β-amyloid. (Angosto & González, 2009). Likewise, it has been concluded that the apoE4 genotype (apolipoprotein E4) influences the formation of Aβ deposition and, therefore, the formation of neurofibrillary tangles.

Although it is not known precisely how Aβ deteriorates cells, it has been determined how Aβ can damage neurons through four situations. First, from the activation of microglia of

the CNS. Second, by activating the inflammatory response leading to the release of neurotoxic cytokines and, finally, by producing oxidative damage in neighboring cells or inducing apoptosis or programmed cell death (Von Bernhardi, 2005; Angosto & González, 2009).

The inflammatory response is marked by an increase of interleukins and tumor necrosis factor α (TNF-α), pro-inflammatory cytokines, which cross the blood-brain barrier (BBB) and trigger a signaling cascade in the CNS. Although the release of pro-inflammatory cytokines and chemokines, activate microglia and astrocytes and protect the body from different pathogens, a prolonged activation of these glial cells could promote neurodegenerative processes (AD) through synaptic phagocytosis and positive regulation of kinases that would favor the hyperphosphorylation of Tau and the oligomerization of Aβ (Uehara, 2020).

3.2.2. Second stage: Activation of glial cells

A second aspect that plays a key role in neurodegeneration, is the activation of microglia and astrocytes (Meraz-Ríos, Toral-Rios, Franco-Bocanegra, Villeda-Hernández, & Campos-Peña, 2013), as an inflammatory response induced by the deposition of Aβ. Glial cells play an important role in neuronal activity, since they are related to neuronal survival, plasticity and nutrition. They are also responsible for detoxification or cytotoxicity, and homeostatic regulation of the extracellular medium.

a) Microglia

In general, microglia cells are generated in the bone marrow, then enter the circulation as monocytes and migrate to the brain during the last phase of embryonic life, establishing their permanent residence there. When the nervous tissue suffers damage; these cells act quickly. In doing so, the microglia will begin to undergo different morphological changes until it becomes “reactive microglia”, generating phagocytosis, synthesis and expression of various molecules related to inflammation, modulation of the immune response and the secretion of high levels of cytokines, proteases and other factors. These cytokines cross the BBB, activate astrocytes and induce the production of α1-antichymotrypsin (ACT), α2-macroglobulin (α2 M), and apolipoprotein. The Microglial reactivity is directly associated with the neuronal damage process as it is a great source of oxygen free radicals, which contributes to oxidative stress and its neurodegenerative effects (Angosto & González, 2009). Reactive oxygen species (ROS), and nitric oxide (NO) have also been implicated in AD (Angosto & González, 2009).

b) Astrocytes

Astrocytes, also called astroglia, like microglia, play a crucial role in the regulation of neuroinflammation (Colombo & Farina, 2016). In the healthy CNS, astrocytes perform several physiological functions involved in ionic homeostasis, neurotransmitter transmission, growth factor secretion, synaptic remodeling, and regulation of oxidative stress (Wyss-Coray & Rogers, 2012). Astrocytes also participate in the maintenance and permeability of the BBB, due to their proximity to blood vessels and their interaction with endothelial cells (Abbott, 2002).

Astrocytic expression of growth factors and cytokines also tightly regulates the permeability of BBB during inflammatory conditions and, in doing so, helps control the passage of immune cells to the CNS (Argaw et al., 2012). In AD, astrocytes are mainly associated with senile plaques in the brain, for example through astrogliosis, a distinctive feature in AD patients in which reactive astrocytes accumulate around amyloid plaques. After activation by Aβ or after a signal of damage, astrocytes can cause neuropathological changes through the expression of a large number of inflammatory factors such as IL-1, IL-1β, IL-6 and TNF-α, and transforming growth factor-β (TGF- β), promoting the neurodegeneration observed in AD (Bai, Su, Piao, Jin, & Jin, 2021).

The exact mechanisms by which astrocytes react with Aβ remain unclear, however it is known that astrocytes express a wide range of receptors, including RAGE, lipoprotein receptor-related proteins (LRPs), membrane-associated proteoglycans and scavenger receptor-like receptors, which recognize and bind to Aβ (Wyss-Coray & Rogers, 2012). On the other hand, Aβ aggregates can stimulate the production of chemotactic molecules, including monocyte chemoattractant protein 1 (MCP-1), that help mediate astrocyte recruitment to the injury site (Wyss-Coray et al., 2003). Aβ has been shown to activate nuclear astroglial factor-kappa B (NF- B), thereby enhancing the production of inflammatory mediators and contributing to the neurodegenerative changes seen in AD. Astrocytes can also swallow large amounts of Aβ that are partially digested, eventually leading to astrocytic defects and neuronal apoptosis (Söllvander et al., 2016). On the other hand, it has been observed that reactive astrocytes participate in the elimination of Aβ in vitro, which suggests a direct role in the attenuation of neurodegenerative processes in AD (Wyss-Coray et al., 2003).

It is known that astrocytes are capable of producing Aβ, thanks to inflammatory factors (Blasko et al., 2000). They are also involved in the formation of the NFTs. Astrocytes reactive by releasing nitric oxide (NO) and other pro-inflammatory cytokines have been reported to accelerate the formation of neurofibrillary tangles (Allaman et al., 2011). Finally, astrocytes have the ability to physically interact with microglia, thus exerting significant control over their activation, phagocytic capacity, and ability to secrete inflammatory mediators (Solà, Casal, Tusell, & Serratosa, 2002).

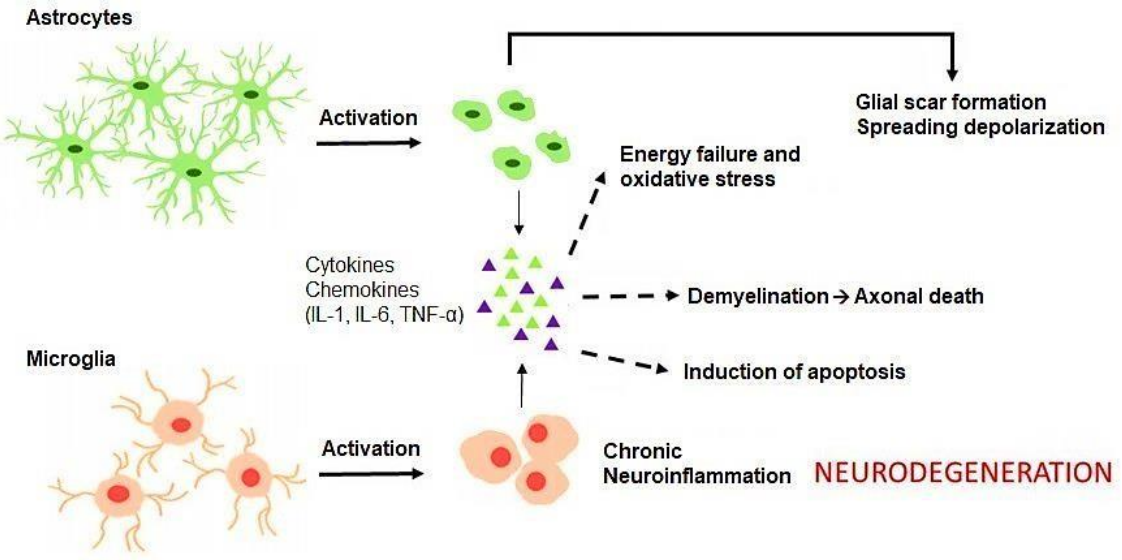

Figure 18. Activation of inflammation mediated by glial cells. Activation of astrocytes and microglia either by Aβ or by some other damaging stimulus, results in the secretion of inflammatory cytokines and chemokines, for example; IL-1, IL-6, and TNF-α. These, in turn, trigger a cascade of events; such as; oxidative stress, demyelination, and apoptosis. All of these elements lead to neurodegeneration and cognitive decline. However, reactive astrocytes also lead to scar formation, generally around injured tissue. For example,

accumulation of astrocytes has been observed around amyloid plaques. From (Fakhoury, 2018).

3.2.3. Third stage: hyperphosphorylation of Tau

Tau, almost absent in dendrites, is a neuronal protein, located mainly in the axon, and to a lesser extent in cell bodies. As described above, this protein, along with others, is associated with microtubules, essential components of the cell cytoskeleton and fundamental for the formation of axons and dendrites, and formation and maintenance of cell morphology and their specific connections (Angosto & González, 2009). Tau hyperphosphorylation affects dendritic and axonal transport, the distribution of proteins and organelles, and cell signaling, therefore neurodegeneration, neuronal death and cognitive deterioration are triggered (Angosto & González, 2009; Uehara, 2020).

Tau hyperphosphorylation is considered in the third stage because the accumulation of Aβ plaques causes the activation of kinases and the inhibition of phosphatases leading to aberrant phosphorylation and the formation of neurofibrillary tangles. As a result, cellular transport and signaling processes are blocked, which causes neurons to become dysfunctional and eventually they die (Von Bernhardi, 2005; Uehara, 2020).

An interesting fact is that, in brains where oxidation is higher, Tau levels are also higher. This will generate an oxidative cross-linking that makes proteins more resistant to proteolysis by inhibition of proteasome activity and contributes significantly to the

accumulation of ubiquitin conjugates in NFTs. It occurs through glycation processes (non-enzymatic addition of reducing sugars to a protein), manifested with a lower capacity of binding to the microtubules of the Tau filaments (Angosto & González, 2009). In this sense, "the Tau filaments undergo glycation". As a consequence of this, the Tau protein generates ROS and oxidative stress in neurons, which leads to the activation of NF-κB. Moderate ROS concentrations affect signaling pathways; whilst high level of ROS causes injury and cell death.

3.2.4. Fourth stage: deficiency in multiple neurotransmitters

A fourth stage of AD is related to the deficiency in multiple neurotransmitters. It is believed that, in the advanced AD stage, the presence of symptoms such as loss of memory, learning, perception of language and behavior are associated with altered levels of synaptic neurotransmitters. Therefore, neuron-to-neuron functioning is disrupted (Kaur et al., 2019).

The most marked characteristic in this stage is the decrease in cholinergic activity; that is, the function of the synapses or nerve endings in which acetylcholine acts as a neurotransmitter on nicotinic or muscarinic receptors. Under normal conditions, the neurotransmitter acetylcholine allows synapse between motor neuronal cells and muscle cells. However, when AD is present, acetylcholine levels drop due to the large amount of neuronal death (Uehara, 2020). This, mainly, is due to the fact that the presynaptic cholinergic terminals, the projection neurons that produce monoamine transmitters, and cortical neurons that produce glutamate, GABA, somatostatin, and neuropeptide begin to be affected (Guimerà, Gironès & Cruz-Sánchez, 2002). The intracellular signaling processes are altered once the neurotransmitters activate the receptors on the cell surface

(Angosto & González, 2009).

Other neurotransmitters, such as glutamate, serotonin, and dopamine, also contribute to the pathophysiology of AD. Recently, these neurotransmitters and their signaling receptors are under intense investigation due to their important contribution to learning and memory phenomena (Strac, Muck-Seler, & Pivac, 2015). This concept arises due to the findings of altered levels of neurotransmitters in the post mortem brains of patients with AD. It is also important to note that some current drugs in AD such as donepezil, rivastigmine, are cholinergic drugs, and function as acetylcholinesterase inhibitors (Kaur et al., 2019).

4. Animal experimental models of AD

Our basic knowledge of the development of AD is increasing rapidly and has now reached a level of maturity where it is possible to evaluate therapeutic procedures to treat this important public health problem. Therefore, important efforts have been made to develop relevant animal models to recapitulate the molecular basis of the pathology and to identify relevant early diagnosis biomarkers. They are almost 200 animal models of AD that can be classified into 2 subtypes: transgenic and non-transgenic. The first developed models are transgenic and they account from more than 80 % of animal models available to date. Although they were useful to better decipher the molecular basis of AD development, they failed to recapitulate accurately the late-onset AD (LOAD) that is the most common form of AD patients. These last 10 years, important progress has been made to fine tune the expression of mutated forms of APP, PSEN or APOE in adult tissue in order to mimic closely AD clinical features. In parallel, non-transgenic models of AD have been also developed and evaluated. Interest of these non-transgenic models rely on the fact that

induction of the pathology arises from a non-genetic affected background and in adult specimens. These animal models were found relevant to evaluate neuroinflammation development and toxicity at late-time points which are well known to be responsible for cognitive impairment and discomfort in patient.

4.1. Transgenic animal models

The sequence homology between wild-type mouse APP (695 isoform) and human APP is about 97%. Three amino acids within the Aβ sequence (Arginine5Glycine, Tyrosine10 Phenylalanine and Histidine13Arginine) result in impairment of Aβ aggregation and prevention of amyloid plaques development in wild-type mice. Therefore, transgenic mice models that express human mutated gene have been built to recapitulate the AD pathology.

4.1.1. Single mutation

The V717F or Indiana mutation

The first mouse model of AD was described in 1995 (Games et al., 1995). This mice model expresses a human mutated APP gene found in patients with Valine 717 substituted by a Phenylalanine (Murrell, Farlow, Ghetti, & Benson, 1991). The transgene is under the control of the Platelet- derived growth factor subunit β (PDGF-β) promoter. This model exhibits lifelong cognitive deficits (3-19 months) showing impairment in working memory (Webster, Bachstetter, Nelson, Schmitt, & Van Eldik, 2014). These deficits precede the appearance of histological senile plaques lesions that appear at 6 months, which are increased with age.

The KM670/671NL or Swedish mutation

The "Swedish mutation" refers to the human KM670/671NL mutation. This is a double mutation of APP: Lysine 670 is substituted by an Asparagine and Methionine 671 is substituted by a Leucine. The first model called Tg2576 was reported in 1996 (Hsiao et al., 1996), It overexpresses a mutant form of APP (APP 695) with the Swedish mutation. In this model the mutated human gene is under the Hamster PrP (Prion protein) promoter. Those mice have deficits in working memory as early as 9 months and are correlated with an increase in Aβ40 and Aβ42. Senile plaques were observed surrounded by glial activation and neuro dystrophy, but not neurofibrillary degeneration (Hsiao et al., 1996).

Figure 15 shows the mutations in APP that were the first causes of early-onset AD to be identified (Goate et al., 1991); These autosomal dominant mutations tend to cluster around the β- and γ- processing sites, thus affecting Aβ production. The transgenic expression of familial APP mutations has made it possible to successfully reproduce amyloid pathology in mice (Games et al., 1995) and therefore create various transgenic and knock-in APP models. The Swedish and Indiana mutations are the most used.

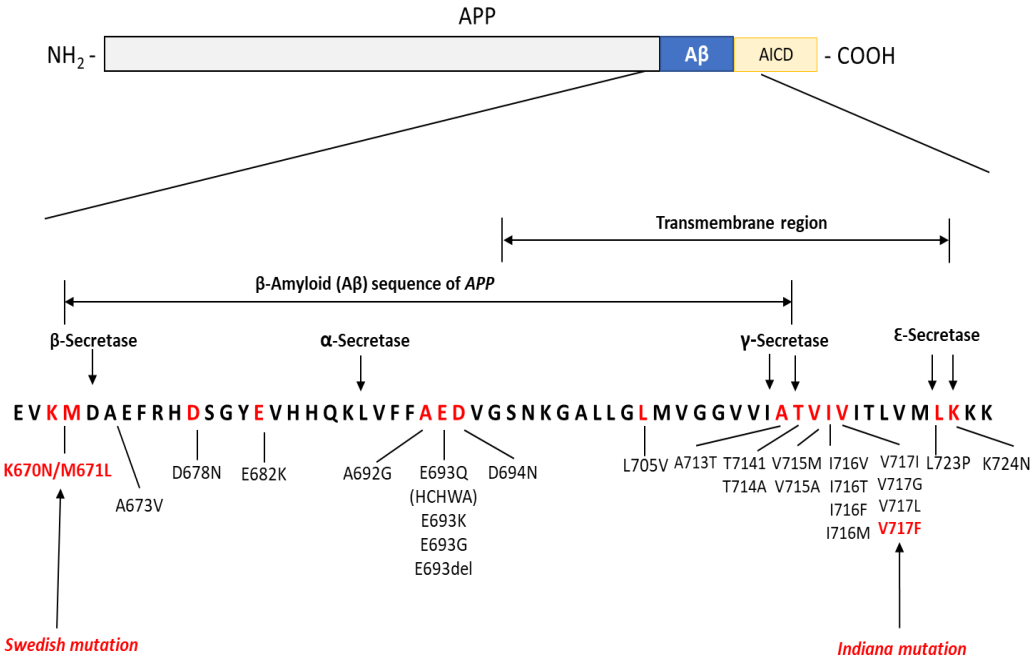

Figure 19. **Representative APP diagram of FAD mutations that have been incorporated into transgenic models of Alzheimer's disease**. The Aβ domain is highlighted in blue, the amino acid sequence is shown, and different mutations are shown with highlighting the two best known mutations as the Swedish mutation and the Indian mutation.

There is also a second mice model called ***APP23*** in which the human APP gene with the Swedish mutation under the control of the Thy-1 mouse promoter. As early as 6 months of age, those mice have senile plaques, which increase with age combined with gliosis and neuro dystrophy. They have also an increase in phosphorylated Tau in the brain compared to wild-type mice, with neurofibrillary degeneration (Sturchler-Pierrat et al., 1997). Those mice have a defect in recognition and spatial memory as early as 3 months and in working memory at 19 month-of age (Dumont, Strazielle, Staufenbiel, & Lalonde, 2004; Lalonde, Dumont, Staufenbiel, Sturchler-Pierrat, & Strazielle, 2002; Prut et al., 2007).

In 2004, Saito's team has produced a model called ***APPNL*** with APP gene was humanized and the human KM670/671NL mutations have been inserted. Those mice do not overexpress human APP and one can observe only the effect of the mutations. This model has an Aβ42/Aβ40 ratio equivalent to that of a wild-type mouse and does not show cognitive deficits even at an advanced age (Saito et al., 2014).

4.1.2. Multiple mutations of the same gene

TgCRN8 and J20 mice models

TgCRN8 (Chishti et al., 2001) and J20 (Mucke et al., 2000) mice models contain both Swedish mutations together with Valine717 to Phenylalanine mutation, but under promoters of PrP and PDGF, respectively. Those mice models have deficits in working, associative and recognition memory as early as 3- month of age. Both models show an increase in Aβ40 and Aβ42 peptides with age with senile plaques combined with gliosis and neuro dystrophy without neurofibrillary degeneration.

The APPNL-F mice model

In this model, the Swedish mutation in exon 16 is combined with the Beyreuther/Iberian mutation, Isoleucine Isoleucine 716 substituted with a Phenylalanine in exon 17 of mouse APP gene (Saito et al., 2014). The mouse APP gene has been humanized and these two human mutations have been inserted. This model has a late working memory deficit at 18 months with senile plaques composed predominantly of Aβ42 peptide. The Beyreuther / Iberian mutation increases γ cleavage at the C- terminal position 42, which specifically

increases the Aβ42 / Aβ40 ratio. These species of peptide are found first in the cortex, then in the hippocampus and are combined with gliosis and synaptic loss. In this model, the Swedish mutation was used because it increases the cleavage of the APP β site, which leads to an increase in the level of APP-CTF-β which in turn increases the levels of Aβ40 and Aβ42.

APPNL -G-F model

This model presents the Swedish mutation, the Iberian mutation, and the Arctic mutation (Glutamic acid 693 to Glycine) (Saito et al., 2014). The combination of these 3 mutations lead to an aggressive pathology than the APPNL-F model with a very early and aggressive Aβ pathology from 2 months of age, including senile plaques in the subcortical structures, due to this the mice also show an earlier onset of neuroinflammation (gliosis and astrogliosis) in comparison with APPNL-F mice. Behavioral evaluations showed memory impairment from 6 months of age. Furthermore, Aβ together with the arctic mutation results in a greater inflammatory response. Mehla et al., characterized this model at a biochemical and behavioral levels in relation to age, using 3, 6, 9 and 12-month-old C57BL / 6J mice as controls (Mehla et al., 2019). They used different tests to evaluate the memory and behavior of the animals such as the Morris water maze (MWM), the recognition of objects and the fear conditioning tests. Open field test was performed to measure the locomotor activity of the mice. Biochemical studies were performed using immunostaining for amyloid plaques (4G8), glial fibrillar acid protein (GFAP), choline acetyltransferase (ChAT), and tyrosine hydroxylase (TH). The results obtained with MWM showed a memory and learning impairment that began at 6 months of age and became more severe at 12 months of age. Although in previous studies shown by Saito et al., no deficits in

learning and memory were observed at 6 months of age, in MWM (Saito et al., 2014), these discrepancies in the results may be due to differences in the protocol followed in these studies. The object recognition test showed a memory deficit at 9 months of age. Regarding locomotor and exploratory activities, there were no significant differences between the APPNL-GF compared with C57BL / 6J. The biochemical evaluation of this model showed an increase in amyloid load in different regions of the brain, which was dependent on age. However, at 3 months no amyloid pathology was found. There was also a significant reduction in ChAT and TH neurons and an increase in GFAP load, also dependent on age.

The APP DSL mice model

The APP DSL model was generated by (H. Li et al., 2014). In this model exons 16 and 17 of mouse APP were replaced, with sequences containing Swedish (K670N, M671L), Dutch (E693Q) and London (V717I) mutations and the sequence of humanized Aβ generated by homologous recombination was used. Homozygous APP DSL mice cannot develop Aβ pathology, but when crossed with PSEN 1 mutant mice they are capable of developing this pathology (Jankowsky & Zheng, 2017), due to this the studies were confronted with APP SL which is an equivalent line but lacking the Dutch mutation, and both lines were crossed in the PS1M146V knock-in background (H. Li et al., 2014).

APP DSL mice has significantly elevated levels of Aβ40 and Aβ42 peptides at advanced age and showing amyloid plaque formation prominent in the hippocampus. They also showed levels of insoluble Aβ40 and Aβ42 in middle age, and increased levels of insoluble Aβ 1-42 in aged mice. APPDSL mice develop minimal CAA at an early age, however, when they reach middle age, they show prominent CAA, which becomes severe as the mice age. Behavioral analyses were evaluated with classical tests MWM, Elevated plus maze,

open arm test, conditioned fear test, the two transgenic lines (APP DSL and APP SL), develop anxiety-like behaviors at a young age, but only APP DSL mice showed a spatial learning deficit and memory impairment in middle-aged animals. Similar results were also shown in other studies (Guo et al., 2013; Guo, Zheng, & Justice,2012). Li et al. concluded that the Dutch mutation in APPDSL mice generates many of the relevant features of AD (vascular amyloid formation characteristic of CAA, decreased cerebral blood flow (CBF), late-onset microhemorrhage, and cognitive impairment) when crossed with a PSEN mutant line, and that these characteristics are accentuated in relation to age (H. Li et al., 2014).

4.1.3. Mice models with mutations in multiple genes

APP/PS1 mice model

One of the widely studied transgenic models is the double transgenic APP/PS1 mice. This model expresses a chimeric mouse/human beta amyloid precursor protein (Mo/HuAPP695swe) and a deletion or at least one mutation of PSEN1 gene. Mutated APP refers to the Swedish mutations Lys 670 → Asn and Met671 → Leu that led to the production of 695 isoform of Aβ precursor protein. Regarding PSEN1 gene, it contains at least one mutation or more depending on the specific type of APP/PS1 model. Other differences between these models are the mode of expression of the mutated transgenes and the promoter used (Drummond & Wisniewski, 2017).

One model associates the Swedish APP mutation with a total deletion of exon 9 of the human PSEN1 gene (http://alzforum.org/mutations) under the control of the PrP mouse promoter (Jankowsky et al., 2004; Jankowsky et al., 2002). This mouse model exhibits

senile plaques as early as 4 months of age, with a progressive increase until 12 months of age. The plaques in this model appear earlier than in Tg 2576 but with a more progressive evolution (Garcia-Alloza et al., 2006). APP/PS1 mice show impairments in working memory as early as 3 months, and in reference and associative memory as early as 6 months (Knafo et al., 2009; Lalonde et al., 2002; Reiserer, Harrison, Syverud, & McDonald, 2007).

Kosel et al., proposed a classification of the APP / PS1 model according to the different mutations used (Kosel, Pelley, & Franklin, 2020). The APPSwe / PS1 A246E refers to the Swedish mutation in the APP gene and carries a punctual mutation of Alanine to Glutamine at the amino acid position 246 in PS1 (Borchelt et al., 1996). The PS1/APP model containing other common mutations such as APPSwe and PSEN1 M146L or Methionine 146→ Lysine (Holcomb et al., 1998), the APPSwe, PSEN1 Methionine 146 → Valine from (McGowan et al., 1999) and more recently the APPSwe, PSEN Leucine 166→Proline created by (Radde et al., 2006), which is one of most commonly used APP/PS1 model. The neuron-specific Thy1promoter was used in this line to restrict APP expression in postnatal brain tissues and to achieve high levels of neuron-specific transgene expression. Overall, this model has shed on light on the highly pathogenic index of the Leucine mutation in amino acid 166 position (Pantieri et al., 2005).

In most of APP/PS1 models, the transgene expression of the mutated human APP transgene was found approximately 3 times greater than that of endogenous murine APP. Cerebral amyloidosis is detected progressively with age, starting from the cerebral cortex between 6 to 8 weeks. Amyloid deposits into the hippocampus could be observed later, between 3 and 4 months of age and into the striatum, the thalamus and brainstem between 4 and 5 months of age. Finally, at age of 7 to 8 months, amyloidosis occurs in all regions of the

brain, except the cerebellum. These transgenic lines generate high levels of soluble Aβ42 and lower levels of Aβ40, both of which increased with age (Maia et al., 2013; Radde et al., 2006).

5xFAD mice model

The FAD model is another relevant model of APP/PS included in classification by (Drummond & Wisniewski, 2017). These transgenic lines are considered as an extreme APP/PS1 model because they carry more than a single mutation in APP and several mutations in PSEN1 gene. The 5xFAD mouse model, has 3 mutations in APP (K670N/M671L + I716V + V717I) and PS1 (M146L + L286V) (Oakley et al., 2006), under the control of the murine Thy-1 promoter. This 5xFAD model exhibits an extreme pathology index as mice begin to express intracellular Aβ 42 at 1.5 months old of age (Holcomb et al., 1998), which evolves into massive response at 2 months characterized by an extracellular Aβ accumulation, senile plaques, extensive neuronal loss and cognitive impairment that increased from 4 to 6 months of age (Esquerda-Canals, Montoliu-Gaya, Güell-Bosch, & Villegas, 2017). On other hand, those animals do not form neurofibrillary tangles (C. Li, Ebrahimi, & Schluesener, 2013; Oakley et al., 2006). In term of behaviour, Jawhar et al, reported that the 5XFAD model develops an age-dependent motor phenotype in addition to the defect in working memory and anxiety levels (Jawhar, Trawicka, Jenneckens, Bayer, & Wirths, 2012).

This 5XFAD animal mouse model is considered as a highly valuable research model of AD due to its ability to recapitulate many of the distinctive features of this pathology and although this model does not have the capacity to produce the formation of neurofibrillary

tangles, it represents a "predominantly amyloid" AD model (Jawhar et al., 2012).

3xTg-AD mice model

This model harbors three individual mutations: the common Swedish mutation, a single mutation in Methionine 146→Valine in presenilin-1 (PS1) and a Tau mutation in Proline 301 to lysine. Importantly, this animal model progressively develops Aβ deposit of two peptide forms (Aβ 1-40 and Aβ 1-42) and a Tau pathology that closely resembles that which appears in the human AD brain (Oddo, Caccamo, Kitazawa, Tseng, & LaFerla, 2003). These two characteristics make this model of great interest and considered one of the most advanced animal models of AD (Esquerda-Canals et al., 2017). Aβ deposition occurs earlier in 3xTgAD mice, prior to any significant cognitive impairments that appear later, around 6 months of age, as evidenced by the spatial memory in the MWM (Ameen-Ali et al., 2017; Billings, Oddo, Green, McGaugh, & LaFerla, 2005). It is noteworthy that impaired synaptic function progresses with age. (Oddo et al., 2003), while the appearance of NFTs develop later, around 12 months of age (Ameen-Ali et al., 2017).

APOE based-mice models

As ApoE4 allele is also a hallmark of AD development, apoE4 transgenic mouse was generated. The coding sequence of mice ApoE gene including a part of exon 2, the entire exons 3 and 4 were replaced by those of human (Hamanaka et al., 2000). Several promoters are employed to drive expression of human ApoE cDNA in neurons and glia (Mann et al., 2004) to mimic the clinical setting with heterogeneous APOE levels described between

patients (Carter et al., 2001; Hamanaka et al., 2000; Holtzman et al., 1999).

There are three types of APOE models: mice invalidated on ApoE gene, called "Knock-Out" or KO, mice in which the gene has been replaced, called "Knock-in" or KI, and mice expressing an ApoE transgene.

Knocking out of APOE gene has allowed to better understand the physiological role of APOE and its involvement in AD. APOE KO mice have diffuse Aβ deposits in the hilus of the dentate gyrus of the hippocampus, even at advanced age (Holtzman et al., 2000). However, they do not present fibrillar deposits of Aβ, which indicates that the elimination of ApoE causes the blockage of the formation of cerebrovascular Aβ, or in the brain parenchyma.

These mice also did not show neuritic plaque formation. Therefore, in this study presented by Hotzman et al. ApoE was shown to facilitate the formation of both neuritic and cerebrovascular plaques, which are pathological features of AD and CAA (Holtzman et al., 2000).

On the other hand, knock-in mice have been created to allow researchers to compare the effects of various human APOE isoforms and to conditionally alter APOE expression. These mice express the full-length human ApoE protein under the control of endogenous mouse regulatory elements. APOE knock-in mice crossed with APP/PS1 mice show APOE immunoreactivity in the center of the plaques and in microglia and astrocytes. Another characteristic is the presence of amyloid deposition, which was more pronounced in female mice that carried the APOE4 sequence than in females that carried the APOE3 sequence ((Huynh et al., 2019); https://www.alzforum.org/research-models/apoe4-knock- floxed-curealz)).

Other studies have evaluated the role of APOE in brain cholesterol metabolism. For example, Mann et al., used APOE knock-in (KI) model in which the human allele is expressed under endogenous regulatory elements, on a defined C57BL6/ J background (Mann et al., 2004). They demonstrated that the KI mice have significantly different steady-state levels of serum cholesterol and APOE levels in the brain, however, these mice had equivalent levels of brain cholesterol. Specifically, they found that the APOE level in the fasting brain and liver of the APOE ε2 KI mice was 2 times higher compared to those of the APOE ε3 KI and APOE ε4 KI animals. The APOE level in the fasting serum of APOE ε2 KI animals was also significantly higher than that found in APOE ε3 KI and APOE ε4 KI animals. The correspondence between genotype and APOE levels in KI mice is similar to that observed in humans (Mann et al., 2004). The evaluation of cholesterol levels showed that APOE ε2 KI animals had the highest cholesterol level (average 234 mg / dl) and APOE ε4 KI animals, the lowest cholesterol (average 67 mg / dl) while APOE ε3 KI animals did not differ significantly from wild type animals. Likewise, it was reported that the triglyceride levels found for ε3 KI, ε4 KI and wild type animals were statistically indistinguishable. Furthermore, they reported that the presence of APOE significantly increases Aβ and cholesterol levels in the brain, but this increase is regardless of the allele. Therefore, there is an independent role for APOE in peripheral cholesterol metabolism in relation to the CNS, and despite the fact that these mice present altered levels of cholesterol and APOE, they are insufficient to influence Aβ metabolism. However, this model has some advantages. Although the abundance of APOE in the brains of ε4 KI animals is low, they present normal levels of serum cholesterol. These animals would allow studying the effects of low APOE levels in the absence of high cholesterol, which is often observed in humans who inherit an ε4 allele. Likewise, ε2 KI animals have high levels of serum cholesterol and high levels of APOE in brain. They could be helpful in determining the

effects of high cholesterol independent of low APOE levels (Mann et al., 2004).

4.2. Regulatable transgenic lines

Although those single and multiples transgenic lines were found more relevant and physiological closer to the clinical setting, they still suffer from drawbacks as early-birth stage development of AD in young animal. Therefore, to induce expression of mutated form of AD markers (Tau, APP, etc) in more-advanced age of animal, regulatable-transgenic lines have been recently evaluated. Most of these transgenic lines relies on theTet/ON-OFF regulatable inducible system.

rTg4510

The rTg4510 mouse is a regulatable expression model, representing the human Tauopathy mutation (TauP301L) (Gamache et al., 2019) associated with frontotemporal dementia and Parkinson disease both linked to chromosome 17 (Ramsden et al., 2005). The general strategy is based on the Tet – Off system in which expression of the mutated form of TauP301L is switched-OFF after the addition of doxycycline in the drinking water of animal. The brain specific CaMKIIα promoter was employed to drive the expression of TauP301L in forebrain tissues in a physiological range of expression. The most representative feature of this model is the development of NFTs that correlated well with the detection of the hyperphosphorylated 64 kDa Tau isoform according to age (Ramsden et al., 2005; Santacruz et al., 2005). For example, phosphorylated Tau pre-tangles is detected at 2-3 months of age and correlated with the appearance of cell death at 4 and 5.5 months of age in the cortex and hippocampus (Ramsden et al., 2005; Santacruz et al., 2005).

Hippocampal neurodegeneration is also visible depending on the age of the mice, starting at approximately 5 months 10 months of age. The rTg4510 mice show severe brain atrophy as well as other Tauopathy- like phenotypes (Gamache et al., 2019; Ramsden et al., 2005; Santacruz et al., 2005), which are not discernible in the standard, not regulatable Tauopathy models (P301L) carrying the same mutation (Götz, Chen, van Dorpe, & Nitsch, 2001). Likewise, cognitive impairment in this model has also been shown to be age-dependent, becoming significant at 4.5 months of age and increasing in older mice. Cognitive impairment is consistent with macroscopic and severe forebrain atrophy and prominent loss of neurons, especially in the CA1 subdivision of the hippocampus of these mice (Ramsden et al., 2005). Interestingly, the addition of doxycycline in the drinking water of the animals to switch-off expression of the mutated form of Tau restored the cognitive impairment in those animals, confirming the specificity of the approach used (Santacruz et al., 2005). Gelman et al., 2018 investigated the synaptic activity of rTg4510 mice compared to the regular APP/ PS1 model (Gelman, Palma, Tombaugh, & Ghavami, 2018). Results indicated substantial differences in term of hippocampal function deficits. Paired pulse facilitation (PPF) deficiency at 6-7 months of age was noted early in rTg4510 mice in contrast to the APP / PS1 model in which it was observed from 8-9 months of age (Ramsden et al., 2005; Santacruz et al., 2005). Long Term Potentiation (LTP) deficiency was also evident at 6 to 7-month in Tg4510 mice and correlated with reduced presynaptic activation at this time. In contrast, any significant difference was visible in term of basal synaptic transmission (BST) activity between the two animal models. However, APP/ PS1 mice aged 2-3 and 8-10 months showed deficits in BST (Gelman et al., 2018). Overall, these data indicate that synaptic transmission deficits in these models progress differentially and that this difference is based on the spatial and temporal expression of the mutated form of Tau in the brain of mice.

rTg3696AB model

Paulson et al., 2008, created another Tet-OFF regulatable transgenic animal model that, unlike to rTg4510, includes APP transgene (Paulson et al., 2008). The rTg3696AB model incorporated the human APP (APPNLI) gene harboring three mutations associated with the early development of AD: the Swedish mutations (K670→N and M671→L) and the London (V717→I) mutation with the aim of improving the production of Aβ 42. The mutated form of Tau was the TauP301→L. As for the rTg4510 line, the CaMKII promoter was used to ensure transgene expression in the forebrain while the temporal transgene expression was achieved by addition of doxycycline. In this model, the main important features of AD were detectable i.e. Aβ plaque formation, neurofibrillary tangles and neurodegeneration which again correlated well with tissue atrophy and neuronal loss. Surprisingly, the expression of the APP transgene in the brain of rTg3696AB mice was 50% of that which could be detected in the Tg2576 model, while the tau expression from P301L was 25% that in rTg4510 (Santacruz et al., 2005). This indicates that the expression levels of mutated forms of APP and Tau, and the type and nature of the mutations are detrimental to the development of AD in animals. In any case, NFTs formation was age-dependent as well as in the rTg4510 model, although transgenic human Tau levels were lower expressed in rTg3696AB compared to rTg4510 mice. At 13 months of age, the presence of senile plaques was observed throughout the forebrain, as well as the presence of NTFs. The acceleration of tangles pathology in this model is probably enhanced by the presence of Aβ. Neuronal loss was also observed in mice older than 11 months and this was significant in CA1. Paulson et al., 2008 did not carry out studies on behavior, but they deduced that this model also presents alterations at the cognitive level.

rTg9191 model

Regarding the two transgenic lines described above, Liu et al., 2015 generated a Tet-OFF transgenic animal, rTg9191 model, carrying the 695 amino acid isoforms of human APP (APPNLI) with the Swedish (K670N and M671L) and London (V717I) mutations (P. Liu et al., 2015). This mouse has 4-fold higher level of mutant human APPNLI, preferably in excitatory forebrain neurons, than endogenous mouse APP which remains constant with age. Amyloid plaque formation was age- dependent and observed from 8 months of age in the cerebral cortex and between 10.5 - 12.5 months of age in the hippocampus. In 25-month-old mice, plaque formation was observed to be distributed in at least 19 % of the cortex. Importantly, density of neuritic plaques in rTg9191 mice was found to be comparable to that found in the brain of AD patients. Formation of Aβ aggregates was also observed to increase with age, with the fibrillar aggregates found majority with low amounts of non-fibrillar aggregates. These mice also develop neuroinflammation, tau misfolding near neuritic plaques and hyperphosphorylation. However, no clear signs of cognitive impairment were detected in these animal models even in old animals. Overall, there were some disadvantages with these regulatable OFF systems. Defective brain development was observed as well as a reduction in forebrain weight. The size of the dentate gyrus was regularly smaller in these animals than in the counterpart animals (P. Liu et al., 2015). Although no clear explanation was drawn from these mice, it has been suggested that the integration tTA promoter into genomic loci, might transcribe, in addition to the tTA gene, other genes located nearly to the integration sites, inducing a global change of gene expression and side effects. A phenomenon widely recognized as “Chromatin position effects” (X. Chen & Zhang, 2016).

4.3. Sporadic AD models

Transgenics models de AD has many advantages, and generally exhibit Aβ aggregation and eventually, senile plaques and show significant cognitive impairment and some other characteristics of this pathology (H. Y. Kim, Lee, Chung, Kim, & Kim, 2016). But they suffer from several limitations. For example, they are uneconomical and time-consuming, taking several months to develop Aβ plaques and even longer to detect Aβ-induced behavioral or synaptic abnormalities (Bryan, Lee, Perry, Smith, & Casadesus, 2009; Elder, Gama Sosa, & De Gasperi, 2010). Moreover, since mutated forms of AD markers are expressed from birth, brain cells could develop rescue mechanisms throughout age to compensate for these defects. This could create some interpretation bias. For instance, the neuroinflammation process that occurs at a late time in AD patient could not be studied with precision in these transgenic lines.

Some alternatives have been explored in animals to closely mimic this specific feature. The general strategy is based on the intracranial injection of neurotoxic or inflammatory molecules into the brain of aged animals. Infusion of Aβ peptides into hippocampal regions as well as inflammatory cytokines have been evaluated. In the next section, we will discuss the impact of these two different approaches in AD.

4.3.1. Aβ infusion models

Several studied have shown that intrahippocampal injection of Aβ 1–42 into the brain of wild-type rat provides an excellent in vivo model which replicates the amyloidopathy (Facchinetti, Bronzuoli, & Scuderi, 2018). Aβ peptide exists in several forms, such as monomeric, oligomeric, proto-fibrillar and/or fibrillar forms in AD brain; soluble peptide, oligomers or fibrils could be precisely infused into specific regions of the brain (Karthick et al., 2019). Results from these infused models indicated that the oligomeric form of the Aβ peptide is the most neurotoxic in the AD pathogenesis (Marr &Hafez, 2014; Sun, Chen, & Wang, 2015). The brain parenchyma and the hippocampus are often chosen as target tissues because these regions are the most affected area in AD neurodegeneration (Facchinetti et al., 2018; Jean, Baleriola, Fà, Hengst, & Troy, 2015; Scuderi et al., 2014). Therefore, the infused model allows to replicate the increase of Aβ peptide spatially and temporally as observed in AD, preventing any compensatory or side effects that can be found with transgenic lines.

Several recent investigations have shown the effects of Aβ 1-42 peptide injection at the cognitive and molecular level. In a study conducted by (Wong, Cechetto, & Whitehead, 2016), a single acute exposure of 150 μM Aβ oligomer (AβO) was performed and the pathological effects were evaluated at different times (1, 3, 7, 21 days) post- surgery. It was found that; bilateral infusion of AβO into the lateral ventricles of the hippocampus induced significant deficits in spatial learning and anxiety- like behavior as evidenced by MWM and open field assays. The pathological outcome was evaluated by immunolabelling of Aβ, Ox-6, and IBA-1 proteins expressed from microglia while Choline acetyltransferase (ChAT) expression was evaluated from basal forebrain cholinergic neurons. Significant behavioral deficits were correlated with a transient increase of Aβ within the corpus

callosum and cingulate gyrus. A significant increase in activated microglia was also observed within these same areas, and a significant decrease in cholinergic neurons within the basal forebrain. This study showed for the first time that acute exposure to AβO resulted in deficits in learning, memory, and behavior, as well as loss of cholinergic cells, sustained activation of microglia, and other pathologies similar to those originating in AD brains. These features were concomitant with a transient increase in Aβ deposition. Therefore, the acute AβO exposure model can be a useful tool to assess the early stages of AD pathogenesis.

Faucher et al., reported the lasting impact of bilateral intrahippocampal infusion of AβO over several days in the dorsal hippocampal CA1 (dCA1). The procedure consisted of daily bilateral injections of AβO at 0.2 μg / μL for 4 days. The objective of this study was to evaluate the effect of AβO on working memory, spatial memory and on the activation of extracellular signal-regulated kinase (ERK) that participates in the metabolism of APP, the production of Aβ, and its relationship to synaptic plasticity and memory formation. Furthermore, it has been described that the alteration of the ERK activation dynamics can also alter memory processes and above all is involved in the origin of memory deficits in AD. The results of this study showed that AβO infusions induced strong deficits in working memory, however, no changes in spatial memory were observed 7 days after the last injection. Furthermore, AβO infusion prevented the sequential activation of ERK in various brain structures, such as the hippocampus, specifically the DG area, the pre-limbic cortex and the medial septum, areas that are involved in the formation of working memory. This study was one of the first to demonstrate that subchronic AβO injections produce the main sign of cognitive impairment corresponding to the early stages of AD, through long-lasting alterations of the ERK / MAPK pathway. The authors suggested that this model is a valuable tool to study the impact of AβO on cognitive decline, which represents a very

early stage of AD (Faucher, Mons, Micheau, Louis, & Beracochea, 2015).

Another study using Aβ peptide injection (15 µM) was performed in a Samaritan rat model. Unlike previous studies, chronic intracerebroventricular injections were performed for 28 days. The authors co-infused peptides with other pro-oxidative substances such as ferrous sulphate heptahydrate (1 mM) and L-buthionine-(S, R)-sulfoximine (12 mM) (Petrasek et al., 2016) to improve the clinical onset of pathology. Different behavioral methods were used to evaluate the impact of these administration procedures. Two independent spatial cognitive tasks, MWM was used to evaluate the long-term memory version and the active allothetic place avoidance (AAPA) task to evaluate the dynamic memory. Spatial learning and memory deficits were reported with two spatial tasks with significant alterations in the cortical glutamatergic and hippocampal cholinergic systems. Generally, Samaritan rats exhibited significant changes in NR2A expression and CHT1 activity compared to controls rats.

Karthick et al., conducted a study to evaluate the time-dependent effect of AβO on mRNA expression of gene encoding N-methyl D-aspartate (NMDA) at 8, 15 and 30 days after surgery. NMDA plays an important role in neurotransmission and memory formation in the CNS, and in the expression of acetylcholine receptors and also in cognitive impairment in the rat model of AD. Synthetic AβO was infused bilaterally into the intrahippocampal region of the rat brain. Behavioral analysis was evaluated using the eight-arm Radial Arm Maze task, while changes in mRNA expression at the glutamatergic and cholinergic receptor were analyzed by qRT-PCR. The results showed that AβO causes decreased expression of the α7 nicotinic acetylcholine receptor and an increased expression of the 2A and -2B subunits of the NMDA receptor. Spatial learning and memory deficits, behavioral disturbances, and neuron loss were also observed 15 days after injection. These findings were correlated with the presence of Aβ 1-42 deposits after 15 days of infusion. The authors

concluded that single exposure to AβO results in modulation of NMDA receptors (NMDAR) and acetylcholine receptors. They also concluded that this model allows the understanding of the molecular mechanisms caused by the temporal effect of AβO in the hippocampus, and therefore, this model is important to characterize the initial stage of AD pathogenesis (Karthick et al., 2019).

Recently, the Aβ infusion model was used to evaluate a therapeutic procedure based on the administration of interferon -β1a (IFNβ1a) employed as an attenuator of cognitive damage and inflammation. The rat model of AD was obtained by intra-hippocampal injection of Aβ 1-42 peptide (23 μg / 2 μL) and 6 days later by infusion of 3.6 μg of IFNβ1a administered subcutaneously for 12 days. The novel object recognition (NOR) test was used to assess cognitive performance. Furthermore, the activity levels of pro-inflammatory or anti-inflammatory cytokines, reactive oxygen species (ROS) and superoxide dismutase (SOD) were analyzed in parallel. Results demonstrated that IFNβ1a treatment was able to reverse memory impairment and to counteract microglia activation and upregulation of pro-inflammatory cytokines (IL-6, IL- 1β) (Mudò et al., 2019).

4.3.2. Neuroinflammation animal models for LOAD

Several chemical compounds can be used to induce neuroinflammation in the brain. These chemical-induced animal models are widely used in several brain diseases and AD. The general strategy is based on the infusion neuroinflammatory or neurotoxic products.

Lipopolysaccharide (LPS)

As example intracerebroventricular (ICV) intrahippocampal or intraperitoneal injection of lipopolysaccharide (LPS) in rats or mice has been widely used as a neuroinflammation model of AD (Herber et al., 2006; Ophir et al., 2003). LPS is a component of the cell wall of the outer membrane of gram-negative bacteria that interacts with the toll- like receptor 4 (TLR-4) (Alpizar et al., 2017; Boonen et al., 2018). Activation of TLR4 by LPS triggers the response of adapters molecules such as; myeloid differentiation primary response protein 88 (MyD88), adapter-inducing interferon-β containing TIR domain (TRIF) and TRIF-related adapter molecule (TRAM) (Ruckdeschel et al., 2004). This process ends with activation of transcription factors for the production of pro-inflammatory genes (Gray et al., 2011).

In addition to its role in inflammation, LPS has been directly related to AD (Zhan, Stamova, & Sharp, 2018). For example, the presence of LPS together with Aβ 1-40 or Aβ1-42 has been reported in amyloid plaques in the gray and white matter of the brains of AD patients (Zhan et al., 2018). LPS has also been found abundantly in the neocortex and hippocampus of AD brains and has been shown to have strong adherence to the membrane of neuronal nuclei in AD patients (Y. Zhao, Cong, Jaber, & Lukiw, 2017).

Different studies have shown that single dose of LPS by intravenous injection (Herber et al., 2006) causes a significant increase in IL-1β and TNF-α (Sly et al., 2001) in various brain regions such as the cortex and hippocampus in wild-type mice, rats or in transgenic mice such as the aged Tg2576 mouse line (L. M. Wang et al., 2018). An increased in inflammatory cytokines (IL-1β, IL-6 and TNF-α) has also been observed in the blood of

rats (L. M. Wang et al., 2018). Other findings revealed that LPS injection is sufficient to activate chronic microglial (L. M. Wang et al., 2018) as evidenced by the increase in glial fibrillar acidic protein (GFAP) expression (Herber et al., 2006). Interestingly, an increase in soluble Aβ and phosphorylated Tau levels has also been observed after LPS injection in wild type animals, indicating that neuroinflammation could aggravate development of AD (L. Ma et al., 2016; L. M. Wang et al., 2018). This was correlated with memory impairment and behavioral changes in the animals. Likewise, successive injections of LPS have been shown to cause neuronal degeneration similar to AD (Behairi et al., 2016). Consecutive injections of LPS repeated three or seven times promoted the accumulation of Aβ 1-42 in the hippocampus and cerebral cortex of mice. Increased of β- and γ-secretase activities were also detected as well as astrocyte activation and cognitive impairment (Lee et al., 2008).

Polyinosinic-polycytidylic acid (Poly(I:C))

Poly I:C administration has also been used to model inflammation in AD (Weintraub et al., 2014; J. D. White et al., 2016). Poly I:C is a synthetic double-stranded RNA that acts through Toll-like receptors 3 (TLR-3) and is commonly used experimentally to replicate the acute phase of a viral infection in animals. This component is capable of increasing the levels of INFα and INFβ and several other pro-inflammatory cytokines (McLinden et al., 2012; Reimer, Brcic, Schweizer, & Jungi, 2008; Weintraub et al., 2014) and chemokines (Kamer et al., 2008; Wyss-Coray & Rogers, 2012). Like Aβ 1-42 infusion, repeated administration of poly I: C has been shown to increase Aβ deposition in the hippocampus of non-transgenic animals (Weintraub et al., 2014). White et al., examined the effect of successive poly I: C injections on cognitive deficits, Aβ accumulation and phosphorylated

Tau at 7-, 14- and 21- days post-treatment. Poly I: C significantly increases Aβ at all times evaluated in correlation with cognitive impairment after 14 and 21 days of administration. Phosphorylated Tau levels were also elevated after 14 days before decreasing at 21 days post- treatment. (J. D. White et al., 2016). Similar results were shown in a study conducted by Weintraub et al., who showed that intraperitoneal injections of poly I: C administered for 7 consecutive days cause an increase in Aβ 1-42 peptide levels, which has also been correlated with significant cognitive deficits evaluated with the contextual fear conditioning (CFC) test (Weintraub et al., 2014).

Streptozotocin (STZ)

STZ is another component used as a model of neuroinflammation (Fine et al., 2017; Grieb, 2016). STZ is a glucosamine-nitrosourea compound isolated from the soil bacterium Streptomyces achromogenes. Initially patented as an antibiotic, it is used as an anticancer agent against rare neuroendocrine tumors (Turner et al., 2010), and it is also used as an inducer of diabetes in animals (Grieb, 2016) due to its toxicity to insulin-producing β cells in the pancreas (G. Francis et al., 2009) via its cellular uptake by the low-affinity glucose transporter protein 2 (GLUT2) located in their cell membranes (Grieb, 2016). STZ causes dysregulation of insulin metabolism, oxidative stress and inflammation (Fine et al., 2017), and in recent years it is used frequently for a sporadic AD model.

This is based on the fact that AD patients have a drop in cerebral oxygen and glucose consumption, poor insulin metabolism, as well as reductions in insulin signaling and glucose uptake (Hoyer, 2004). Single or constant dose intracerebroventricular (icv) injections of STZ have been shown to chronically decrease glucose uptake in the brain and

generate deficiencies such as those found in AD patients (Grieb, 2016) for example; neuroinflammation and oxidative damage resulting in behavioral deficits, memory loss, impaired locomotion, as well as impaired glucose metabolism, reduced glycolytic enzymes, cerebral amyloid angiopathy, reduced insulin transcription, increased phosphorylated Tau concentration (Barilar, Knezovic, Grünblatt, Riederer, & Salkovic-Petrisic, 2015; Salkovic-Petrisic et al., 2011) and mitochondrial oxidative damage (Du et al., 2015; Prakash, Kalra, & Kumar, 2015). Grieb et al., concluded that ICV STZ can damage brain glucose insulin- producing cells and / or brain glucose sensors.

5. MicroRNAs biomarkers in AD

MicroRNAs (miRNAs) are small, non-coding, conserved RNA sequences, long from 20 to 22 nucleotides that play important roles in the regulation of gene through a post-transcriptional mechanism inducing mRNA degradation and/or translation arrest. Several investigations have reported that deregulation of miRNAs is a hallmark of multifactorial disease such as cancer, cardiovascular and neurodegenerative diseases. Currently more than 2 000 human miRNAs have been identified. Almost 70 % of them are expressed in the human brain where they regulate different key neurological functions such as neurite growth, neuronal differentiation and synaptic plasticity. Impairment of microRNA function is closely related to AD pathogenesis. A panel of miRNA have been specifically annotated to AD as miRNA-15, -107, -181, -146, -9 and-106 and thus are considered as relevant therapeutic agents and biomarkers for this disease type. In the field of research directed towards the search for non-invasive biomarkers for the diagnosis of diseases, it has been demonstrated that miRNAs are stably expressed in various body fluids such as serum, plasma, saliva and urine, etc. This makes them interesting as biomarkers of AD. In this section, we will focus our discussion on the role of miRNAs as circulating biomarkers of this disease. For this, we will compare the expression of circulating miRNAs in transgenic, non-transgenic animal models and in patients.

5.1. Biogenesis

MicroRNAs are transcribed by RNA polymerase II and then form nascent "capped" and polyadenylated primary transcripts (3'), called "pri-miRNA," ranging from hundreds to thousands of ribonucleotides. These transcripts can be monocistronic (single hairpin) or polycistronic (various hairpins). Then, the pri-microRNA is cut to shorter precursors (~ 70 nucleotides, now called, pre- microRNAs) by Drosha (RNase type III) giving rise to pre-microRNAs and shortly after they are directed from the nucleus to the cytoplasm by exportin-5. In the cytoplasm, Dicer cleavage pre- microRNAs resulting in smaller double-stranded RNAs of ~22 nt. Next, in the canonical pathway, one of the strands is taken by Argonaute (Ago) protein through a mechanism still needed to understand. Once taken by Ago, is formed the miRNA induced silencing complex known as miRISC; this complex is targeted to the messenger RNA (mRNA) (Xiao & MacRae, 2019; Zlotorynski, 2019). The post-transcriptional suppression is achieved by binding of the microRNA- RISC complex in the 3'-untranslated region (3'-UTR) of the mRNA commonly named as the “seed region” of about 6-8 nucleotides. It is essential to mention that one miRNA can regulate several mRNAs at the same time and different miRNAs targets a particular mRNA. Bioinformatics, in vivo and in vitro studies have shown that miRNAs regulate the majority of mammalian mRNAs, thus representing a crucial role in cell physiology (S. Kumar & Reddy, 2016; Xiao& MacRae, 2019). Figure 20. shows a summary of miRNA production and mechanism of action.

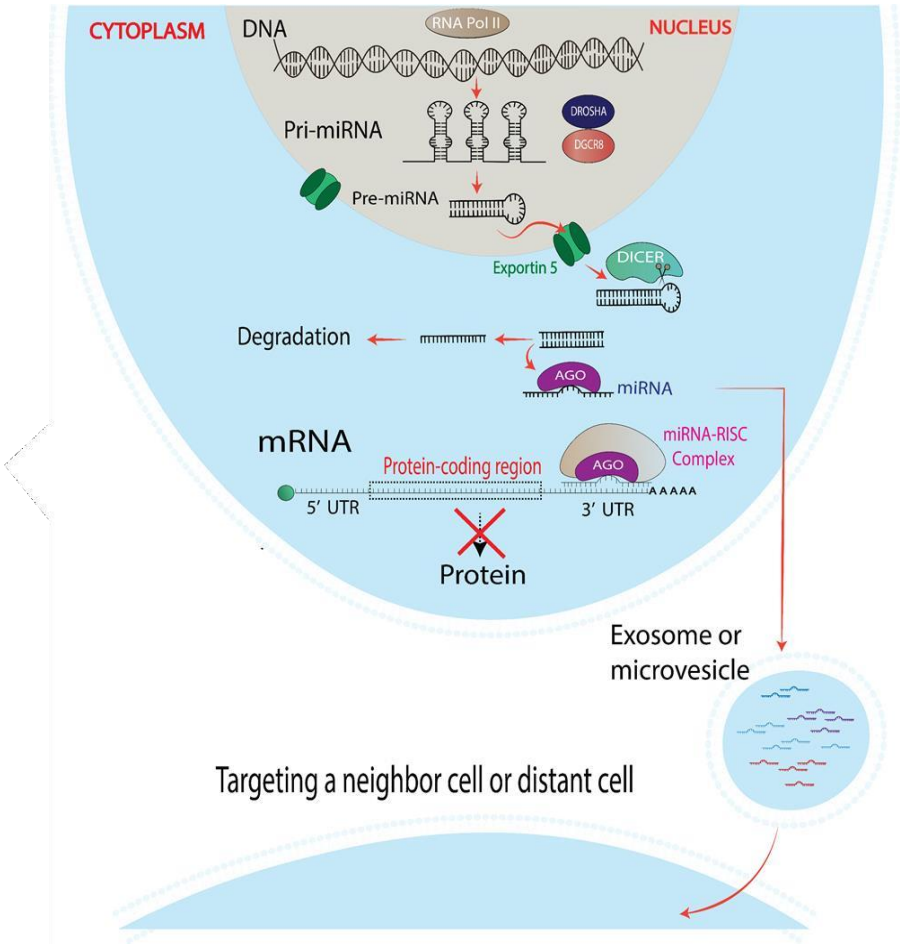

Figure 20. microRNA biogenesis

5.2. miRNA Dysregulation in Alzheimer's Disease

Many of deregulated pathways described above led to important changes in the expression of miRNAs in brain tissues of AD patients. More than hundreds of miRNAs are altered in AD brain. Here, we review the most reported deregulated miRNAs in AD with a particular focus on their involvement in pathological mechanisms that contribute to AD development.

miR-29 family

The miR-29 family includes miR-29a, miR-29b and miR-29c isomiRs. They share the same seed sequences and differ by 2 to 3 nucleotides located in supplementary binding sites of miRNAs sequence. The miR-29 family has been shown to target multiple genes in Alzheimer's disease (Hébert et al., 2008; Wu et al., 2017; G. Yang et al., 2015).

BACE regulation by miR-29 isomirs is by far the most consistent and reproducible results published until now. Inverse relationship of expression between miR-29a and -29b and BACE-1 mRNA has been indeed reported in several independent cohort of brain tissues of AD patients as well as in related blood samples (Hébert et al., 2008; Nunez-Iglesias, Liu, Morgan, Finch, & Zhou, 2010; Shioya et al., 2010; L. B. Yang et al., 2003). MiR- 29 family are significantly reduced in AD tissues and principally in the human AD parietal lobe and frontal cortex as compared to age-matched control (Nunez-Iglesias et al., 2010; Shioya et al., 2010). This down-regulation is systematically correlated with higher level of BACE-1 (β-site APP cleaving enzyme-1) expression (Jahangard et al., 2020; Shioya et al., 2010; Zong et al., 2011). As mentioned before cleavage of APP by BACE-1 is the first and rate-limiting step Aβ production and a hallmark of Alzheimer's disease pathogenicity.

Downregulation of BACE1 expression by miR-29a (Hébert et al., 2008) and later miR-29c (Lei, Lei, Zhang, Zhang, & Cheng, 2015) was validated through an in vitro functional assay using the miR-OFF luciferase system. Putative binding sites complementary to the seed sequence of miR-29 family were identified in the 3'UTR part of BACE1 mRNA (Lei et al., 2015). Direct experimental proof of implication of miR-29 family in development of AD was brought by Hebert and collaborators (Hébert et al., 2008) who reported that modulation of miR-29a in human neuroblastoma SH-SY5Y cells promoted production of Aβ. It is known more widely admitted that loss of miR-29 family, contribute to increased BACE1 expression that favorite Aβ production and accumulation in brain tissues of AD patients.

Beyond the roles of miR-29 isomiRs in control of the amyloidogenic pathway, these miRNAs play also important role in survival of neuronal cells. Puma (p53 upregulated modulator of apoptosis), Bim (Bcl-2-like protein 11), Bmf (Bcl-2-modifying factor), Hrk (Activator of apoptosis harakiri) and N-Bak (neuronal Bak) and VDAC1 (Voltage Dependent Anion Channel 1) (Jahangard et al., 2020; Kole, Swahari, Hammond, & Deshmukh, 2011; Roshan et al., 2014) are commonly targeted by miR-29 isomiRs. Consequently down- regulation of miR-29 family in AD tissues is detrimental for patients as it might facilitate up-regulation of these pro-apoptotic genes. Roshan et al., 2014 showed that loss of miR-29 resulted in upregulation of VDAC1 in the hippocampus, cerebellum, and cortex of ataxia animal model following miRNA knockdown. Partial restoration of apoptosis was achieved by down-regulation of VDAC1 in miR-29 knockdown cells (Roshan et al., 2014). In addition, miRNA 29 isomirs are reported to regulate as well formation of synapse and synaptic plasticity. ARPC3 (Actin Related Protein 2/3 Complex Subunit 3) (Lippi et al., 2011) and NAV3 (Neuron Navigator 3) (Zong et al., 2015) are direct transcriptional regulators to miR-29 that fine tunes structural plasticity by regulating

actin network and axon guidance of brain cells respectively.

miR-146a

The miR-146a is a brain-enriched miRNA with known function as regulator of inflammatory response in various neurodegenerative diseases including AD (Y. Y. Li, Cui, Hill, et al., 2011; Lukiw, Surjyadipta, Dua, & Alexandrov, 2012; Taganov, Boldin, Chang, & Baltimore, 2006). Expression of miR-146a is more widely expressed in microglial cells than in neurons in which it exerts its inflammatory functions by modulating the NF-κB signalling pathway.

In context of AD, upregulation of miR-146a is easily detected in hippocampus and temporal cortex brain regions of AD patients. Interestingly expression of miR-146a expression tends to increase with age of AD patients (Y. Y. Li, Cui, Hill, et al., 2011). The same was reported in age-related animal models of AD. It was concluded that this miRNA might play dual role, e;g in inflammatory response in one part, and cellular senescence in other part (Deng, Du, Zhao, & Du, 2017; Olivieri et al., 2013). The miR-146a regulates many transcriptional targets as TLR2 and TLR4 (Toll 2 or Toll 4 receptor), CFH (complement factor H), IRAK1 & 2 (interleukin- receptor-associated kinase 1 & 2), TRAF6 (TNF Receptor Associated Factor 6) and the TSPAN12 (Tetraspanin12). TLR2 is considered as the principal cellular receptor to oligomeric amyloid beta (OAβ) and as a potent activator of the downstream-associated NF-κB -cell signaling pathway. This specific TLR2-OAβ interaction in M2 macrophages is expected to facilitate amyloid internalization and brain clearing, exemplifying, as such, its anti-inflammatory functions (Ravari, Mirzaei, Kennedy, & Kazemi Arababadi, 2017). While direct correlation was early demonstrated

between expression of miR-146a and the NF-κB cell signalling activation in glial cells, the exact role of this miRNA is the control of this pathway is complex and somewhere controversial.

Several NF-kB (p50/p65) recognition binding sites has been detected in the proximal promoter of miR-146 gene which are responsible for the de novo expression of this miRNAs in cells treated with pro-inflammatory cytokines (Lukiw, Zhao, & Cui, 2008; Taganov et al., 2006). It was therefore first suggested that this miRNA might play pro-inflammatory functions as other NF-KB transcriptional targets such as IL-1β, IFN-γ, iNOS, IL-6, and TNF-α (Lukiw et al., 2008; Taganov et al., 2006). However, observation that IRAK-1, -2 and TRAF-6, three main effectors of the NF- κB signalling pathway and direct transcriptional targets of miR-146, that are significantly down- regulated in these neuronal cells lead to suggest rather that this miRNA might play a negative feedback regulation loop of control of the NF-κB cell signalling (Cui, Li, Zhao, Bhattacharjee, & Lukiw, 2010; Lukiw et al., 2008). As demonstrated by Taganov et al. the upregulation of miR-146a, negatively regulates the expression of IRAK1 and TRAF6 (Taganov et al., 2006) that was correlated with the reduction in the translocation of p65 NF-κB submit to the nucleus (Srinivasan & Lahiri, 2015). As consequence, miR-146a suppresses the production of pro-inflammatory cytokines in these cells such as IL-1β, IFN-γ, iNOS, IL-6, and TNF-α. Similar results were generated by transfection of miR-146a mimic in neuronal cells treated with cytokines with Aβ 1- 42 (Cui et al., 2010; Lukiw et al., 2008). It is therefore likely that miR- 146a antagonize the TLR signalling pathways activated in glial cells in response to OAβ, alleviating as such neuroinflammation and glial activation. These experimental studies indicated that miR-146a therapeutic might be a promising approach for AD treatment. This point has been evaluated in a recent and elegant study by Hui Mai et al (Mai et al., 2019). Authors demonstrated that intranasal delivery of miR-146a mimic

(agomiR-146) in the APP/PS1 animal model of AD improved the overall pathological state of AD. Reduction of neuroinflammation, glia activation, Aβ deposit, and Tau phosphorylation was found in hippocampus of mice treated with this agomiR. The authors concluded that overexpression of miR-146a reduced the overall neurotoxic effects of exacerbated inflammation in the brain of APP/PS1 animal model of AD. Several other novel transcriptional targets were identified in this study among them, Srsf6 (Serine And Arginine Rich Splicing Factor 6), a splicing factor frequently altered in the brains of Huntington's disease patients. Down- regulation of this hallmark marker of neurocognitive disorder that led to neuronal degeneration might also contribute to the positive outcome of this miR-146-based therapy.

On other hand, other studies have reported that miR-146a overexpression in the brain potentiates fairly neuroinflammation. Expression of CFH (complement factor H) is frequently inversely correlated with miR-146a expression in AD patients (Hye et al., 2006; Y. Y. Li et al., 2012; Lukiw & Alexandrov, 2012; Lukiw et al., 2008). CFH is a potent repressor of the amplification cascade of the alternative pathway of complement activation (Makou, Herbert, & Barlow, 2013) and therefore considered as major negative regulator of the innate immune and inflammatory response. Transfection of miR-146a mimics in neuronal and glial cells down-regulated CFH expression at both mRNA and protein levels through direct 3′-UTR binding of CFH mRNA. On opposite, treatment of brain cells with antisense oligonucleotide to miR-146a restore expression of CFH mRNA (Lukiw, Alexandrov, Zhao, Hill, & Bhattacharjee, 2012; Lukiw et al., 2008). Therefore, elevated expression of miR-146a coupled to down-regulation of CFH in brain cells of AD patients is expected to exacerbate the pathogenicity of AD disease (Lukiw, Surjyadipta, et al., 2012). Another target of miR-146a that might turn on development of AD pathology is TSPAN12. TSPAN12 is an essential regulator of ADAM10 α-secretase that plays role in

ADAM10-dependent processing of beta-amyloid precursor protein (βAPP) in neuroblastoma cells (Lukiw et al., 2005; Pogue et al., 2009; Pogue & Lukiw, 2004; L. L. Wang, Huang, Wang, & Chen, 2012; Xu, Sharma, & Hemler, 2009). Studies demonstrated that TSPAN12 down-regulation by miR-146a induction leads to significant increase in catabolism rate of βAPP by the non-amyloidogenic pathways. As consequence more neurotoxic Aβ42 peptides is generated in these cells.

miR-181c

miR-181 is significantly enriched in brain tissues as compared to several other tissues (C.Z. Chen, Li, Lodish, & Bartel, 2004). Beyond the well-established roles of this miRNA in CNS (Hutchison et al., 2013). Several independent studies have frequently reported downregulation of miR-181 expression in different regions of brain of sporadic AD patients. The same was also reported in several transgenic animal models of AD (Cogswell et al., 2008; Hébert et al., 2008; Nunez-Iglesias et al., 2010; Takousis et al., 2019).

Interestingly, mouse primary hippocampal neurons cells treated with Aβ 1-42 led to significant reduction of miR-181 expression (Schonrock et al., 2010). By searching for mRNA targets regulated by miR-181, Geekiyanage et al., identified a putative binding site in the 3-UTR of SPTLC1 (long-chain base subunit of serine palmitoyltransferase 1) (Geekiyanage & Chan, 2011). SPTLC1 encodes for a component of the SPT heterodimer, a first rate-limiting enzyme involved in de novo ceramide synthesis pathway (Hannun & Obeid, 2008). Interestingly a significant negative correlation has been detected between the low expression level of miR-181c and the high expression levels of SPTLC1 in the frontal cortices of the brains of AD patients. This, correlated with higher abundance of Aβ

1-42 in these specific brain regions (X. He, Huang, Li, Gong, & Schuchman, 2010). Upregulation of ceramide, a sphingolipid expressed in cell membrane, is consistently observed in AD patients (X. He et al., 2010). It was speculated that such an increase in ceramide levels could contribute to the initiation of AD pathology by facilitating the mislocation of BACE1 and γ-secretase in lipid rafts. As previously discussed, mislocation or abnormal expression of BACE1 and γ-secretase contribute to Aβ -formation and aggregation, in vivo and in vitro (Vetrivel et al., 2005).

Experimentally, it was shown that exogenous addition of ceramide in tissue culture of astroglia cells increased Aβ production and tau hyperphosphorylation (Patil, Melrose, & Chan, 2007). This connection link between ceramide levels induced by miR-181 and Aβ deposit have also been observed in another study. Transfection of primary astrocytes deriving from the human APP Swedish mutation animal model of AD with miR-181 led to down-regulation of SPTLC1 that correlated with reduction of Aβ production in these cells (Geekiyanage, Upadhye, & Chan, 2013). Taken together these studies indicate that deregulated level of ceramide production is an important risk factor for sporadic AD and that down-regulation of miR-181 aggravate this negative outset of this pathology.

miR-125b

miR-125b is also a miRNA enriched in the CNS (Millan, 2017) in which it plays neuroinflammation roles (Lukiw & Alexandrov, 2012). In AD, miR-125b is positively correlated with AD progression both in early and late onset of this pathology (Herrera-Espejo et al., 2019; Lukiw, 2012; McKeever et al., 2018; Pogue & Lukiw, 2018). Multiple functions have been assigned to miR-125b in AD pathogenesis.

In a first study (Banzhaf-Strathmann et al., 2014), it was shown that overexpression of miR-125b in primary neuronal cells induced Tau hyperphosphorylation and upregulation of p35, cdk5, and p44/42-MAPK, well-known regulators of cell cycle progression. On opposite, phosphatases DUSP6 and PPP1CA as well as the anti-apoptotic factor Bcl-W were found to be significantly down-regulated through direct binding to the 3'UTR of some of these transcriptional targets. Involvement of miR-125b in Tau phosphorylation and apoptosis have been confirmed in other independent studies.

For instance, Ma et al., showed that the overexpression of miR-125b in neurons increased the phosphorylation of Tau (X. Ma, Liu, & Meng, 2017) by activation of CDK5, a kinase, which promotes the phosphorylation of Tau (Mazanetz & Fischer, 2007). Pogue et al., reported that the upregulation of miR-125b can down-regulate the cyclin-dependent kinase inhibitor 2A (CDKN2A), a cell cycle inhibitor (Pogue et al., 2010). FOXQ1 is a member of the FOX family of genes involved in embryonic development, cell cycle regulation, cell signaling and tumorigenesis (Shimeld, Degnan, & Luke, 2010). Ma et al., 2017 also showed that FOXQ1 is a direct target gene for miR- 125b, and this promotes neuronal cell apoptosis and phosphorylation of Tau.

On other hand, the expression of sphingosine kinase 1 (SphK1) is as well directly regulated by miR- 125b. SphK1 is a key enzyme responsible for the phosphorylation of sphingosine to sphingosine- 1-phosphate (S1P) that plays important roles in ceramide production at the cellular membrane and regulation of proinflammatory cytokines in activated microglia (Lv, Zhang, Dai, Zhang, & Zhang, 2016). The production imbalance between ceramide and S1P is closely associated with cell death and survival and is a hallmark of AD pathogenesis by modulating Aβ production, as mentioned above for miR-181 and SPTLC1 (X. He et al., 2010). Because of this dual role of miR-125b in astrogliosis and inflammation as well in

excessive Aß production, it was anticipated that miR-125- based therapy might be beneficial for AD treatment. Very recently Xiao C et al., evaluated this point (Xiao & Chauhan, 2020), in the 5XFAD transgenic mice model of AD by intranasal infusion of 2'-O-Methyl/locked nucleic acid (LNA)-modified antagomiR-125b oligonucleotide (AMO 125 inhibitor oligonucleotide). Results demonstrated remarkable improvement in cognitive performance of mice in the Morris Water Maze (MWM) test assay, mainly in working memory ability of animals, which correlated with reduction of oligomeric Aβ accumulation in the brain. Decreased in the phosphorylated status of Tau in cerebral tissues examined as well as ablation of astrogliosis was also observed that correlated with decreased in the expression of inflammatory markers (Xiao & Chauhan, 2020).

miR-191

miR-191-5p has been shown to be one of the best biomarker candidates for predicting Alzheimer's disease with> 95% accuracy (P. Kumar et al., 2013). Among its functions in AD, miR-191 has been shown to target tropomodulin-2 (Tmod2), a neuron-specific member of the tropomodulin family (Hu et al., 2014). Tropomodulins are proteins that cap the ends of actin filaments and therefore regulate the dynamics, length and quantity of actin filaments (F-actin) (Fischer & Fowler, 2003). Tmod2 may also play a role in actin regulation during long-term depression (LTD). Tmod2 that decreases in response to increased expression of miR-191 after N-methyl-D-aspartate receptor (NMDAR) activity during LTD (Hu et al., 2014). N-methyl-D-aspartate (NMDA) receptor- dependent LTD (NMDAR-LTD) is a form of synaptic plasticity important for learning and memory. Impairment of LTD in mice caused by deactivation of NMDA receptor subunits or inhibition of NMDA receptor signalling pathways is associated with cognitive deficits,

such as dysfunctions in spatial learning, working memory, and behavioral flexibility (Brigman et al., 2010). The induction of NMDAR-LTD is accompanied by contraction and loss of the dendritic spine (Hu et al., 2014).

miR-106b

The miR-106 was first discovered by Hebert and collaborators (Hébert et al., 2009) when looking for potential miRNA target sites located into the 3′UTR of APP mRNA. The miR-20a, -17-5p and
-106b belonging to the miR-20 family were identified as negative regulator of APP expression in human neuronal cell lines. In this study, confirmed by subsequent reports, an inverse relationship between miR-106 downregulation and APP upregulation was reported in brain tissues with sporadic AD compared to control tissues.

In a follow-up study, Wang et al., anticipated a possible link between miR-106 expression and the TGF-β signaling pathway (H. Wang et al., 2010). This cell signaling pathway is frequently deregulated in AD. In the CNS, TGF-β signaling acts as multifunctional pro survival cytokines, exerting neuroprotective functions by stimulating the growth and survival of neurons. The essential role of TGF-β signaling in CNS survival was strongly demonstrated by the observation that invalidation of TGF-β1 signaling in transgenic mice induced extensive neurodegeneration (Brionne, Tesseur, Masliah, & Wyss-Coray, 2003). In the context of AD, dysfunction of TGF-β1 signaling has been shown to increase Aβ accumulation and neurodegeneration in AD models, whereas the addition of TGF-β1 is sufficient to reverse Aβ-induced neurotoxicity, in the brain of rats (Caraci et al., 2011). Of interest, an inverse relationship between miR-106b expression and TGF-β receptor type II (TβR II) expression was reported for the first time in the APPswe / PSΔE9 transgenic

double line animal model. Treatment of SH-SY5Y neuronal cells with Aβ42 oligomers induced the expression of miR-106b that was correlated with the down-regulation of the TβRII protein. Finally, two putative miR-106 binding sites were found in the 3'UTR of the TβR II receptor mRNA. The transfection of miR-106 in these neuronal cells reduced the expression of TβR II that could be abrogated when specific mutations were inserted in one of the putative miR-106b binding sites. As a direct consequence, the phosphorylated form of one of the main effectors of TGF-β signaling, Smad2 / 3, was found to be significantly reduced, which induced neurodegeneration in tissue culture. It was concluded that reduction of miR-106b expression in AD tissues might promote neuronal survival by keeping constant the pro-survival TGF-β signaling pathway. Another transcriptional target of miR-106 has been identified. In the study by Kin et al., (J. Kim et al., 2012), miR-106b was identified as a regulator of the ATP-binding cassette transporter A1 (ABCA1) and of Aβ metabolism. ABCA1 is a cholesterol transporter that recycles excess cellular cholesterol into lipid-poor apolipoproteins. Several studies (W. S. Kim et al., 2007; Koldamova et al., 2003) have reported that ABCA1 decreases the levels of Aβ and CTFβ. In this study, Kin et al., Demonstrated that miR-106b significantly decreased ABCA1 levels in neuronal cells and altered cellular cholesterol output. As a consequence, miR-106b transfection increased Aβ production levels in neuronal cells and at the same time prevented Aβ clearance.

More recently, a novel biological function was assigned to miR-106b in regard of Tau hyperphosphorylation. Liu et al., demonstrated (W. Liu, Zhao, & Lu, 2016) that expression level of miR-106b was decreased in the frontal cortex of AD patients. This spatial regulation was correlated with inversed expression of Fyn mRNA. Fyn is a non-receptor type tyrosine kinase that exerts variety of biological actions as, T-cell development and activation, brain development, neuroinflammation, synaptic function, and plasticity. In

AD, the Fyn protein is co-localized with Tau in neurons with neurofibrillary tangles (Nygaard, van Dyck & Strittmatter, 2014). Mechanically, it was found that in the Tau-overexpressed SH-SY5Y cell line (SH-SY5Y / Tau), miR-106b transfection inhibited phosphorylation of Tau in Tyr18 induced by the treatment of these cells with Aβ42. These inhibitory effects could be recapitulated when Fyn expression was silenced and, at opposite, could be rescued by inhibition of miR-106b expression using specific inhibitor. It was concluded that miR-106b inhibit Aβ42 induced Tau phosphorylation at Tyr18 via regulating the expression of Fyn (W. Liu et al., 2016).

miR-135a

Expression level studies have shown that miR-135a is downregulated in both serum and gray matter of AD patients (C. G. Liu et al., 2014; W. X. Wang, Huang, Hu, Stromberg, & Nelson, 2011). Initially, miR-135 has been reported to be a regulator of BACE-1 activity (C. G. Liu et al., 2014). It has also been shown that miR-135a targets the 3'UTR region of thrombospondin 1 (THBS1) suggesting a role of miR-135a in the angiogenesis process of AD development (Ko et al., 2015). Years later, miR-135a-5p was shown to be up-regulated in long-term depression (LTD) (Ge et al., 2010). In 2018, van Battun et al. reported that miR-135a-5p regulates synaptic functions in CNS axon regeneration (van Battum et al., 2018). In adult mice, intravitreal infusion of miR-135 facilitated CNS axon regeneration after nerve injury by modulating axon growth, branching, development and cortical neuronal migration. These processes were related to down-regulation of the Krüppel-like factor 4 (KLF4), a well-known endogenous inhibitor of axon regeneration. This work was the first to report a novel axis of miRNA regulation controlled by miR-135 that involves

the KLF4 signaling pathway (van Battum et al., 2018). Recently Zheng et al., (Zheng et al., 2021) evaluated the functions of miR-135a in synaptic activity in context of AD development. The results of this study revealed that the loss of expression of miR-135a-5p in brain tissues of an animal model of AD resulted in increased of the activity of Rho-associated coiled-coil containing protein kinase 2 (Rock2) that correlated with dendritic abnormalities and memory impairment. Rock2 activation is known to promote morphological changes in dendrites and dendritic spines by modulating the depolymerization of actin filaments (P. Sharma & Roy, 2020). To search for possible Rock2 substrates, a bioinformatic analysis was performed. Adducin was identified (Add1). Experimental studies demonstrated that miRNA-135 down-regulation led to up-regulation of Rock2 activity and Add1 hyperphosphorylation. This study provides an alternative pathway of regulation controlled by miR-135a-5p that implicated Rock2 and Add1 as partners in memory modulation /synaptic disorders in AD.

Another interesting finding of this study is that the decrease in the expression of miR-135a-5p was prominent in excitatory neurons and was induced by a decrease in factor de transcription in the expression of Forkhead box D3 (Foxd3). Foxd3 is a well-known transcriptional factor that is important for the development of the vertebrate nervous system, including the migration, and differentiation of neural crest lineages (Sommer, 2011). The authors also demonstrated that the loss of miR-135a expression is Tau-dependent and mediated by Foxd3. Finally, the dysregulation of miR-135a-5p was less evident in older mice of the AD model, e.g. 9 months, compared to younger mice (6 months of age). This later finding suggests that miR-135a-5p downregulation is more likely involved in the relatively early stages of AD (Zheng et al., 2021). In other studies, it was confirmed that the expression of miR-135a and also miR-200b and -429, was significantly reduced in the hippocampus of APP / PS1 transgenic mice and, more importantly, also in

samples from AD patients.

Functional studies performed in primary mouse hippocampal neurons, SH-SY5Y and HEK293 cells indicated that miR-135a could repress the expression and activity of BACE-1 by binding to the 3′– UTR of this target (C. G. Liu et al., 2014). Interestingly, downregulation of miR-135a-5p in the amygdala of mice was found to induce an increase in anxiety-like behavior in animals, indicating a regulatory role for miR-135a-5p in the presynaptic function of this brain region. Given that anxiety is one of the most prevalent psychiatric manifestations in the early stage of AD, the administration of synthetic miR-135a-5p might represent a promising therapeutic approach to treat both, emotional and cognitive disorders relating to AD etiology (Mannironi et al., 2018).

5.3. Challenges of selecting circulating miRNAs as biomarkers of AD

One of the main problems in the management of neurodegenerative diseases and specifically AD, is that the symptomatic clinical detection of this disease occurs late because the pathology is characterized by a slow dynamic pathological process with a long asymptomatic period. In fact, the first clinical symptoms appear in a late stage of the disease and, therefore, the possibility of reversing the pathology is compromised by the death of neurons, loss of important synaptic function, irreversible alteration of glial cells.

Usually, the diagnosis of Alzheimer's disease is based on invasive and expensive methods, such as analysis of cerebrospinal fluid or neuroimaging techniques. These monitoring methods lack of sensitivity and specificity and, again, do not offer sufficient resolution for a therapeutic intervention. In this context, the detection of biomarkers in body fluids have

attracted strong interests in the field of clinical diagnosis. One of the main advantages of miRNAs as a diagnostic marker for AD is that this class of non-coding RNA has already been approved as relevant clinical biomarkers for diagnosing cancer patients. Furthermore, miRNAs are stable molecules, resistant to changes in freezing, thawing and pH conditions and can easily be detected in any body biofluids using appropriate methods.

5.3.1. Circulating miRNAs in patients

Here, we report, what we consider as the most representative studies, human clinical studies that included a minimal of 30 patients diagnosed with either early or late symptom of AD compared also with a significant number of controls-matched donor. We review the literature of the last 10 years and selected 6 important studies.

MicroRNA signature in blood samples: impact of cohort size.

In a major study from Tan et al., a total of 413 people were included in this biomarker analysis and separated into two cohorts (Tan, Yu, Tan, et al., 2014). The first cohort included 208 people diagnosed with probable AD, while the second cohort included 205 age- and sex-matched control subjects diagnosed with some neurological disorder or common illnesses. Patients in the first cohort were classified with the classic Mini Mental State Examination (MMSE) based on cognitive tests to distinguish patients with pre-symptomatic, medium and severe cognitive impairments. This meta-analysis clinical study was performed over a 3-year follow-up study conducted in three constitutive steps. In the first stage, serum samples were collected from 50 probable AD patients and 50 healthy controls and miRNAs were extracted for subsequently sequencing using the Illumina

HiSeq 2000 sequencing technology. The differential expression profile of miRNA between the two cohorts of people was defined according to the detection of at least 10 copies of miRNA in serum sample and a threshold value corresponding to at least a 2-fold change between the two groups. The second stage consisted of confirming the RNAseq result using a qRT-PCR approach with a specific primer performed on the same patient sample used as in the first stage (AD = 50, Control = 50). The third stage consisted of the final validation procedure also performed by qRT-PCR but, this time, on a greater number of patients (AD = 158, Control = 155) due to the relevance of the statistical analysis. Results of this study indicated that a pool of 90 miRNAs was identified as significantly differentially expressed between the probable patients with AD group compared to control matched donor. A novel miRNA biomarker, e.g miR-36, was identified from this whole RNA sequencing approach that was not originally included in miRBase (Release 19) highlighting the performance of the RNAseq approach to detect novel biomarker. Among the 90 miRNAs detected in samples, 14 of them were also selected as the most deregulated microRNAs. Ten of them were down-regulated as; miR-36, miR-98-5p, miR-885-5p, miR-485-5p, miR-483-3p, miR-342-3p, miR-30e-5p, miR-191-5p, let-7g-5p, let-7d-5p whereas the 4 of them- miR-3158-3p, miR-27a-3p, miR-26b-3p, miR-151b- showed upregulation in AD patients compared to controls. At the second stage of the screening procedure only 6 over the 10 most down regulated miRNAs were found consistently reduced in the group of AD patients whereas none of 4 upregulated miRNAs from the first screening process were found consistent. At the final stage of this clinical study, **miR-98-5p, miR-885-5p, miR-483-3p, miR-342-3p, miR-191-5p and miR-let-7d-5p** were detected as the most relevant and distinguishable downregulated miRNA between the 2 groups while the **miR- 342-3p** showed the highest precision with a sensitivity of 81.5% and a specificity of 70.1%.

MiR-9-5p as regulator of the metabolic cascade of APP amyloidogenic pathway

In a second study by Souza et al., The miRNA pattern was examined in a cohort of female patientsolder than 55 years old diagnosed with late-onset Alzheimer's disease syndromes, attested by the presence of homozygous or heterozygous mutation in ApoE Ɛ4 allele (Souza et al., 2020).

A total of 74 women (38 controls and 36 patients with probable AD) were enrolled in the study according to specific and selective inclusion criteria related to the MMSE cognitive evaluation test, criteria from the American Psychiatric Association/Diagnostic and Statistical Manual of Mental Disorders and severity of dementia determined by the Clinical Dementia Rating scale. Lifestyle habits, psychiatric disorders, common illnesses and medication use were also included in the evaluation. Next, an original strategy was developed to define a list of miRNAs to evaluate their expression in body fluid samples from these patients.

A bioinformatics approach was employed to list potential miRNA candidates based on their prediction binding to the 3'UTR region of mRNA encoded from late-onset AD-related genes such as ApoE, APP, PS1 and PS2, MAPT, Clusterin, Picalm and BACE1. The second selection criteria were based on the previous experimental validation of these miRNAs in animal models or in AD patients. Finally, the Kyoto Encyclopedia of Genes and Genomes was used as a final selection filter of 25 miRNAs. Intriguingly, over the 25 miRNAs evaluated in blood serum sample of patients, comprising miR-I-3p, miR-I-2-5p, miR-9-5p, miR-16-2-3p, miR-21-5p,miR-27b-3p, miR-29b- 3p, miR-30a-3p, miR-34a-5p, miR-34c-5p, miR-92a-3p, miR-100- 5p, miR-126-3p, miR-130a-3p, miR-141-3p, miR-145-5p, miR-146a-5p, miR-155-5p, miR-181a-5p, miR-181c-5p, miR-183-5p, miR-200a-

3p, miR-221-3p, miR- 371-3p, miR-373-5p, only **miR-9-5p was found to be significantly differentially represented between the group of patient with an average of 3-fold decrease**. Interestingly miRNA-9 has been reported several times as differentially represented in AD samples from APP23 transgenic mice model and patient's cohort (Delay et al., 2012; Kiko et al., 2014; Lukiw, 2007; Schonrock et al., 2010), and this, independently of the biological nature ofbody fluids (serum, plasma or CSF). Overall, this clinical study is another valuable source of information for considering that the circulating form of miR-9 is a relevant marker for non- invasivediagnosis of AD. The miR-9 is an enriched miRNA in the adult brain (Souza et al., 2020) as it plays several key biological processes in apoptosis, inflammation and oxidative stress in neuronal cells. It was reported that this miRNA regulates the expression of multiple genes involved in the metabolic cascade of the APP amyloidogenic pathway responsible for accumulation of the Aβ 1- 42 production. Those genes include BACE1, PSEN1, Calcium / calmodulin-dependent protein kinase kinase 2 (CAMKK2), Sirtuin 1 (SIRT1), Transforming growth factor-beta (TGFβ), Tripartite motif-containing protein 2 (TRIM2). In functional studies, showed that the down- regulation of miR-9 in AD is a negative prognostic factor of this pathology. Down-regulation of this miR is systematically associated with increase in expression of BACE1 and subsequently overproduction of Aβ 1-42 (Hébert et al., 2008). Other studies reported that miR-9 down-regulation increased neurotoxicity through the modulation of the CAMKK2-AMPK pathway and increase the phosphorylated form of Tau (P-Tau) and amyloidogenesis (F. Chang, Zhang, Xu, Jing, & Zhan, 2014; Salminen, Kaarniranta, Haapasalo, Soininen, & Hiltunen, 2011).

miRNA signature from mild cognitive impairment to AD

An interesting study by Siedlecki-Wullich et al., evaluated miRNAs from plasma levels of two different cohorts of people (Siedlecki-Wullich et al., 2019). The first cohort included 14 healthy subjects, 26 subjects with mild cognitive impairment (MCI) and 56 patients with sporadic AD. The second cohort included 24 healthy subjects and 27 patients with frontotemporal dementia (FTD). The clinical diagnosis of the patients was performed by neurologists using the international neurological diagnostic criteria of National Institute on Aging-Alzheimer's association (NIA-AA). This study is quite interesting because unlike most of studies focused on miRNAs regulating specific AD-related proteins, a particular emphasis was given in this study to select a panel of miRNAs known to regulate synaptic proteins, especially glutamatergic synapses. Indeed, the dysfunction of synaptic proteins might be related to early cognitive dysfunction in experimental AD models (Casaletto et al., 2017; Miñano-Molina et al., 2011; Reddy et al., 2005; Roselli, Hutzler, Wegerich, Livrea, & Almeida, 2009).

The miRNAs profiling in samples was performed by qRT-PCR using specific primers to detect expression of selected miRNAs. The results of this study revealed a significant increase of **miR- 92a-3p, miR-181c-5p and miR-210-3p in plasma of AD patients compared to healthy subjects**.A significant upregulation of miRNA-181c-5p and miR-210-3p was also observed in plasma from people with MCI whereas an increasing but not significant trend was observed for miR-92a-3p. Furthermore, these 3 microRNAs had a better diagnostic value for patients with MCI than patients with AD syndromes. Therefore, it was proposed that these microRNAs could represent a molecular signature for the early diagnosis of patients experiencing the development of AD with a history of MCI. This assumption was reinforced by the observation that patients with a history of MCI who

progressed to AD had higher levels of these miRNAs compared to MCI patients who did not develop AD. Interestingly, none of these three microRNAs were altered in FTD patients, therefore, the expression of these microRNAs was specific for MCI and AD patients.

Another recent study describes the miRNA expression pattern of blood samples from 465 individuals from two different geographically distributed patient cohorts; i.e Germany and the USA. Samples consist of 145 sera from people diagnosed with AD (AD), 38 diagnosed with Mild cognitive impairment (MCI), 68 diagnosed with other neurological disease (OND) and 68 healthy control subjects (HC). The authors selected a set of 21 miRNAs from their previous studies and from a literature review and evaluated their abundance in blood samples by qRT-PCR using the small-nucleolar RNA, RNU48 as endogenous control because it is the most stable expressed non- coding RNA in all of patient groups. Results of a Machine Learning approach combined with stringent statistical analysis (Benjamini-Hochberg adjusted p value below 0.001) indicated that over the 21 miRNAs investigated (miR-17-3p, -5010-3p, let-7d-3p, -532-5p, -345-5p, -1285-5p, -34a- 5p, -1468-5p, -26b-5p, -151-3p, -26a-5p, -139-5p, -103a-3p, -28-3p, -486-5p, let-7f- 5p, -3157-3p,

-4482-3p, -5006-3p and -107), 20 of them were consistently de-regulated in the US and German cohorts. Interestingly, 18 miRNAs were significantly correlated with neurodegeneration with highest significance for miR-532-5p, which was markedly decreased levels in AD patients, and slightly decreased levels in patients with OND and MCI.

The second most significant deregulated miRNA was miR-17-3p which had a similar abundance pattern to miR-532-5p. The third and fourth most important deregulated

miRNAs were miR-103a- 3p and miR-107, respectively. They are less abundant in the groups of patients with AD compared to HC. By contrast, the miR-1468-5 shows an opposite expression pattern, being more abundant in AD patients with regard to HC. One question raised by authors was: is it possible to distinguish MCI patients from AD patients based on their miRNA's expression profile. Data indicated that 11 miRNAs had significant differential expression in MCI versus AD patients. In fact, miR-17-3p, - 26b- 5p, -532-5p, -103a-3p, -107, -345-5p, let-7f-5p, -26a-5p were less abundant in AD patients compared to HC while let-7d-3p, miR-1468-5p and -139-5p which were found more abundant in the AD groups of patients. Interestingly miR-26a, 26b-5p, and let-7f- 5p, showed the highest representative miRNA correlated to MMSE. Surprisingly none of the 20 miRNAs investigated were significantly correlated with gender and age of patients and this independently of groups of patients. The specificity of this meta-analysis study was validated with the bioinformatics study indicating that same miRNA profiles can be obtained when the USA and the Germany cohorts were analyzed separately or combined. Finally, authors investigated the distribution of miRNAs expression pattern in blood components such as peripheral blood cells, serum, exosomes using a recently released miRNA blood cell type atlas (Juzenas et al., 2017). Interestingly, the miRNAs with lower abundance in AD patients were enriched in monocytes and T-helper cells, while those miRNAs more abundant AD patients were enriched in serum, exosomes, cytotoxic T cells, and β-cells. Therefore, this report highlights the existence of complex regulatory pattern of miRNAs expression among different blood cell compounds that can be taken in consideration when searching for accessible tool to detect miRNA biomarkers as well for better understanding miRNA functions in diseases development. Furthermore, this study was the first that correlates the expression pattern of miR-532-5p to AD. Downregulation of miR-532-5p expression has been reported in several cancer types as epithelial ovarian

cancer (Wei, Tang, Zhang, Sun, & Ding, 2018), bladder cancer (Xie, Pan, Han, & Chen, 2019) and renal cell carcinoma (Yamada et al., 2019). This miRNA acts as tumor suppressor miRNA where its negatively regulates proliferation and migration of cancer cells though transcriptional repression of HMGB3, a member of the high-mobility group box family known to play key roles in DNA replication, recombination and repair, as well as the transcriptional factor TWIST. A closed interplay relationship between miR-532-5p and Wnt/β-catenin signaling has been suggested as HMGB3 and TWIST are two key regulators of this frequently deregulated cell signaling pathway in cancer. Moreover, miR-532-5p expression has been also associated to sporadic amyotrophic lateral sclerosis (Liguori et al., 2018) and is detected in exosomes from patients with multiple sclerosis (Selmaj et al., 2017) and geriatric fragility syndrome (Ipson, Fletcher, Espinoza, & Fisher, 2018). The exact role of miR-532-5p in development of AD remains to be determined. Recently a machine learning approach (X. Zhao et al., 2020) was applied to 96 serum samples collected from the Oxford Project to Investigate Memory and Aging (OPTIMA) program in the UK. This OPTIMA program enrolled 32 serum samples from patients with AD classified according to the Alzheimer's Disease and Related Disorders Association criteria, 13 serum samples from patient diagnosed as mild cognitive impairment (MCI) according to the Petersen practice parameter (Petersen et al., 1999) and 51 serum controls diagnosed with any neurocognitive impairment or deficiency. A list a 12 miRNA was first selected over a first machine learning test cohorts split in a ratio of 70:30 of AD and control patients to identify the most discriminable miRNAs from the 566 total miRNAs detected by a multiplex RT-qPCR serum analysis. Results indicated that miRNA-346, - 345, and -122 were upregulated in AD compared to controls, whereas miR- 208b, miR-499a, and miR-206 were downregulated in AD. The threshold p significant statistical values were adjusted to ≤ 0.02 in this study.

The expression pattern of these miRNAs allowed to diagnose AD patient from control subject with 90.0% sensitivity, 66.7% specificity, and 76.0% accuracy in an independent and separated cohort attesting the reliability of this bio-informatics blinded approach that does not rely on biological matters or literature consensus but rather over distribution of miRNAs in samples of different types or groups of patients. When the same strategy was applied to MCI serum samples to identify relevant miRNA biomarkers unable to discriminate MCI patients from control, none of the 12 selected miRNAs selected pass through the multivariable tests of statistical analysis. The authors conclude that the alteration of serum miRNA signature identified between AD and control groups probably occurred latter to the MCI symptoms and therefore could not be used to accurately diagnose the early stage of AD progression. In addition, the few numbers of MCI samples included in the analysis was recognized as a limit.

MicroRNAs in cerebrospinal fluid

The expression levels of 754 miRNAs were analyzed from CSF samples of patients with AD and control subjects (Dangla-Valls et al., 2017). AD patients were diagnosed according to the revised criteria of the National Institute on Aging- Alzheimer's association (NIA-AA) in addition to clinical, neuropsychological and magnetic resonance examinations.

Age and sex-matched controls enrolled in this clinical study, were evaluated for normal cognitive performances based on specific tests, clinical dementia and absence of psychiatric symptoms or history of neurological disease. In addition, molecular and biochemical markers of AD such as Aβ42 production and phosphorylated form of Tau were also evaluated at the time of CSF collection from lumbar punctures performed in the two

groups of patients. The TaqMan Array Human MicroRNA cards technology, covering 384 human mature miRNA per card was employed to screen for the differential expression pattern of miRNA in the CSF sample. In the first stage, a cohort of 10 AD and 10 matched control CSF samples were analyzed to profile the expression pattern of miRNA in these samples. Twelve miRNAs were selected and then screened in a second and larger independent cohort of samples consisting in 37 AD and 32 matches control CSF samples. Then, 9 miRNA candidates were selected for a last screening procedure performed on AD samples and matched control. Results of this clinical trial evaluation indicated that 68 over the 750 miRNAs spotted on the TaqMan Array Human MicroRNA cards have a detectable expression level in samples and that 9 of them; **miRNA-21, miRNA-126, miR-138, miR-146a, miR-146b, miR-205, miR-222, miR-375 and miR-885-5p,** showed the most different distribution pattern (downregulated) between the AD samples and matched donor control groups. The miR-125b and miR-222 were the most significantly upregulated in the AD group. Interestingly positive regulation of miR-222 in AD was reported for the first time. In contrast, the miR-125b has been frequently detected in patients with Alzheimer's disease while its biological functions have been correlated with astrogliosis in neurodegeneration (Pogue et al., 2010).

5.3.2 Common pattern of microRNAs between patients and in AD animal models

Regarding the expression profile of miRNAs, the coincidence between species is not elusive. Animal models continue to be so widely used in bioassays that they allow extrapolation of results in humans, it has been observed some expression profiles of consensus miRNAs in specific organs and their deregulation in pathological state, more

specifically it has been shown that the brains of AD mice reveal the same characteristics as the brains of humans with AD (Reddy et al., 2012).

The miRNA expression studies in mouse models with AD have helped to reveal, for example, that dysregulation in miRNA expression in AD brain correlates directly or indirectly with Aβ production and phosphorylated Tau, they have also allowed us evaluate whether the observed changes in miRNA levels in humans are a cause or a consequence of the neurodegenerative process (Delay & Hébert, 2011). In addition, it has made it possible to compare the changes in miRNAs expression with the alterations at the cognitive level (Pepeu & Giovannini, 2004). Although the expression profile of miRNAs has been investigated in transgenic or non- transgenic rodent models of AD, and the results have shown a similar expression profile in humans, not all microRNAs found in animal models have been validated in humans. This stage would be essential to translate the molecular observations from mice to humans, as has been done in recent years.

As in AD patients, most studies on miRNAs expression have been performed in brain tissue from transgenic mice (H. Wang et al., 2010) showed global miRNA profiles in an APP/PS1 (APPSwe- PS1M146L) transgenic mouse model using microarray analysis. Of the 37 differently expressed miRNAs, 5 microRNAs (miR-20a, miR29a, miR-125b, miR-128a and miR-106b) were down- regulated, while 4 (miR-34a, let-7, miR-28 and miR-98) were upregulated. The following investigations have also shown that some miRNAs present an expression similar to that found in the brain of humans with AD (Hébert et al., 2009; Hébert et al., 2008; Nunez-Iglesias et al., 2010; Shioya et al., 2010; W. X. Wang et al., 2011).

Several animal models have been developed that could continue to be used and exploited their potential to examine and verify microRNAs profiles in blood, serum and plasma, with

the aim of searching for AD biomarkers and also to test and validate microRNA-based therapies.

5.3.3. Circulating microRNAs in transgenic animal models

To our knowledge, few reports have examined the expression pattern of circulating microRNAs in body fluids of animal models of AD. Most of the published studies focused on the biological functions of deregulated microRNAs in AD brain tissues or cell cultures as highlighted in the previous paragraphs. The first published study dedicated to the analysis of circulating microRNAs in animal models of AD was performed by (Garza-Manero, Arias, Bermúdez-Rattoni, Vaca, & Zepeda, 2015). The authors evaluated the expression pattern of plasma miRNAs in the 3xTg- AD triple transgenic mouse model as compared to the wild-type, littermate control mice. The samples were collected at different times according to the chronic development of the pathology throughout the age. The evaluation was carried out at different time points in the evolution of the pathology in this model. 4 groups were evaluated; Group 1) Wt mice of 2 to 3 months of age (n = 6), Group 2) Wt mice of 14 to 15 months of age (n = 7), Group 3) 3xTg-AD mice of 2 to 3 months (n = 6) and Group 4) 3xTg-AD mice aged 14 to 15 months (n = 6). The miScript miRNA PCR Array System that contained the Pathway-Focused miScript miRNA PCR Array "Neurological Development and Disease" was used, which included 84 miRNAs that have been associated with different neuropathologies, including AD. The initial results showed that the majority of the 84 miRNAs evaluated were detected in the plasma of the mice of all the groups analyzed, however, the highly abundant miRNAs detected belonged to the let-7 family, the miR-15 family, the miR-30 family, miR-24-27 group, miR-29 group, miR17- 92 group and their paralogs miR-106a-363 and miR-106b -25. A group of less

detected or undetected miRNAs was also found, such as miR-135b, miR-302a / b, miR-488 and miR-9, however the comparisons of miRNAs abundance between both young groups, that is, 3xTg- AD and control group of 2 to 3 months, did not show significant differences in the profile of circulating miRNAs.

In a second stage, they compared the profile of circulating miRNAs between young and old mice for both the WT and 3xTg-AD groups. They showed that changes in the plasma levels of a certain group of microRNAs are associated with aging, with significant differences found in the levels of 33 miRNAs between old WT mice and young WT mice. In addition, significant differences were found in 40 miRNA levels when comparing old versus young 3xTg-AD mice (reviewed in Garza- Manero et al., 2015); 19 of these miRNAs were common in both comparisons and include family members of let-7, miR-30, miR-17- 92 cluster and their paralogs. miR-132, miR-138, miR-146a, miR-146b, miR-22, miR-24, miR-29a, miR29c, and miR-34a was found by comparing young and old 3xTg-AD mice, showing significant differences between plasma microRNAs only in the transgenic group, thus suggesting age-related changes that occur specifically in 3xTg-AD mice.

In 2017, Hong and collaborators published a comparative study (Hong, Li, & Su, 2017) between expression of circulating miRNAs previously detected in body fluids samples from AD patients with that could be detected in the APP/PS1 transgenic animal model of AD. Results indicated that miR-125b, -9 and -191-5p were significantly downregulated in the serum of APP/PS1 mouse model as was also found in AD human serum samples. The miR-28-3p was also upregulated in sera sample of human AD patients and APP/PS1 transgenic mice model. The miR-181c, and - 26b-3p did not show significant differences between the groups of animals although these miRNAs were detected as up- and down-regulated in human serum sample from AD patients. Pearson's correlation analysis revealed

a positive correlation between miR-125b expression and the cognitive function of the APP/PS1 animal model. Interestingly, authors evaluated whether treatment of APP/ PS1 mice with the epigallocatechin gallate (EGCG), an abundant bioactive polyphenol found in solid green tea extract with well characterized anti- inflammatory properties (Chu, Deng, Man, & Qu, 2017) and protective effects against neuronal damage and cerebral edema (Schaffer, Asseburg, Kuntz, Muller, & Eckert, 2012; Unno et al., 2007), could reverse the expression pattern of circulating miRNAs detected in APP / PS1 transgenic AD model. As anticipated, levels of serum miR-125b, -9, and - 191-5p were reversed in EGCG-treated APP/PS1 transgenic mouse models. It is worth to note that the neuroprotective effect of EGCG against cognitive impairments of patients with AD is currently evaluated in clinical trial (e.g., Sunphenon EGCg (Epigallocatechin- Gallate) in the Early Stage of Alzheimer´s Disease (SUN-AK)). As miR-125b was the most consistent deregulated miRNA in AD samples from human and mouse and one of most reversed miRNAs following treatment of APP / PS1 transgenic mice with EGCG, the level of miR-125b was also evaluated in the SH-SY5Y neuroblastoma cell line treated with EGCG. The results of this study indicated that although the detection of miR-125b in cell culture supernatant was found difficult, treatment of cells with EGCG markedly increased this miRNA, i.e., the results were consistent with those found in the APP/PS1 model treated with EGCG. Authors concluded that circulating miR- 125b is the most likely relevant biomarker of AD.

In another major and elegant recent study (Ryan, Guévremont, Mockett, Abraham, & Williams, 2018), the expression level of circulating microRNAs related to age and to amyloid-β plaque deposition was evaluated in the APPswe/PSEN1dE9 AD transgenic mouse model. A custom designed Taqman microRNA arrays representing 185 neuropathology-related microRNAs was employed to evaluate the kinetic of miRNA

expression over the chronic development of pathology, at 4, 8, and 15 months of age. The results revealed that 8 microRNAs (miR-27b-3p, miR-30b-5p, miR-93-3p, miR-143-3p, miR-361-5p, miR-382-5p, miR-421-3p, miR-423-5p) were significantly affected by age alone in wild-type animals. Twelve microRNAs were altered in APPswe/PSEN1dE9 mice, either prior to amyloid-β plaque deposition detected at 4 months, or later during course of AD development, i.e., detected between 8 to 15 months of age. When the pattern of miRNA expressions was analysed precisely at each time points, differing sets of microRNAs were identified. At 4 months of age there was a significant decrease in the expression of miR-200b- 3p, miR-139-5p and miR-27b-3p while it was found that the expression levels of miR-205-3p and miR-320-3p increased significantly. Functional analysis of this early-time miRNONE profile combined with bioinformatics tools to predict the enrichment of specific miRNA pathways, as well as targeted genes regulated by these miRNAs revealed alterations in common pathways related to inflammatory response, cell death and survival, molecular transport and protein synthesis. Of note, a specific enrichment of the TGFb / Smad signaling pathway was detected at this 4-month time point for which Aβ plaque deposition was not detected in the brains of these mice. It was then proposed that this early-time response might reflect an early neuroprotective response to AD development. Later, at time point superior to 8 months of age, miR-140-3p, -486-3p, -339-5p and - 744-5p were upregulated in APPswe/PSEN1dE9 mice compared to control, littermate mice. On opposite; miR-143-3p and miR-34a-5p were found downregulated. This altered miRNAs patterns of expression and corresponding deregulated genes were more closely associated to chronic amyloidosis response with significant enrichment of inflammatory response genes focused to the TNF signaling pathway. Free Radical Scavenging, immunological Disease, and apoptosis signaling were also more specifically enriched at this time point that further increased till 15 months of age. This specific late-time response reflected more

a neurodegeneration signature that fitted well with the presence of important amyloid-β plaque deposition in brains of in APPswe/PSEN1dE9 mice compare to control, littermate mice.

Finally, very Recently Kim et al., (Y. J. Kim et al., 2020) investigated change in expression of miR-16-5p in the 5xFAD animal model of AD. Panel of miRNA expression was evaluated using the Affymetrix Gene Chip miRNA 4.0 array from plasma samples collected from 1, 2, 3, 4, 6, and 9-month-old of 5xFAD mice and were compared to WT mice of the same age. Among the 84 miRNAs found as deregulated between the 5xFAD and WT mice, miRNAs miR-140-5p, -106b-5p and -16-5p were identified as the most significantly deregulated miRNAs. From them, the miRNA-16-5p was upregulated at a much higher level than the other miRNAs and was found as a better discriminating circulating biomarker between 5xFAD and WT mice. Spatial expression pattern of miR16-5p in brain tissues of 5xFAD mice revealed enrichment of this miRNA in the cortex, hippocampus and thalamus and, remarkably, near to Aβ plaques deposition and neuronal loss as evidenced by FISH and immunohistochemistry analysis. Interestingly, the level of miR-16-5p was significantly higher in 6- and 9-month-old 5xFAD mouse brains compared to those of age-matched WT mice. This increased in the expression of miR-16-5p coincided furthermore with the loss of neurons in the cortex, hippocampus and thalamus reinforcing again a direct link of correlation between expression of miR-16-5p, Aβ deposit and neurodegeneration. To investigate whether expression of miR-16-5p was induced in neuronal cells undergoing to cell death, primary cultured of cortical neurons and the human neuroblastoma SH-SY5Y cells were treated with a toxic form of Aβ. Results indicated that miR-16-5p expression was upregulated in Aβ-treated cortical and SH-SY5Y neuronal cells. MiRNA data base interrogation combined with miRNA reporter assay identified a putative binding site in 3'UTR part of the anti-apoptotic factor, B cell lymphoma- 2 (BCL-2) which

was significantly downregulated, both at the mRNA and protein level in SH- SY5Y transfected cells with miR-16-5p. All together this data support previous experiment (showing that upregulation of miR-16-5p in brain tissues of AD patients and animal model is a bad prognosis marker of AD development and an important risk factor for neuronal cells death in AD.

Chapter 2 Material and Methods

This chapter describes the different materials and protocols that we use during the execution of this project. We receive important collaborations, for example, Dr. Marc Dhenain from The Molecular Imaging Research Center (Fontenay-aux-Roses, Paris), who has donated serum samples from transgenic APP / PS1 mice. Another collaboration was made with the staff of the Novaxia pathology laboratory (Saint-Laurent-Nouan, France), who performed the histological analyses.

a. Animals

Sprague-Dawley rats (aged 8-12 weeks) with a body weight of 200-380 g were obtained from the Bioterium of the Research and Development Laboratory located in the Universidad Peruana Cayetano Heredia (Lima, Peru). Animals were maintained under controlled laboratory temperature (25 ± 2°C) and humidity (60 %) conditions, with a controlled light cycle (12 hours light/12 hours dark). Water and food were available ad libitum throughout the experiment. The animal handling and experimental procedures were approved by Ethics Committee of the Universidad Peruana Cayetano Heredia (CIEA-102069). The animal behaviors were monitored daily by the animal care staff to ensure that the animals were safe and healthy.

b. Preparation of amyloid-β 1-42 peptide

Aβ1-42 (amyloid-β1-42) peptides were obtained from Sigma–Aldrich (A9810) and solubilized in Dimethyl Sulphoxide (DMSO), prepared at concentration to 2 mM, to generate a stock solution at a concentration of 10 µg/µl. The solution was then stored at -20°C until use. The working solutions were then diluted in Phosphate Buffered Saline (PBS) at the final concentration of 0.5, 1 and 2.5 µg/µL, and incubated for 1 week at 37°C (Wu et al., 2017), to produce the fibrillar form of Aβ 1-42 peptide. This form of Aβ 1-42 peptide were called FAβ and was injected intracerebrally into the hippocampus of the rats as described below.

c. Model of Alzheimer disease generated by intracranial injection of FAβ

The general procedure to administrate the Aβ in the brains of rats was from (Wu et al., 2017) with some modifications. At first, rats were anesthetized with an intraperitoneal injection of 10 % (vol/vol) of chloral hydrate prepared in distilled water at a dose of 400 mg / kg of body weight per animal. Anesthetized animals were thereafter placed on a stereotaxic apparatus (KOPF ® 900, David Kopf Instruments). The head of rats were shaved, disinfected using a chlorhexidine 0.5 % (w/vol, Sigma Aldrich). An anterior-posterior incision of 2.5 cm starting from the midline of the scalp through a longitudinal incision was performed between the eyes until the back of the ears. The Bregma was used as reference to perforate the skull and inject the Aβ peptide into the hippocampus using the following coordinates: 2.6 mm lateral, 3.0 mm back, 3.0 mm deep from the bregma (Figure 1). The groups of animals (n = 11±2) were injected at the level of the CA1 region of the hippocampus, according to the Paxinos and Watson rat brain stereotaxic coordinate atlas,

fourth edition (Paxinos and Watson, 1998). A maximum of 3 µL of Aβ solution prepared at final concentrations of 0.5, 1 and 2.5 µg/µl were then infused in the two hemispheres of the hippocampus using a microsyringe Hamilton® (Qiagen, Hilden, Germany). The control group of animals were injected with PBS of same volume in the same area. The solution was injected slowly over a 6 min time period using the following standardized procedure; for each microliter of Aβ solution inoculated over 1 min, the microsyringe was left intact for an additional 1 min before inoculating the next microliter of Aβ solution. This procedure was repeated until the total volume of Aβ solution was inoculated. At the end of the inoculation, the microsyringe was held in place for an additional 3 min to ensure that the solution properly dispersed into the ventricles and that the injected volume was not re-aspirated when the microsyringe was removed. Then, the holes in the skulls were filled with dental acrylic solution prepared from a dental powder commercially available, and dissolved in sterile distilled water. The dental acrylic was placed on the perforated region using a sterile spatula until the powder solidified at room temperature. Finally, the scalp was sutured using saturation threads and sterilized using a commercially available silver sulfadiazine cream (Sigma- Aldrich). Rats were held alone in a single cage until they were fully awake and monitored for viability. The rats were thereafter returned to cages (n=8) and monitored every day until the time of experimentation.

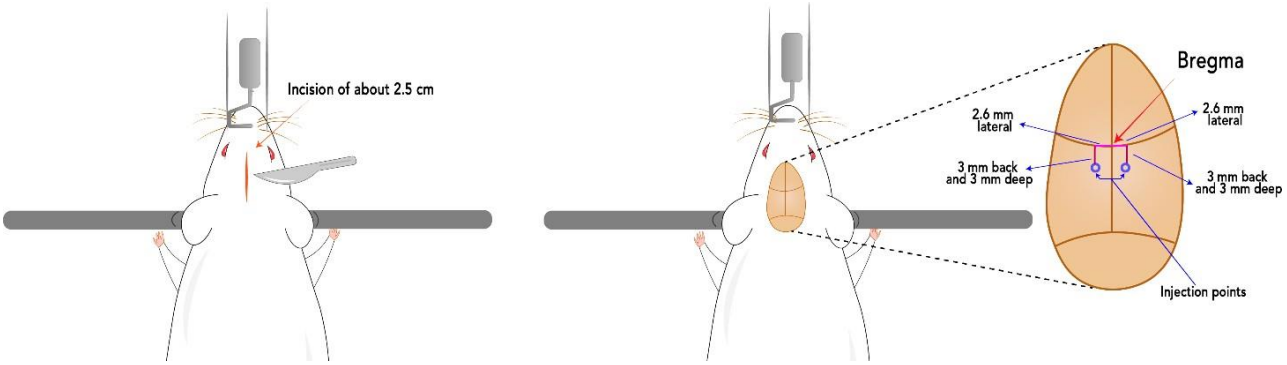

Figure 1. Scheme of stereotaxic coordinates for the injection of Aβ 1-42 peptides.

d. Morris Water Maze test

4.1. Presentation of the experimental procedure

The Morris Water Maze test (MWM) was used to evaluate the spatial memory of rats injected with Aβ peptides or with the PBS control solution. The general procedure was derived from (Wenk, 2004) with modifications. MWM was performed 14 days after the infusion of Aβ or PBS. The animals were assigned in 3 different groups (n=11); one treated group infused with 3 µl of Aβ (0.5 µg/µL), a second group infused with 3 µl of Aβ (1 µg/µL) and a control group infused with 3 µL of PBS. The Maze was built at the Universidad Peruana Cayetano Heredia using a circular black plastic circular pool of 126 cm in diameter and 75 cm in high filled with water at 21-22 °C to generate a swimming pool of 35 cm in high. The pool was divided with imaginary lines to delimitate four quadrants: Northeast (NE), Northwest (NW), Southeast (SE), Southwest (SW). The pool contained a transparent plastic platform of 10 cm in diameter and 33 cm in high located in the SE quadrant and 10 cm away from the pool wall. The pool had geometric figures (triangle, circle, rhombus and square) in walls located in each quadrant. Swimming trajectories used by the rats to reach the platform were monitored using a webcam connected to a computer to collect video every 90 seconds (Figure 2).

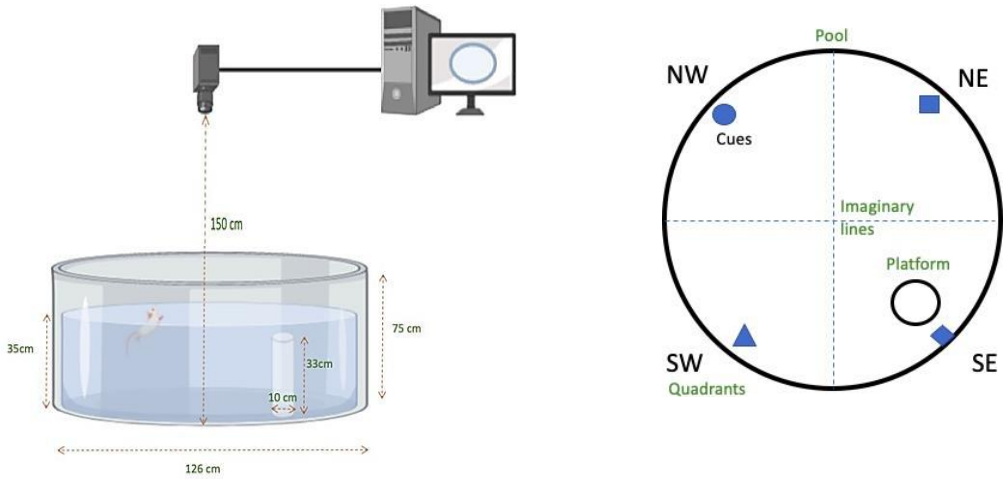

Figure 2. Morris water maze test. A) Dimensions of the pool and camera linked to the computer for tracking record of the path. B) Geometric cues and quadrants in the pool.

4.2. Morris water maze evaluation and video recording

To evaluate the effect of Aβ 1-42 peptides on memory performance of rats, we used a memory protocol consisting in familiarization, acquisition and memory sessions steps. In all sessions, the rats were randomly placed in the maze, while the location of the platform remained constant during the procedure. We also kept a constant 5 min time interval period between the three different memory sessions.

Familiarization session was performed the first day of training. The objective of this session was to familiarize the animals to the maze and the platform. The procedure consisted in placing the rats in a quadrant of the pool and to perform at least 4 trials per rat. The video was switched-ON when the rats were placed in the pool until the time when the animals found and climbed the platform. We assigned a maximal arbitral time of 90 seconds for the rats to reach the platform. Above this time period, meaning that the rats did not climb onto the platform within 90 seconds, the trial was terminated. Then, an experimenter guided the

rat to the platform.

The acquisition session was performed the day after the familiarization session and was performed over four days. The objective of this session was to evaluate the spatial learning of the animals according to their treatment with the Aβ or PBS solutions. To do that, the rat was placed in different quadrants of the pool. A total of 8 trials were recorded per rat. The video was switched-on when the rats were placed into the pool and until the time when the animals found and climbed the platform. Again, we assigned a maximal arbitral time of 90 seconds for the rats to reach the platform and if the rat rats did not climb onto the platform, an experimenter placed the rat on the platform before starting the next trail. Videos were used to record and monitor the exact time and trajectories used by the animals to reach the platform

The memory session was done on the sixth day. The objective of this session was to evaluate the reference memory of rats according to their treatment with Aβ or PBS solutions. To do that, the rats were placed in the pool without any platform. One trial per rat was used in this specific session. The trajectory and time the rats spent swimming to the platform area were also recorded over a 90 seconds time period.

4.3. Video acquisition and data monitoring

The videos were processed with a RatsTrack plug-in, designed and settled up from both, the School of Engineering of the University of Ibague in Colombia and the Universidad Peruana Cayetano Heredia. RactsTrack consists a new image processing plug-in to evaluate automatically the variables of distance, time and velocity in the Morris water maze test in rats. This free access plug-in was implemented using ImageJ software and is currently being considered for publication: RatsTrack: New automatic method for tracking rats in a

pool in the Morris water maze. Forero et al.

e. Body fluid collection and sampling

i. Blood collection and serum separation

Blood samples were collected in BD Vacutainer® tubes coated with silica as coagulation activator according to the procedure described by (Vigneron et al., 2016). Samples were collected from 8 rats at 7, 14, 21 days post-injection with Aβ 1-42 or PBS solutions. Blood was collected using the cardiac puncture technique described by (Beeton, Garcia, & Chandy, 2007) to collect a sufficient amount of blood samples. Blood samples were left at room temperature for 30 to 40 min for blood clot formation. Then, the serum was collected by centrifugation at 1 900 x g for 10 min at 4°C. The supernatant corresponding to the serum was clarified through a second high speed centrifugation (16 000 x g for 10 min and 4°C). The clarified serum was carefully transferred into a new Eppendorf tube and stored at - 80 °C until used. Absence of hemolysis was visually inspected. Hemolyzed samples were discarded from the study.

ii. Cerebrospinal fluid collection and preparation

CSF was collected 14 days after the inoculation of Aβ 1-42 from the cisterna magna of the rats according to procedure described by (Blanco, Mayo, Bandiera, De Pietri Tonelli, & Armirotti, 2020; Pegg, He, Stroink, Kattner, & Wang, 2010). Before CSF extraction, the animals were anesthetized by an intraperitoneal injection of ketamine (100 mg / kg) and

xylazine (10 mg / kg). Afterwards, the base of the skull was shaved and disinfected with a 70 % of alcohol solution. The animal was then positioned on a flat surface with the head manually placed in a position to form an angle of 135° with the body of the animal. In this position, the cisterna magna became more visible facilitating the extraction of the CSF (Blanco et al., 2020). The procedure to extract the CSF consisted in using an infusion system equipped with a 25-gauge butterfly needle to precisely collect the CSF into the dura mater/ atlanto-occipital membrane according to procedure (L. Liu & Duff, 2008; L. Liu, Herukka, Minkeviciene, van Groen, & Tanila, 2004). Precaution was taken during the procedure to avoid contaminating CSF samples with blood. Then the CSF was loaded in a 0.5 mL Eppendorf tube, stand for 1 hour before to centrifuge the tubes at 1 000 x g for 5 min at 4 ° C to remove cellular debris. The clarified CSF samples were stored at -80 ° C until use.

6. Analysis of circulating microRNAs expression in animal models of AD

6.1. Procedure presentation and normalization strategy

The procedure used to quantify the expression of miRNA in serum samples derived from a general procedure described by (Tan, Yu, Liu, et al., 2014; Vigneron et al., 2016) and was adapted to my studies. The procedure consisted in a 4 main steps: 1) total RNAs extraction from body fluids, 2) addition of a fixed amount of synthetic exogenous miRNAs to normalize the relative expression of circulating miRNA in samples, 3) reverse transcriptase step to generate cDNA and 4) qPCR analysis using specific primers.

An absolute prerequisite in qPCR analysis is the selection of an adequate housekeeper RNA to normalize the relative expression of molecular target of interest according to

sample variations due to both experimental errors introduced during sample preparation and processing and biological variations. Whereas U6 or SNORD44 small nucleolar RNAs and the 5S ribosomal RNA (5S rRNA) are commonly used in “solid sample” as tissues or cells to normalize expression of miRNA, these RNA molecules cannot be used as circulating housekeeper miRNA. Several studies have reported that these conventional housekeeping miRNAs are variably secreted from cells and degraded in serum, plasma or CSF samples. Therefore, they cannot be used as reliable circulating housekeeping miRNA in body fluids. To palliate to this issue, one of alternative procedures, although being still debated, is to add a fixed and constant amount of synthetic oligonucleotide miRNAs in all samples to be analyzed. These exogenous miRNAs also frequently referred as spiked-in miRNAs can be used as circulating housekeeping miRNA to normalize the relative expression of target miRNA in samples according to experimental variation (technical and instrumentation errors, sample preparation and processing). In our study, we decided to follow recommendation from Vigneron et al. and to add 3 different spike-in miRNA deriving from C. elegans: Cel-miR-39-3p, Cel-miR-238- and cel-miR-248. The choice of those spike-in miRNAs is justified by the fact that 1) those miRNAs are not phylogenic conserved in rat and 2) have GC content in sequence closed to 50 % meaning that they can be easily amplified by RT-qPCR. Sequences of these spike-in miRNAs were obtained from the miRBase database and synthesized by Eurogentec (Eurogentec, Lieja, Belgicum). The SDS-PAGE purified oligonucleotides were suspended in water at a fixed concentration of 200 amol/µL. Then 2.5 µL spike-in / 100 µL samples was added after the denaturation step of the extraction procedure in such way that the final concentration of these spike-in miRNAs in the sample was similar to concentration of circulating miRNA in samples (Vigneron et al., 2016).

We evaluated two different methods to extract the total RNA fraction from bloody fluid

samples. The first method was based on the miRNeasy Serum/Plasma Kit from Qiagen, while the second method derived from kit NucleoSpin® miRNA Plasma from Macherey-Nagel, Hoerdt, France). The total RNA extraction was performed from serum and CSF samples collected from the animal model of AD generated and also from serum samples collected from APP/PS1dE9 transgenic mice of AD. These latter were provided by Dr Marc Dhenain (PhD. Group Leader, Molecular Imaging Research Center, Fontenay-aux-Roses, Paris). In this specific case, bloods from 4- and 15-month-old transgenic mice were pooled, when necessary, to obtain a minimal final volume of 130 µL of serum and to generate at least 5 animals by groups e.g APP/PS1dE9 transgenic mice and their littermate, not transgenic mice. Total RNA extraction was performed with the miRNeasy Serum / Plasma Kit, as this is less demanding in term of starting blood volumes required for serum preparation and for extract circulating miRNAs.

6.2. Total RNA extraction from body fluids

6.2.1. Total RNA extraction from serum samples

The method from the miRNeasy Serum/Plasma Kit (Qiagen, Hilden, Germany) consists in extracting the total RNA from 200 µL of serum samples. One mL of QIAzol lysis reagent was added to the sample and vortexed vigorously before leaving the samples at room temperature (15– 25 °C) for 5 min. Then, 5 µL of each exogenous miRNAs (cel-miR-39- 3p, cel-miR-238- and cel- miR-248) prepared at 200 amol/µL were added to the sample. Samples were vortexed and incubated a further 5 min at room temperature. The proteins were precipitated by the addition of 200 µL of chloroform solution followed by a vortexing step and an incubation period of 3 min at room temperature. The tubes were

centrifuged at 12 000 g for 15 min at 4 ° C to collect the upper aqueous phase containing the total RNAs. The intermediate and lower phases containing the proteins and the organic solvent were discarded. The upper aqueous phase (approximately 600 µL) was transferred to a new Eppendorf tube before adding 900 µL of a 100 % ethanol solution. After mixing the solution by inversion, 700 µL of the sample was transferred to a RNeasy MinElute spin column and then centrifuged at 8000 g for 15 s at RT. Then 700 µl of RWT washing Buffer was added to the column before to centrifuge the tube at 8000 x g for 15 s. A second RPE washing buffer (500 µl) was performed followed by a final wash with 500 µl of 80 % ethanol solution. After centrifugation, the column was carefully removed, placed in a new Eppendorf tube and centrifuged at 12 000 x g for 5 min to remove any trace of solvent and to dry the column. The column was placed in a new Eppendorf tube before adding 14 µl of RNase free water on the center of the column membrane and left at RT for 1 min to allow the elution volume to disperse into the full membrane surface. Finally, the tube was centrifuged for 1 min at 8 000 x g to elute the miRNA from the column. The sampleswere stored at -80 ° C until use.

The method from NucleoSpin® miRNA Plasma kit (Macherey-Nagel, Hoerdt, France) consists in extracting the total RNA from 300 µL of serum samples. At first, 90 µL MLP buffer (Buffer Lysis) was added to the samples to denature the proteins then the samples were vortexed for 5 s and incubated for 3 min at room temperature. Then, 7.5 µL of each exogenous miRNA (cel-miR-39-3p, cel-miR-238- and cel-miR-248) prepared at 200 amol/µL was added to the sample. Thereafter, 32.2 µL of Buffer MPP was loaded to the samples to precipitate proteins by centrifugation at 11 000 x g for 3 min. The supernatant was transferred to new tube before addition of 430 µL of isopropanol and vortexing the tube vigorously for 1 min. The samples were then loaded into a NucleoSpin® miRNA

Column to capture RNA. After an incubation of 2 min at RT, the tubes were centrifuged at 11 000 x g for 30 s. A first wash was performed by addition of 700 µL of Buffer MW2 followed by a centrifugation step at 11,000 x g for 30 s. A second wash was performed by addition of 250 µL of Buffer MW2 followed by a centrifugation step 11,000 x g for 2 min. Then, 50 µL of recombinant DNase solution supplied in the kit was loaded onto the column to digest genomic DNA. After an incubation period of 15 min at RT, a first wash was performed by addition of 100 µL of MW1 buffer followed by a centrifugation step at 11000 x g for 30 s. A second wash was performed by addition of 700 µL of MM2 buffer followed by a centrifugation step at 11000 x g at 30 s. Finally, a third wash was performed by addition of 250 µL of MM2 buffer followed by a centrifugation step at 11000 x g for 2 min to completely dry the membrane. The column was placed in a new Eppendorf tube before adding 30µl of RNase free water in the center of the column for 1 min to allow the solution to disperse into the membrane. Last, the tube was centrifuged for 1 minute at 8 000 x g to elute the miRNA from the column. The samples were stored at -80 ° C until use. The total RNA fractions eluted from the 2 extraction methods were quantified using nanodrop spectrophotometer (Nanodrop 2000, Thermo Scientific). Concentration and purity of the samples were evaluated by reading absorbance of sample at 260, 280 and 230 nm. Samples with absorbance ratio values ranging from 1.8 to 2 at 260/280 nm and with absorbance ratio values ranging from 1.8 to 2.2 at 260/230 nm were considered for the experiments.

6.2.2. RNA extraction from CSF samples

After preliminary optimization procedures, we finally selected the miRNeasy Serum / Plasma Kit as the extraction method. This procedure allows us to extract and to quantify

miRNAs from as few as 50 µL of CSF sample. Moreover, to further optimize the yield of miRNA recovery from these small volume samples, 5 µg of glycogen solution prepared at concentration of 0.1 µg/µL was added as recommended by (Duy, Koehler, Honko, & Minogue, 2015). The RT and qRT-PCR procedures were performed with the miRScript system (Qiagen, Hilden, Germany) as described in the details below.

6.3. Reverse transcription reaction (RT)

Total RNAs were reverse transcribed into cDNA using the miScript II RT Kit (Qiagen) according to the manufacturer's instructions. Fifty ng of total RNAs prepared at concentration of 10 ng / µL were polyadenylated by a poly (A) polymerase and then reverse transcribed to cDNA by using oligo-dT primers. The RT-reactions were performed with a final volume of 20 µl containing 4 µL of 5X miScript HiSpec Buffer, 2 µL of 10X miScript Nucleic Mix, 2 µL of miScript Reverse Transcriptase Mix. The RT reaction was initiated at 37°C for 60 min followed by a final step at 95°C for 5 min. The cDNAs were then stored at -20°C until use.

6.4. Real time quantitative RT-PCR (qRT-PCR)

qRT-PCR was performed with the miScript SYBR® Green PCR Kit (Qiagen) according to the manufacturer's instructions (Figure 3). A volume of 2.5 µL corresponding to 50 ng of cDNA were loaded in a final volume of 10 µL containing 5 µL of 2X QuantiTect SYBR Green PCR Master Mix, 1 µL of 10X miScript Universal Primer and 10X miScript Primer Assay and 0.5 µL of RNase- free water. The quantification of PCR products (amplicon)

was collected using the Light Cycler® 480 (Roche Diagnostics Corporation, Indianapolis, IN, USA) according to the manufacturer's instructions. All miRNA specific forward primers (miScript Primer Assays) were purchased from Qiagen. The list of primer used is available in Table 1. The miScript Universal Primer from the kit was used as reverse primer. RNase-free water was used as negative control. Cycling conditions for real-time PCR were 95◦C for 15 min, 45 cycles of 94°C for 15 s, 55°C for 30 s, and 70 °C for 30 s followed by a melt-curve analysis to evaluate PCR specificity. All samples were analyzed in triplicate and the geometric mean of the Ct values of each sample was calculated. The relative expression level of miRNAs was calculated using the relative threshold cycle and the comparative threshold cycle method. The miRNAs expression was calculated according to Livak and Schmittgen method (Livak & Schmittgen, 2001) after normalization by 3 cel-miRs exogenous. The results were finally expressed as ($2^{-\Delta\Delta Ct}$) in which $\Delta\Delta Ct$ = Ct (miRNAs of interest) – Ct (miRNAs cel-miRs exogenous). Each experimental group consisted of 8 samples from the control and treated animal.

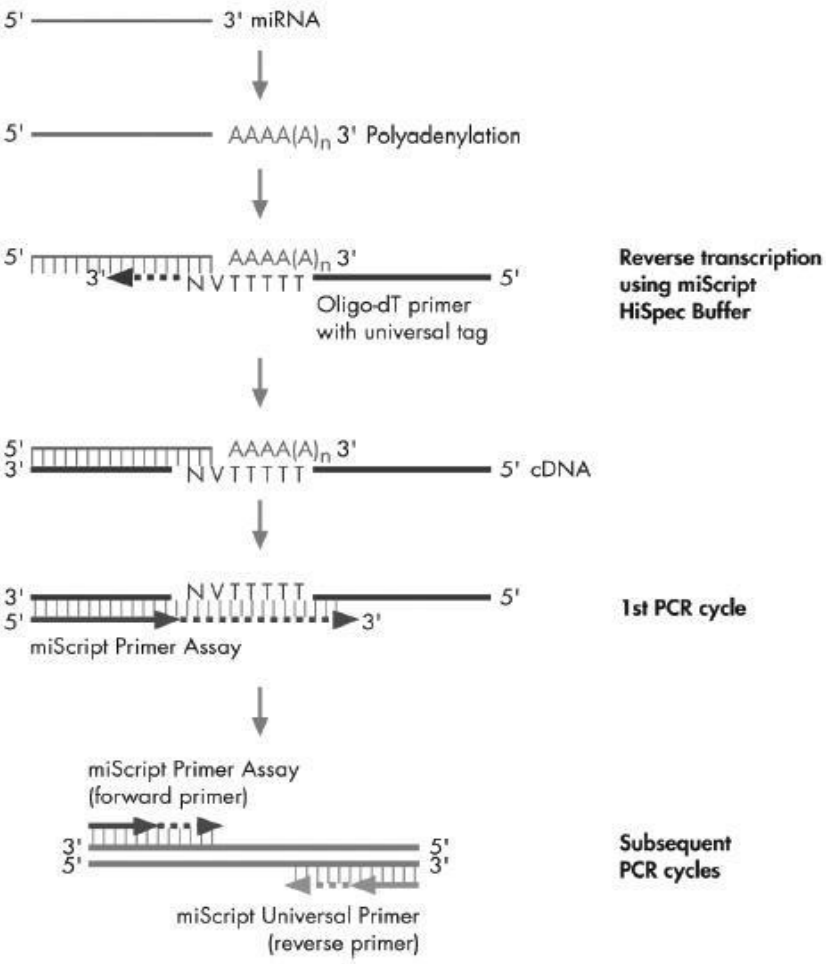

Figure 3. Selective conversion of mature miRNAs into cDNA using the miScript system. In a reverse transcription reaction with miScript HiSpec Buffer, mature miRNAs are polyadenylated by poly(A) polymerase and converted into cDNA by reverse transcriptase with oligo-dT priming. The cDNA is then used for real-time PCR quantification of mature miRNA expression using specific primer and a universal primer. https://www.qiagen.com/fr/resources/resourcedetail?id=7954ef25-3a39-4b0a-a27e-42689dbb4f5f&lang=en

Table 1. Sequence of microRNAs

mature microRNA	Sequence	Sanger Accesion	Catalog number
rno-miR-9a-5p	UCUUUGGUUAUCUAGCUGUAUGA	MIMAT0000781	MS00013951
rno-miR-146a- 5p	UGAGAACUGAAUUCCAUGGGUU	MIMAT0000852	MS00000441
rno-miR-29a-3p	UAGCACCAUCUGAAAUCGGUUA	MIMAT0000802	MS00033397
rno-miR-29c-3p	UAGCACCAUUUGAAAUCGGUUA	MIMAT0000803	MS00000175
cel-miR-39-3p	UCACCGGGUGUAAAUCAGCUUG	MIMAT0000010	MS00019789
cel-miR-238-3p	UUUGUACUCCGAUGCCAUUCAGA	MIMAT0000293	MS00019439
cel-miR-248	AUACACGUGCACGGAUAACGCUCA	MIMAT0000304	MS00019516

7. Brain tissues collection

To collect the tissues from the brain of the animals, a general routine procedure developed by the staff of the laboratory of Neuroscience located in the Universidad Peruana Cayetano Heredia was used. First, rats were anesthetized by an intraperitoneal injection of sodium pentobarbital (90 mg/Kg) before infusing them with an injection system composed of a 16-gauge blunt cannula and a manometry pump. A lateral incision of approximately 5 cm was made through the integument of the animal to make accessible the diaphragm. A second incision was thereafter made on each side of the clavicle to expose the heart. Finally, a last small incision was made at the posterior end of left ventricle to the heart to insert the cannula into the ascending aorta. The cannula and the heart were clamped with a haemostatic forceps before cutting the right atrium and to inject 300 mL of a washing solution consisting of a saline solution containing 0,9 % NaCl. Thereafter, 200 mL of a fixing solution containing 4 % paraformaldehyde prepared in 0.2

M PBS was injected under of 80 mm Hg pressure guided by manometry pump. The injection was performed quickly and uniformly. Then brains of animals were removed manually and kept for 24 hours at 4°C in a 4 % paraformaldehyde solution. The next day, brains were washed 3 times with PBS and finally stored in PBS at 4 °C until the organs were embedded in paraffin for histological examination.

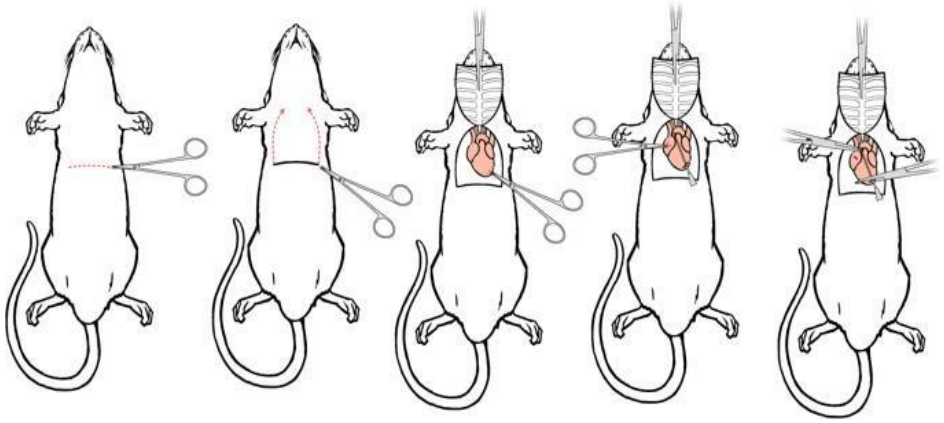

Figure 4. Perfusion Surgery. The positioning of the forceps to have access to the diaphragm and then to the entire thoracic cage are shown. Lateral incisions were done to expose the pleural cavity and the heart. Then a cannula was inserted into the ascending aorta. Image from (Gage, Kipke, & Shain, 2012).

8. Histology and immunofluorescence analysis of brain samples

8.1. Tissue sections and histology staining

Paraffin blocks containing brain tissue were cut into 5 µm thick sections and mounted on glass slides. Hematoxylin-eosin (HE) and Cresyl violet staining were performed according to routine histology procedure performed by the staff of the Novaxia pathology laboratory (Saint-Laurent- Nouan, France).

8.2. Immunofluorescence staining

Sections (5 µm) of brain tissues mounted on glass slides were subjected to deparaffinization and re-hydration procedures before staining the tissues with specific antibodies. Briefly, the deparaffinization step was performed by 3 sequential xylene baths of 5 min each followed by a rehydration step of tissue sections in sequential alcohol baths at 100 %, 95 % and 75 % of 5 min each. A final wash with distilled water was carried out for 1 min. Immunostaining was performed following the protocol described in (Reverchon et al., 2020). At first, the slides were incubated in citrate buffer (1 M citric acid, 1 M sodium citrate, pH 6 at 80 °C for 30 min to unmask the epitopes induced by brain fixation with the 4 % paraformaldehyde fixative solution. Then, tissue slides were rinsed 3 times in a TBS solution containing 0.3 % (vol/vol) Triton X-100 (TBST) and then incubated for 2 h in a humid chamber at room temperature with a blocking TBS solution containing 1 % (w/v) BSA; 10 % (vol/vol) Fetal Calf Serum (FCS); 0.3 % (vol/vol) Triton X-100 and 1% NaN3. The sections were then incubated with primary antibodies; anti-GFAP (Dako, Agilent, Santa Clara, USA, Z0334; 1: 500) or anti-Iba-1 (Abcam, Cambridge, England, ab5076; 1: 500) at 4 °C overnight. The next day, the sections were washed 3 times in TBST and incubated 2 hours at RT with a secondary anti-rabbit Alexa 488 antibody (Abcam, ab150077, 1: 1000) for GFAP labelling or with secondary anti-goat Alexa 488 antibody (Abcam, ab150129, 1: 1000) for IBA-1 labelling. After 3 washes in TBST buffer, the slides were stained with DAPI (14.3 mM) for 10 min and washed before mounting with Fluoromount-G (SouthernBiotech, Birmingham, England). Then, the slides were dried overnight and visually inspected using the ZEISS AXIOVERT 200 M Apotome microscope (Zeiss, Oberkochen, Germany) connected to a

digital camera located at the Pacyfic Platform (CBM, Orléans). Serial sections were analyzed at 20x magnification to reconstruct the whole hippocampus of the brain using the ZEN2.1 software (Zeiss). Images were collected as serial Z stack series of from 18 optical slices. Once the images were reconstructed, GFAP and IBA-1 labelled positive cells were counted manually. In parallel, the DAPI fluorescence counting was performed. Both analyses were performed for each area of the hippocampus, i.e., cornu ammonis (CA) 1/CA2, CA3 and the dentate gyrus (DG) using Image J -Fiji software (Schindelin et al., 2019). A total of 40 slides were analyzed, corresponding to treated group (n=5) and control group (n=5).

9. *In vitro* assessment of the impact of OAβ and FAβ treatment on rat primary astrocytes

9.1. Primary astrocytes preparation and culture

Primary astrocyte cultures were prepared following the protocols described in (Galland et al., 2019; Y. J. Gao et al., 2009). Six brains were collected aseptically from newborn 3-day-old Sprague Dawley rats ordered from Janvier Labs (Le Genest-Saint-Isle, France), prior to isolating the cerebral hemispheres manually.

The tissues were put into small Petri dishes containing cold Hanks' Balanced Salt Solution buffer (Sigma-Aldrich, Saint-Quentin Fallavier, France). Then, the meninges were carefully removed under microscope before dissociating tissues mechanically using a pipette and scalpel. The solution was then centrifuged at 1 000 x g for 5 min. The supernatant was removed and the cell pellet was resuspended in DMEM medium

(Dulbecco's Modified Eagle's Medium containing 4 g/L of glucose, Sigma-Aldrich) supplemented with 10% FCS, and 1 % of penicillin and 10 mM of L-Glutamine. The cells were seeded in 24-wells plate at density of 1.5 x 105 cells /cm2 and cultured for approximately 14 days in a humidified incubator in 5 % CO2 at 37 °C to reach 80 % of confluency. The medium was changed every 3-4 days. A GFAP staining was then performed to validate presence of astroglia cells in this primary tissue culture.

9.2. Preparation of Aβ 1-42 peptide

Aβ 1-42 peptides obtained from Sigma – Aldrich (Sigma-Aldrich, Saint - Quentin Fallavier, France, A9810) were solubilized in 2 mM DMSO to generate a first stock solution at 220 mM and stored at -20 °C. This stock solution was then diluted in PBS at the final concentration of 100 µM. The beta amyloid oligomer (OAβ) or fibrillar (FAβ) was generated according to procedures described in several publications (Dahlgren et al., 2002; Heo et al., 2007; J. A. White, Manelli, Holmberg, Van Eldik, & Ladu, 2005) and adapted to our study. Briefly, OAβ was generated by incubation of the 100 µM working Aβ1-42 solution at 4 °C for 24 hours whereas the FAβ was generated by incubating the 100 µM working Aβ1-42 solution at 37 °C for 4 days.

9.3. Treatment of primary astrocytes with OAβ, FAβ, LPS, and BMS

Experiments were performed after 14 days of culture, when the primary astrocytes monolayer reached 90 % confluence. Before treatment, cells monolayer was washed 2 times with 1 mL of D- PBS (Dulbecco's Phosphate Buffered Saline, Invitrogen, Carlsbad,

CA) and then incubated with the OAβ or FAβ preparation at final concentration of 5, 1 and 2 µM for 3 days at 37°C. Cells incubated with 2 µM of DMSO solution were used as controls. Additional conditions were performed by incubating cells with 1 µM FAβ or 1µM OAβ and DMSO as control for 7 days and a renewal of the 1 µM FAβ work solution on day 3.5. In parallel; cells were also treated with a NF-κB inhibitor (BMS-345541, Sigma-Aldrich, France) used at the final concentration of 5 µM. When specified, the cells were pre-incubated for 1 hour in tissue culture with the BMS-345541 inhibitor before treatment with the OAβ or LPS solution for 3 days as described in here (Burke et al., 2003; Owens et al., 2017).

9.4. Cell Viability Assay

Cell viability analysis was performed with the Alamar Blue™ HS reagent according to manufacturer's instructions (Invitrogen, Carlsbad, CA, A50101). A 1/10 dilution of Alamar blue solution was prepared in serum –free DMEM culture medium. Then, 500 µL was added to each well of the 24-well plate for 2 h at 37 °C. After incubation, 5 aliquots of 50 µL of cell supernatant were transferred to a 96-well white plate for monitoring fluorescence intensity (λ-excitation: 560 nm and λ-emission: 605 nm using a microplate reader (VICTOR3™ Multilabel Plate Reader, Perkin Elmer). The fluorescence value from the untreated cells (NT) was set up as the arbitral value of 100 %.

9.5. miRNA and mRNA quantification from primary astrocytes culture

For miRNA quantification from the primary cells, total RNA was isolated with the miRNeasy kit (Qiagen, Hilden, Germany) following the manufacturer's instructions.

Reverse transcription was performed with 100 ng of total RNA as starting material using miScript II RT Kit (Qiagen, Hilden, Germany) as described in section 6.3. We performed the quantitative RT-PCR with 100 ng of cDNA using the miScript PCR System and specific primer miScript Primer Assay as described in section 6.4. The relative expression of miRNAs of interest was normalized to the relative expression of U6 using the miScript Primer Assay purchased from Qiagen (Hs_RNU6-2_11) (Qiagen, Hilden, Germany, MS00033740). Final results were expressed using the 2-ΔΔCt as described in section 6.4. For mRNA quantification from the primary cells, we isolated the total RNA using Trizol reagent (Invitrogen, Carlsbad, CA). Briefly, cell monolayers were washed in PBS and then lysed by adding 800 µL of Trizol solution. Then, 80 µL (1/10 volume) of chloroform was added to each sample and the content vortexed vigorously followed by 5 min incubation at RT. Then, the tubes were centrifuged at 12,000 x g for 15 min at 4 °C before collecting the aqueous upper phase containing the total RNA. One volume of 70% ethanol solution was added and the mixture was gently mixed by inverting the tube several times. We loaded the samples onto a RNeasy mini-columns (Qiagen, Hilden, Germany) and centrifuged at 12 000 x g for 15 s. Columns were washed 2 times with 500 µL of RPE buffer (Qiagen, Hilden, Germany) followed by a final centrifugation step at 11 000 x g for 2 min to dry the membrane. total RNAs were eluted in a column by adding 20 µL of nuclease-free H2O (Qiagen, Hilden, Germany) followed by a centrifugation step for 1 min at 12 000 x g. The total RNA was quantified using the Nanodrop spectrophotometer (NanoDrop™ 2000 / 2000c, ThermoFisher) as described above in the section 6.2.1. The RT and qPCR procedures were rigorously the same as previously described above (sections 6.3 and 6.4). The primers used to quantify the relative expression of IRAK1, TRAF6 and IRAK2 were purchased from Qiagen (Qiagen, Hilden, Germany). The other primers specifics for IL-6, IL-1β, TNF-α were designed in our laboratory according to a routine procedure. The

GAPDH housekeeping gene and corresponding primers were used to normalize the relative expression of mRNA in all samples. Finally, the data were expressed as 2-ΔΔCt according to method from (Livak & Schmittgen, 2001).

Table 2. Primers for qRT-PCR

Gene (Rat)	Forward primer (5'–>3')	Reverse primer (5'–>3')	Reference
IL-6	TCCAGTTGCCTTCTTGGGAC	AGTCTCCTCTCCGGACTTGT	10.1038/s41598-018-26421-5
IL-1β	TTCATCTTTGAAGAAGAGCCCAT	TCGGAGCCTGTAGTGCAGTT	10.1038/s41598-018-26421-5
TNF- α	CAAGGAGGAGAAGTTCCCAA	TGATCTGAGTGTGAGGGTCTG	10.3390/cells8121553
GAPDH	GATGACATCAAGAAGGTGGTGA	ACCCTGTTGCTGTAGCCATATTC	10.1007/s10753-019-01029-7

9.6. Sandwich enzyme-linked immunosorbent assay

A sandwich enzyme-linked immunosorbent assay (ELISA) system was used to measure the concentrations of IL-1B, IL-6, TNF-α and CXCL1, from the astrocytes culture medium, using paired antibodies according to the manufacturer's instructions. The procedures were carried out in collaboration with the laboratory; «Immunologie et Neurogénétique Expérimentales et Moléculaires» (INEM).

10. Statistical analysis

To ensure robustness of our analysis, two different statistical analysis were employed. The first analysis consists in evaluating the statistical significance of the OAβ treatment in Test de Morris and the second in serum samples and in cell culture samples.

10.1. Statistical analysis of Morris test

The quantitative variables were: distance, time spent by rats in each quadrant, distance travelled by rats in each quadrant, acceleration and velocity. The Stata 13.0 software was employed to analyze the data. GraphPrism 8.0 software was used to elaborate the graphs. The data obtained from the MWM test were analyzed with the Kruskal Wallis test. This non-parametric test (data did not follow the normal distribution), was used to evaluate the statistical difference between the three groups (0.5 µg / µl, 1 µg / µl and control group), P <0.05 was considered significant.

10.2. Statistical analysis of microRNAs

The relative expression of miRNAs and mRNAs were expressed as mean ± SEM. XLSTAT statistical software was used to analyze the data and the GraphPrism 8.0 software to elaborate the graphs. At first, the Grubbs test was run to identify outlier values. Then, after eliminating the outliers, the values were processed for a test of normality using 4 different statistical tests: Shapiro-Wilk, Anderson-Darling, Lilliefors and Jarque-Bera tests. If the statistical analysis indicated that groups of values followed a normal distribution then a parametric test was fixed and the t-student unilateral test was used. Conversely, if the result of 4 tests indicated that the data followed a non-parametric distribution then the Mann-Whitney unilateral test was used. In all cases $p < 0.05$ was considered as significant and $p < 0.01$ as highly significant.

Chapter 3 Results

This chapter is composed of two parts:

I. Identification of circulating microRNAs in rat model produced by intrahippocampal injection of Aβ 1-42.
II. Mechanistic study of miR-146a-5p in primary astrocytes model of AD

I. Results Part 1: Animal model of AD generated by intrahippocampal injection of Aβ 1-42 leads to memory impairment

I.1. Rational procedure for intrahippocampal infusion of Aβ 1-42 peptides

Procedures to infuse Aβ 1-42 peptide in the brain of animals were derived from different publications with some modifications. Indeed, several reports indicated that a single, bilateral intra- hippocampal infusion of Aβ peptide at a concentration ranging from 0.5 to > 5 µg/µL is sufficient to affect the working memory and cognitive performance of infused animals (Karthick et al., 2019; McLarnon & Ryu, 2008; Morroni, Sita, Tarozzi, Rimondini, & Hrelia, 2016; S. Sharma, Verma, Kapoor, Saini, & Nehru, 2016; Wong et al., 2016; Wuet al., 2017). In addition, other publications indicated that a repetitive infusion of Aβ 1-42 peptide with varying concentrations also generates similar results (Faucher et al., 2015; Fekete et al., 2019; Forny-Germano et al., 2014). Here, we decided to evaluate the impact of bilateral intrahippocampal infusion of the Aβ 1-42 peptide both on the cognitive performance of the animals and on the amounts of miRNA circulating in the blood (serum) and CSF. Since microRNAs can be useful as early AD biomarkers, our objective was to directly correlate the level of circulating miRNAs with the presence of the Aβ 1-42 peptide

in fibrillar state, a major component of AD pathogenesis. Considering that the current diagnosis of AD uses cumbersome and expensive methods, the quantification of circulating microRNAs in serum with non-invasive methods is essential. It has been suggested that fibrillar insoluble form of Aβ 1-42 peptide (FAβ 1–42), rather than the oligomeric soluble form (OAβ 1–42) is more neurodegenerative and responsible for synaptic and cognitive dysfunctions. The FAβ aggregated form of the Aβ 1-42 peptide precedes the formation of amyloid plaques and deposits and is considered to be one of the main pathological hallmarks of AD. Again, the procedure for the preparation of Aβ was also subject to significant divergences in the literature (Dahlgren et al., 2002; Heo et al., 2007; H. Y. Kim et al., 2016; Lecanu & Papadopoulos, 2013). In this project, we produced the FAβ by spontaneous aggregation of the Aβ 1-42 peptide for 7 days at 37°C (Lane- Donovan & Herz, 2017; Wu et al., 2017). Then, we infused the FAβ into the two hemispheres of hippocampus and more precisely in the bilateral CA1 region. It is known that this region is primarily involved in long-term memory storage and is widely affected in AD patients with the presence of significant deposits of amyloid plaques (Karthick et al., 2019; Mattsson et al., 2012). The infusion into the hippocampus was performed by stereotaxic surgery, following the standard procedures that have been described in the Materials and Methods. The Figure 1 shows a schematic representation of the general procedure used.

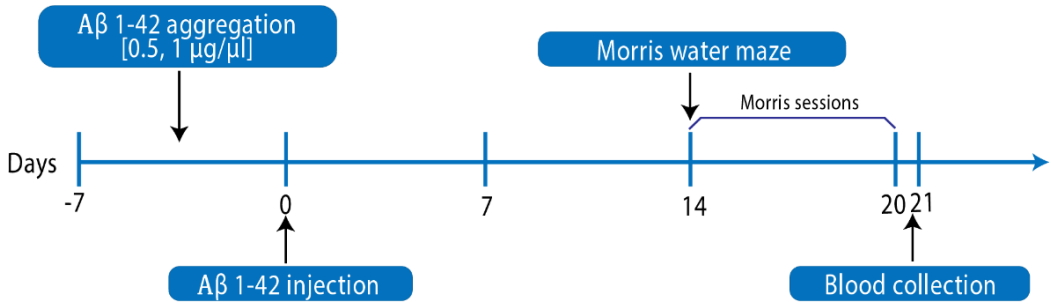

Figure 1. Schematic representation of the first experimental design of the intrahippocampal injection of Aβ 1-42 at 0.5 and 1 µg/µL prepared as FAβ 1-42. Rats were injected with 3 µL of FAβ 1–42 (Aβ-treated group) or PBS as vehicle solution (Control group). Cognitive behavior was evaluated on day 14 and sample collection was performed on day 21.

I.2. Cognitive impairments of rats inoculated with 1 µg/µL of FAβ

Our rat animal model of AD, induced by intrahippocampal infusion of Aβ 1-42 peptide solution as shown in Figure 1, was challenged for the first time using the classic Morris Water Maze test to assess memory performance and behavior of treated animals (Wenk, 2004).

Procedures and methods used to record the trajectories and times for the animals to reach the platform are described in details in Materials & Methods. In collaboration with colleagues from the Faculty of Engineering of the University of Ibague (Ibagué, Tolima, Colombia Colombia), we developed a novel plugin called “RatsTrack” to automatically extract trajectories of rats in maze from video recorded by a camera placed on the top of the maze (Figure 2). An example of trajectory used by a rat to reach the platform is shown in Figure

2C.

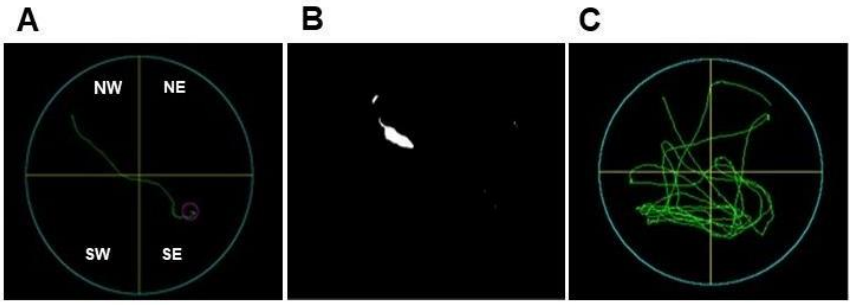

Figure 2. Automatic monitoring of trajectory used by a rat to reach a platform during a Morris water maze test. (A) Maze designed with quadrant orientation and platform localization (pink circle) **(B)** Video detection of an animal in the maze **(C)** Automatic trajectory recording using the novel plug-in "RatsTrack" developed during this study.

For each rat, we monitored the distance travelled and the latency escape as variables of cognitive performance (Figure 3). During the familiarization session, no statistically significant differences were found on day 1 of the training session between all groups, indicating that animals in both groups have similar visual and motor skills.

Conversely, significant differences were found in the lengths of the trajectories from day 2 to day 5 (Figure 3A). Evaluations in the NW quadrant showed that Aβ-treated rats used longer distances to find the platform during these 4-day time interval compared to PBS-treated rats (Figure S1A). When rats were placed in the NE quadrant, significant differences were only observed on day 4 and day 5 (Figure S1B). For rats placed in the SW quadrant, Aβ-treated rats used longer distances compared to the control group of animals, but the differences were not statistically significant (Figure S1C). In the SE quadrant, the path lengths of Aβ treated-group were significantly different to those of the control group from day 2 to day 4 (Figure S1D).

When the reference memory was evaluated on day 6, the difference between the Aβ treated-group was statistically significant to that of PBS-treated group. In the NW and SE quadrants, the Aβ treated-group performed wider distances compared to the control, but the difference was not statistically significant (Figure 3B).

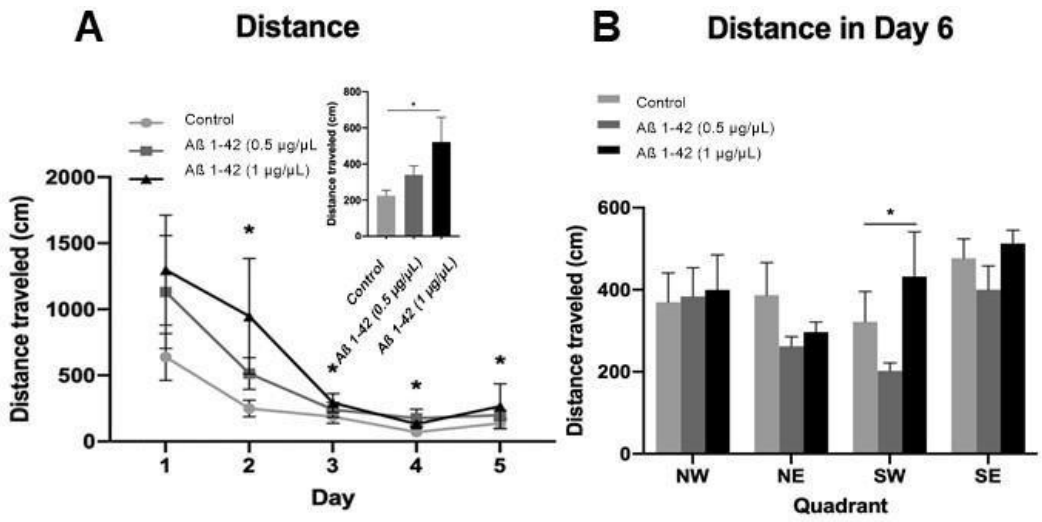

Figure 3. Effects of FAβ 1-42 injection on memory and learning, evaluated by the MWM test. The distance performed by rats injected with FAβ prepared with 0.5 and 1 µg / µL of Aβ 1- 42 to find the platform was evaluated on day 14 after injection. **(A)** Total distance traveled duringthe 5 days of training. **(B)** Reference memory evaluated in each quadrant on day 6 of the MWM test. Control group (n=10); group injected with FAβ made with 0.5 µg/µL of Aβ 1-42 (n=11); group injected with FAβ made with 1 µg/µL of Aβ 1-42 (n=13). Data are represented as mean ± SEM. Statistical comparisons were performed using Kruskal-Wallis. *p≤0.05, **p≤0.01, ***p≤0.001.

Figure 4 corresponds to the escape latency evaluated as second variable. The escape latency of each rat was evaluated in 4 quadrants. The groups of animals infused with FAβ 1-42

showed a longer escape latency compared to the control group with a significant difference on day 4 and 5 ($p < 0.05$) (Figure 4A). The results of the reference memory evaluation on day 6 were not statistically significant between the groups (Figure 4B). When the same test was evaluated on 28 days post treatment, no statistically significant differences were observed, indicating that the effect of Aβ on cognitive performance is likely reversible due to peptide clearance (data not shown).

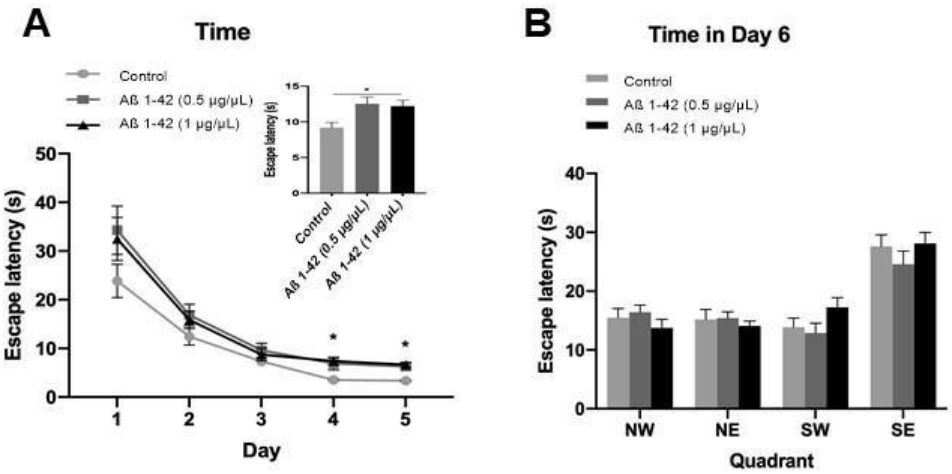

Figure 4. Effects of Aβ 1-42 injection on memory and learning, evaluated by the MWM test. The escape latency to find the platform was evaluated on day 14 post- treatment. **(A)** Total escapelatency during the 5 days of training. **(B)** Reference memory evaluated in each quadrant on day 6 of the MWM test. Control group (n=10); group injected with FAβ made with 0.5 µg/µL of Aβ 1- 42 (n=11); group injected with FAβ made with 1 µg/µL of Aβ 1-42 (n=13). Data are represented as mean ± SEM. Statistical comparisons were performed using Kruskal-Wallis. *p≤0.05, **p≤0.01, ***p≤0.001.

I.3. Intrahippocampal injection of Aβ 1-42 leads to dysregulation of circulating microRNAs

Our next objective was to evaluate whether the defective cognitive performance of the FAβ peptide- infused rats could be associated with the dysregulation of the circulating miRNAs detected in the serum of these animals collected on day 21, the last day of the MWM test. We selected from the literature a panel of circulating miRNAs reported as frequently dysregulated in the blood of AD patients and / or in transgenic animal models of AD. Those microRNAs are: miR-9a-5p, miR-146a-5p, miR-29a-3p, miR-29c-3p, miR-125b-5p, miR-181c-5p, miR-191-5p, -miR-106b-5p and miR-135a-5p. The results obtained by qRT-PCR indicated that among the 9 microRNAs evaluated, only the amount of one miRNA, miR-146a-5p, was statistically different in sera from Aβ-treated animals compared to those of PBS-treated animals ($p < 0.05$) (Figure 5). Nevertheless, the amounts of miR-9a-5p, miR-29a-3p, and miR-29c-3p tend to be lower in the Aβ-treated group compared to the control group, although the difference was not statistically significant, it was very close to 0.05 (Figure 5).

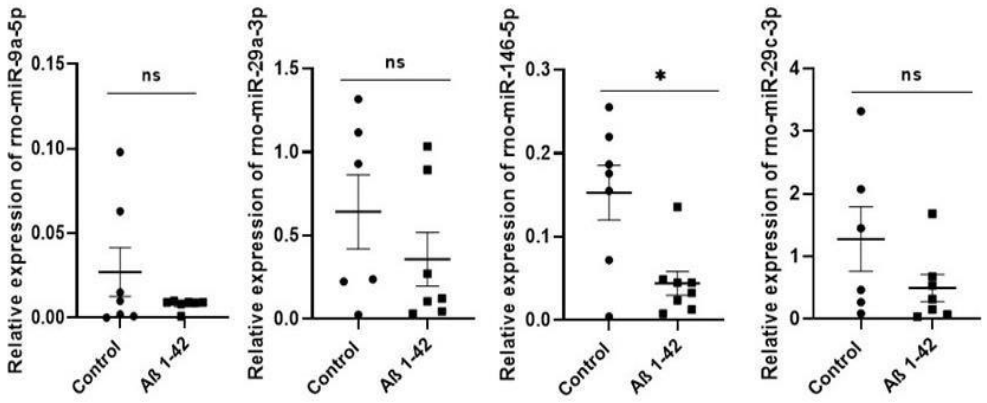

Figure 5. **Relative expression of circulating miR-9a-5p, miR-29a-3p, miR-146a-5p, miR-29c-3p in serum samples.** Sera from rats infused with FAβ (treated group) or PBS (Control group) were collected 21 days post-treatment. MicroRNA were extracted and quantified by qRT-PCR. Data are represented as mean ± SEM of 7-8 samples evaluated in triplicate. Statistical comparisons between Aβ 1-42 and PBS groups were performed using the Mann-Whitney test * $p \leq 0.05$, ** $p \leq 0.01$, *** $p \leq 0.001$.

I.4. Increasing the amount of Aβ 1-42 peptide infused into hippocampus of rats enhanced the relative abundance of circulating miRNA in serum samples.

Our first results prompted us to evaluate whether increasing the amount of Aβ 1-42 peptide infused into the brain of rats could also increase the expression level of miRNAs in serum samples of these animals. We assessed this point in a second cohort of rats infused intrahippocampally with 3 µL of FAβ made with 2.5 µg/µl of Aβ 1-42 peptide. A schematic representation of procedure and experimentsperformed in this second cohort of animal is

shown in Figure 6.

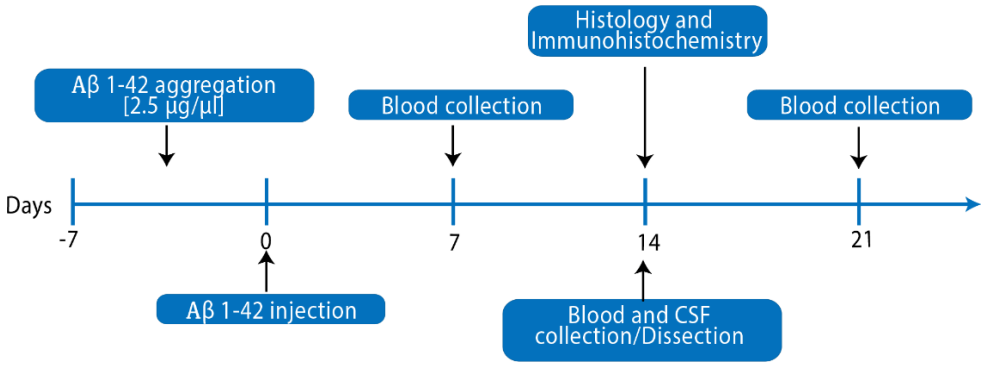

Figure 6. Schematic representation of the second experimental design of the intrahippocampal injection of FAβ made with Aβ 1-42 at 2.5 µg/µL. Rats were injected 3 µL with FAβ or vehicle solution (PBS). Samples collection was performed at 7, 14- and 21-days post-injection. n =8 rats in each group.

Data from the qRT-PCR analysis performed on serum samples collected on day 21 indicated that 3 of 4 circulating miRNAs (miR-29a-3p, miR-146a-5p and miR-29c-3p) were significantly reduced in the FAβ-treated group compared to the control group. By contrast, the relative abundance of miR-9 did not change upon infusion of 2.5 times more FAβ peptides (Figure. 7 *versus* Figure 5).

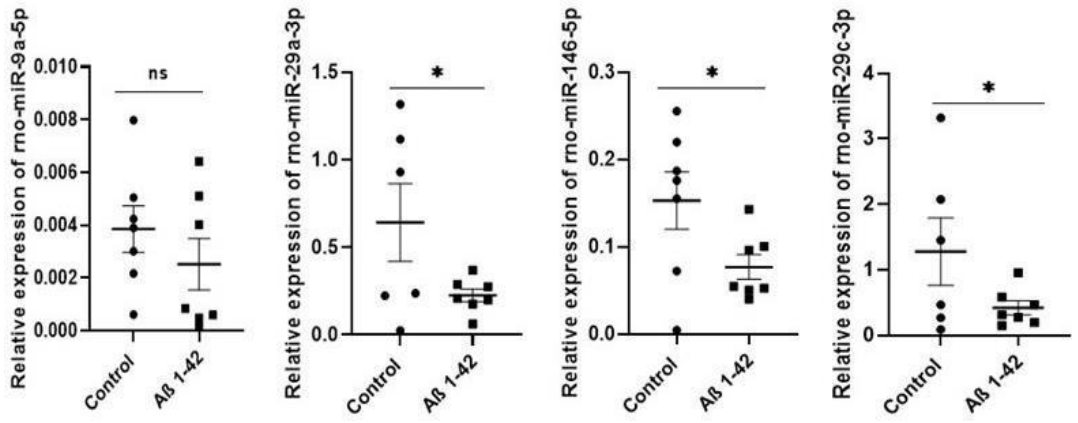

Figure 7. Relative expression of circulating miR-9a-5p, miR-29a-3p, miR-146a-5p, miR-29c-3p in serum of rat infused with FAβ made with Aβ at 2.5 µg/µL. Serum samples were collected 21 days post-infusion. MicroRNAs were extracted and quantified by qRT-PCR. Data are represented as mean ± SEM of 7-8 samples evaluated in triplicate. Statistical comparisons between Aβ 1-42 and PBS groups were performed using the Mann-Whitney test * $p \leq 0.05$, ** $p \leq 0.01$, *** $p \leq 0.001$.

I.5. Kinetics of miRNAs detection in the rat model of AD

To the best of our knowledge, there are very few studies reporting the kinetics of circulating miRNAs in sera from animal models with AD. For this purpose, we collected rat serum samples at various time points after inoculation of FAβ prepared with Aβ 1-42 at 2.5 µg / µL. Figure 8 shows the kinetics of miRNAs detected in serum samples. Concerning to miR-9-5p in Aβ-treated group, its profile tends to be lower as a function of time compared to the control group, but again without significant differences (Figure 8A). In contrast, the miR-29a-3p and miR-29c-3p profiles were statistically reduced at all evaluation times compared to the control group and the difference is higher on day 7 ($p = 0.016$ and $p < 0.01$ for miR-29a-3p and miR-

29c-3p, respectively. Figure 8B and 8C).

The amount of miR-146a was significantly reduced on both day 14 and day 21 in serum samples from Aβ-infused rats ($p = 0.022$ and $p = 0.027$, respectively, Figure 8D) compared to the control group. Of note, for all kinetics drawn up for this analysis, it becomes apparent that, a at late time

e.g on day 21, the expression of all investigated miRNAs tended to return to the baseline expression level detected on day 0. This indicates, as observed in Morris water maze test, that effect of Aβ infused in hippocampus of rats seems reversible.

The amount of miR-146a was significantly reduced on both day 14 and day 21 in serum samples from Aβ-infused rats ($p = 0.022$ and $p = 0.027$, respectively, Figure 8D) compared to the control group. Of note, for all kinetics drawn up for this analysis, it becomes apparent that, an at late time e.g on day 21, the expression of all investigated miRNAs tended to return to the baseline expression level detected on day 0. This indicates, as observed in Morris water maze test, that effect of Aβ infused in hippocampus of rats seems reversible.

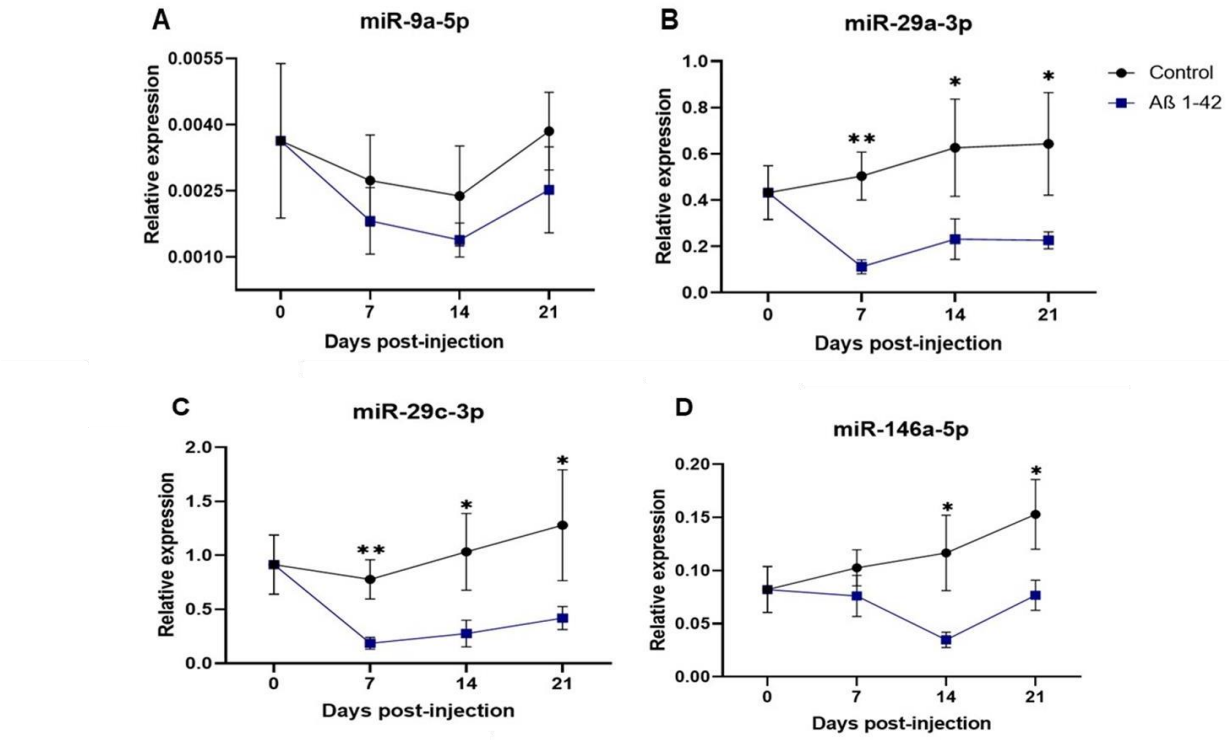

Figure 8. Kinetics of circulating microRNAs detected in serum. The quantification of microRNAs in serum was investigated at 0-, 7-, 14- and 21-days post-infusion with FAβ or PBS **(A-D)**. Relative expression profiles for **(A)** miR-9a-5p, **(B)** miR-29a-3p, **(C)** miR-146a-5p, **(D)** miR-29c-3p are shown. The amount of each microRNAs was evaluated by quantitative real time qRT-PCR and normalized with exogenous cel-miRNAs. Data are expressed as mean ± SEM of result obtained from each serum assessed in triplicate (for each time, n = 8 rats per group). Statistical comparisons between groups at each time were made using the Mann-Whitney test. * $p \leq 0.05$, ** $p \leq 0.01$, *** $p \leq 0.001$.

I.6. Aβ 1-42 infusion leads to an inflammatory response in the hippocampus of rats

Next, we evaluated whether the altered expression of circulating miRNAs found in serum samples could be corroborated with altered morphology of brain tissues and a modification in the activated status of astrocytes and microglia. The evaluation was done in FAβ-treated and control groups at 14 days post-infusion. We first looked at the appearance and the structure of the two hemispheres of hippocampus by Cresyl violet staining. As shown in Figure 9, no structural and/or cellular damage was detected in the CA1/CA2/ CA3 and DG regions of hippocampus in both groups of rats. However, in both groups, the impact of the intrahippocampal injection procedure led to some local damages in the CA1 region of the rat's hippocampus and along the whole trajectory of the Hamilton needle to reach the target region.

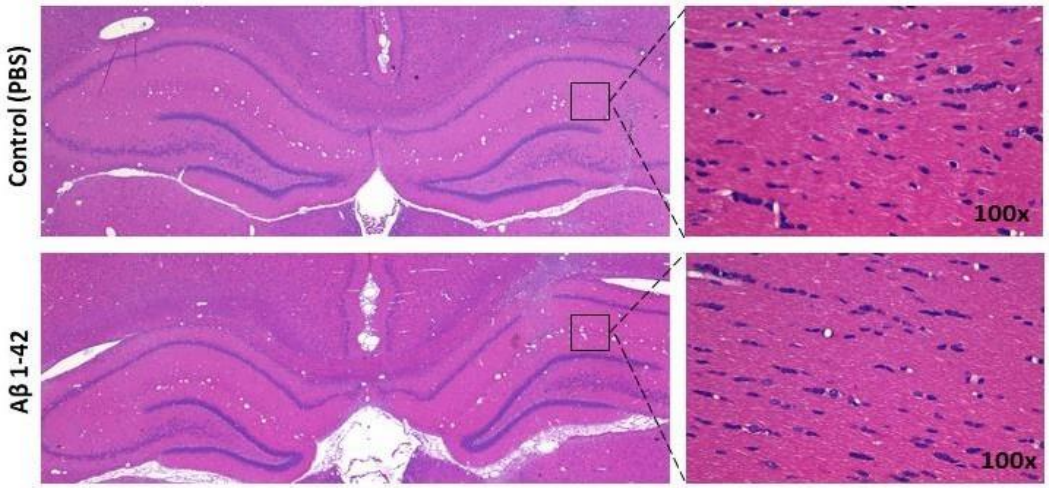

Figure 9. Histological staining of rat's brains infused with FAβ made with 2.5 µg/µL of Aβ 1-42. Cresyl violet staining was performed to assess neuronal viability on hippocampal sections from rats injected with FAβ or PBS 14 days post-surgery. Right panel: representative sections at 100x magnification of the entire hippocampus from rats injected with FAβ or PBS are shown.

We then presumed that discrete events, difficult to be observed by histological staining analysis, might be detected in these tissues by an immunohistochemical procedure using specific markers. Astrogliosis is a universally recognized feature of AD characterized by cellular hypertrophy and increased GFAP expression (Bagyinszky, Youn, An, & Kim, 2014). Therefore, we performed GFAP fluorescence labelling of brain tissues of rats extracted at 14 days post-infusion. Representative immunofluorescence images are shown in Figure 10A. Compared to brain sections from control group, a more pronounced fluorescence staining was detected in the whole hippocampus tissues with a pronounced staining in the CA1/CA2/ CA3 and DG regions in brain sections from FAβ- treated rats. The quantification of GFAP+ cells, indicated that 2-fold more GFAP positive cells were found in the whole hippocampus tissues of Aβ rats compared to control rats, precisely 2.1-fold more in CA1/CA2 and CA3 and 1.7-fold more in DG regions.

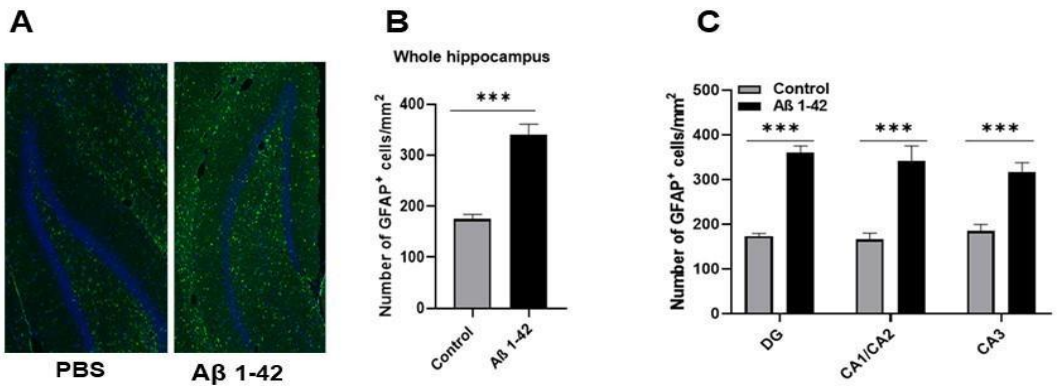

Figure 10. Quantification of astrocytes and microglial cells in the hippocampal areas. Brain sections from rats injected with FAβ 1-42 or PBS were analyzed 14 days post injection. **(A)** Representative immunohistochemical staining (DAPI in blue and GFAP in green) in the DG area (40x magnification). **(B)** Histograms showing the number of GFAP + cells per mm2 quantified in the total hippocampus and **(C)** in each area of the hippocampus (CA1 / CA2, CA3 and DG). The quantification of GFAP + and IBA1 + cells was analyzed in 4-5 sections per animal (n = 5 for each group). In rats injected with FAβ 1-42, the number of GFAP+ cells and microglial cells increased in all areas of the hippocampus. Statistical comparisons between both groups were analyzed using Student's t-test. * $P \leq 0.05$, ** $P \leq 0.01$, *** $P \leq 0.001$.

I.7. Analysis of circulating miRNA expression in the APP/PS1delE9 transgenic model of AD

Next, we sought to evaluate whether the alteration profile of circulating microARNs detected in the rat animal model generated by hippocampal infusion of FAβ could also be observed in the APP/PS1delE9 transgenic mice expressing two constitutive mutant forms of APP and PSEN1. APP/PS1delE9 mice model is one of the most commonly used transgenic animal model of AD. These transgenic mice develop Aβ deposits at 6-months of age, with abundant plaques in the hippocampus and cortex at 9 months (Jankowsky et al., 2004). Plaques continue to increase up to around 12 months of age (Garcia-Alloza et al., 2006). We evaluated the expression pattern of the 9 miRNAs mentioned above from serum samples prepared from blood collected from APP/PS1delE9 transgenic mice of 4- and 15-months of age.

The results obtained indicated that the amount of miRNAs detected in the serum samples of APP / PS1delE9 mice of 4 months of age, were not significantly different from those found in control group (littermate mice). By contrast, in serum samples from 15-months old mice, 4 over 9 miRNAs were found significantly downregulated in the APP/PS1delE9 mice (Figure 11). Interestingly, 2 of these 4 deregulated miRNAs (miR-29a-3p and miR-29c-3p) were also down-regulated in rats injected with FAβ in the hippocampus.

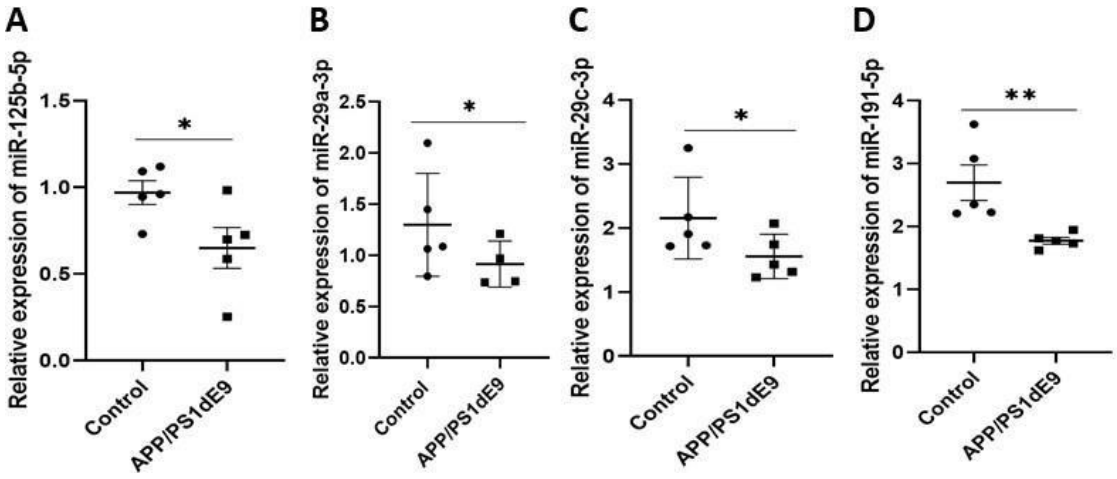

Figure 11. Relative expression of circulating miR-125b-5p, miR-29a, miR-29c and miR-191-5p in the serum of APP/PS1delE9 transgenic animal model of AD. Serum samples from transgenic animals were extracted at 15 months of age and selected miRNAs were quantified by qRT-PCR. **(A)** miR-125b-5p, **(B)** miR-29a-3p, **(C)** miR-29c-3p, **(D)** miR-191-5p. Data are represented as mean ± SEM of 5 samples performed in triplicate. Statistical comparisons between the transgenic and control group were performed using the Mann-Whitney test. * $p \leq 0.05$, ** $p \leq 0.01$, *** $p \leq 0.001$

I.8. Intrahippocampal injection of FAβ 1-42 leads to an increased expression of miR-146a in CSF

We were intrigued by the fact that the kinetic of miR-146a-5p expression was not significantly altered in serum sample of Aβ-injected rats at an early time point such as on day 7 post- injection and the down regulation peak detected on day 14 in contrast to other miRNAs (Figure 8). Therefore, we decided to focus our following experiments on the investigation of biological role of miR-146a-5p in our rat animal model. First because this miRNA was not found to be deregulated in APP/PS1 transgenic mice and second because

this miRNA is reported to be a key regulator of innate immune (Mattsson et al., 2012) and inflammatory responses in astrocytes (Angelucci et al., 2019, Y. Y. Li, Cui, Dua, et al., 2011; Lukiw et al., 2008, (Bartel, 2004; Johanson et al., 2014) and microglia. Regarding the negative impact of inflammation in AD development, better knowledge of mechanism of action of an inflammamiR as miR-146a-5p is of interest for potential therapeutic translation.

First, we evaluated the expression pattern of miR-146a-5p in CSF samples collected 14 days after Aβ infusion into rat brains. Our results indicated that, in contrast to serum samples in which its expression was found to be significantly down-regulated (Figure 5; p = 0.022), the amount of miR-146a-5p in the CSF samples from FAβ-treated group was significantly up-regulated (p= 0.004) compared to those obtained from the control group (Figure 12).

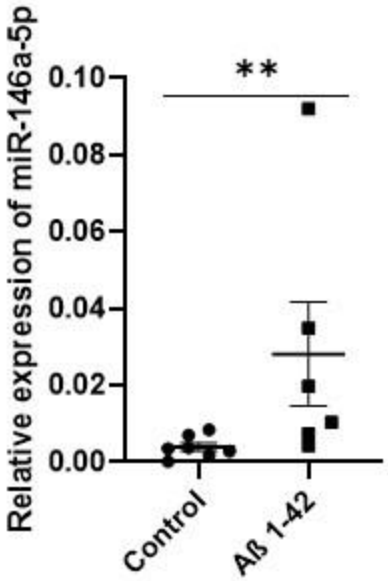

Figure 12. Relative expression of circulating miR-146a-5p in CSF of rats infused with FAβ 1-42. CSF samples from rats infused with FAβ or PBS solutions were collected at 14

days post-injection. miR-146-5p amounts was quantified by qRT-PCR. Data are represented as mean ± SEM of n = 7 samples performed in triplicate. Statistical comparisons between Aβ-infused and control group were performed using the Mann-Whitney test * $P \leq 0.05$, ** $p \leq 0.01$, *** $P \leq 0.00.1$.

Altogether, our data indicate that there is a discrepancy between the presence of miR-146a in serum versus CSF samples.

II. Mechanistic study of miR-146a-5p in primary astrocytes model of AD

II.1. The upregulation of miR-146a is dependent on the state of aggregation and the concentration of Aβ 1-42 in astrocyte cell culture.

Next, we evaluated the biological effects of Aβ 1-42 in primary astrocytes cell culture to recapitulate, at least partially, an AD-like environment. Astrocytes are considered to promote the first line of neuroinflammation response by regulating the expression of key mediators of innate and adaptive immune responses in the CNS (Johanson et al., 2014). We performed primary astrocytes cell cultures (Figure 13A) to evaluate the impact generated with the treatment of Aβ 1-42 peptides There are controversial results in the literature concerning the impact of Aβ 1-42 peptide aggregation states on the induction of neuroinflammation in AD. Therefore, we compared biological effects of 2 well known aggregation state of Aβ 1-42 peptides: oligomeric (OAβ) and fibrillary (FAβ) forms. The oligomeric form of Aβ 1-42 peptides was generated by incubating peptides for a short period of time, e.g., 24 hours, at 4°C, whereas the fibrillar form of the Aβ 1-42 peptides was generated by incubating peptides for a longer incubation period, e.g., 4 days, at 37 ° C.

First, we evaluated the relative toxicity index of OAβ and FAβ made with several concentrations of Aβ 1-42 peptides on the viability of primary astrocytes cultured for 3 days. As shown in Figure 13B and 13C, none of concentrations evaluated in this study were toxic to cells.

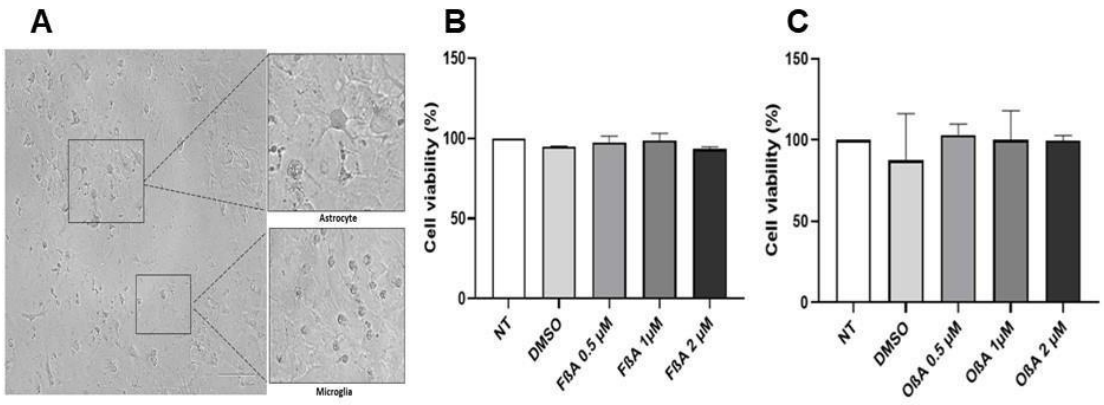

Figure 13. **Incubation of primary astrocytes cell culture with OAβ or FAβ made at the indicated concentration of Aβ does not lead to any cell toxicity**. **(A)** Representative bright-field image of primary astrocytes culture (40x magnification). Primary Astrocyte cell culture were obtained from neocortex of new-born animals. **(B)** Alamar Blue cell viability assay of primary Astrocyte cell culture treated with FAβ or (C) OAβ at 0.5, 1 and 2 µM. The fluorescence value from the untreated cells (NT) was set up as the arbitral value of 100%.

Next, we monitored the expression of miR-146a-5p in these cells after treatment with OAβ or FAβ. The qPCR results revealed that treatment of cells with OAβ for 3 days increased the expression of miR-146a at all concentrations evaluated (Fig. 14A). Maximum induction of miR-146a expression was detected when 1 µM OAβ was used. The treatment of cells with FAβ for 3 days also resulted in upregulation of miR-146a-5p with a maximum induction obtained with 2 µM of FAβ (Figure 14B). Then, we sought to increase the incubation time of FAβ to see if this could further enhance the expression of miR-146a. Astrocytes were treated 2 times with 1µM of FAβ for 3.5 days (7 days in total) before monitoring miR-146a expression. As shown in Figure 14C, miR-146a-5p expression was found to be significantly upregulated after this incubation time compared to that obtained in control cells (7 days). However, the induction level was not statistically different from the fold change value detected in cells treated once for 3 days only (Figure 14C *versus* B).

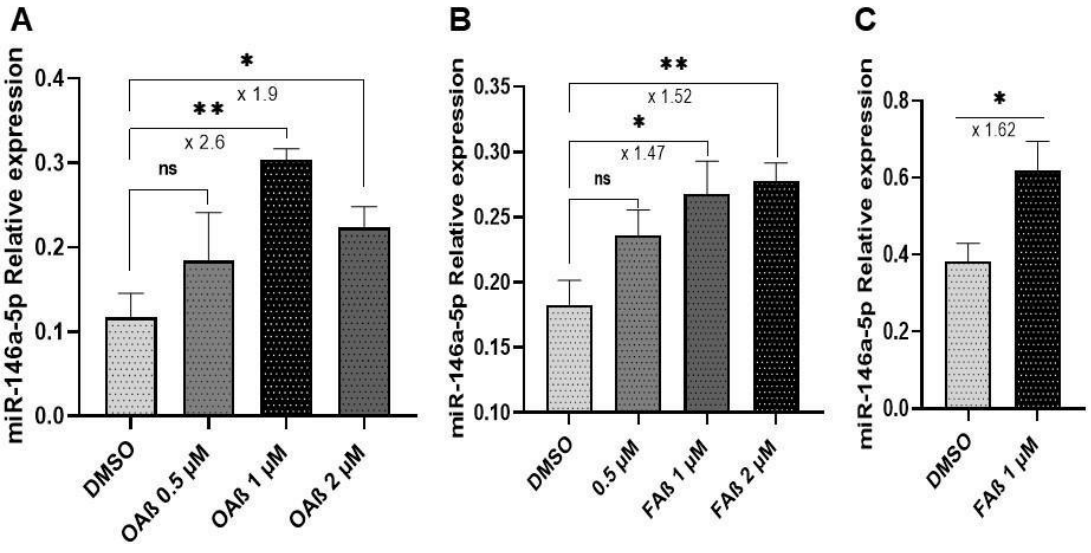

Figure 14. miR-146a-5p is up-regulated in OAβ and FAβ-treated primary astrocytes. Cells were treated with the OAβ or FAβ made at 0.5, 1 and 2 µM for 3 days. **(A)** Relative expression of miR-146a-5p in primary astrocytes treated with OAβ or **(B)**

FAβ during 3 days at different concentrations. **(C)** Relative expression of miRNA 146a-5p in primary astrocyte culture treated with FAβ for 7 days at 1 µM. The expression of miR-146a-5p was evaluated by quantitative real-time qRT-PCR. Small nuclear RNA U6 (RNU6) expression was used for normalization. Data are represented as the mean ± SEM performed in triplicate. Statistical comparisons between OAβ or FAβ treated cells or DMSO treated cells were made with the student's t-test. * $p \leq 0.05$, ** $p \leq 0.01$, *** $p \leq 0.001$.

II.2. OAβ induces miR-146a expression through the NF-κB cell signaling pathway

The expression of miRNA-146a has been reported to be upregulated in several CNS cells in response to TNF-α, IL-1β or LPS through activation of NF-κB cell signaling pathway. Therefore, we evaluated whether OAβ and FAβ treatments might be sufficient to induce the expression of miRNA-146a in primary astrocytes using the same cell signaling pathway. Cells were treated with OAβ or FAβ in presence or absence of the well-known pharmacological inhibitor BMS-345541 of NF-κB pathway for 3 days. As positive control, cells were treated with LPS (Johanson et al., 2014).

Results in the Figure 15 demonstrated, that treatment of primary astrocytes with 1 µM OAβ induced the expression of miR-146a-5p by 3.33-fold compared to control cells. This expression can be inhibited by pre-treatment with 1 µM of BMS-345541 inhibitor before incubation with OAβ. The expression level of miR-146a dropped-down significantly and reached the basal expression level detected in non-treated cells. As expected, LPS treatment of primary astrocytes significantly increased miRNA-146a expression by 3.50-

fold, which could also be significantly reversed by treatment with the BMS-345541 inhibitor.

The same results were generated with FAβ (data not shown). Taken together, these results indicate that both OAβ and FAβ could increase the basal expression level of miR-146 through transcriptional regulation of the NF-κB pathway, as well as pro-inflammatory cytokines (YY Li, Cui, Dua, et al..,2011; Lukiw et al., 2008) or LPS, but to a lesser extent.

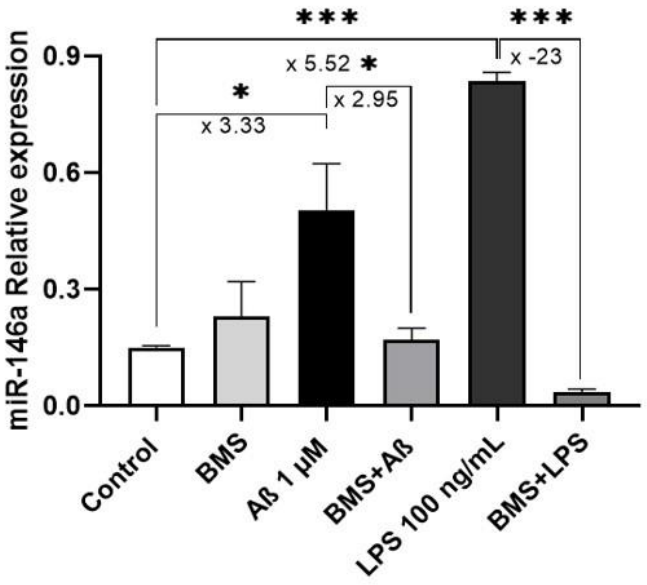

Figure 15. miRNA-146a expression is dependent on the NF-κB pathway. The effects of NF-κB inhibition on miR-146a expression were evaluated in OAβ-treated primary astrocytes culture. Primary astrocytes were stimulated with OAβ at 1µM and LPS at 100 ng/mL from Escherichia coli (Positive Control) with or without pre-incubation with IκB kinase inhibitors (BMS-345541) for 3 days. Data are represented as the mean ± SEM performed in triplicate. Statistical comparisons between OAβ treated cells or DMSO treated cells were made with the student's t-test. * $p \leq 0.05$, ** $p \leq 0.01$, ***$p \leq 0.001$.

II.3.OAβ or FAβ treatment did not induce any inflammatory cytokines expression

Based on the above results, we checked whether the expression level of pro-inflammatory cytokines produced in primary astrocyte cells could also be induced in response to OAβ and FAβ treatments. Surprisingly, as shown in Figure 16, none of the cytokines evaluated as IL-6, TNF-α and IL-1β were transcriptionally induced by FAβ or OAβ treatment for 3 days (Figure 16). Same results were obtained when the expression level of these cytokines was evaluated at the protein level by sandwich ELISA (Data not shown). Long term treatment of astrocyte cells with FAβ for 7 days did not change these outcomes (data not shown). A significant and high induction level of those cytokines (IL-6, TNF-α, and IL-1β) were detected in cells upon treatment with LPS for 3 days, as expected (Fig. 16D, 16E, 16F).

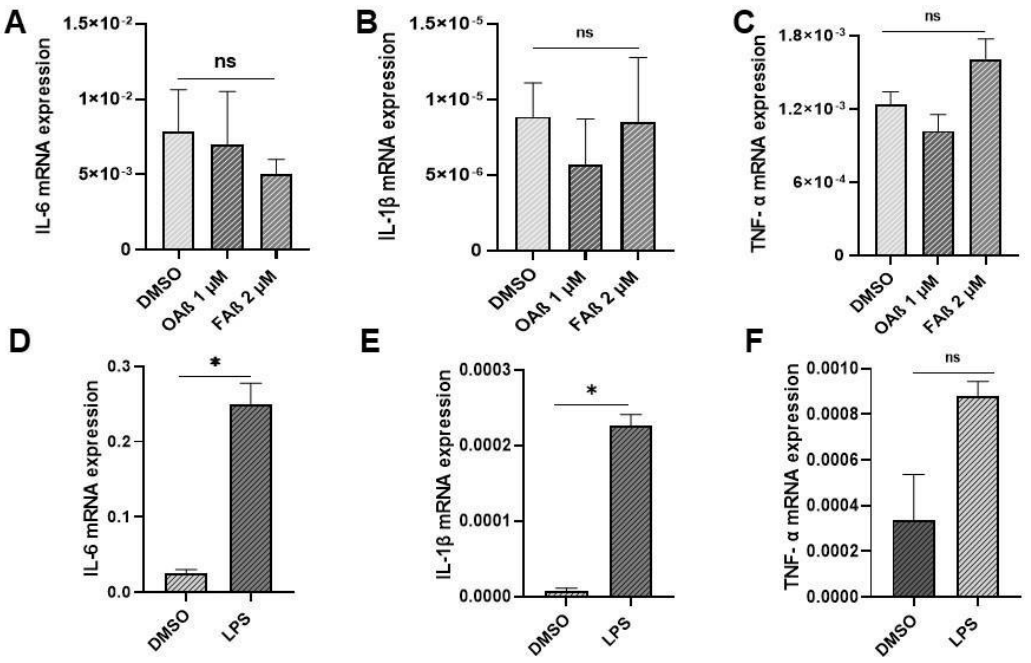

Figure 16. Expression of mRNA of inflammatory markers in cell culture of primary astrocytes stimulated with OAβ or FAβ. Three days post-stimulation with OAβ and FAβ, the expression of inflammatory cytokines was evaluated by RT-qPCR. mRNA expression of pro- inflammatory markers (A) IL-6 (B) IL-1β (C) TNF-α. GAPDH expression was used for normalization. Astrocytes were also stimulated with LPS at 100 ng/ mL (positive control). Data are represented as mean ± SEM of experiments made in triplicate. Statistical comparisons between groups were made using the student's t-test. * $P \leq 0.05$, ** $P \leq 0.01$, *** $P \leq 0.001$.

II.4.miRNA-146a induction more likely counteracts NF-κB signaling pathway in astrocyte cells through down-regulation of IRAK-1 and upregulation of IRAK-2 as a compensatory mechanism.

It was intriguing to find out that miR-146a expression was induced in OAβ- and FAβ-treated cells through the activation of the NF-κB pathway but without inducing cytokines production. To assess the specificity of this result and to go further, we evaluated the expression of IRAK-1 and TRAF- 6, two transcriptional targets of miR-146a. These proteins are part of the NF-κB pathway (Figure 17A) (Edsbagge et al., 2017). We selected OAβ treatment to conduct this investigation. As shown in Figure 17B, the relative expression of IRAK-1 was significantly down regulated (1.5- fold) in OAβ-treated cells compared to control cells, and IRAK-2 was increased in OAβ-treated cells. Surprisingly, the relative expression of TRAF-6, a direct downstream effector of the IRAK- 1/2 complex, was found unchanged in OAβ-treated cells compared to control cells (Figure 17C).

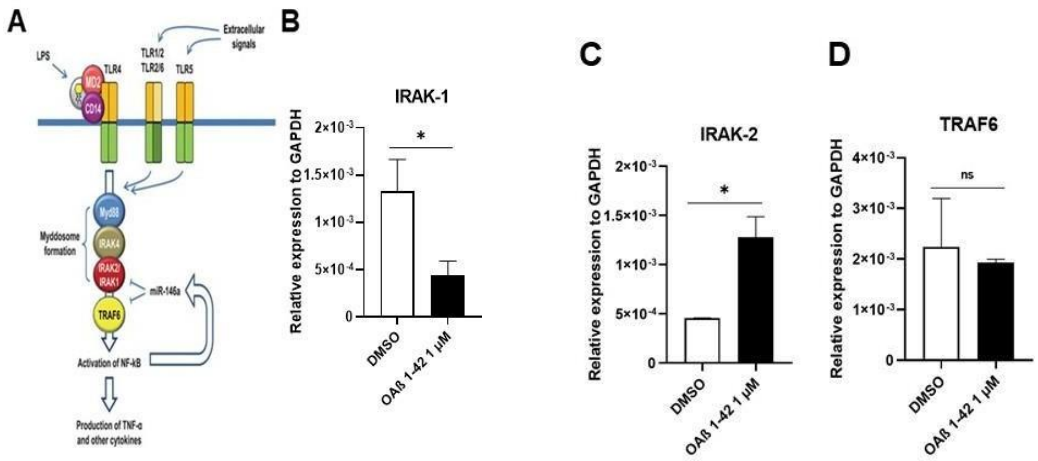

Figure 17. The expression of miR-146a counteracts the activation of the NF-κB cellular pathway through the regulation of its IRAK-1, IRAK-2 and TRAF-6 targets. **(A)** Schematic representation of NF-κB signaling pathway **(B)** The relative levels of IRAK-1 mRNA **(C)** IRAK-2 **(D)** TRAF-6 in primary astrocytes incubated with OAβ at 1 µM or cells treated with DMSO for 3 days were detected by qRT-PCR. GAPDH expression was used for normalization. Data are represented as the mean ± SEM of experiments performed in triplicate. Statistical comparisons were made between OAβ-treated cells and DMSO-treated cells with Student's t-test. * $p \leq 0.05$, ** $p \leq 0.01$, *** $p \leq 0.001$.

The downregulation of IRAK-1 was found to be not significant and unaltered expression of TRAF- 6 was also detected in FAβ-treated cells (Figure 18). Furthermore, no up-regulation of IRAK-2 was detected compared to OAβ-treatment. This different results between OAβ- to FAβ-treated cells on IRAK-2 regulation might be a direct consequence of the lower expression level of miR-146a-5p in FAβ-treated cells as compared to OAβ-treated cells. Indeed, the level of induction of miR-146a in FAβ-treated cells was only 1.52-fold versus 2.6-fold for OAβ-treated cells. Furthermore, it is worth noting that the level of

IRAK-1 downregulation is also more pronounced in OAβ-treated cells than in FAβ-treated cells. Beyond this consideration, the level of TRAF-6 expression does not change in FAβ- or OAβ-treated cells compared to control cells. This could be corroborated with the absence of production of cytokines detected in primary astrocyte cells upon treatment with FAβ or OAβ.

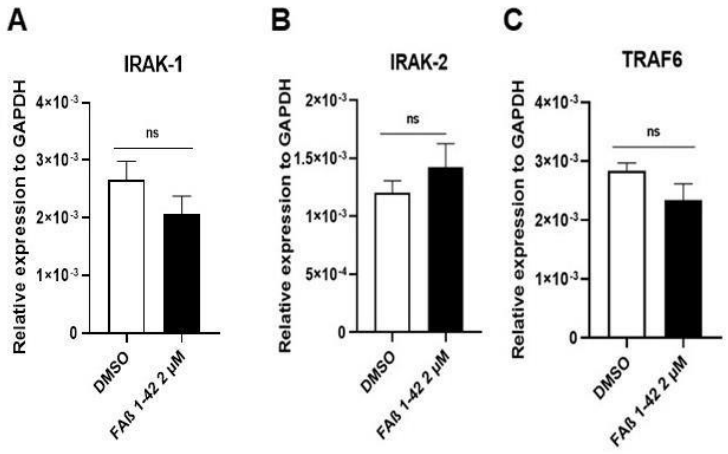

Figure 18. IRAK-1, IRAK-2 and TRAF-6 expression in FAβ-treated astrocytes. (A) The relative levels of IRAK-1 **(B)** IRAK-2 **(C)** TRAF-6 mRNA in cultures of primary astrocytes incubated with FAβ at 2 µM or cells treated with DMSO for 3 days were quantified by qRT-PCR. GAPDH expression was used for normalization. Data are represented as the mean ± SEM of experiments performed in triplicate. Statistical comparisons were made between FAβ-treated cells and DMSO-treated cells with Student's t-test. * $P \leq 0.05$, ** $P \leq 0.01$, *** $P \leq 0.001$.

Based on these last results, it is tempting to speculate that upregulation of miR-146a by the NF-κB transcription factor activated in response to OAβ or FAβ might play a negative feedback loop of control of NF-κB signaling pathway by down-regulation of IRAK-1 and up-regulation of IRAK-2. As a consequence of this retro-control loop of NF-κB pathway,

an abrogation of the expression of pro-inflammatory cytokines as IL-6, TNF-α, and IL-1β occurred by keeping constant the expression level of TRAF-6. This, is in line with reports showing that miRNA expression can act as a negative feed-back regulator of the same signaling pathway used for its own induction, thereby preventing an overstimulation of the inflammatory response (Mattsson et al., 2012).

II.5.OAβ and FAβ treatments stimulate the chemokines production

Since the treatment of cells with either OAβ or FAβ was sufficient to induce transcriptional changes in IRAK-1 and 2, this prompted us to postulate if other mechanistic events or signaling pathways different than NF-κB signaling might be activated by those treatments. We focused on expression level of chemokine as CXCL1 as potential candidate. Chemokines are considered to play active role in pro-inflammatory response by recruiting immune cells of sites of injury. In AD, it is well established that astrocyte and microglia can be activated by Aβ to produce chemokines as MCP-1, MIP-1α, CCL4, IL-8 and CXCL-1 (M. Wang, Qin, & Tang, 2019). We evaluated the production of CXCL-1 by primary astrocytes following treatment with either OAβ or FAβ for 3 days at several concentrations. ELISA assay data shown in Figure 20, revealed a slight, but significant, dose- response of CXCL-1 production by astrocytes in response to increased concentration of OAβ. The maximum level of CXCL-1 production was detected in cells treated with 1 μM of OAβ that correlated well and again with the maximum induction of miR-146a expression detected at the same concentration. In contrast in FAβ-treated cells, no significant production, different to control cells treated with DMSO, was detected. This later result indicated again that the overall effect of FAβ on the astrocyte cells is weaker than OAβ.

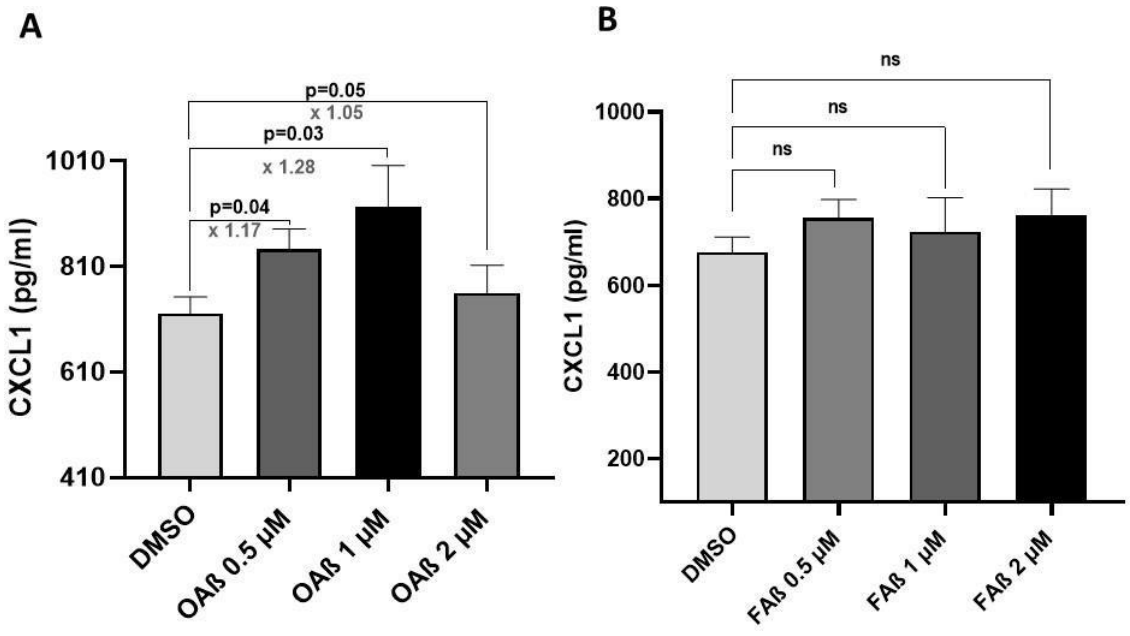

Figure 19. CXCL-1 secretion by OAβ-treated primary astrocytes. CXCL-1 expression was evaluated by ELISA assays on supernatants from primary astrocytes stimulated with **(A)** OAβ at 0.5, 1 and 2 µM or **(B)** FAβ at 0.5, 1 and 2 µM for 3 days. Data are represented as the mean ± SEM of experiments made in triplicate. Statistical comparisons were made between OAβ-treated cells and DMSO-treated cells with Student's t-test. * $p \leq 0.05$, ** $p \leq 0.01$, *** $p \leq 0.001$.

Chapter 4

Discussion and Conclusions

1. Discussion

1.1. General aspects of Alzheimer's disease

AD is the most common form of primary degenerative dementia, whose pathophysiology is multifactorial due to the interaction between the APP, TAU, PSEN1, PSEN2, APOE proteins, among others. This brain pathology is characterized mainly by the formation of amyloid plaques and neurofibrillary tangles. The majority of AD cases correspond to 60-80% of all dementia cases, and have been established as LOAD, which represents 95% of AD cases (Lecanu & Papadopoulos, 2013). This form of AD occurs between 60 and 65 years of age, and is driven by a complex interaction between genetic and environmental factors and ~ 70% of risk is believed to be attributed genetic factors, with the APOE gene being the most important genetic risk factor (Bagyinszky et al., 2014; Lane-Donovan & Herz, 2017). The complex interaction between genetic and environmental factors has hampered the identification of early biomarkers for LOAD cases (Mattsson et al., 2012). Currently, there is no therapeutic agent capable of curing or preventing AD (Angelucci et al., 2019) and at the same time the need to predict developing symptomatic AD (MCI or dementia) is increasing in asymptomatic individuals (Shaffer et al., 2013). Therefore, the search for biomarkers for diagnosis is essential and is currently an active field of research. MiRNAs are a subclass of small non-coding RNAs that play an important role in the regulation of post- transcriptional gene expression, binding to complementary sequences of target messenger RNA (mRNA) (Friedman et al., 2009), and thus repress the translation (Bartel, 2004). miRNAs are present in most body tissues, including brain tissue, CSF, or serum (Friedman et al., 2009). Under pathological conditions, a dysregulation of miRNAs is

generated. The miRNAs that are present in biofluids are called circulating miRNAs (Gilad et al., 2008), and could reflect the composition of the fluid in the extracellular space of the brain and serve as biomarkers of disease (Edsbagge et al., 2017). The miRNAs are stable enough in biological fluids, including serum, plasma and CSF. Furthermore, many of them directly target genes involved in the pathophysiology of AD (Keifer, Zheng, & Ambigapathy, 2015; M. Wang et al., 2019). The detection of miRNAs in biofluids is a relatively simple procedure (Kalogianni, Kalligosfyri, Kyriakou, & Christopoulos, 2018) and is considered a type of non-invasive diagnosis, it has been described that its detection is highly sensitive, for example when they are amplified by PCR (S. Kumar & Reddy, 2016). On the other hand, the current diagnosis of AD uses cumbersome and expensive methods such as structural magnetic resonance imaging (MRI) and molecular neuroimaging with positron emission tomography (PET) (Angelucci et al., 2019). The main objective of our research was to evaluate the microRNAs in serum (circulating microRNAs), using an animal model of AD, which consists of the injection of the Aβ 1-42 peptide. The search for microRNAs in serum corresponds to non- invasive procedures that could be extrapolated in humans. This model, unlike transgenic models, is favorable for studying the direct effect on the expression of microRNAs in a single- component; Aβ 1-42, in this pathology.

1.2. Challenge for the detection of early diagnosis markers/ Importance of detecting early markers of AD

Since AD comprises an asymptomatic stage, the search for early biomarkers is crucial. Clinico- pathological studies support the notion that this pathology begins 10-20 years before a significant neuronal death and the subsequent appearance of any cognitive and behavioral symptoms (Bateman et al., 2012). Several animal models have been created for AD research, with transgenic animal models being the most popular. However, there are several

drawbacks that have been observed. Indeed, an animal model of AD must imitate all the cognitive, behavioral and neuropathological characteristics of the pathology, i.e., it must recapitulate the phenotype of the disease with high fidelity. The models that are currently used are called partial models, because they mimic only some components of AD. However, transgenic animal models of AD have been created based on the genetic origins of familial AD or EOAD and have contributed significantly to the understanding of the molecular mechanisms involved in the pathology, but the use of these models does not represent the majority of AD cases (LOAD) (Lecanu & Papadopoulos, 2013). On the other hand, the different genetic background of these models constitutes a real issue (Kaushal, Wani, Anand, & Gill, 2013). Due to these drawbacks, relevant non-transgenic animal models have been developed to study the LOAD or AD sporadic form (Lecanu & Papadopoulos, 2013). They have one or more distinctive characteristics such as senile plaques similar to AD, NFTs, oxidative stress and cognitive impairment (Kaushal et al., 2013). Amongst them, one model consists of injecting Aβ peptide into the brain of rodents. Previous studies have shown that Aβ causes learning and memory deficits in treated animals, the formation of amyloid plaque, and the disruption of long-term potentiation and behavior (Faucher et al., 2015; Karthick et al., 2019; Kaushal et al., 2013). Furthermore, Aβ is the first component to appear in the long preclinical stage of AD, and the aggregated form is believed to gradually lead to the development of AD pathology (Sadigh-Eteghad et al., 2015). These characteristics make it an interesting model for the search for early markers such as microRNAs.

1.3. Rationale of using Aβ 1-42 intrahippocampal injected rat model

Various investigations have shown that the Aβ peptide plays a central role in the appearance and AD progression (Findeis, 2007). Aβ peptide is also produced in normal individuals, or in young brains but thanks to the balance between its production and its elimination, a constant level or a steady state is maintained (Shankar & Walsh, 2009). By contrast, in aging and pathological conditions such as AD, there is an imbalance between production and elimination (Harkany et al., 2000) leading to the accumulation of Aβ in the brain and the formation of senile plaques upon the formation of aggregates (Qiu, Kivipelto, & von Strauss, 2009; Sadigh-Eteghad et al., 2015).

In the present study, we injected the Aβ 1-42 peptide into the CA1 region of the hippocampus instead of injecting it in other brain regions such as the ventricles (Faucher et al., 2015) or the neocortex (Bolmont et al., 2007). We chose the hippocampus because it plays an important role in memory formation (Faucher et al., 2015; Karthick et al., 2019) and we performed the injection in the CA1 subregion, since it is one of the first hippocampal areas affected in AD (Masurkar, 2018). The choice of the form of Aβ 1- 42 peptide was a real issue in our study. Being prone to aggregation, Aβ 1-42 peptide can be found as oligomer or fibrillar forms. Although Aβ aggregation states are known to play an important role in this pathology, it is not clear which is the most important in this process. Nevertheless, many reports have shown that Aβ oligomers trigger synapse dysfunction in AD (Bao et al., 2012; Esparza et al., 2013; Ono, 2018). Furthermore, small and stable oligomers of Aβ 1-42 have been isolated from the brain, the plasma and CSF of AD patients and they have been correlated with the severity of neurodegeneration in AD (Dahlgren et al., 2002). Nevertheless, there are studies that indicate that Aβ fibrillation or formation of mature fibrils

(FAβ) is the main agent of neuronal dysfunction in AD and can cause neuronal damage by acting directly on synapses and indirectly activating astrocytes and microglia (Hardy & Selkoe, 2002). Bilateral intrahippocampal injections of fibrillar form of Aβ did result in a reduction in neuronal density, an increase in the intensity of the glial fibrillar acid protein and caused deficiencies in behavioral performance (Chacón, Barría, Soto, & Inestrosa, 2004; Y. He et al., 2012). Borbely et al., demonstrated that intrahippocampal administration of synthetic FAβ simultaneously decreases both the spatial learning capacity in MWM and the density of the dendritic column in the CA1 region of the rat hippocampus (Borbély et al., 2014). There is still debate as the reports published so far showed evidence that both Aβ oligomers and fibrils can play the major role in inducing synaptic loss and causing AD-associated dementia (Dahlgren et al., 2002; Haass & Steiner, 2001; Klein, Krafft, & Finch, 2001).

Looking carefully at the literature on the preparation of these forms, we have found heterogeneous and even contradictory reports regarding the solubilization protocols and the preparation of Aβ aggregation. Some authors only mentioned that the state of aggregation is carried out by incubating the Aβ peptide for 7 days at 37°C without specifying whether the oligomeric or fibrillar forms were obtained with this preparation (J. Li et al., 2010). Other authors have described the oligomerization of Aβ by incubation at 37°C for 3 days (Karthick et al., 2019). However, we noticed that the majority of publications use oligomerization protocols based on the protocol published by Dahlgren et al., 2002. They have indicated that the oligomerization state is carried out by incubating Aβ at 4°C for 1 day, and the fibrils are performed at 37°C. Note that the incubation times varied from 1 day to 7 days. In our study, we adapted the preparation and aggregation of the Aβ 1-42 peptide based on the different protocols). We injected the fibrillar form of Aβ 1-42, which was obtained by incubation at 37°C for 7 days. We also performed a single injection of Aβ 1-42 and tested different

concentrations of 0.5, 1, and 2.5 µg/µL.

1.4. Impacts on the memory, microRNA expression and mechanistic studies

We used MWM to assess the effect of Aβ injection into the hippocampus in rats on spatial learning and working memory, as it is well known that the memory impairment is a central symptom of AD. When performing MWM, it is crucial to have very powerful tools to analyze the acquisitions without any ambiguity. Our data was analyzed using a plugin called "RatsTrack", compatible with the imageJ software and developed in partnership with researchers from a Colombian university. This plugin was created due to the difficulty of using other commonly used software programs such as Ethovision or MouBeat. Unlike these, this plugin allows to automatically obtain the trajectory of the rat in the Morris test, without user's intervention. Our results showed a deterioration of learning and memory capacity in animals treated with Aβ 1-42. On day 1, the absence of significant differences between the injected and control groups with regard to the distance travelled or the latency escape (Figure 3A and 4A), indicates that all animals are similar for the beginning of the learning and memory tasks. During the subsequent days of evaluation, the results showed that rats treated with 0.5 µg/µL and 1 µg/µL of Aβ presented a memory loss, evidenced by a greater distance and time (escape latency) required to find the platform, unlike the control group (Figure 3A and 4A). MWM was performed 14 days post- surgery based on reports showing that the deterioration is visibly significant at this time. Indeed, Karthick et al., have found an impact on learning memory 15 days post-injection (Karthick et al., 2019). Another study using Aβ oligomers revealed an impaired spatial learning memory on day 12 post-injection (Wong et al., 2016). When verified earlier, for example 8 days post- injection, no significant differences were observed between groups (Nell, Whitehead, & Cechetto, 2015).

The short period may not have been sufficient to affect spatial learning. In addition to the evaluation of cognitive impairment, we also evaluated the inflammatory processes caused by the injection of 2.5 µg/µL of Aβ 1-42. We first perfor a histological staining using the Cresyl violet stain, commonly used for neuronal tissue evaluation as it binds to the acidic components of the neuronal cytoplasm reflecting the number of viable neurons (Kasza et al., 2017). No differences were found in neuronal viability between the treated group and the control group (Figure 9). However, we decided to complete our evaluation by immunofluorescence staining. We investigated Aβ 1-42-induced astrocyte reactivity in the hippocampus by staining for the GFAP marker on day 14 after injection (Verkhratsky et al., 2012). It has been shown that abnormal accumulation and shedding of Aβ can lead to localized inflammation involving reactive astrocytes with increased GFAP expression (Kamphuis et al., 2012). This process called gliosis occurs after brain injury and is characteristic of neurodegenerative disorders such as AD (Verkhratsky et al., 2012). Immunofluorescence staining analysis revealed that animals injected with Aβ1-42 had a higher number of astrocytes in all regions of the hippocampus CA1 / CA2, CA3 and DG, suggesting an activated morphology in contrast to the control group animals with a lower number of astrocytes. Each area contained approximately twice the number of astrocytes, compared to the areas of the control animals (Figure 10A, 10B, 10C). Our data are in line with those of different studies showing an increase in astrocytes in a model of injection of fibrillar Aβ in the hippocampus of AD model rats (Chacón et al., 2004; Y. He et al., 2012; Scuderi et al., 2014).

The amounts of circulating microRNAs in serum samples were assessed in rats injected with 1 µg/µL of Aβ 1-42, which had exhibited cognitive impairment. We evaluated a total of 9 microRNAs frequently expressed in AD patients and / or in transgenic animal models. Amongst them, miR-9a, miR-29a, miR-29c and miR-146a were deregulated in animals

injected with Aβ 1-42. Only miR- 146a was found to be statistically significant, while the other miRs were not statistically different, but had p-values close to statistical significance (Figure 7C). Based on this rationale, we hypothesized that increasing the concentration of Aβ 1-42 would result in a more significant deregulated expression of microRNAs. The concentration of Aβ was increased 2.5 times more, i.e., 2.5 µg / µL. Moreover, previous studies have shown that to achieve adequate memory impairment in animals, these aggregated forms of Aβ must be used in higher doses (Townsend, Shankar, Mehta, Walsh, & Selkoe, 2006). As expected, in rats injected with 2.5 µg/µL of Aβ, a dysregulation of 3 circulating microRNAs (miR-146a, miR-29a, miR29c) was observed on 21 days post injection.

With this second step of evaluation, miR-146a, miR-29a, miR-29c and miR-9 were significantly down regulated. For miR-9, no statistic difference was seen between the experimental group and the control group (Figure 7). Knowing that microRNA acts as a temporary regulator of different biological processes, we evaluated the kinetics of microRNA expression on days 7, 14 and 21 (Figure 8). Our data show that there is a clear down-regulation tendency for all microRNAs in treated rats compared to controls. Concerning miR-9, the expression kinetics of the treated group was different in relation to the control group, but these differences were not statistically significant (Figure 8A). MiR-9 is known to regulate BACE1 expression; lowering miR-9 levels resulted in an increase of BACE1 expression, thereby increasing Aβ 1-42 production. (Souza et al., 2020). The reduced expression of miR-9 in the CNS would promote amyloidogenic processing, leading to a pronounced Aβ aggregation and its deposition in senile plaques (Miya Shaik et al., 2018). Comparative study of miR-9 levels in the serum of AD patients, with mild cognitive impairment and controls subjects has shown that the circulating levels of miR-9 in AD was

the lowest (Souza et al., 2020). Our results suggest that although Aβ 1-42 aggregates were passively introduced into the hippocampus region, their presence was sufficient to alter microRNAs expression resulting in miR-9 down-regulation.

The reduced amount of miR-9 has also been found in plasma from 3xTg-AD and APP / PS1 transgenic mice models (Garza-Manero et al., 2015; Hong et al., 2017). Different studies carried out with human samples have also shown a down-regulation of miR-9 in whole blood, in serum and CSF enriched with exosomes (Geekiyanage, Jicha, Nelson, & Chan, 2012; Kiko et al., 2014; Riancho et al., 2017). Recently, Souza et al. evaluated samples of women carrying the ApoE e4 allele and showed that miR-9 concentration is also altered in whole blood; supporting the hypothesis, that miR-9 may constitute an accessible biomarker for AD (Souza et al., 2020).

The members of the miR-29 family showed similar trend, there is a strong dysregulation in the Aβ-injected group at 7 days compared to control group. At 14 and 21 days, the deregulation was maintained but the curve began to rise very slightly, suggesting a reverse phase (Figure 8C and 8D). The down regulation of miR-29a and miR-29c is consistent with many previous reports that have evaluated serum and / or plasma from AD patients (Geekiyanage & Chan, 2011; Geekiyanage et al., 2012; Kiko et al., 2014; P. Kumar et al., 2013; Wu et al., 2017). Interestingly, miR-29 a/b cluster has been reported to be correlated with BACE1/β- secretase expression (Hébert et al., 2008).Combined with the miR-9 data, it can be suggested that a passive introduction of Aβ aggregates is sufficient to retro-control the level of microRNAs. Overall, our data are in the same line as those recently reported by Calvo-Flores et al., which suggest that that the injection of synthetic Aβ 1-42 peptide could have a transient effect (Calvo-Flores Guzmán et al., 2020).

Regarding the expression of miR-146a, it was down-regulated at all evaluated times.

However, the difference was not significant at 7 days post- injection in contrast to days 14 and 21 (Figure 8B). MicroRNA-146a has been shown to be characteristic of AD, as it participates in the inflammatory response and neuroinflammation (Lukiw et al., 2008).

To our knowledge, our study reports for the first time the expression of circulating microRNAs in an Aβ 1-42 injection model. Nevertheless, our results are consistent with different studies that evaluated the circulating expression profile of miR-146a in transgenic animal models or in humans. Garza-Manero et al., Have reported the same profile for miR-146a in the transgenic model 3xTg- AD from 14 to 15 months compared to young mice (Garza-Manero et al., 2015)

Studies carried out in humans have also shown that the circulating profile of miR-146a is decreased in AD (Kiko et al., 2014; Müller et al., 2014). It is interesting to note that miR-146a levels in the blood of MCI patients were also downregulated in MCI patients progressing to AD (Ansari et al., 2019).

Next, we compared the microRNA expression profile of the in vivo Aβ 1-42 injection model with the APPswe / PSEN1dE9 transgenic model, also known as APP / PS1. These mice recapitulate the early AD phenotype, and are characterized by an increased Aβ in the brain (Ryan et al., 2018). These animals express a human / mouse chimeric APP and a human presenilin-1 and have early synaptic dysfunction (Ahmad et al., 2017) and chronic Aβ deposition, neuroinflammation and cognitive impairment from 6 months (Jankowsky et al., 2004; Savonenko et al., 2005). We checked the expression of 9 microRNAs in serum obtained from 4 and 15-month-old animals. We did not find any significant changes in the expression of microRNAs in the serum of 4- month-old mice. In the sera of 15-month-old animals, there was a significant downregulation of miR-125b, miR- 191-5p, miR-29a and miR-29c but not miR-146a (Figure 11). Although this model and ours show expression of different microRNAs, interestingly we find that they share the down-regulation of the miR-

29 family in serum. Therefore, each animal model of AD, which represents specific components of the disease, reflects the dysregulation of certain microRNAs that are more closely related to these components. To conclude, each AD model has some advantages and limitations. They must be carefully selected according to our objective and must be compared with those obtained from human samples.

In this study, we also evaluated the expression of miR-146a in CSF obtained from rats injected with 2.5 μg / μL of Aβ 1-42 at 14 days post injection. We found an upregulation of miR-146a in Aβ 1- 42 treated animals compared to the control group (Figure 12). This is in line with reports showing high levels of miR-146a expression in human CSF samples from AD patients (Alexandrov et al., 2012; Denk et al., 2015). Due to its direct and intimate relationship with brain tissue, CSF reflects neurophysiological changes in AD (Denk et al., 2015).

In the last part of the project, we conducted functional studies and used an in vitro AD model, generated by incubation of Aβ at different concentrations in a primary astrocytes culture. The main objective was to investigate the role of miR-146a and its relationship with inflammation. Neuroinflammation is characterized by the accumulation of reactive astrocytes and activated microglia, and these intervene in the severity and progression of the disease by exacerbating the inflammatory response (Garwood, Pooler, Atherton, Hanger, & Noble, 2011). Moreover, the severity of glial activation is correlated with the degree of brain atrophy and cognitive impairment. We chose to use primary astrocytes because they are the most abundant cell type in the CNS (Giovannoni & Quintana, 2020) and they are important modulators of the innate and inflammatory immune response of the brain of AD patients (Bai et al., 2021; Bell & Zlokovic, 2009; Y. Zhao, Cui, & Lukiw, 2006). It is known that the inflammatory cascade promoted by astrocytes, results in the pathological accumulation of the Tau protein (Birch et al., 2014). These characteristics make them important players in

Aβ-induced inflammation. We also took the opportunity to assess the impact of oligomers (OAβ) and fibrils (FAβ) on astrocytes. We compared which of these forms would cause a greater dysregulation of miR-146a expression because it is not clear which of them is the most important in the pathogenesis of AD, especially in inflammation. We first checked that the Aβ concentrations used (0,5, 1 and 2 μM) were not toxic for cell viability (Figure 13). Both OAβ and FAβ incubation induced upregulation of miR-146a compared to control cells (Figure 14A and 14B). These findings are consistent with previous studies in human astrocytes that showed up- regulation of miR-146a when incubated with Aβ. However, Aβ aggregation form was not specified in this study. Similarly, Li et al., demonstrated that miR-146a was positively regulated in human neuronal-glial (HNG), human astroglial (HAG) and human microglial (HMG) cells treated with Aβ 1-42 and TNF-α in compared to untreated controls (Y. Y. Li, Cui, Dua, et al., 2011). Similar results were obtained when human neuronal primary cell culture was treated with inflammatory molecules such as Aβ 1-42, IL-1β, and H_2O_2 (Lukiw et al., 2008).

It is known that miR-146a expression is under the transcriptional control of NF-κB (Lukiw, 2020; Lukiw et al., 2008). When NF-κB pathway was inhibited by BMS-345541, the upregulation of miR- 146a expression was abolished corroborating the involvement of this pathway (Figure 15). To go further in the dissection of OAβ and FAβ impacts on astrocytes, we quantified the expression of inflammatory cytokines such as IL-6, IL-1β, and TNF-α, which are known to be increased following astrocytes activation and they aberrantly expressed in AD brain (Garwood et al., 2011; Sudduth, Schmitt, Nelson, & Wilcock, 2013; Tuppo & Arias, 2005) Surprisingly, we did not find expression of inflammatory cytokines (Figure 16), which are different from those previous findings.

To understand the absence of inflammatory cytokines expression, we analyzed the expression of miR-146a targets (Figure 17 and 18). The role of this microRNA in the regulation of inflammation has been shown to be associated with the regulation of Toll-like (TLR) and interleukin-1 receptors (ILRs) signaling (Cui et al., 2010; Granic, Dolga, Nijholt, van Dijk, & Eisel, 2009; Kawagoe et al., 2008; Reverchon et al., 2020; Taganov et al., 2006). Furthermore, it is known that miR-146a causes direct repression of interleukin-1 receptor associated kinase 1 (IRAK1), and Tumor necrosis factor receptor associated factor 6 (TRAF6).

Different reports made with human astrocytes showed that concurrent with the positive regulation of miR-146a in cells exposed to Aβ, a decrease in IRAK-1 associated with a compensatory increase in the expression of Interleukin-1 receptor-associated kinase-like 2 (IRAK-2) were induced leading to a sustained inflammatory response (Cui et al., 2010; Kawagoe et al., 2008; Pogue et al., 2009). The decrease of IRAK-1 gene was also reported when HNG, HAG, HMG cells were stressed by Aβ 1-42 and TNF-α (Y. Y. Li, Cui, Dua, et al., 2011). These studies are consistent with our results as we found that in OAβ-treated cells, IRAK1 expression was downregulated whilst IRAK- 2 was upregulated (Figure 17). With FAβ treatment, IRAK1 tends as well to decrease whilst it was not statistically significant compared to control cells (Figure 18).

It is known that upon activation of TLR/ILR, a molecular cascade including IRAK-1/IRAK-2 and TRAF6 leads to phosphorylation and degradation of IκBα allowing the activation of NF-κB and its nuclear import (Taganov et al., 2006). The activation of NF-κB induces the transcription of many genes, including miRNA precursors, such as pri-miR-146a. Once pri-miR-146a is transferred to the cytoplasm and loaded into the RISC complex, mature miR-146a acts in a negative feedback loop by binding to IRAK1 and TRAF6 mRNAs (Rusca & Monticelli, 2011). These two targets are upstream of the NF-κB signaling pathway, and consequently abolish signal transduction of NF-κB pathway by reducing the production of

IL-6, IL-8, IL-1β, and TNF-α (Y. Y. Li, Cui, Dua, et al., 2011; Taganov et al., 2006). At this stage, there is an attenuation of inflammation (mild inflammation). Therefore, the non-expression of cytokines in our experiments could reflect the negative feedback caused by miR-146a on IRAK1 and TRAF6 targets. In advanced AD, there is a chronic inflammation due to many factors that activate different receptors, which induce several signaling pathways. The activation of inflammation is not only triggered by OAβ or FAβ but also by others danger signals (herpes virus, bacteria for instance) leading to the production of many cytokines and chemokines. Under such a condition, the neuronal cells are overwhelmed, and miR- 146a upregulation failed to resolve the inflammation contributing to the cognitive impairment and AD progression (Boldin & Baltimore, 2012; Cui et al., 2010; Granic et al., 2009; Sen, 2011). These mechanisms are recapitulated in Figure 1.

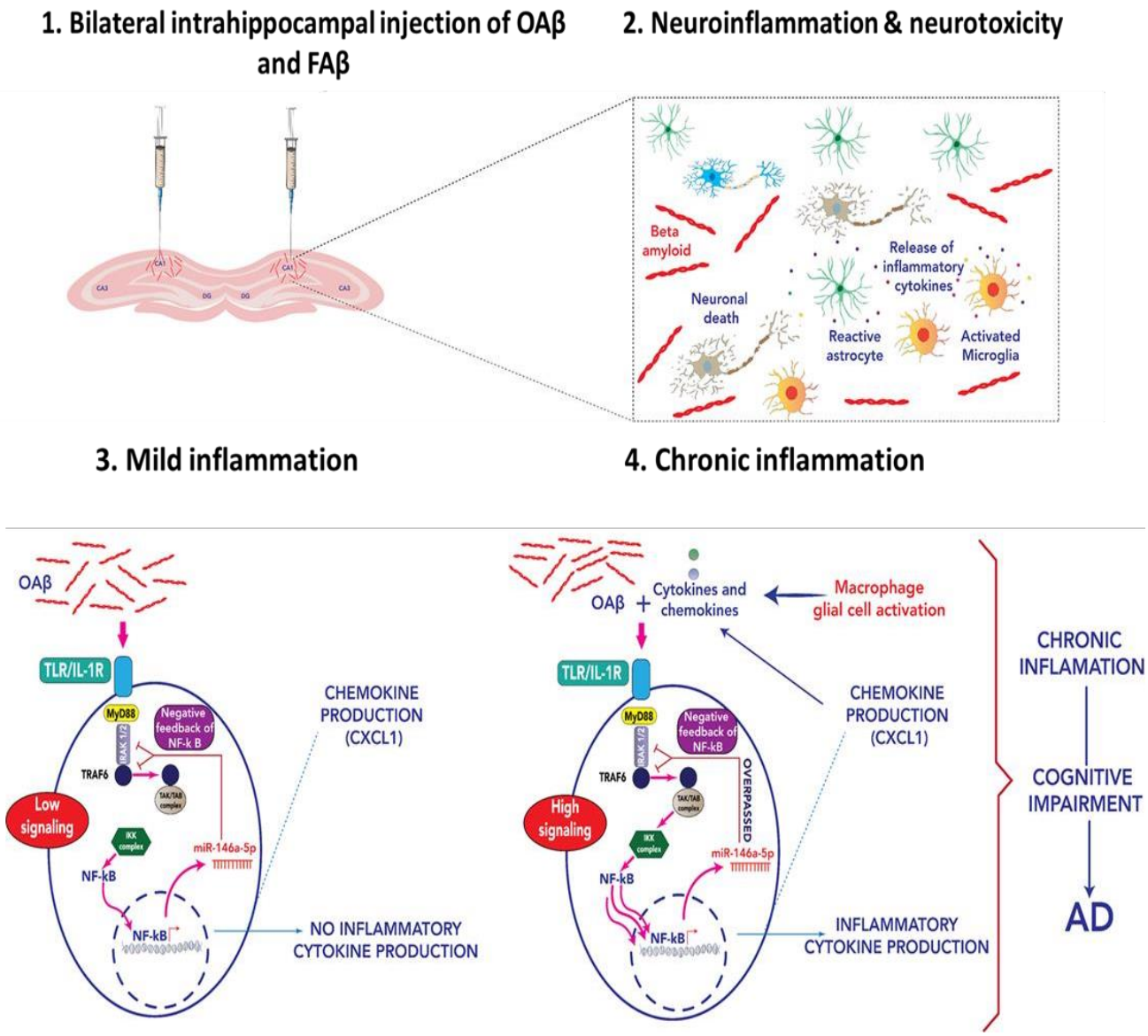

Figure 1. Overview of the injection of OAβ and FAβ in the hippocampus of rats and the role of miR-146a in mild and chronic inflammation.

2. Conclusion

AD affects millions of people in the world due to progressive and irreversible neuronal damage in the brain. This multifactorial disease is characterized by the deregulation of many keys regulators proteins. Despite extensive research, the etiology of the disease is still not fully understood. Many studies have brought experimental evidences that one of main cause of AD is closely associated with the aggregation of the Aβ peptide that accumulate in the extracellular matrix of the brain and trigger a variety of biochemical pathways such as formation of NFTs, the interruption of synaptic connections, the activation of neuro-inflammatory processes and finally neuronal loss. Due to the fact that the pathology is initiated at least 20 years before these symptoms become clinically detectable, the identification of early diagnosis markers is essential and a challenge to improve the management of this disease. In this context, circulating microRNAs have been proposed as promising diagnostic agents due to their relatively easy detection in patients body fluid samples and also because some of the circulating microARNs are closely associated in the clinic with the early development of other disease types such as cancer for instance. In recent years, several animal models have been developed to better understand the molecular events that govern the etiology of this disease and to identify circulating biomarkers. The most widely used AD animal models are those derived from transgenic animal models harboring targeted mutations in APP, PSEN1/2, APOE and Tau. Although they are relevant to recapitulate the main molecular characteristic of the AD development, these genetic forms of disease represent only 5% of AD cases. Therefore, other animal models of AD are required and notably those enabling to develop clinical symptoms of this disease in the adult stage that represent 95% of AD form. In this work,

we developed an animal model of AD by intracranial infusion of aggregated form (fibrillar amyloid beta) of peptide Aβ 1- 42 (FAβ) into the hippocampus of wild type adult rats.

We demonstrate that increasing the amount of FAβ infused into the brain also increased the amount of deregulated circulating miRNAs in blood samples from animals that correlated with cognitive impairments of the animal such as loss of spatial and reference memory.

We established the kinetic of expression of 3 selected circulating miRNAs (miR-29a, miR-29c, miR-146a) and demonstrated that one of them, the miR-146a, exhibits a distinct expression pattern when compared to other miRNAs. Importantly, some of those miRNAs were also found to be deregulated in the APP/PS1dE9 animal model, indicating that the miRNAs pattern detected in our AD animal model is more likely to be associated with the pathogenicity of FAβ/OAβ accumulation in the brain and therefore, could represent early diagnosis markers of this pathology. We evaluated a possible defect in neuronal viability in the hippocampal regions by Cresyl violet staining and demonstrated that although none abnormal coloration was detected, GFAP immunohistochemistry analysis revealed the presence of astrogliosis. Finally, we examine a possible correlation link between astrogliosis and deregulated expression of miRNA-146a in serum and CSF samples as well as in primary rat astrocyte culture. We demonstrated that treatment of astrocytes with either OAβ or FAβ was sufficient to induce upregulation of miR-146a in astrocytes, which in turn downregulated the expression of IRAK-1, a known molecular target of miR- 146a involved in the initiation of NF-κB pathway signaling.

However, this event was found insufficient to down regulate the expression of TRAF-6, a key effector of this cell signaling pathway. To finally assess whether NF-κB signaling was activated in these cells, we evaluated expression of pro-inflammatory cytokines at the transcriptional and translational levels. No changes in the expression of IL-6, TNF-α, IL-1β were detected, although a slight but significant change in the expression of CXCL1 was detected.

Based on these data and those reported in the literature, we assume that miR-146a upregulation in astrocyte cells is more likely to play an anti-inflammatory role through negative feedback of the NF-κB pathway. Taken together, our data indicated that miR-146a could be seen as a possible early- diagnostic circulating biomarker correlated with OAβ / FAβ accumulation in the brain, and may play an anti-inflammatory role in AD by counteracting initiation of the NF-κB signaling pathway.

3. Supplementary Data

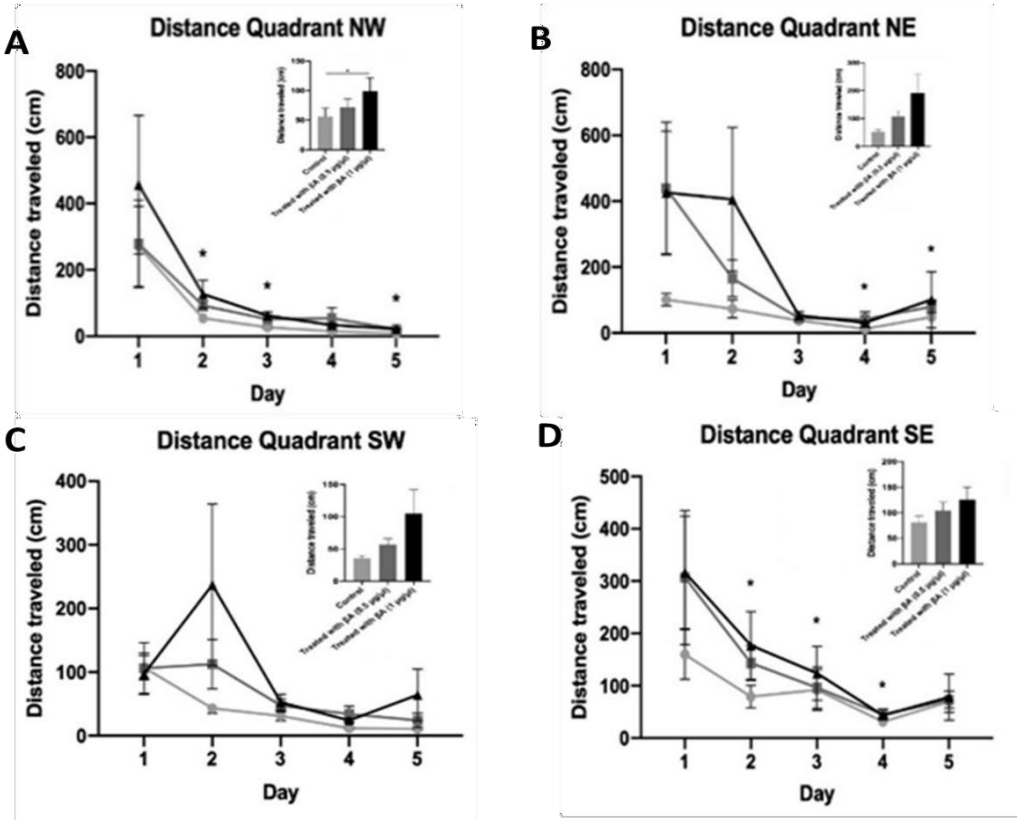

Figure S1. Effects of FAβ 1-42 injection on memory and learning, evaluated by the Morris Water Maze (MWM) test. The distance performed by rats injected with FAβ made with 0.5 and 1 µg/µL of Aβ1-42 to find the platform was evaluated, at day 14 post-injection. Distance (A) in the quadrant NW (B) in the quadrant NE, (C) in the quadrant SW (D), in the target quadrant SE. Control group (n=10); group injected with FAβ made with 0.5 µg/µL Aβ 1-42 (n=11); group injected with FAβ made with 1 µg/µL Aβ 1-42 (n=13). Data are represented as mean ± SEM. Statistical comparisons were performed using Kruskal-Wallis. *p≤0.05, **p≤0.01, ***p≤0.001.

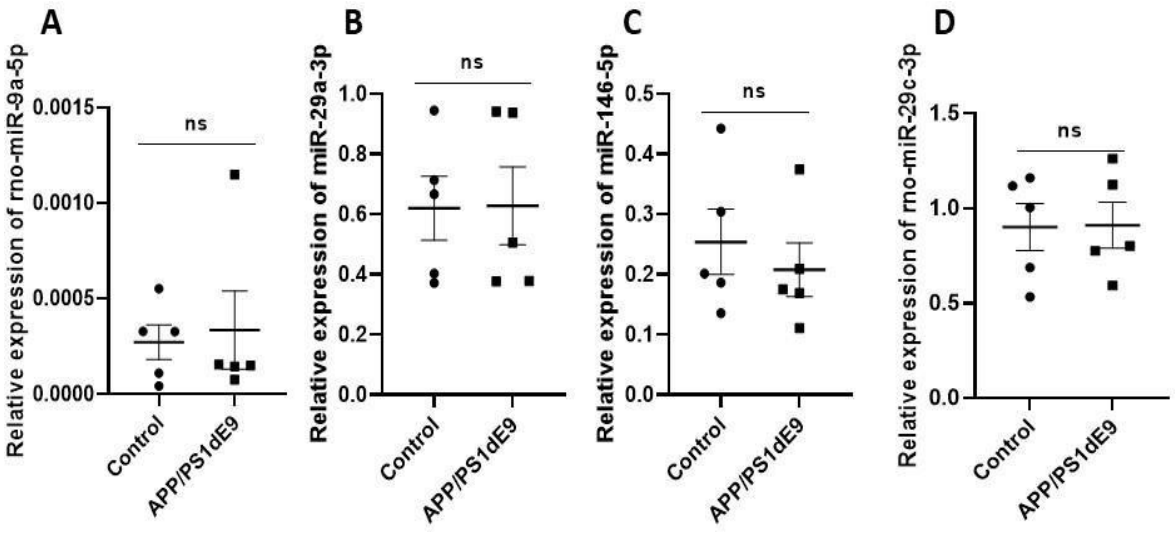

Figure S2. Relative expression of circulating miR-9a-5p, miR-29a-3p, miR-146a-5p and miR-29c-3p in serum of APP/PS1delE9 transgenic animal model of AD. Serum samples from transgenic animals at 4 months of age were extracted and selected miRNA were quantified by qRT-PCR. (A) miR-9a-5p, (B) miR-29a-3p, (C) miR-146a-5p, (D) miR-29c-3p. Data are represented as mean ± SEM of 5 samples performed in triplicate. Statistical comparisons between the transgenic and control group were performed using the Mann-Whitney test. * $p \leq 0.05$, ** $p \leq 0.01$, *** $p \leq 0.001$

4. References

Abbott, N. J. (2002). Astrocyte-endothelial interactions and blood-brain barrier permeability. *J Anat, 200*(6), 629-638. doi: 10.1046/j.1469-7580.2002.00064.x

Agostinho, P., Pliássova, A., Oliveira, C. R., & Cunha, R. A. (2015). Localization and Trafficking of Amyloid-β Protein Precursor and Secretases: Impact on Alzheimer'sDisease. *J Alzheimers Dis, 45*(2), 329-347. doi: 10.3233/jad-142730

Agrawal, V., Sawhney, N., Hickey, E., & McCarthy, J. V. (2016). Loss of Presenilin 2 Function Is Associated with Defective LPS-Mediated Innate Immune Responsiveness. *Mol Neurobiol, 53*(5), 3428-3438. doi: 10.1007/s12035-015-9285-0

Ahmad, F., Singh, K., Das, D., Gowaikar, R., Shaw, E., Ramachandran, A., . . . Ravindranath, V. (2017). Reactive Oxygen Species-Mediated Loss of Synaptic Akt1 Signaling Leads to Deficient Activity-Dependent Protein Translation Early in Alzheimer's Disease. *Antioxid Redox Signal, 27*(16), 1269-1280. doi: 10.1089/ars.2016.6860

Alexandrov, P. N., Dua, P., Hill, J. M., Bhattacharjee, S., Zhao, Y., & Lukiw, W. J. (2012). microRNA (miRNA) speciation in Alzheimer's disease (AD) cerebrospinal fluid (CSF) and extracellular fluid (ECF). *Int J Biochem Mol Biol, 3*(4), 365-373.

Almansoub, Hamm, Tang, H., Wu, Y., Wang, D. Q., Mahaman, Y. A. R., Wei, N., . . . Liu, D. (2019). Tau Abnormalities and the Potential Therapy in Alzheimer's Disease. *JAlzheimers Dis, 67*(1), 13-33. doi: 10.3233/jad-180868

Alpizar, Y. A., Boonen, B., Sanchez, A., Jung, C., López-Requena, A., Naert, R., . . . Talavera, K. (2017). TRPV4 activation triggers protective responses to bacterial lipopolysaccharides in airway epithelial cells. *Nat Commun, 8*(1), 1059. doi: 10.1038/s41467-017-01201-3

Ameen-Ali, K. E., Wharton, S. B., Simpson, J. E., Heath, P. R., Sharp, P., & Berwick, J. (2017). Review: Neuropathology and behavioural features of transgenic murine models of Alzheimer's disease. *Neuropathol Appl Neurobiol, 43*(7), 553-570. doi: 10.1111/nan.12440

Andrews-Zwilling, Y., Bien-Ly, N., Xu, Q., Li, G., Bernardo, A., Yoon, S. Y., . . . Huang, Y.(2010). Apolipoprotein E4 causes age- and Tau-dependent impairment of GABAergic interneurons, leading to learning and memory deficits in mice. *J Neurosci, 30*(41), 13707-13717. doi: 10.1523/jneurosci.4040-10.2010

Angelucci, F., Cechova, K., Valis, M., Kuca, K., Zhang, B., & Hort, J. (2019). MicroRNAs in Alzheimer's Disease: Diagnostic Markers or Therapeutic Agents? *Front Pharmacol, 10*, 665. doi: 10.3389/fphar.2019.00665

Anoop, A., Singh, P. K., Jacob, R. S., & Maji, S. K. (2010). CSF Biomarkers for Alzheimer's Disease Diagnosis. *Int J Alzheimers Dis, 2010*. doi: 10.4061/2010/606802

Ansari, A., Maffioletti, E., Milanesi, E., Marizzoni, M., Frisoni, G. B., Blin, O., . . . Bocchio-Chiavetto, L. (2019). miR-146a and miR-181a are involved in the progression of mild cognitive impairment to Alzheimer's disease. *Neurobiol Aging, 82*, 102-109. doi: 10.1016/j.neurobiolaging.2019.06.005

Argaw, A. T., Asp, L., Zhang, J., Navrazhina, K., Pham, T., Mariani, J. N., . . . John, G. R.(2012). Astrocyte-derived VEGF-A drives blood-brain barrier disruption in CNS inflammatory disease. *J Clin Invest, 122*(7), 2454-2468. doi: 10.1172/jci60842

Bagyinszky, E., Youn, Y. C., An, S. S., & Kim, S. (2014). The genetics of Alzheimer's disease. *Clin Interv Aging, 9*, 535-551. doi: 10.2147/cia.s51571

Bai, Y., Su, X., Piao, L., Jin, Z., & Jin, R. (2021). Involvement of Astrocytes and microRNADysregulation in Neurodegenerative Diseases: From Pathogenesis to Therapeutic Potential. *Front Mol Neurosci, 14*, 556215. doi: 10.3389/fnmol.2021.556215

Baldassarre, A., Felli, C., Prantera, G., & Masotti, A. (2017). Circulating microRNAs and Bioinformatics Tools to Discover Novel Diagnostic Biomarkers of Pediatric Diseases. *Genes (Basel), 8*(9). doi: 10.3390/genes8090234

Banzhaf-Strathmann, J., Benito, E., May, S., Arzberger, T., Tahirovic, S., Kretzschmar,

H.,. . . Edbauer, D. (2014). MicroRNA-125b induces tau hyperphosphorylation and cognitive deficits in Alzheimer's disease. *EMBO J, 33*(15), 1667-1680. doi: 10.15252/embj.201387576

Bao, F., Wicklund, L., Lacor, P. N., Klein, W. L., Nordberg, A., & Marutle, A. (2012). Different β-amyloid oligomer assemblies in Alzheimer brains correlate with age ofdisease onset and impaired cholinergic activity. *Neurobiol Aging, 33*(4), 825 e821-813. doi: 10.1016/j.neurobiolaging.2011.05.003

Barilar, J. O., Knezovic, A., Grünblatt, E., Riederer, P., & Salkovic-Petrisic, M. (2015). Nine-month follow-up of the insulin receptor signalling cascade in the brain of streptozotocin rat model of sporadic Alzheimer's disease. *J Neural Transm (Vienna), 122*(4), 565-576. doi: 10.1007/s00702-014-1323-y

Bartel, D. P. (2004). MicroRNAs: genomics, biogenesis, mechanism, and function. *Cell, 116*(2), 281-297. doi: 10.1016/s0092-8674(04)00045-5

Bateman, R. J., Xiong, C., Benzinger, T. L., Fagan, A. M., Goate, A., Fox, N. C., . . . Morris, J. C. (2012). Clinical and biomarker changes in dominantly inherited Alzheimer's disease. *N Engl J Med, 367*(9), 795-804. doi: 10.1056/NEJMoa1202753

Beeton, C., Garcia, A., & Chandy, K. G. (2007). Drawing blood from rats through the saphenous vein and by cardiac puncture. *J Vis Exp*(7), 266. doi: 10.3791/266

Behairi, N., Belkhelfa, M., Rafa, H., Labsi, M., Deghbar, N., Bouzid, N., . . . Touil-Boukoffa, C. (2016). All-trans retinoic acid (ATRA) prevents lipopolysaccharide-induced neuroinflammation, amyloidogenesis and memory impairment in aged rats. *J Neuroimmunol, 300*, 21-29. doi: 10.1016/j.jneuroim.2016.10.004

Bekris, L. M., Yu, C. E., Bird, T. D., & Tsuang, D. W. (2010). Genetics of Alzheimer disease. *J Geriatr Psychiatry Neurol, 23*(4), 213-227. doi: 10.1177/0891988710383571

Bell, R. D., & Zlokovic, B. V. (2009). Neurovascular mechanisms and blood-brain barrier disorder in Alzheimer's disease. *Acta Neuropathol, 118*(1), 103-113. doi: 10.1007/s00401-009-0522-3

Bentahir, M., Nyabi, O., Verhamme, J., Tolia, A., Horré, K., Wiltfang, J., . . . De Strooper, B. (2006). Presenilin clinical mutations can affect gamma-secretase activity by different mechanisms. *J Neurochem, 96*(3), 732-742. doi: 10.1111/j.1471- 4159.2005.03578.x

Bhute, S., Sarmah, D., Datta, A., Rane, P., Shard, A., Goswami, A., . . . Bhattacharya, P.(2020). Molecular Pathogenesis and Interventional Strategies for Alzheimer's Disease: Promises and Pitfalls. *ACS Pharmacol Transl Sci, 3*(3), 472-488. doi: 10.1021/acsptsci.9b00104

Bien-Ly, N., Andrews-Zwilling, Y., Xu, Q., Bernardo, A., Wang, C., & Huang, Y. (2011). C- terminal-truncated apolipoprotein (apo) E4 inefficiently clears amyloid-beta (Abeta) and acts in concert with Abeta to elicit neuronal and behavioral deficits in mice. *Proc Natl Acad Sci U S A, 108*(10), 4236-4241. doi: 10.1073/pnas.1018381108

Biffi, A., Sonni, A., Anderson, C. D., Kissela, B., Jagiella, J. M., Schmidt, H., . . . Rosand, J. (2010). Variants at APOE influence risk of deep and lobar intracerebral hemorrhage. *Ann Neurol, 68*(6), 934-943. doi: 10.1002/ana.22134

Billings, L. M., Oddo, S., Green, K. N., McGaugh, J. L., & LaFerla, F. M. (2005). Intraneuronal Abeta causes the onset of early Alzheimer's disease-related cognitive deficits in transgenic mice. *Neuron, 45*(5), 675-688. doi: 10.1016/j.neuron.2005.01.040

Blanco, M. E., Mayo, O. B., Bandiera, T., De Pietri Tonelli, D., & Armirotti, A. (2020). LC- MS/MS analysis of twelve neurotransmitters and amino acids in mouse cerebrospinal fluid. *J Neurosci Methods, 341*, 108760. doi: 10.1016/j.jneumeth.2020.108760

Blasko, I., Veerhuis, R., Stampfer-Kountchev, M., Saurwein-Teissl, M., Eikelenboom, P., & Grubeck-Loebenstein, B. (2000). Costimulatory effects of interferon-gamma andinterleukin-1beta or tumor necrosis factor alpha on the synthesis of Abeta1-40 andAbeta1-42 by human astrocytes. *Neurobiol Dis, 7*(6 Pt B), 682-689. doi: 10.1006/nbdi.2000.0321

Boldin, M. P., & Baltimore, D. (2012). MicroRNAs, new effectors and regulators of NF-κB. *Immunol Rev, 246*(1), 205-220. doi: 10.1111/j.1600-065X.2011.01089.x

Bolmont, T., Clavaguera, F., Meyer-Luehmann, M., Herzig, M. C., Radde, R., Staufenbiel,M., . . . Jucker, M. (2007). Induction of tau pathology by intracerebral infusion of amyloid-beta -containing brain extract and by amyloid-beta deposition in APP x Tau transgenic mice. *Am J Pathol, 171*(6), 2012-2020. doi: 10.2353/ajpath.2007.070403

Boonen, B., Alpizar, Y. A., Sanchez, A., López-Requena, A., Voets, T., & Talavera, K. (2018). Differential effects of lipopolysaccharide on mouse sensory TRP

channels.*Cell Calcium, 73*, 72-81. doi: 10.1016/j.ceca.2018.04.004

Borbély, E., Horváth, J., Furdan, S., Bozsó, Z., Penke, B., & Fülöp, L. (2014). Simultaneous changes of spatial memory and spine density after intrahippocampal administration of fibrillar aβ1-42 to the rat brain. *Biomed Res Int, 2014*, 345305. doi: 10.1155/2014/345305

Borchelt, D. R., Thinakaran, G., Eckman, C. B., Lee, M. K., Davenport, F., Ratovitsky, T.,. . . Sisodia, S. S. (1996). Familial Alzheimer's disease-linked presenilin 1 variants elevate Abeta1-42/1-40 ratio in vitro and in vivo. *Neuron, 17*(5), 1005-1013. doi: 10.1016/s0896-6273(00)80230-5

Borroni, B., Di Luca, M., & Padovani, A. (2006). Predicting Alzheimer dementia in mild cognitive impairment patients. Are biomarkers useful? *Eur J Pharmacol, 545*(1), 73-80. doi: 10.1016/j.ejphar.2006.06.023

Braak, H., & Braak, E. (1991). Neuropathological stageing of Alzheimer-related changes. *Acta Neuropathol, 82*(4), 239-259. doi: 10.1007/bf00308809

Brecht, W. J., Harris, F. M., Chang, S., Tesseur, I., Yu, G. Q., Xu, Q., . . . Huang, Y. (2004). Neuron-specific apolipoprotein e4 proteolysis is associated with increased tau phosphorylation in brains of transgenic mice. *J Neurosci, 24*(10), 2527-2534. doi: 10.1523/jneurosci.4315-03.2004

Brigman, J. L., Wright, T., Talani, G., Prasad-Mulcare, S., Jinde, S., Seabold, G. K., . . . Holmes, A. (2010). Loss of GluN2B-containing NMDA receptors in CA1 hippocampus and cortex impairs long-term depression, reduces dendritic spine density, and disrupts learning. *J Neurosci, 30*(13), 4590-4600. doi: 10.1523/jneurosci.0640-10.2010

Brionne, T. C., Tesseur, I., Masliah, E., & Wyss-Coray, T. (2003). Loss of TGF-beta 1 leads to increased neuronal cell death and microgliosis in mouse brain. *Neuron, 40*(6), 1133-1145. doi: 10.1016/s0896-6273(03)00766-9

Bryan, K. J., Lee, H. G., Perry, G., Smith, M. A., & Casadesus, G. (2009). *Transgenic Mouse Models of Alzheimer's Disease: Behavioral Testing and Considerations Methods of Behavior Analysis in Neuroscience*. Boca Raton FL: © Taylor & Francis Group,LLC.

Bu, G. (2009). Apolipoprotein E and its receptors in Alzheimer's disease: pathways, pathogenesis and therapy. *Nat Rev Neurosci, 10*(5), 333-344. doi: 10.1038/nrn2620

Buée, L., Bussière, T., Buée-Scherrer, V., Delacourte, A., & Hof, P. R. (2000). Tau proteinisoforms, phosphorylation and role in neurodegenerative disorders. *Brain Res Brain Res Rev, 33*(1), 95-130. doi: 10.1016/s0165-0173(00)00019-9

Burke, J. R., Pattoli, M. A., Gregor, K. R., Brassil, P. J., MacMaster, J. F., McIntyre, K. W.,. . . Zusi, F. C. (2003). BMS-345541 is a highly selective inhibitor of I kappa B kinase that binds at an allosteric site of the enzyme and blocks NF-kappa B-dependent transcription in mice. *J Biol Chem, 278*(3), 1450-1456. doi: 10.1074/jbc.M209677200

Calvo-Flores Guzmán, B., Elizabeth Chaffey, T., Hansika Palpagama, T., Waters, S., Boix,J., Tate, W. P., . . . Kwakowsky, A. (2020). The Interplay Between Beta-Amyloid 1-42 (Aβ(1-42))-Induced Hippocampal Inflammatory Response, p-tau, Vascular Pathology, and Their Synergistic Contributions to Neuronal Death and Behavioral Deficits. *Front Mol Neurosci, 13*, 522073. doi: 10.3389/fnmol.2020.552073

Caraci, F., Battaglia, G., Bruno, V., Bosco, P., Carbonaro, V., Giuffrida, M. L., . . . Copani, A. (2011). TGF-β1 pathway as a new target for neuroprotection in Alzheimer's disease. *CNS Neurosci Ther, 17*(4), 237-249. doi: 10.1111/j.1755-5949.2009.00115.x

Carter, D. B., Dunn, E., McKinley, D. D., Stratman, N. C., Boyle, T. P., Kuiper, S. L., . . . Gurney, M. E. (2001). Human apolipoprotein E4 accelerates beta-amyloid deposition in APPsw transgenic mouse brain. *Ann Neurol, 50*(4), 468-475. doi: 10.1002/ana.1134

Casaletto, K. B., Elahi, F. M., Bettcher, B. M., Neuhaus, J., Bendlin, B. B., Asthana, S., . .. Kramer, J. H. (2017). Neurogranin, a synaptic protein, is associated with memoryindependent of Alzheimer biomarkers. *Neurology, 89*(17), 1782-1788. doi: 10.1212/wnl.0000000000004569

Cerf, E., Gustot, A., Goormaghtigh, E., Ruysschaert, J. M., & Raussens, V. (2011). High ability of apolipoprotein E4 to stabilize amyloid-β peptide oligomers, the pathological entities responsible for Alzheimer's disease. *FASEB J, 25*(5), 1585-1595. doi: 10.1096/fj.10-175976

Cogswell, J. P., Ward, J., Taylor, I. A., Waters, M., Shi, Y., Cannon, B., . . . Richards, C. A. (2008). Identification of miRNA changes in Alzheimer's disease brain and

CSFyields putative biomarkers and insights into disease pathways. *J Alzheimers Dis, 14*(1), 27-41. doi: 10.3233/jad-2008-14103

Cohen, T. J., Guo, J. L., Hurtado, D. E., Kwong, L. K., Mills, I. P., Trojanowski, J. Q., & Lee, V. M. (2011). The acetylation of tau inhibits its function and promotes pathological tau aggregation. *Nat Commun, 2*, 252. doi: 10.1038/ncomms1255

Colombo, E., & Farina, C. (2016). Astrocytes: Key Regulators of Neuroinflammation. *Trends Immunol, 37*(9), 608-620. doi: 10.1016/j.it.2016.06.006

Contino, S., Porporato, P. E., Bird, M., Marinangeli, C., Opsomer, R., Sonveaux, P., . . . Kienlen-Campard, P. (2017). Presenilin 2-Dependent Maintenance of Mitochondrial Oxidative Capacity and Morphology. *Front Physiol, 8*, 796. doi: 10.3389/fphys.2017.00796

Corder, E. H., Saunders, A. M., Strittmatter, W. J., Schmechel, D. E., Gaskell, P. C., Small, G. W., . . . Pericak-Vance, M. A. (1993). Gene dose of apolipoprotein E type 4 allele and the risk of Alzheimer's disease in late onset families. *Science, 261*(5123), 921-923. doi: 10.1126/science.8346443

Cui, J. G., Li, Y. Y., Zhao, Y., Bhattacharjee, S., & Lukiw, W. J. (2010). Differential regulation of interleukin-1 receptor-associated kinase-1 (IRAK-1) and IRAK-2 by microRNA-146a and NF-kappaB in stressed human astroglial cells and in Alzheimer disease. *J Biol Chem, 285*(50), 38951-38960. doi: 10.1074/jbc.M110.178848

Chacón, M. A., Barría, M. I., Soto, C., & Inestrosa, N. C. (2004). Beta-sheet breaker peptide prevents Abeta-induced spatial memory impairments with partial reduction of amyloid deposits. *Mol Psychiatry, 9*(10), 953-961. doi: 10.1038/sj.mp.4001516

Chang, F., Zhang, L. H., Xu, W. P., Jing, P., & Zhan, P. Y. (2014). microRNA-9 attenuatesamyloidβ-induced synaptotoxicity by targeting calcium/calmodulin-dependent protein kinase kinase 2. *Mol Med Rep, 9*(5), 1917-1922. doi: 10.3892/mmr.2014.2013

Chang, S., ran Ma, T., Miranda, R. D., Balestra, M. E., Mahley, R. W., & Huang, Y. (2005).Lipid- and receptor-binding regions of apolipoprotein E4 fragments act in concert to cause mitochondrial dysfunction and neurotoxicity. *Proc Natl Acad*

Sci U S A, 102(51), 18694-18699. doi: 10.1073/pnas.0508254102

Chen, C. Z., Li, L., Lodish, H. F., & Bartel, D. P. (2004). MicroRNAs modulate hematopoietic lineage differentiation. *Science, 303*(5654), 83-86. doi: 10.1126/science.1091903

Chen, G. F., Xu, T. H., Yan, Y., Zhou, Y. R., Jiang, Y., Melcher, K., & Xu, H. E. (2017). Amyloid beta: structure, biology and structure-based therapeutic development. *Acta Pharmacol Sin, 38*(9), 1205-1235. doi: 10.1038/aps.2017.28

Chen, H. K., Ji, Z. S., Dodson, S. E., Miranda, R. D., Rosenblum, C. I., Reynolds, I. J., . .. Mahley, R. W. (2011). Apolipoprotein E4 domain interaction mediates detrimental effects on mitochondria and is a potential therapeutic target for Alzheimer disease. *J Biol Chem, 286*(7), 5215-5221. doi: 10.1074/jbc.M110.151084

Chen, J., Li, Q., & Wang, J. (2011). Topology of human apolipoprotein E3 uniquely regulates its diverse biological functions. *Proc Natl Acad Sci U S A, 108*(36), 14813-14818. doi: 10.1073/pnas.1106420108

Chen, X., Ba, Y., Ma, L., Cai, X., Yin, Y., Wang, K., . . . Zhang, C. Y. (2008). Characterization of microRNAs in serum: a novel class of biomarkers for diagnosis of cancer and other diseases. *Cell Res, 18*(10), 997-1006. doi: 10.1038/cr.2008.282

Chen, X., & Zhang, J. (2016). The Genomic Landscape of Position Effects on Protein Expression Level and Noise in Yeast. *Cell Syst, 2*(5), 347-354. doi: 10.1016/j.cels.2016.03.009

Chishti, M. A., Yang, D. S., Janus, C., Phinney, A. L., Horne, P., Pearson, J., . . . Westaway, D. (2001). Early-onset amyloid deposition and cognitive deficits in transgenic mice expressing a double mutant form of amyloid precursor protein 695.*J Biol Chem, 276*(24), 21562-21570. doi: 10.1074/jbc.M100710200

Chu, C., Deng, J., Man, Y., & Qu, Y. (2017). Green Tea Extracts Epigallocatechin-3-gallate for Different Treatments. *Biomed Res Int, 2017*, 5615647. doi: 10.1155/2017/5615647

Dahlgren, K. N., Manelli, A. M., Stine, W. B., Jr., Baker, L. K., Krafft, G. A., & LaDu, M. J. (2002). Oligomeric and fibrillar species of amyloid-beta peptides differentially affect neuronal viability. *J Biol Chem, 277*(35), 32046-32053. doi: 10.1074/jbc.M201750200

Dangla-Valls, A., Molinuevo, J. L., Altirriba, J., Sánchez-Valle, R., Alcolea, D., Fortea, J.,. . . Antonell, A. (2017). CSF microRNA Profiling in Alzheimer's Disease: a Screening and Validation Study. *Mol Neurobiol, 54*(9), 6647-6654. doi: 10.1007/s12035-016-0106-x

Dawkins, E., & Small, D. H. (2014). Insights into the physiological function of the β-amyloid precursor protein: beyond Alzheimer's disease. *J Neurochem, 129*(5), 756-769. doi: 10.1111/jnc.12675

De-Paula, V. J., Radanovic, M., Diniz, B. S., & Forlenza, O. V. (2012). Alzheimer's disease. *Subcell Biochem, 65*, 329-352. doi: 10.1007/978-94-007-5416-4_14

Delay, C., & Hébert, S. S. (2011). MicroRNAs and Alzheimer's Disease Mouse Models: Current Insights and Future Research Avenues. *Int J Alzheimers Dis, 2011*, 894938. doi: 10.4061/2011/894938

Delay, C., Mandemakers, W., & Hébert, S. S. (2012). MicroRNAs in Alzheimer's disease. *Neurobiol Dis, 46*(2), 285-290. doi: 10.1016/j.nbd.2012.01.003

Deng, M., Du, G., Zhao, J., & Du, X. (2017). miR-146a negatively regulates the induction of proinflammatory cytokines in response to Japanese encephalitis virus infection in microglial cells. *Arch Virol, 162*(6), 1495-1505. doi: 10.1007/s00705-017-3226- 3

Denk, J., Boelmans, K., Siegismund, C., Lassner, D., Arlt, S., & Jahn, H. (2015). MicroRNAProfiling of CSF Reveals Potential Biomarkers to Detect Alzheimer`s Disease. *PLoS One, 10*(5), e0126423. doi: 10.1371/journal.pone.0126423

Domingues, C., da Cruz, E. Silva O. A. B., & Henriques, A. G. (2017). Impact of Cytokines and Chemokines on Alzheimer's Disease Neuropathological Hallmarks. *Curr Alzheimer Res, 14*(8), 870-882. doi: 10.2174/1567205014666170317113606

Drechsel, D. N., Hyman, A. A., Cobb, M. H., & Kirschner, M. W. (1992). Modulation of the dynamic instability of tubulin assembly by the microtubule-associated protein tau. *Mol Biol Cell, 3*(10), 1141-1154. doi: 10.1091/mbc.3.10.1141

Drummond, E., & Wisniewski, T. (2017). Alzheimer's disease: experimental models and reality. *Acta Neuropathol, 133*(2), 155-175. doi: 10.1007/s00401-016-1662-x

Du, L. L., Chai, D. M., Zhao, L. N., Li, X. H., Zhang, F. C., Zhang, H. B., . . . Zhou, X. W. (2015). AMPK activation ameliorates Alzheimer's disease-like pathology and spatial memory impairment in a streptozotocin-induced Alzheimer's disease modelin rats. *J Alzheimers Dis, 43*(3), 775-784. doi: 10.3233/jad-140564

Dumont, M., Strazielle, C., Staufenbiel, M., & Lalonde, R. (2004). Spatial learning and exploration of environmental stimuli in 24-month-old female APP23 transgenic mice with the Swedish mutation. *Brain Res, 1024*(1-2), 113-121. doi: 10.1016/j.brainres.2004.07.052

Duy, J., Koehler, J. W., Honko, A. N., & Minogue, T. D. (2015). Optimized microRNA purification from TRIzol-treated plasma. *BMC Genomics, 16*(1), 95. doi: 10.1186/s12864-015-1299-5

Edbauer, D., Winkler, E., Regula, J. T., Pesold, B., Steiner, H., & Haass, C. (2003). Reconstitution of gamma-secretase activity. *Nat Cell Biol, 5*(5), 486-488. doi: 10.1038/ncb960

Edsbagge, M., Andreasson, U., Ambarki, K., Wikkelsø, C., Eklund, A., Blennow, K., . . . Tullberg, M. (2017). Alzheimer's Disease-Associated Cerebrospinal Fluid (CSF) Biomarkers do not Correlate with CSF Volumes or CSF Production Rate. *J Alzheimers Dis, 58*(3), 821-828. doi: 10.3233/jad-161257

Eisenberg, D. T., Kuzawa, C. W., & Hayes, M. G. (2010). Worldwide allele frequencies ofthe human apolipoprotein E gene: climate, local adaptations, and evolutionary history. *Am J Phys Anthropol, 143*(1), 100-111. doi: 10.1002/ajpa.21298

Elder, G. A., Gama Sosa, M. A., & De Gasperi, R. (2010). Transgenic mouse models of Alzheimer's disease. *Mt Sinai J Med, 77*(1), 69-81. doi: 10.1002/msj.20159

Elliott, D. A., Kim, W. S., Jans, D. A., & Garner, B. (2007). Apoptosis induces neuronal apolipoprotein-E synthesis and localization in apoptotic bodies. *Neurosci Lett, 416*(2), 206-210. doi: 10.1016/j.neulet.2007.02.014

Elliott, D. A., Tsoi, K., Holinkova, S., Chan, S. L., Kim, W. S., Halliday, G. M., . . . Garner, B. (2011). Isoform-specific proteolysis of apolipoprotein-E in the brain. *Neurobiol Aging, 32*(2), 257-271. doi: 10.1016/j.neurobiolaging.2009.02.006

Escamilla-Ayala, A., Wouters, R., Sannerud, R., & Annaert, W. (2020). Contribution of thePresenilins in the cell biology, structure and function of γ-secretase. *Semin Cell Dev Biol, 105*, 12-26. doi: 10.1016/j.semcdb.2020.02.005

Esparza, T. J., Zhao, H., Cirrito, J. R., Cairns, N. J., Bateman, R. J., Holtzman, D. M., & Brody, D. L. (2013). Amyloid-β oligomerization in Alzheimer dementia versus high-pathology controls. *Ann Neurol, 73*(1), 104-119. doi: 10.1002/ana.23748

Esquerda-Canals, G., Montoliu-Gaya, L., Güell-Bosch, J., & Villegas, S. (2017). Mouse

Models of Alzheimer's Disease. *J Alzheimers Dis, 57*(4), 1171-1183. doi: 10.3233/jad-170045

Fá, M., Puzzo, D., Piacentini, R., Staniszewski, A., Zhang, H., Baltrons, M. A., . . . Arancio, O. (2016). Extracellular Tau Oligomers Produce An Immediate Impairment of LTPand Memory. *Sci Rep, 6*, 19393. doi: 10.1038/srep19393

Facchinetti, R., Bronzuoli, M. R., & Scuderi, C. (2018). An Animal Model of Alzheimer Disease Based on the Intrahippocampal Injection of Amyloid β-Peptide (1-42). *Methods Mol Biol, 1727*, 343-352. doi: 10.1007/978-1-4939-7571-6_25

Fakhoury, M. (2018). Microglia and Astrocytes in Alzheimer's Disease: Implications for Therapy. *Curr Neuropharmacol, 16*(5), 508-518. doi: 10.2174/1570159x15666170720095240

Farrer, L. A., Cupples, L. A., Haines, J. L., Hyman, B., Kukull, W. A., Mayeux, R., . . . vanDuijn, C. M. (1997). Effects of age, sex, and ethnicity on the association between apolipoprotein E genotype and Alzheimer disease. A meta-analysis. APOE and Alzheimer Disease Meta Analysis Consortium. *JAMA, 278*(16), 1349-1356.

Faucher, P., Mons, N., Micheau, J., Louis, C., & Beracochea, D. J. (2015). Hippocampal Injections of Oligomeric Amyloid β-peptide (1-42) Induce Selective Working Memory Deficits and Long-lasting Alterations of ERK Signaling Pathway. *Front Aging Neurosci, 7*, 245. doi: 10.3389/fnagi.2015.00245

Fekete, C., Vastagh, C., Dénes, Á, Hrabovszky, E., Nyiri, G., Kalló, I., . . . Sárvári, M. (2019). Chronic Amyloid β Oligomer Infusion Evokes Sustained Inflammation andMicroglial Changes in the Rat Hippocampus via NLRP3. *Neuroscience, 405*, 35- 46. doi: 10.1016/j.neuroscience.2018.02.046

Fernandez, C. G., Hamby, M. E., McReynolds, M. L., & Ray, W. J. (2019). The Role of APOE4 in Disrupting the Homeostatic Functions of Astrocytes and Microglia in Aging and Alzheimer's Disease. *Front Aging Neurosci, 11*, 14. doi: 10.3389/fnagi.2019.00014

Findeis, M. A. (2007). The role of amyloid beta peptide 42 in Alzheimer's disease. *Pharmacol Ther, 116*(2), 266-286. doi: 10.1016/j.pharmthera.2007.06.006

Fine, J. M., Forsberg, A. C., Stroebel, B. M., Faltesek, K. A., Verden, D. R., Hamel, K. A.,. . . Hanson, L. R. (2017). Intranasal deferoxamine affects memory loss, oxidation,and the insulin pathway in the streptozotocin rat model of Alzheimer's

disease. *J Neurol Sci, 380*, 164-171. doi: 10.1016/j.jns.2017.07.028

Fischer, R. S., & Fowler, V. M. (2003). Tropomodulins: life at the slow end. *Trends Cell Biol, 13*(11), 593-601. doi: 10.1016/j.tcb.2003.09.007

Forny-Germano, L., Lyra e Silva, N. M., Batista, A. F., Brito-Moreira, J., Gralle, M., Boehnke, S. E., . . . De Felice, F. G. (2014). Alzheimer's disease-like pathology induced by amyloid-β oligomers in nonhuman primates. J Neurosci, 34(41), 13629- 13643. doi: 10.1523/jneurosci.1353-14.2014

Francis, G., Martinez, J., Liu, W., Nguyen, T., Ayer, A., Fine, J., . . . Toth, C. (2009). Intranasal insulin ameliorates experimental diabetic neuropathy. *Diabetes, 58*(4), 934-945. doi: 10.2337/db08-1287

Francis, R., McGrath, G., Zhang, J., Ruddy, D. A., Sym, M., Apfeld, J., . . . Curtis, D. (2002). aph-1 and pen-2 are required for Notch pathway signaling, gamma-secretase cleavage of betaAPP, and presenilin protein accumulation. *Dev Cell, 3*(1), 85-97. doi: 10.1016/s1534-5807(02)00189-2

Frandemiche, M. L., De Seranno, S., Rush, T., Borel, E., Elie, A., Arnal, I., . . . Buisson, A. (2014). Activity-dependent tau protein translocation to excitatory synapse is disrupted by exposure to amyloid-beta oligomers. *J Neurosci, 34*(17), 6084-6097.doi: 10.1523/jneurosci.4261-13.2014

Friedman, R. C., Farh, K. K., Burge, C. B., & Bartel, D. P. (2009). Most mammalian mRNAsare conserved targets of microRNAs. *Genome Res, 19*(1), 92-105. doi: 10.1101/gr.082701.108

Gage, G. J., Kipke, D. R., & Shain, W. (2012). Whole animal perfusion fixation for rodents. *J Vis Exp*(65). doi: 10.3791/3564

Galland, F., Seady, M., Taday, J., Smaili, S. S., Gonçalves, C. A., & Leite, M. C. (2019). Astrocyte culture models: Molecular and function characterization of primary culture, immortalized astrocytes and C6 glioma cells. *Neurochem Int, 131*, 104538.doi: 10.1016/j.neuint.2019.104538

Gamache, J., Benzow, K., Forster, C., Kemper, L., Hlynialuk, C., Furrow, E., . . . Koob, M. D. (2019). Factors other than hTau overexpression that contribute to tauopathy- like phenotype in rTg4510 mice. *Nat Commun, 10*(1), 2479. doi: 10.1038/s41467-019-10428-1

Games, D., Adams, D., Alessandrini, R., Barbour, R., Berthelette, P., Blackwell, C., . . . etal. (1995). Alzheimer-type neuropathology in transgenic mice overexpressing V717F beta-amyloid precursor protein. *Nature, 373*(6514), 523-527. doi:

10.1038/373523a0

Gao, Y. J., Zhang, L., Samad, O. A., Suter, M. R., Yasuhiko, K., Xu, Z. Z., . . . Ji, R. R. (2009). JNK-induced MCP-1 production in spinal cord astrocytes contributes to central sensitization and neuropathic pain. *J Neurosci, 29*(13), 4096-4108. doi: 10.1523/jneurosci.3623-08.2009

Gao, Y. L., Wang, N., Sun, F. R., Cao, X. P., Zhang, W., & Yu, J. T. (2018). Tau in neurodegenerative disease. *Ann Transl Med, 6*(10), 175. doi: 10.21037/atm.2018.04.23

Gao, Y., Tan, L., Yu, J. T., & Tan, L. (2018). Tau in Alzheimer's Disease: Mechanisms and Therapeutic Strategies. *Curr Alzheimer Res, 15*(3), 283-300. doi: 10.2174/1567205014666170417111859

Garcia-Alloza, M., Robbins, E. M., Zhang-Nunes, S. X., Purcell, S. M., Betensky, R. A., Raju, S., . . . Frosch, M. P. (2006). Characterization of amyloid deposition in the APPswe/PS1dE9 mouse model of Alzheimer disease. *Neurobiol Dis, 24*(3), 516-524. doi: 10.1016/j.nbd.2006.08.017

Garwood, C. J., Pooler, A. M., Atherton, J., Hanger, D. P., & Noble, W. (2011). Astrocytes are important mediators of Aβ-induced neurotoxicity and tau phosphorylation in primary culture. *Cell Death Dis, 2*(6), e167. doi: 10.1038/cddis.2011.50

Garza-Manero, S., Arias, C., Bermúdez-Rattoni, F., Vaca, L., & Zepeda, A. (2015). Identification of age- and disease-related alterations in circulating miRNAs in a mouse model of Alzheimer's disease. *Front Cell Neurosci, 9*, 53. doi: 10.3389/fncel.2015.00053

Ge, Y., Dong, Z., Bagot, R. C., Howland, J. G., Phillips, A. G., Wong, T. P., & Wang, Y. T.(2010). Hippocampal long-term depression is required for the consolidation of spatial memory. *Proc Natl Acad Sci U S A, 107*(38), 16697-16702. doi: 10.1073/pnas.1008200107

Geekiyanage, H., & Chan, C. (2011). MicroRNA-137/181c regulates serine palmitoyltransferase and in turn amyloid β, novel targets in sporadic Alzheimer's disease. *J Neurosci, 31*(41), 14820-14830. doi: 10.1523/jneurosci.3883-11.2011

Geekiyanage, H., Jicha, G. A., Nelson, P. T., & Chan, C. (2012). Blood serum miRNA: non-invasive biomarkers for Alzheimer's disease. *Exp Neurol, 235*(2), 491-496. doi: 10.1016/j.expneurol.2011.11.026

Geekiyanage, H., Upadhye, A., & Chan, C. (2013). Inhibition of serine

palmitoyltransferase reduces Aβ and tau hyperphosphorylation in a murine model: a safe therapeutic strategy for Alzheimer's disease. *Neurobiol Aging, 34*(8), 2037-2051. doi: 10.1016/j.neurobiolaging.2013.02.001

Gelman, S., Palma, J., Tombaugh, G., & Ghavami, A. (2018). Differences in Synaptic Dysfunction Between rTg4510 and APP/PS1 Mouse Models of Alzheimer's Disease. *J Alzheimers Dis, 61*(1), 195-208. doi: 10.3233/jad-170457

Gerson, J., Castillo-Carranza, D. L., Sengupta, U., Bodani, R., Prough, D. S., DeWitt, D. S., . . . Kayed, R. (2016). Tau Oligomers Derived from Traumatic Brain Injury Cause Cognitive Impairment and Accelerate Onset of Pathology in Htau Mice. *J Neurotrauma, 33*(22), 2034-2043. doi: 10.1089/neu.2015.4262

Giau, V. V., Bagyinszky, E., An, S. S., & Kim, S. Y. (2015). Role of apolipoprotein E in neurodegenerative diseases. *Neuropsychiatr Dis Treat, 11*, 1723-1737. doi: 10.2147/ndt.s84266

Gilad, S., Meiri, E., Yogev, Y., Benjamin, S., Lebanony, D., Yerushalmi, N., . . . Chajut, A.(2008). Serum microRNAs are promising novel biomarkers. *PLoS One, 3*(9), e3148. doi: 10.1371/journal.pone.0003148

Giovannoni, F., & Quintana, F. J. (2020). The Role of Astrocytes in CNS Inflammation. *Trends Immunol, 41*(9), 805-819. doi: 10.1016/j.it.2020.07.007

Goate, A., Chartier-Harlin, M. C., Mullan, M., Brown, J., Crawford, F., Fidani, L., . . . et al.(1991). Segregation of a missense mutation in the amyloid precursor protein gene with familial Alzheimer's disease. *Nature, 349*(6311), 704-706. doi: 10.1038/349704a0

Götz, J., Chen, F., van Dorpe, J., & Nitsch, R. M. (2001). Formation of neurofibrillary tangles in P301l tau transgenic mice induced by Abeta 42 fibrils. *Science, 293*(5534), 1491-1495. doi: 10.1126/science.1062097

Granic, I., Dolga, A. M., Nijholt, I. M., van Dijk, G., & Eisel, U. L. (2009). Inflammation andNF-kappaB in Alzheimer's disease and diabetes. *J Alzheimers Dis, 16*(4), 809-821.doi: 10.3233/jad-2009-0976

Gray, P., Dagvadorj, J., Michelsen, K. S., Brikos, C., Rentsendorj, A., Town, T., . . . Arditi, M. (2011). Myeloid differentiation factor-2 interacts with Lyn kinase and is tyrosinephosphorylated following lipopolysaccharide-induced activation of the TLR4 signaling pathway. *J Immunol, 187*(8), 4331-4337. doi: 10.4049/jimmunol.1100890

Grela, A., Turek, A., & Piekoszewski, W. (2012). Application of matrix-assisted laser

desorption/ionization time-of-flight mass spectrometry (MALDI-TOF MS) in Alzheimer's disease. *Clin Chem Lab Med, 50*(8), 1297-1304. doi: 10.1515/cclm-2011-0550

Grieb, P. (2016). Intracerebroventricular Streptozotocin Injections as a Model of Alzheimer's Disease: in Search of a Relevant Mechanism. *Mol Neurobiol, 53*(3), 1741-1752. doi: 10.1007/s12035-015-9132-3

Guo, Q., Li, H., Cole, A. L., Hur, J. Y., Li, Y., & Zheng, H. (2013). Modeling Alzheimer's disease in mouse without mutant protein overexpression: cooperative and independent effects of Aβ and tau. *PLoS One, 8*(11), e80706. doi: 10.1371/journal.pone.0080706

Guo, Q., Zheng, H., & Justice, N. J. (2012). Central CRF system perturbation in an Alzheimer's disease knockin mouse model. *Neurobiol Aging, 33*(11), 2678-2691. doi: 10.1016/j.neurobiolaging.2012.01.002

Haass, C., & Steiner, H. (2001). Protofibrils, the unifying toxic molecule of neurodegenerative disorders? *Nat Neurosci, 4*(9), 859-860. doi: 10.1038/nn0901-859

Hamanaka, H., Katoh-Fukui, Y., Suzuki, K., Kobayashi, M., Suzuki, R., Motegi, Y., . . . Fujita, S. C. (2000). Altered cholesterol metabolism in human apolipoprotein E4 knock-in mice. *Hum Mol Genet, 9*(3), 353-361. doi: 10.1093/hmg/9.3.353

Hannun, Y. A., & Obeid, L. M. (2008). Principles of bioactive lipid signalling: lessons fromsphingolipids. *Nat Rev Mol Cell Biol, 9*(2), 139-150. doi: 10.1038/nrm2329

Hardy, J., & Selkoe, D. J. (2002). The amyloid hypothesis of Alzheimer's disease: progress and problems on the road to therapeutics. *Science, 297*(5580), 353-356. doi: 10.1126/science.1072994

Harkany, T., Abrahám, I., Timmerman, W., Laskay, G., Tóth, B., Sasvári, M., . . . Luiten, P. G. (2000). beta-amyloid neurotoxicity is mediated by a glutamate-triggered excitotoxic cascade in rat nucleus basalis. *Eur J Neurosci, 12*(8), 2735-2745. doi: 10.1046/j.1460-9568.2000.00164.x

Harris, F. M., Brecht, W. J., Xu, Q., Tesseur, I., Kekonius, L., Wyss-Coray, T., . . . Huang, Y. (2003). Carboxyl-terminal-truncated apolipoprotein E4 causes Alzheimer's disease-like neurodegeneration and behavioral deficits in transgenic mice. *Proc Natl Acad Sci U S A, 100*(19), 10966-10971. doi: 10.1073/pnas.1434398100

Hashimoto, T., Serrano-Pozo, A., Hori, Y., Adams, K. W., Takeda, S., Banerji, A. O., . . . Hyman, B. T. (2012). Apolipoprotein E, especially apolipoprotein E4, increases theoligomerization of amyloid β peptide. *J Neurosci, 32*(43), 15181-15192. doi: 10.1523/jneurosci.1542-12.2012

He, X., Huang, Y., Li, B., Gong, C. X., & Schuchman, E. H. (2010). Deregulation of sphingolipid metabolism in Alzheimer's disease. *Neurobiol Aging, 31*(3), 398-408.doi: 10.1016/j.neurobiolaging.2008.05.010

He, Y., Zheng, M. M., Ma, Y., Han, X. J., Ma, X. Q., Qu, C. Q., & Du, Y. F. (2012). Soluble oligomers and fibrillar species of amyloid β-peptide differentially affect cognitive functions and hippocampal inflammatory response. *Biochem Biophys Res Commun, 429*(3-4), 125-130. doi: 10.1016/j.bbrc.2012.10.129

Hébert, S. S., Horré, K., Nicolaï, L., Bergmans, B., Papadopoulou, A. S., Delacourte, A., & De Strooper, B. (2009). MicroRNA regulation of Alzheimer's Amyloid precursor protein expression. *Neurobiol Dis, 33*(3), 422-428. doi: 10.1016/j.nbd.2008.11.009

Hébert, S. S., Horré, K., Nicolaï, L., Papadopoulou, A. S., Mandemakers, W., Silahtaroglu, A. N., . . . De Strooper, B. (2008). Loss of microRNA cluster miR-29a/b-1 in sporadic Alzheimer's disease correlates with increased BACE1/beta-secretase expression. *Proc Natl Acad Sci U S A, 105*(17), 6415-6420. doi: 10.1073/pnas.0710263105

Henriksen, K., O'Bryant, S. E., Hampel, H., Trojanowski, J. Q., Montine, T. J., Jeromin, A.,. . . Weiner, M. W. (2014). The future of blood-based biomarkers for Alzheimer's disease. *Alzheimers Dement, 10*(1), 115-131. doi: 10.1016/j.jalz.2013.01.013

Heo, C., Chang, K. A., Choi, H. S., Kim, H. S., Kim, S., Liew, H., . . . Suh, Y. H. (2007). Effects of the monomeric, oligomeric, and fibrillar Abeta42 peptides on the proliferation and differentiation of adult neural stem cells from subventricular zone.*J Neurochem, 102*(2), 493-500. doi: 10.1111/j.1471-4159.2007.04499.x

Herber, D. L., Maloney, J. L., Roth, L. M., Freeman, M. J., Morgan, D., & Gordon, M. N. (2006). Diverse microglial responses after intrahippocampal administration of lipopolysaccharide. *Glia, 53*(4), 382-391. doi: 10.1002/glia.20272

Herrera-Espejo, S., Santos-Zorrozua, B., Álvarez-González, P., Lopez-Lopez, E., & Garcia-Orad, Á. (2019). A Systematic Review of MicroRNA Expression as

Biomarker of Late-Onset Alzheimer's Disease. *Mol Neurobiol, 56*(12), 8376-8391.doi: 10.1007/s12035-019-01676-9

Holcomb, L., Gordon, M. N., McGowan, E., Yu, X., Benkovic, S., Jantzen, P., . . . Duff, K.(1998). Accelerated Alzheimer-type phenotype in transgenic mice carrying both mutant amyloid precursor protein and presenilin 1 transgenes. *Nat Med, 4*(1), 97-100. doi: 10.1038/nm0198-097

Holtzman, D. M., Bales, K. R., Wu, S., Bhat, P., Parsadanian, M., Fagan, A. M., . . . Paul, S. M. (1999). Expression of human apolipoprotein E reduces amyloid-beta deposition in a mouse model of Alzheimer's disease. *J Clin Invest, 103*(6), R15-R21. doi: 10.1172/jci6179

Holtzman, D. M., Fagan, A. M., Mackey, B., Tenkova, T., Sartorius, L., Paul, S. M., . . . Hyman, B. T. (2000). Apolipoprotein E facilitates neuritic and cerebrovascular plaque formation in an Alzheimer's disease model. *Ann Neurol, 47*(6), 739-747.

Hong, H., Li, Y., & Su, B. (2017). Identification of Circulating miR-125b as a Potential Biomarker of Alzheimer's Disease in APP/PS1 Transgenic Mouse. *J Alzheimers Dis, 59*(4), 1449-1458. doi: 10.3233/jad-170156

Hoyer, S. (2004). Causes and consequences of disturbances of cerebral glucose metabolism in sporadic Alzheimer disease: therapeutic implications. *Adv Exp MedBiol, 541*, 135-152. doi: 10.1007/978-1-4419-8969-7_8

Hsiao, K., Chapman, P., Nilsen, S., Eckman, C., Harigaya, Y., Younkin, S., . . . Cole, G. (1996). Correlative memory deficits, Abeta elevation, and amyloid plaques in transgenic mice. *Science, 274*(5284), 99-102. doi: 10.1126/science.274.5284.99

Hu, Z., Yu, D., Gu, Q. H., Yang, Y., Tu, K., Zhu, J., & Li, Z. (2014). miR-191 and miR-135 are required for long-lasting spine remodelling associated with synaptic long-termdepression. *Nat Commun, 5*, 3263. doi: 10.1038/ncomms4263

Huang, Y., & Mucke, L. (2012). Alzheimer mechanisms and therapeutic strategies. *Cell, 148*(6), 1204-1222. doi: 10.1016/j.cell.2012.02.040

Humpel, C. (2011). Identifying and validating biomarkers for Alzheimer's disease. *TrendsBiotechnol, 29*(1), 26-32. doi: 10.1016/j.tibtech.2010.09.007

Hutchison, E. R., Kawamoto, E. M., Taub, D. D., Lal, A., Abdelmohsen, K., Zhang, Y., . . . Mattson, M. P. (2013). Evidence for miR-181 involvement in neuroinflammatory responses of astrocytes. *Glia, 61*(7), 1018-1028. doi: 10.1002/glia.22483

Huynh, T. V., Wang, C., Tran, A. C., Tabor, G. T., Mahan, T. E., Francis, C. M., . . .

Holtzman, D. M. (2019). Lack of hepatic apoE does not influence early Aβ deposition: observations from a new APOE knock-in model. *Mol Neurodegener, 14*(1), 37. doi: 10.1186/s13024-019-0337-1

Hye, A., Lynham, S., Thambisetty, M., Causevic, M., Campbell, J., Byers, H. L., . . . Lovestone, S. (2006). Proteome-based plasma biomarkers for Alzheimer's disease. *Brain, 129*(Pt 11), 3042-3050. doi: 10.1093/brain/awl279

Ipson, B. R., Fletcher, M. B., Espinoza, S. E., & Fisher, A. L. (2018). Identifying Exosome-Derived MicroRNAs as Candidate Biomarkers of Frailty. *J Frailty Aging, 7*(2), 100-103. doi: 10.14283/jfa.2017.45

Iqbal, K., Liu, F., & Gong, C. X. (2016). Tau and neurodegenerative disease: the story sofar. *Nat Rev Neurol, 12*(1), 15-27. doi: 10.1038/nrneurol.2015.225

Ittner, L. M., Ke, Y. D., & Götz, J. (2009). Phosphorylated Tau interacts with c-Jun N-terminal kinase-interacting protein 1 (JIP1) in Alzheimer disease. *J Biol Chem, 284*(31), 20909-20916. doi: 10.1074/jbc.M109.014472

Jahangard, Y., Monfared, H., Moradi, A., Zare, M., Mirnajafi-Zadeh, J., & Mowla, S. J. (2020). Therapeutic Effects of Transplanted Exosomes Containing miR-29b to a Rat Model of Alzheimer's Disease. *Front Neurosci, 14*, 564. doi: 10.3389/fnins.2020.00564

Jankowsky, J. L., Fadale, D. J., Anderson, J., Xu, G. M., Gonzales, V., Jenkins, N. A., . . .Borchelt, D. R. (2004). Mutant presenilins specifically elevate the levels of the 42 residue beta-amyloid peptide in vivo: evidence for augmentation of a 42-specific gamma secretase. *Hum Mol Genet, 13*(2), 159-170. doi: 10.1093/hmg/ddh019

Jankowsky, J. L., Savonenko, A., Schilling, G., Wang, J., Xu, G., & Borchelt, D. R. (2002).Transgenic mouse models of neurodegenerative disease: opportunities for therapeutic development. *Curr Neurol Neurosci Rep, 2*(5), 457-464. doi: 10.1007/s11910-002-0073-7

Jankowsky, J. L., & Zheng, H. (2017). Practical considerations for choosing a mouse model of Alzheimer's disease. *Mol Neurodegener, 12*(1), 89. doi: 10.1186/s13024-017-0231-7

Jawhar, S., Trawicka, A., Jenneckens, C., Bayer, T. A., & Wirths, O. (2012). Motor deficits,neuron loss, and reduced anxiety coinciding with axonal degeneration and intraneuronal Aβ aggregation in the 5XFAD mouse model of Alzheimer's disease. Neurobiol Aging, 33(1), 196 e129-140. doi:

10.1016/j.neurobiolaging.2010.05.027

Jayadev, S., Leverenz, J. B., Steinbart, E., Stahl, J., Klunk, W., Yu, C. E., & Bird, T. D. (2010). Alzheimer's disease phenotypes and genotypes associated with mutations in presenilin 2. *Brain, 133*(Pt 4), 1143-1154. doi: 10.1093/brain/awq033

Jean, Y. Y., Baleriola, J., Fà, M., Hengst, U., & Troy, C. M. (2015). Stereotaxic Infusion of Oligomeric Amyloid-beta into the Mouse Hippocampus. *J Vis Exp*(100), e52805. doi: 10.3791/52805

Johanson, T. M., Skinner, J. P., Kumar, A., Zhan, Y., Lew, A. M., & Chong, M. M. (2014).The role of microRNAs in lymphopoiesis. *Int J Hematol, 100*(3), 246-253. doi: 10.1007/s12185-014-1606-y

Jouanne, M., Rault, S., & Voisin-Chiret, A. S. (2017). Tau protein aggregation in Alzheimer's disease: An attractive target for the development of novel therapeutic agents. *Eur J Med Chem, 139*, 153-167. doi: 10.1016/j.ejmech.2017.07.070

Juzenas, S., Venkatesh, G., Hübenthal, M., Hoeppner, M. P., Du, Z. G., Paulsen, M., . . . Hemmrich-Stanisak, G. (2017). A comprehensive, cell specific microRNA catalogue of human peripheral blood. *Nucleic Acids Res, 45*(16), 9290-9301. doi: 10.1093/nar/gkx706

Kalogianni, D. P., Kalligosfyri, P. M., Kyriakou, I. K., & Christopoulos, T. K. (2018). Advances in microRNA analysis. *Anal Bioanal Chem, 410*(3), 695-713. doi: 10.1007/s00216-017-0632-z

Kamer, A. R., Dasanayake, A. P., Craig, R. G., Glodzik-Sobanska, L., Bry, M., & de Leon, M. J. (2008). Alzheimer's disease and peripheral infections: the possible contribution from periodontal infections, model and hypothesis. *J Alzheimers Dis, 13*(4), 437-449. doi: 10.3233/jad-2008-13408

Kamphuis, W., Mamber, C., Moeton, M., Kooijman, L., Sluijs, J. A., Jansen, A. H., . . . Hol, E. M. (2012). GFAP isoforms in adult mouse brain with a focus on neurogenic astrocytes and reactive astrogliosis in mouse models of Alzheimer disease. *PLoSOne, 7*(8), e42823. doi: 10.1371/journal.pone.0042823

Karthick, C., Nithiyanandan, S., Essa, M. M., Guillemin, G. J., Jayachandran, S. K., & Anusuyadevi, M. (2019). Time-dependent effect of oligomeric amyloid-β (1-42)-induced hippocampal neurodegeneration in rat model of Alzheimer's disease. *Neurol Res, 41*(2), 139-150. doi: 10.1080/01616412.2018.1544745

Kasza, Á, Penke, B., Frank, Z., Bozsó, Z., Szegedi, V., Hunya, Á, . . . Fülöp, L. (2017). Studies for Improving a Rat Model of Alzheimer's Disease: Icv Administration of Well-Characterized β-Amyloid 1-42 Oligomers Induce Dysfunction in Spatial Memory. *Molecules, 22*(11). doi: 10.3390/molecules22112007

Kaushal, A., Wani, W. Y., Anand, R., & Gill, K. D. (2013). Spontaneous and induced nontransgenic animal models of AD: modeling AD using combinatorial approach. *Am J Alzheimers Dis Other Demen, 28*(4), 318-326. doi: 10.1177/1533317513488914

Kawagoe, T., Sato, S., Matsushita, K., Kato, H., Matsui, K., Kumagai, Y., . . . Akira, S. (2008). Sequential control of Toll-like receptor-dependent responses by IRAK1 andIRAK2. *Nat Immunol, 9*(6), 684-691. doi: 10.1038/ni.1606

Keifer, J., Zheng, Z., & Ambigapathy, G. (2015). A MicroRNA-BDNF Negative Feedback Signaling Loop in Brain: Implications for Alzheimer's Disease. *Microrna, 4*(2), 101-108. doi: 10.2174/2211536604666150813152620

Kiko, T., Nakagawa, K., Tsuduki, T., Furukawa, K., Arai, H., & Miyazawa, T. (2014). MicroRNAs in plasma and cerebrospinal fluid as potential markers for Alzheimer'sdisease. *J Alzheimers Dis, 39*(2), 253-259. doi: 10.3233/jad-130932

Kim, H. Y., Lee, D. K., Chung, B. R., Kim, H. V., & Kim, Y. (2016). Intracerebroventricular Injection of Amyloid-β Peptides in Normal Mice to Acutely Induce Alzheimer-like Cognitive Deficits. *J Vis Exp*(109). doi: 10.3791/53308

Kim, J., Yoon, H., Ramírez, C. M., Lee, S. M., Hoe, H. S., Fernández-Hernando, C., & Kim, J. (2012). MiR-106b impairs cholesterol efflux and increases Aβ levels by repressing ABCA1 expression. *Exp Neurol, 235*(2), 476-483. doi: 10.1016/j.expneurol.2011.11.010

Kim, W. S., Rahmanto, A. S., Kamili, A., Rye, K. A., Guillemin, G. J., Gelissen, I. C., . . . Garner, B. (2007). Role of ABCG1 and ABCA1 in regulation of neuronal cholesterol efflux to apolipoprotein E discs and suppression of amyloid-beta peptide generation. *J Biol Chem, 282*(5), 2851-2861. doi: 10.1074/jbc.M607831200

Kim, Y. J., Kim, S. H., Park, Y., Park, J., Lee, J. H., Kim, B. C., & Song, W. K. (2020). miR-16-5p is upregulated by amyloid β deposition in Alzheimer's disease models and induces neuronal cell apoptosis through direct targeting and suppression of BCL-2. *Exp Gerontol, 136*, 110954. doi: 10.1016/j.exger.2020.110954

Klein, W. L., Krafft, G. A., & Finch, C. E. (2001). Targeting small Abeta oligomers: the solution to an Alzheimer's disease conundrum? *Trends Neurosci, 24*(4), 219-224. doi: 10.1016/s0166-2236(00)01749-5

Knafo, S., Venero, C., Merino-Serrais, P., Fernaud-Espinosa, I., Gonzalez-Soriano, J., Ferrer, I., . . . DeFelipe, J. (2009). Morphological alterations to neurons of the amygdala and impaired fear conditioning in a transgenic mouse model of Alzheimer's disease. *J Pathol, 219*(1), 41-51. doi: 10.1002/path.2565

Ko, C. Y., Chu, Y. Y., Narumiya, S., Chi, J. Y., Furuyashiki, T., Aoki, T., . . . Wang, J. M. (2015). CCAAT/enhancer-binding protein delta/miR135a/thrombospondin 1 axis mediates PGE2-induced angiogenesis in Alzheimer's disease. *Neurobiol Aging, 36*(3), 1356-1368. doi: 10.1016/j.neurobiolaging.2014.11.020

Koistinaho, M., Lin, S., Wu, X., Esterman, M., Koger, D., Hanson, J., . . . Paul, S. M. (2004).Apolipoprotein E promotes astrocyte colocalization and degradation of deposited amyloid-beta peptides. *Nat Med, 10*(7), 719-726. doi: 10.1038/nm1058

Kolarova, M., García-Sierra, F., Bartos, A., Ricny, J., & Ripova, D. (2012). Structure and pathology of tau protein in Alzheimer disease. *Int J Alzheimers Dis, 2012*, 731526.doi: 10.1155/2012/731526

Koldamova, R. P., Lefterov, I. M., Ikonomovic, M. D., Skoko, J., Lefterov, P. I., Isanski, B.A., . . . Lazo, J. S. (2003). 22R-hydroxycholesterol and 9-cis-retinoic acid induce ATP-binding cassette transporter A1 expression and cholesterol efflux in brain cells and decrease amyloid beta secretion. *J Biol Chem, 278*(15), 13244-13256. doi: 10.1074/jbc.M300044200

Kole, A. J., Swahari, V., Hammond, S. M., & Deshmukh, M. (2011). miR-29b is activated during neuronal maturation and targets BH3-only genes to restrict apoptosis. *Genes Dev, 25*(2), 125-130. doi: 10.1101/gad.1975411

König, G., Mönning, U., Czech, C., Prior, R., Banati, R., Schreiter-Gasser, U., . . . Beyreuther, K. (1992). Identification and differential expression of a novel alternative splice isoform of the beta A4 amyloid precursor protein (APP) mRNA inleukocytes and brain microglial cells. *J Biol Chem, 267*(15), 10804-10809.

Kosel, F., Pelley, J. M. S., & Franklin, T. B. (2020). Behavioural and psychological symptoms of dementia in mouse models of Alzheimer's disease-related pathology. *Neurosci Biobehav Rev, 112*, 634-647. doi: 10.1016/j.neubiorev.2020.02.012

Kumar, A., & Thakur, M. K. (2012). Presenilin 1 and 2 are expressed differentially in

the cerebral cortex of mice during development. *Neurochem Int, 61*(5), 778-782. doi: 10.1016/j.neuint.2012.07.001

Kumar, P., Dezso, Z., MacKenzie, C., Oestreicher, J., Agoulnik, S., Byrne, M., . . . Oda, Y. (2013). Circulating miRNA biomarkers for Alzheimer's disease. *PLoS One, 8*(7),e69807. doi: 10.1371/journal.pone.0069807

Kumar, S., & Reddy, P. H. (2016). Are circulating microRNAs peripheral biomarkers for Alzheimer's disease? *Biochim Biophys Acta, 1862*(9), 1617-1627. doi: 10.1016/j.bbadis.2016.06.001

LaDu, M. J., Gilligan, S. M., Lukens, J. R., Cabana, V. G., Reardon, C. A., Van Eldik, L. J., & Holtzman, D. M. (1998). Nascent astrocyte particles differ from lipoproteins in CSF. *J Neurochem, 70*(5), 2070-2081. doi: 10.1046/j.1471-4159.1998.70052070.x

Lalonde, R., Dumont, M., Staufenbiel, M., Sturchler-Pierrat, C., & Strazielle, C. (2002). Spatial learning, exploration, anxiety, and motor coordination in female APP23 transgenic mice with the Swedish mutation. *Brain Res, 956*(1), 36-44. doi: 10.1016/s0006-8993(02)03476-5

Lane-Donovan, C., & Herz, J. (2017). ApoE, ApoE Receptors, and the Synapse in Alzheimer's Disease. *Trends Endocrinol Metab, 28*(4), 273-284. doi: 10.1016/j.tem.2016.12.001

Lanfranco, R. G., Manríquez-Navarro, P., Avello, L. G., & Canales-Johnson, A. (2012). [Early evaluation of Alzheimer's disease: biomarkers and neuropsychological tests]. *Rev Med Chil, 140*(9), 1191-1200. doi: 10.4067/s0034-98872012000900014

Lanoiselée, H. M., Nicolas, G., Wallon, D., Rovelet-Lecrux, A., Lacour, M., Rousseau, S.,. . . Campion, D. (2017). APP, PSEN1, and PSEN2 mutations in early-onset Alzheimer disease: A genetic screening study of familial and sporadic cases. *PLoS Med, 14*(3), e1002270. doi: 10.1371/journal.pmed.1002270

Larner, A. J. (2011). Presenilin-1 mutation Alzheimer's disease: a genetic epilepsy syndrome? *Epilepsy Behav, 21*(1), 20-22. doi: 10.1016/j.yebeh.2011.03.022

Lecanu, L., & Papadopoulos, V. (2013). Modeling Alzheimer's disease with non-transgenicrat models. *Alzheimers Res Ther, 5*(3), 17. doi: 10.1186/alzrt171

Lee, J. W., Lee, Y. K., Yuk, D. Y., Choi, D. Y., Ban, S. B., Oh, K. W., & Hong, J. T. (2008). Neuro-inflammation induced by lipopolysaccharide causes cognitive impairment through enhancement of beta-amyloid generation. *J*

Neuroinflammation, 5, 37. doi:10.1186/1742-2094-5-37

Lei, X., Lei, L., Zhang, Z., Zhang, Z., & Cheng, Y. (2015). Downregulated miR-29c correlates with increased BACE1 expression in sporadic Alzheimer's disease. *Int J Clin Exp Pathol, 8*(2), 1565-1574.

Li, C., Ebrahimi, A., & Schluesener, H. (2013). Drug pipeline in neurodegeneration basedon transgenic mice models of Alzheimer's disease. *Ageing Res Rev, 12*(1), 116- 140. doi: 10.1016/j.arr.2012.09.002

Li, H., Guo, Q., Inoue, T., Polito, V. A., Tabuchi, K., Hammer, R. E., . . . Zheng, H. (2014).Vascular and parenchymal amyloid pathology in an Alzheimer disease knock-in mouse model: interplay with cerebral blood flow. *Mol Neurodegener, 9*, 28. doi: 10.1186/1750-1326-9-28

Li, J., Wang, C., Zhang, J. H., Cai, J. M., Cao, Y. P., & Sun, X. J. (2010). Hydrogen-rich saline improves memory function in a rat model of amyloid-beta-induced Alzheimer's disease by reduction of oxidative stress. *Brain Res, 1328*, 152-161. doi: 10.1016/j.brainres.2010.02.046

Li, Y. Y., Alexandrov, P. N., Pogue, A. I., Zhao, Y., Bhattacharjee, S., & Lukiw, W. J. (2012). miRNA-155 upregulation and complement factor H deficits in Down's syndrome. *Neuroreport, 23*(3), 168-173. doi: 10.1097/WNR.0b013e32834f4eb4

Li, Y. Y., Cui, J. G., Dua, P., Pogue, A. I., Bhattacharjee, S., & Lukiw, W. J. (2011). Differential expression of miRNA-146a-regulated inflammatory genes in human primary neural, astroglial and microglial cells. *Neurosci Lett, 499*(2), 109-113. doi:10.1016/j.neulet.2011.05.044

Li, Y. Y., Cui, J. G., Hill, J. M., Bhattacharjee, S., Zhao, Y., & Lukiw, W. J. (2011). Increasedexpression of miRNA-146a in Alzheimer's disease transgenic mouse models. *Neurosci Lett, 487*(1), 94-98. doi: 10.1016/j.neulet.2010.09.079

Liguori, M., Nuzziello, N., Introna, A., Consiglio, A., Licciulli, F., D'Errico, E., . . . Simone, I. L. (2018). Dysregulation of MicroRNAs and Target Genes Networks in PeripheralBlood of Patients With Sporadic Amyotrophic Lateral Sclerosis. *Front Mol Neurosci, 11*, 288. doi: 10.3389/fnmol.2018.00288

Lippi, G., Steinert, J. R., Marczylo, E. L., D'Oro, S., Fiore, R., Forsythe, I. D., . . . Young, W. (2011). Targeting of the Arpc3 actin nucleation factor by miR-29a/b regulates dendritic spine morphology. *J Cell Biol, 194*(6), 889-904. doi: 10.1083/jcb.201103006

Liu, C. G., Wang, J. L., Li, L., Xue, L. X., Zhang, Y. Q., & Wang, P. C. (2014).

MicroRNA-135a and -200b, potential Biomarkers for Alzheimer's disease, regulate βsecretase and amyloid precursor protein. *Brain Res, 1583*, 55-64. doi: 10.1016/j.brainres.2014.04.026

Liu, C., & Götz, J. (2013). Profiling murine tau with 0N, 1N and 2N isoform-specific antibodies in brain and peripheral organs reveals distinct subcellular localization, with the 1N isoform being enriched in the nucleus. *PLoS One, 8*(12), e84849. doi:10.1371/journal.pone.0084849

Liu, F., Grundke-Iqbal, I., Iqbal, K., & Gong, C. X. (2005). Contributions of protein phosphatases PP1, PP2A, PP2B and PP5 to the regulation of tau phosphorylation. *Eur J Neurosci, 22*(8), 1942-1950. doi: 10.1111/j.1460-9568.2005.04391.x

Liu, L., & Duff, K. (2008). A technique for serial collection of cerebrospinal fluid from the cisterna magna in mouse. *J Vis Exp*(21). doi: 10.3791/960

Liu, L., Herukka, S. K., Minkeviciene, R., van Groen, T., & Tanila, H. (2004). Longitudinal observation on CSF Abeta42 levels in young to middle-aged amyloid precursor protein/presenilin-1 doubly transgenic mice. *Neurobiol Dis, 17*(3), 516-523. doi: 10.1016/j.nbd.2004.08.005

Liu, P., Paulson, J. B., Forster, C. L., Shapiro, S. L., Ashe, K. H., & Zahs, K. R. (2015). Characterization of a Novel Mouse Model of Alzheimer's Disease--Amyloid Pathology and Unique β-Amyloid Oligomer Profile. *PLoS One, 10*(5), e0126317. doi: 10.1371/journal.pone.0126317

Liu, W., Zhao, J., & Lu, G. (2016). miR-106b inhibits tau phosphorylation at Tyr18 by targeting Fyn in a model of Alzheimer's disease. *Biochem Biophys Res Commun, 478*(2), 852-857. doi: 10.1016/j.bbrc.2016.08.037

Livak, K. J., & Schmittgen, T. D. (2001). Analysis of relative gene expression data using real-time quantitative PCR and the 2(-Delta Delta C(T)) Method. *Methods, 25*(4), 402-408. doi: 10.1006/meth.2001.1262

Lukiw, W. J. (2007). Micro-RNA speciation in fetal, adult and Alzheimer's disease hippocampus. *Neuroreport, 18*(3), 297-300. doi: 10.1097/WNR.0b013e3280148e8b

Lukiw, W. J. (2012). NF-κB-regulated, proinflammatory miRNAs in Alzheimer's disease. *Alzheimers Res Ther, 4*(6), 47. doi: 10.1186/alzrt150

Lukiw, W. J. (2020). microRNA-146a Signaling in Alzheimer's Disease (AD) and Prion Disease (PrD). *Front Neurol, 11*, 462. doi: 10.3389/fneur.2020.00462

Lukiw, W. J., & Alexandrov, P. N. (2012). Regulation of complement factor H (CFH)

by multiple miRNAs in Alzheimer's disease (AD) brain. *Mol Neurobiol, 46*(1), 11-19. doi: 10.1007/s12035-012-8234-4

Lukiw, W. J., Alexandrov, P. N., Zhao, Y., Hill, J. M., & Bhattacharjee, S. (2012). Spreadingof Alzheimer's disease inflammatory signaling through soluble micro-RNA. *Neuroreport, 23*(10), 621-626. doi: 10.1097/WNR.0b013e32835542b0

Lukiw, W. J., Cui, J. G., Marcheselli, V. L., Bodker, M., Botkjaer, A., Gotlinger, K., . . . Bazan, N. G. (2005). A role for docosahexaenoic acid-derived neuroprotectin D1 in neural cell survival and Alzheimer disease. *J Clin Invest, 115*(10), 2774-2783. doi: 10.1172/jci25420

Lukiw, W. J., Surjyadipta, B., Dua, P., & Alexandrov, P. N. (2012). Common micro RNAs (miRNAs) target complement factor H (CFH) regulation in Alzheimer's disease (AD) and in age-related macular degeneration (AMD). *Int J Biochem Mol Biol, 3*(1),105-116.

Lukiw, W. J., Zhao, Y., & Cui, J. G. (2008). An NF-kappaB-sensitive micro RNA-146a-mediated inflammatory circuit in Alzheimer disease and in stressed human brain cells. *J Biol Chem, 283*(46), 31315-31322. doi: 10.1074/jbc.M805371200

Lv, M., Zhang, D., Dai, D., Zhang, W., & Zhang, L. (2016). Sphingosine kinase 1/sphingosine-1-phosphate regulates the expression of interleukin-17A in activated microglia in cerebral ischemia/reperfusion. *Inflamm Res, 65*(7), 551-562.doi: 10.1007/s00011-016-0939-9

Ma, L., Zhang, H., Liu, N., Wang, P. Q., Guo, W. Z., Fu, Q., . . . Mi, W. D. (2016). TSPO ligand PK11195 alleviates neuroinflammation and beta-amyloid generation induced by systemic LPS administration. *Brain Res Bull, 121*, 192-200. doi:10.1016/j.brainresbull.2016.02.001

Ma, X., Liu, L., & Meng, J. (2017). MicroRNA-125b promotes neurons cell apoptosis and Tau phosphorylation in Alzheimer's disease. *Neurosci Lett, 661*, 57-62. doi: 10.1016/j.neulet.2017.09.043

Maeda, S., Sahara, N., Saito, Y., Murayama, S., Ikai, A., & Takashima, A. (2006). Increased levels of granular tau oligomers: an early sign of brain aging and Alzheimer's disease. *Neurosci Res, 54*(3), 197-201. doi: 10.1016/j.neures.2005.11.009

Mahley, R. W. (1988). Apolipoprotein E: cholesterol transport protein with expanding rolein cell biology. *Science, 240*(4852), 622-630. doi: 10.1126/science.3283935

Mahley, R. W., & Rall, S. C., Jr. (2000). Apolipoprotein E: far more than a lipid transport

protein. *Annu Rev Genomics Hum Genet, 1*, 507-537. doi: 10.1146/annurev.genom.1.1.507

Mai, H., Fan, W., Wang, Y., Cai, Y., Li, X., Chen, F., . . . Cui, L. (2019). Intranasal Administration of miR-146a Agomir Rescued the Pathological Process and Cognitive Impairment in an AD Mouse Model. *Mol Ther Nucleic Acids, 18*, 681-695. doi: 10.1016/j.omtn.2019.10.002

Maia, L. F., Kaeser, S. A., Reichwald, J., Hruscha, M., Martus, P., Staufenbiel, M., & Jucker, M. (2013). Changes in amyloid-β and Tau in the cerebrospinal fluid of transgenic mice overexpressing amyloid precursor protein. *Sci Transl Med, 5*(194),194re192. doi: 10.1126/scitranslmed.3006446

Makou, E., Herbert, A. P., & Barlow, P. N. (2013). Functional anatomy of complement factor H. *Biochemistry, 52*(23), 3949-3962. doi: 10.1021/bi4003452

Mandelkow, E., von Bergen, M., Biernat, J., & Mandelkow, E. M. (2007). Structural principles of tau and the paired helical filaments of Alzheimer's disease. *Brain Pathol, 17*(1), 83-90. doi: 10.1111/j.1750-3639.2007.00053.x

Mann, K. M., Thorngate, F. E., Katoh-Fukui, Y., Hamanaka, H., Williams, D. L., Fujita, S.,& Lamb, B. T. (2004). Independent effects of APOE on cholesterol metabolism andbrain Abeta levels in an Alzheimer disease mouse model. *Hum Mol Genet, 13*(17),1959-1968. doi: 10.1093/hmg/ddh199

Mannironi, C., Biundo, A., Rajendran, S., De Vito, F., Saba, L., Caioli, S., . . . Presutti, C. (2018). miR-135a Regulates Synaptic Transmission and Anxiety-Like Behavior inAmygdala. *Mol Neurobiol, 55*(4), 3301-3315. doi: 10.1007/s12035-017-0564-9

Mantile, F., & Prisco, A. (2020). Vaccination against β-Amyloid as a Strategy for the Prevention of Alzheimer's Disease. *Biology (Basel), 9*(12). doi: 10.3390/biology9120425

Marques, M. A., Owens, P. A., & Crutcher, K. A. (2004). Progress toward identification ofprotease activity involved in proteolysis of apolipoprotein e in human brain. *J Mol Neurosci, 24*(1), 73-80. doi: 10.1385/jmn:24:1:073

Marr, R. A., & Hafez, D. M. (2014). Amyloid-beta and Alzheimer's disease: the role of neprilysin-2 in amyloid-beta clearance. *Front Aging Neurosci, 6*, 187. doi: 10.3389/fnagi.2014.00187

Masurkar, A. V. (2018). Towards a circuit-level understanding of hippocampal CA1 dysfunction in Alzheimer's disease across anatomical axes. *J Alzheimers Dis*

Parkinsonism, 8(1).

Mattsson, N., Rosén, E., Hansson, O., Andreasen, N., Parnetti, L., Jonsson, M., . . . Zetterberg, H. (2012). Age and diagnostic performance of Alzheimer disease CSF biomarkers. *Neurology, 78*(7), 468-476. doi: 10.1212/WNL.0b013e3182477eed

Mazanetz, M. P., & Fischer, P. M. (2007). Untangling tau hyperphosphorylation in drug design for neurodegenerative diseases. *Nat Rev Drug Discov, 6*(6), 464-479. doi: 10.1038/nrd2111

McGowan, E., Sanders, S., Iwatsubo, T., Takeuchi, A., Saido, T., Zehr, C., . . . Duff, K. (1999). Amyloid phenotype characterization of transgenic mice overexpressing both mutant amyloid precursor protein and mutant presenilin 1 transgenes. *Neurobiol Dis, 6*(4), 231-244. doi: 10.1006/nbdi.1999.0243

McKeever, P. M., Schneider, R., Taghdiri, F., Weichert, A., Multani, N., Brown, R. A., . . . Tartaglia, M. C. (2018). MicroRNA Expression Levels Are Altered in the Cerebrospinal Fluid of Patients with Young-Onset Alzheimer's Disease. *Mol Neurobiol, 55*(12), 8826-8841. doi: 10.1007/s12035-018-1032-x

McLarnon, J. G., & Ryu, J. K. (2008). Relevance of abeta1-42 intrahippocampal injection as an animal model of inflamed Alzheimer's disease brain. *Curr Alzheimer Res, 5*(5), 475-480. doi: 10.2174/156720508785908874

McLinden, K. A., Kranjac, D., Deodati, L. E., Kahn, M., Chumley, M. J., & Boehm, G. W. (2012). Age exacerbates sickness behavior following exposure to a viral mimetic.*Physiol Behav, 105*(5), 1219-1225. doi: 10.1016/j.physbeh.2011.04.024

Medeiros, R., Baglietto-Vargas, D., & LaFerla, F. M. (2011). The role of tau in Alzheimer'sdisease and related disorders. *CNS Neurosci Ther, 17*(5), 514-524. doi: 10.1111/j.1755-5949.2010.00177.x

Mehla, J., Lacoursiere, S. G., Lapointe, V., McNaughton, B. L., Sutherland, R. J., McDonald, R. J., & Mohajerani, M. H. (2019). Age-dependent behavioral and biochemical characterization of single APP knock-in mouse (APP(NL-G-F/NL-G- F)) model of Alzheimer's disease. *Neurobiol Aging, 75*, 25-37. doi: 10.1016/j.neurobiolaging.2018.10.026

Meraz-Ríos, M. A., Toral-Rios, D., Franco-Bocanegra, D., Villeda-Hernández, J., & Campos-Peña, V. (2013). Inflammatory process in Alzheimer's Disease. *Front Integr Neurosci, 7*, 59. doi: 10.3389/fnint.2013.00059

Millan, M. J. (2017). Linking deregulation of non-coding RNA to the core pathophysiologyof Alzheimer's disease: An integrative review. *Prog Neurobiol,*

156, 1-68. doi: 10.1016/j.pneurobio.2017.03.004

Mineur, Y. S., McLoughlin, D., Crusio, W. E., & Sluyter, F. (2005). Genetic mouse models of Alzheimer's disease. *Neural Plast, 12*(4), 299-310. doi: 10.1155/np.2005.299

Miñano-Molina, A. J., España, J., Martín, E., Barneda-Zahonero, B., Fadó, R., Solé, M., .. . Rodríguez-Alvarez, J. (2011). Soluble oligomers of amyloid-β peptide disrupt membrane trafficking of α-amino-3-hydroxy-5-methylisoxazole-4-propionic acid receptor contributing to early synapse dysfunction. *J Biol Chem, 286*(31), 27311- 27321. doi: 10.1074/jbc.M111.227504

Miya Shaik, M., Tamargo, I. A., Abubakar, M. B., Kamal, M. A., Greig, N. H., & Gan, S. H. (2018). The Role of microRNAs in Alzheimer's Disease and Their Therapeutic Potentials. *Genes (Basel), 9*(4). doi: 10.3390/genes9040174

Morroni, F., Sita, G., Tarozzi, A., Rimondini, R., & Hrelia, P. (2016). Early effects of Aβ1- 42 oligomers injection in mice: Involvement of PI3K/Akt/GSK3 and MAPK/ERK1/2 pathways. *Behav Brain Res, 314*, 106-115. doi: 10.1016/j.bbr.2016.08.002

Mucke, L., Masliah, E., Yu, G. Q., Mallory, M., Rockenstein, E. M., Tatsuno, G., . . . McConlogue, L. (2000). High-level neuronal expression of abeta 1-42 in wild-typehuman amyloid protein precursor transgenic mice: synaptotoxicity without plaque formation. *J Neurosci, 20*(11), 4050-4058. doi: 10.1523/jneurosci.20-11-04050.2000

Mudò, G., Frinchi, M., Nuzzo, D., Scaduto, P., Plescia, F., Massenti, M. F., . . . Grimaldi, M. (2019). Anti-inflammatory and cognitive effects of interferon-β1a (IFNβ1a) ina rat model of Alzheimer's disease. *J Neuroinflammation, 16*(1), 44. doi: 10.1186/s12974-019-1417-4

Mukrasch, M. D., Bibow, S., Korukottu, J., Jeganathan, S., Biernat, J., Griesinger, C., . . .Zweckstetter, M. (2009). Structural polymorphism of 441-residue tau at single residue resolution. *PLoS Biol, 7*(2), e34. doi: 10.1371/journal.pbio.1000034

Mullard, A. (2016). Alzheimer amyloid hypothesis lives on. *Nat Rev Drug Discov, 16*(1), 3-5. doi: 10.1038/nrd.2016.281

Muñoz, S. S., Garner, B., & Ooi, L. (2019). Understanding the Role of ApoE Fragments inAlzheimer's Disease. *Neurochem Res, 44*(6), 1297-1305. doi: 10.1007/s11064-018-2629-1

Muralidar, S., Ambi, S. V., Sekaran, S., Thirumalai, D., & Palaniappan, B. (2020). Role

oftau protein in Alzheimer's disease: The prime pathological player. *Int J Biol Macromol, 163*, 1599-1617. doi: 10.1016/j.ijbiomac.2020.07.327

Murrell, J., Farlow, M., Ghetti, B., & Benson, M. D. (1991). A mutation in the amyloid precursor protein associated with hereditary Alzheimer's disease. *Science, 254*(5028), 97-99. doi: 10.1126/science.1925564

Nadler, Y., Alexandrovich, A., Grigoriadis, N., Hartmann, T., Rao, K. S., Shohami, E., & Stein, R. (2008). Increased expression of the gamma-secretase components presenilin-1 and nicastrin in activated astrocytes and microglia following traumaticbrain injury. *Glia, 56*(5), 552-567. doi: 10.1002/glia.20638

Nakamura, T., Watanabe, A., Fujino, T., Hosono, T., & Michikawa, M. (2009). Apolipoprotein E4 (1-272) fragment is associated with mitochondrial proteins and affects mitochondrial function in neuronal cells. *Mol Neurodegener, 4*, 35. doi: 10.1186/1750-1326-4-35

Naseri, N. N., Wang, H., Guo, J., Sharma, M., & Luo, W. (2019). The complexity of tau in Alzheimer's disease. *Neurosci Lett, 705*, 183-194. doi: 10.1016/j.neulet.2019.04.022

Nell, H. J., Whitehead, S. N., & Cechetto, D. F. (2015). Age-Dependent Effect of β-Amyloid Toxicity on Basal Forebrain Cholinergic Neurons and Inflammation in the Rat Brain. *Brain Pathol, 25*(5), 531-542. doi: 10.1111/bpa.12199

Nunez-Iglesias, J., Liu, C. C., Morgan, T. E., Finch, C. E., & Zhou, X. J. (2010). Joint genome-wide profiling of miRNA and mRNA expression in Alzheimer's disease cortex reveals altered miRNA regulation. *PLoS One, 5*(2), e8898. doi: 10.1371/journal.pone.0008898

Nygaard, H. B., van Dyck, C. H., & Strittmatter, S. M. (2014). Fyn kinase inhibition as a novel therapy for Alzheimer's disease. *Alzheimers Res Ther, 6*(1), 8. doi: 10.1186/alzrt238

O'Brien, R. J., & Wong, P. C. (2011). Amyloid precursor protein processing and Alzheimer's disease. *Annu Rev Neurosci, 34*, 185-204. doi: 10.1146/annurev-neuro-061010-113613

Oakley, H., Cole, S. L., Logan, S., Maus, E., Shao, P., Craft, J., . . . Vassar, R. (2006). Intraneuronal beta-amyloid aggregates, neurodegeneration, and neuron loss in transgenic mice with five familial Alzheimer's disease mutations: potential factors in amyloid plaque formation. *J Neurosci, 26*(40), 10129-10140. doi: 10.1523/jneurosci.1202-06.2006

Oddo, S., Caccamo, A., Kitazawa, M., Tseng, B. P., & LaFerla, F. M. (2003). Amyloid deposition precedes tangle formation in a triple transgenic model of Alzheimer's disease. *Neurobiol* Aging, 24(8), 1063-1070. doi: 10.1016/j.neurobiolaging.2003.08.012

Olivieri, F., Lazzarini, R., Recchioni, R., Marcheselli, F., Rippo, M. R., Di Nuzzo, S., . . . Procopio, A. D. (2013). MiR-146a as marker of senescence-associated pro-inflammatory status in cells involved in vascular remodelling. *Age (Dordr), 35*(4), 1157-1172. doi: 10.1007/s11357-012-9440-8

Olsson, F., Schmidt, S., Althoff, V., Munter, L. M., Jin, S., Rosqvist, S., . . . Lundkvist, J. (2014). Characterization of intermediate steps in amyloid beta (Aβ) production under near-native conditions. *J Biol Chem, 289*(3), 1540-1550. doi: 10.1074/jbc.M113.498246

Ono, K. (2018). Alzheimer's disease as oligomeropathy. *Neurochem Int, 119*, 57-70. doi: 10.1016/j.neuint.2017.08.010

Ophir, G., Meilin, S., Efrati, M., Chapman, J., Karussis, D., Roses, A., & Michaelson, D. M. (2003). Human apoE3 but not apoE4 rescues impaired astrocyte activation in apoE null mice. Neurobiol Dis, 12(1), 56-64. doi: 10.1016/s0969-9961(02)00005-0

Owens, R., Grabert, K., Davies, C. L., Alfieri, A., Antel, J. P., Healy, L. M., & McColl, B. W. (2017). Corrigendum: Divergent Neuroinflammatory Regulation of Microglial TREM Expression and Involvement of NF-κB. *Front Cell Neurosci, 11*, 256. doi: 10.3389/fncel.2017.00256

Pangalos, M. N., Shioi, J., Efthimiopoulos, S., Wu, A., & Robakis, N. K. (1996). Characterization of appican, the chondroitin sulfate proteoglycan form of the Alzheimer amyloid precursor protein. *Neurodegeneration, 5*(4), 445-451. doi: 10.1006/neur.1996.0061

Pantieri, R., Pardini, M., Cecconi, M., Dagna-Bricarelli, F., Vitali, A., Piccini, A., . . . Tabaton, M. (2005). A novel presenilin 1 L166H mutation in a pseudo-sporadic case of early-onset Alzheimer's disease. *Neurol Sci, 26*(5), 349-350. doi: 10.1007/s10072-005-0499-1

Patil, S., Melrose, J., & Chan, C. (2007). Involvement of astroglial ceramide in palmitic acid-induced Alzheimer-like changes in primary neurons. *Eur J Neurosci, 26*(8), 2131-2141. doi: 10.1111/j.1460-9568.2007.05797.x

Patterson, K. R., Remmers, C., Fu, Y., Brooker, S., Kanaan, N. M., Vana, L., . . . Binder,

L. I. (2011). Characterization of prefibrillar Tau oligomers in vitro and in Alzheimer disease. *J Biol Chem, 286*(26), 23063-23076. doi: 10.1074/jbc.M111.237974

Paulson, J. B., Ramsden, M., Forster, C., Sherman, M. A., McGowan, E., & Ashe, K. H. (2008). Amyloid plaque and neurofibrillary tangle pathology in a regulatable mouse model of Alzheimer's disease. *Am J Pathol, 173*(3), 762-772. doi: 10.2353/ajpath.2008.080175

Pegg, C. C., He, C., Stroink, A. R., Kattner, K. A., & Wang, C. X. (2010). Technique for collection of cerebrospinal fluid from the cisterna magna in rat. *J Neurosci Methods, 187*(1), 8-12. doi: 10.1016/j.jneumeth.2009.12.002

Pepeu, G., & Giovannini, M. G. (2004). Changes in acetylcholine extracellular levels duringcognitive processes. *Learn Mem, 11*(1), 21-27. doi: 10.1101/lm.68104

Petersen, R. C., Smith, G. E., Waring, S. C., Ivnik, R. J., Tangalos, E. G., & Kokmen, E. (1999). Mild cognitive impairment: clinical characterization and outcome. *Arch Neurol, 56*(3), 303-308. doi: 10.1001/archneur.56.3.303

Petrasek, T., Skurlova, M., Maleninska, K., Vojtechova, I., Kristofikova, Z., Matuskova, H.,. . . Stuchlik, A. (2016). A Rat Model of Alzheimer's Disease Based on Abeta42 and Pro-oxidative Substances Exhibits Cognitive Deficit and Alterations in Glutamatergic and Cholinergic Neurotransmitter Systems. *Front Aging Neurosci, 8*, 83. doi: 10.3389/fnagi.2016.00083

Pluta, R., Kocki, J., Ułamek-Kozioł, M., Bogucka-Kocka, A., Gil-Kulik, P., Januszewski, S.,. . . Czuczwar, S. J. (2016). Alzheimer-associated presenilin 2 gene is dysregulatedin rat medial temporal lobe cortex after complete brain ischemia due to cardiac arrest. *Pharmacol Rep, 68*(1), 155-161. doi: 10.1016/j.pharep.2015.08.002

Pogue, A. I., Cui, J. G., Li, Y. Y., Zhao, Y., Culicchia, F., & Lukiw, W. J. (2010). Micro RNA-125b (miRNA-125b) function in astrogliosis and glial cell proliferation. *Neurosci Lett, 476*(1), 18-22. doi: 10.1016/j.neulet.2010.03.054

Pogue, A. I., Li, Y. Y., Cui, J. G., Zhao, Y., Kruck, T. P., Percy, M. E., . . . Lukiw, W. J. (2009). Characterization of an NF-kappaB-regulated, miRNA-146a-mediated down-regulation of complement factor H (CFH) in metal-sulfate-stressed human brain cells. *J Inorg Biochem, 103*(11), 1591-1595. doi: 10.1016/j.jinorgbio.2009.05.012

Pogue, A. I., & Lukiw, W. J. (2004). Angiogenic signaling in Alzheimer's disease.

Neuroreport, 15(9), 1507-1510. doi: 10.1097/01.wnr.0000130539.39937.1d

Pogue, A. I., & Lukiw, W. J. (2018). Up-regulated Pro-inflammatory MicroRNAs (miRNAs)in Alzheimer's disease (AD) and Age-Related Macular Degeneration (AMD). *Cell Mol Neurobiol, 38*(5), 1021-1031. doi: 10.1007/s10571-017-0572-3

Poirier, J. (2008). Apolipoprotein E represents a potent gene-based therapeutic target for the treatment of sporadic Alzheimer's disease. *Alzheimers Dement, 4*(1 Suppl 1), S91-97. doi: 10.1016/j.jalz.2007.11.012

Prakash, A., Kalra, J. K., & Kumar, A. (2015). Neuroprotective effect of N-acetyl cysteine against streptozotocin-induced memory dysfunction and oxidative damage in rats. *J Basic Clin Physiol Pharmacol, 26*(1), 13-23. doi: 10.1515/jbcpp-2013-0150

Prut, L., Abramowski, D., Krucker, T., Levy, C. L., Roberts, A. J., Staufenbiel, M., & Wiessner, C. (2007). Aged APP23 mice show a delay in switching to the use of a strategy in the Barnes maze. *Behav Brain Res, 179*(1), 107-110. doi: 10.1016/j.bbr.2007.01.017

Qiu, C., Kivipelto, M., & von Strauss, E. (2009). Epidemiology of Alzheimer's disease: occurrence, determinants, and strategies toward intervention. *Dialogues Clin Neurosci, 11*(2), 111-128. doi: 10.31887/DCNS.2009.11.2/cqiu

Qu, X., Yuan, F. N., Corona, C., Pasini, S., Pero, M. E., Gundersen, G. G., . . . Bartolini, F. (2017). Stabilization of dynamic microtubules by mDia1 drives Tau-dependent Aβ(1-42) synaptotoxicity. *J Cell Biol, 216*(10), 3161-3178. doi: 10.1083/jcb.201701045

Querfurth, H. W., & LaFerla, F. M. (2010). Alzheimer's disease. *N Engl J Med, 362*(4), 329-344. doi: 10.1056/NEJMra0909142

Radde, R., Bolmont, T., Kaeser, S. A., Coomaraswamy, J., Lindau, D., Stoltze, L., . . . Jucker, M. (2006). Abeta42-driven cerebral amyloidosis in transgenic mice reveals early and robust pathology. *EMBO Rep, 7*(9), 940-946. doi: 10.1038/sj.embor.7400784

Ramsden, M., Kotilinek, L., Forster, C., Paulson, J., McGowan, E., SantaCruz, K., . . . Ashe, K. H. (2005). Age-dependent neurofibrillary tangle formation, neuron loss, and memory impairment in a mouse model of human tauopathy (P301L). *J Neurosci, 25*(46), 10637-10647. doi: 10.1523/jneurosci.3279-05.2005

Ravari, A., Mirzaei, T., Kennedy, D., & Kazemi Arababadi, M. (2017).

Chronoinflammagingin Alzheimer; A systematic review on the roles of toll like receptor 2. *Life Sci, 171*,16-20. doi: 10.1016/j.lfs.2017.01.003

Recuero, M., Serrano, E., Bullido, M. J., & Valdivieso, F. (2004). Abeta production as consequence of cellular death of a human neuroblastoma overexpressing APP. *FEBS Lett, 570*(1-3), 114-118. doi: 10.1016/j.febslet.2004.06.025

Reddy, P. H., Mani, G., Park, B. S., Jacques, J., Murdoch, G., Whetsell, W., Jr., . . . Manczak, M. (2005). Differential loss of synaptic proteins in Alzheimer's disease: implications for synaptic dysfunction. *J Alzheimers Dis, 7*(2), 103-117; discussion 173-180. doi: 10.3233/jad-2005-7203

Reddy, P. H., Tripathi, R., Troung, Q., Tirumala, K., Reddy, T. P., Anekonda, V., . . . Manczak, M. (2012). Abnormal mitochondrial dynamics and synaptic degeneration as early events in Alzheimer's disease: implications to mitochondria-targeted antioxidant therapeutics. *Biochim Biophys Acta, 1822*(5), 639-649. doi: 10.1016/j.bbadis.2011.10.011

Reimer, T., Brcic, M., Schweizer, M., & Jungi, T. W. (2008). poly(I:C) and LPS induce distinct IRF3 and NF-kappaB signaling during type-I IFN and TNF responses in human macrophages. *J Leukoc Biol, 83*(5), 1249-1257. doi: 10.1189/jlb.0607412

Reiserer, R. S., Harrison, F. E., Syverud, D. C., & McDonald, M. P. (2007). Impaired spatial learning in the APPSwe + PSEN1DeltaE9 bigenic mouse model of Alzheimer's disease. Genes Brain Behav, 6(1), 54-65. doi: 10.1111/j.1601-183X.2006.00221.x

Reverchon, F., de Concini, V., Larrigaldie, V., Benmerzoug, S., Briault, S., Togbé, D., . . . Menuet, A. (2020). Hippocampal interleukin-33 mediates neuroinflammation- induced cognitive impairments. *J Neuroinflammation, 17*(1), 268. doi: 10.1186/s12974-020-01939-6

Riancho, J., Vázquez-Higuera, J. L., Pozueta, A., Lage, C., Kazimierczak, M., Bravo, M.,. . . Sánchez-Juan, P. (2017). MicroRNA Profile in Patients with Alzheimer's Disease: Analysis of miR-9-5p and miR-598 in Raw and Exosome Enriched Cerebrospinal Fluid Samples. *J Alzheimers Dis, 57*(2), 483-491. doi: 10.3233/jad-161179

Roberts, G. W., Gentleman, S. M., Lynch, A., Murray, L., Landon, M., & Graham, D. I. (1994). Beta amyloid protein deposition in the brain after severe head injury: implications for the pathogenesis of Alzheimer's disease. *J Neurol Neurosurg*

Psychiatry, 57(4), 419-425. doi: 10.1136/jnnp.57.4.419

Rohan de Silva, H. A., Jen, A., Wickenden, C., Jen, L. S., Wilkinson, S. L., & Patel, A. J. (1997). Cell-specific expression of beta-amyloid precursor protein isoform mRNAsand proteins in neurons and astrocytes. *Brain Res Mol Brain Res, 47*(1-2), 147- 156. doi: 10.1016/s0169-328x(97)00045-4

Rohn, T. T. (2013). Proteolytic cleavage of apolipoprotein E4 as the keystone for the heightened risk associated with Alzheimer's disease. *Int J Mol Sci, 14*(7), 14908-14922. doi: 10.3390/ijms140714908

Rohn, T. T., Catlin, L. W., Coonse, K. G., & Habig, J. W. (2012). Identification of an amino-terminal fragment of apolipoprotein E4 that localizes to neurofibrillary tangles of the Alzheimer's disease brain. *Brain Res, 1475*, 106-115. doi: 10.1016/j.brainres.2012.08.003

Roselli, F., Hutzler, P., Wegerich, Y., Livrea, P., & Almeida, O. F. (2009). Disassembly of shank and homer synaptic clusters is driven by soluble beta-amyloid(1-40) through divergent NMDAR-dependent signalling pathways. *PLoS One, 4*(6), e6011. doi: 10.1371/journal.pone.0006011

Roshan, R., Shridhar, S., Sarangdhar, M. A., Banik, A., Chawla, M., Garg, M., . . . Pillai, B. (2014). Brain-specific knockdown of miR-29 results in neuronal cell death and ataxia in mice. *RNA, 20*(8), 1287-1297. doi: 10.1261/rna.044008.113

Ruckdeschel, K., Pfaffinger, G., Haase, R., Sing, A., Weighardt, H., Häcker, G., . . . Heesemann, J. (2004). Signaling of apoptosis through TLRs critically involves toll/IL-1 receptor domain-containing adapter inducing IFN-beta, but not MyD88, inbacteria-infected murine macrophages. *J Immunol, 173*(5), 3320-3328. doi: 10.4049/jimmunol.173.5.3320

Rusca, N., & Monticelli, S. (2011). MiR-146a in Immunity and Disease. *Mol Biol Int, 2011*,437301. doi: 10.4061/2011/437301

Ryan, M. M., Guévremont, D., Mockett, B. G., Abraham, W. C., & Williams, J. M. (2018). Circulating Plasma microRNAs are Altered with Amyloidosis in a Mouse Model of Alzheimer's Disease. *J Alzheimers Dis, 66*(2), 835-852. doi: 10.3233/jad-180385

Sadigh-Eteghad, S., Sabermarouf, B., Majdi, A., Talebi, M., Farhoudi, M., & Mahmoudi, J.(2015). Amyloid-beta: a crucial factor in Alzheimer's disease. *Med Princ Pract, 24*(1), 1-10. doi: 10.1159/000369101

Saito, T., Matsuba, Y., Mihira, N., Takano, J., Nilsson, P., Itohara, S., . . . Saido, T. C.

(2014). Single App knock-in mouse models of Alzheimer's disease. *Nat Neurosci,17*(5), 661-663. doi: 10.1038/nn.3697

Salkovic-Petrisic, M., Osmanovic-Barilar, J., Brückner, M. K., Hoyer, S., Arendt, T., & Riederer, P. (2011). Cerebral amyloid angiopathy in streptozotocin rat model of sporadic Alzheimer's disease: a long-term follow up study. *J Neural Transm (Vienna), 118*(5), 765-772. doi: 10.1007/s00702-011-0651-4

Salminen, A., Kaarniranta, K., Haapasalo, A., Soininen, H., & Hiltunen, M. (2011). AMP- activated protein kinase: a potential player in Alzheimer's disease. *J Neurochem, 118*(4), 460-474. doi: 10.1111/j.1471-4159.2011.07331.x

Santacruz, K., Lewis, J., Spires, T., Paulson, J., Kotilinek, L., Ingelsson, M., . . . Ashe, K. H. (2005). Tau suppression in a neurodegenerative mouse model improves memory function. *Science, 309*(5733), 476-481. doi: 10.1126/science.1113694

Savonenko, A., Xu, G. M., Melnikova, T., Morton, J. L., Gonzales, V., Wong, M. P., . . . Borchelt, D. R. (2005). Episodic-like memory deficits in the APPswe/PS1dE9 mouse model of Alzheimer's disease: relationships to beta-amyloid deposition and neurotransmitter abnormalities. *Neurobiol Dis, 18*(3), 602-617. doi: 10.1016/j.nbd.2004.10.022

Scuderi, C., Stecca, C., Valenza, M., Ratano, P., Bronzuoli, M. R., Bartoli, S., . . . Steardo, L. (2014). Palmitoylethanolamide controls reactive gliosis and exerts neuroprotective functions in a rat model of Alzheimer's disease. *Cell Death Dis, 5*(9), e1419. doi: 10.1038/cddis.2014.376

Schaffer, S., Asseburg, H., Kuntz, S., Muller, W. E., & Eckert, G. P. (2012). Effects of polyphenols on brain ageing and Alzheimer's disease: focus on mitochondria. *MolNeurobiol, 46*(1), 161-178. doi: 10.1007/s12035-012-8282-9

Schonrock, N., Ke, Y. D., Humphreys, D., Staufenbiel, M., Ittner, L. M., Preiss, T., & Götz, J. (2010). Neuronal microRNA deregulation in response to Alzheimer's disease amyloid-beta. *PLoS One, 5*(6), e11070. doi: 10.1371/journal.pone.0011070

Selkoe, D. J. (2001). Alzheimer's disease: genes, proteins, and therapy. *Physiol Rev, 81*(2), 741-766. doi: 10.1152/physrev.2001.81.2.741

Selmaj, I., Cichalewska, M., Namiecinska, M., Galazka, G., Horzelski, W., Selmaj, K. W.,& Mycko, M. P. (2017). Global exosome transcriptome profiling reveals biomarkers for multiple sclerosis. *Ann Neurol, 81*(5), 703-717. doi: 10.1002/ana.24931

Sen, R. (2011). The origins of NF-κB. *Nat Immunol, 12*(8), 686-688. doi: 10.1038/ni.2071

Sengupta, U., Portelius, E., Hansson, O., Farmer, K., Castillo-Carranza, D., Woltjer, R., .. . Kayed, R. (2017). Tau oligomers in cerebrospinal fluid in Alzheimer's disease. *Ann Clin Transl Neurol, 4*(4), 226-235. doi: 10.1002/acn3.382

Shaffer, J. L., Petrella, J. R., Sheldon, F. C., Choudhury, K. R., Calhoun, V. D., Coleman, R. E., & Doraiswamy, P. M. (2013). Predicting cognitive decline in subjects at riskfor Alzheimer disease by using combined cerebrospinal fluid, MR imaging, and PET biomarkers. *Radiology, 266*(2), 583-591. doi: 10.1148/radiol.12120010

Shahani, N., & Brandt, R. (2002). Functions and malfunctions of the tau proteins. *Cell MolLife Sci, 59*(10), 1668-1680. doi: 10.1007/pl00012495

Shankar, G. M., & Walsh, D. M. (2009). Alzheimer's disease: synaptic dysfunction andAbeta. *Mol Neurodegener, 4*, 48. doi: 10.1186/1750-1326-4-48

Sharma, P., & Roy, K. (2020). ROCK-2-selective targeting and its therapeutic outcomes. *Drug Discov Today, 25*(2), 446-455. doi: 10.1016/j.drudis.2019.11.017

Sharma, S., Verma, S., Kapoor, M., Saini, A., & Nehru, B. (2016). Alzheimer's disease likepathology induced six weeks after aggregated amyloid-beta injection in rats: increased oxidative stress and impaired long-term memory with anxiety-like behavior. *Neurol Res, 38*(9), 838-850. doi: 10.1080/01616412.2016.1209337

Shimeld, S. M., Degnan, B., & Luke, G. N. (2010). Evolutionary genomics of the Fox genes: origin of gene families and the ancestry of gene clusters. *Genomics, 95*(5), 256-260. doi: 10.1016/j.ygeno.2009.08.002

Shioya, M., Obayashi, S., Tabunoki, H., Arima, K., Saito, Y., Ishida, T., & Satoh, J. (2010). Aberrant microRNA expression in the brains of neurodegenerative diseases: miR- 29a decreased in Alzheimer disease brains targets neurone navigator 3. *Neuropathol Appl Neurobiol, 36*(4), 320-330. doi: 10.1111/j.1365-2990.2010.01076.x

Siedlecki-Wullich, D., Català-Solsona, J., Fábregas, C., Hernández, I., Clarimon, J., Lleó,A., . . . Miñano-Molina, A. J. (2019). Altered microRNAs related to synaptic functionas potential plasma biomarkers for Alzheimer's disease. *Alzheimers Res Ther, 11*(1), 46. doi: 10.1186/s13195-019-0501-4

Sly, L. M., Krzesicki, R. F., Brashler, J. R., Buhl, A. E., McKinley, D. D., Carter, D. B., & Chin, J. E. (2001). Endogenous brain cytokine mRNA and inflammatory responsesto lipopolysaccharide are elevated in the Tg2576 transgenic mouse

model of Alzheimer's disease. *Brain Res Bull, 56*(6), 581-588. doi: 10.1016/s0361- 9230(01)00730-4

Smith, A. D. (2002). Imaging the progression of Alzheimer pathology through the brain. *Proc Natl Acad Sci U S A, 99*(7), 4135-4137. doi: 10.1073/pnas.082107399

Solà, C., Casal, C., Tusell, J. M., & Serratosa, J. (2002). Astrocytes enhance lipopolysaccharide-induced nitric oxide production by microglial cells. *Eur J Neurosci, 16*(7), 1275-1283. doi: 10.1046/j.1460-9568.2002.02199.x

Söllvander, S., Nikitidou, E., Brolin, R., Söderberg, L., Sehlin, D., Lannfelt, L., & Erlandsson, A. (2016). Accumulation of amyloid-β by astrocytes result in enlarged endosomes and microvesicle-induced apoptosis of neurons. *Mol Neurodegener, 11*(1), 38. doi: 10.1186/s13024-016-0098-z

Sommer, L. (2011). Generation of melanocytes from neural crest cells. *Pigment Cell Melanoma Res, 24*(3), 411-421. doi: 10.1111/j.1755-148X.2011.00834.x

Souza, V. C., Morais, G. S., Jr., Henriques, A. D., Machado-Silva, W., Perez, D. I. V., Brito, C. J., . . . Nóbrega, O. T. (2020). Whole-Blood Levels of MicroRNA-9 Are Decreased in Patients With Late-Onset Alzheimer Disease. *Am J Alzheimers Dis Other Demen, 35*, 1533317520911573. doi: 10.1177/1533317520911573

Sperling, R. A., Aisen, P. S., Beckett, L. A., Bennett, D. A., Craft, S., Fagan, A. M., . . . Phelps, C. H. (2011). Toward defining the preclinical stages of Alzheimer's disease: recommendations from the National Institute on Aging-Alzheimer's Association workgroups on diagnostic guidelines for Alzheimer's disease. *Alzheimers Dement, 7*(3), 280-292. doi: 10.1016/j.jalz.2011.03.003

Srinivasan, M., & Lahiri, D. K. (2015). Significance of NF-κB as a pivotal therapeutic targetin the neurodegenerative pathologies of Alzheimer's disease and multiple sclerosis. *Expert Opin Ther Targets, 19*(4), 471-487. doi: 10.1517/14728222.2014.989834

Strac, D. S., Muck-Seler, D., & Pivac, N. (2015). Neurotransmitter measures in the cerebrospinal fluid of patients with Alzheimer's disease: a review. *Psychiatr Danub,27*(1), 14-24.

Sturchler-Pierrat, C., Abramowski, D., Duke, M., Wiederhold, K. H., Mistl, C., Rothacher, S., . . . Sommer, B. (1997). Two amyloid precursor protein transgenic mouse models with Alzheimer disease-like pathology. *Proc Natl Acad Sci U S A, 94*(24), 13287-13292. doi: 10.1073/pnas.94.24.13287

Sudduth, T. L., Schmitt, F. A., Nelson, P. T., & Wilcock, D. M. (2013). Neuroinflammatoryphenotype in early Alzheimer's disease. *Neurobiol Aging, 34*(4), 1051-1059. doi: 10.1016/j.neurobiolaging.2012.09.012

Sun, X., Chen, W. D., & Wang, Y. D. (2015). β-Amyloid: the key peptide in the pathogenesis of Alzheimer's disease. *Front Pharmacol, 6*, 221. doi: 10.3389/fphar.2015.00221

Swarbrick, S., Wragg, N., Ghosh, S., & Stolzing, A. (2019). Systematic Review of miRNAas Biomarkers in Alzheimer's Disease. *Mol Neurobiol, 56*(9), 6156-6167. doi: 10.1007/s12035-019-1500-y

Taganov, K. D., Boldin, M. P., Chang, K. J., & Baltimore, D. (2006). NF-kappaB-dependentinduction of microRNA miR-146, an inhibitor targeted to signaling proteins of innateimmune responses. *Proc Natl Acad Sci U S A, 103*(33), 12481-12486. doi:10.1073/pnas.0605298103

Takami, M., Nagashima, Y., Sano, Y., Ishihara, S., Morishima-Kawashima, M., Funamoto,S., & Ihara, Y. (2009). gamma-Secretase: successive tripeptide and tetrapeptide release from the transmembrane domain of beta-carboxyl terminal fragment. *J Neurosci, 29*(41), 13042-13052. doi: 10.1523/jneurosci.2362-09.2009

Takousis, P., Sadlon, A., Schulz, J., Wohlers, I., Dobricic, V., Middleton, L., . . . Bertram, L. (2019). Differential expression of microRNAs in Alzheimer's disease brain, blood, and cerebrospinal fluid. *Alzheimers Dement, 15*(11), 1468-1477. doi: 10.1016/j.jalz.2019.06.4952

Tan, L., Yu, J. T., Liu, Q. Y., Tan, M. S., Zhang, W., Hu, N., . . . Tan, L. (2014). CirculatingmiR-125b as a biomarker of Alzheimer's disease. *J Neurol Sci, 336*(1-2), 52-56. doi: 10.1016/j.jns.2013.10.002

Tan, L., Yu, J. T., Tan, M. S., Liu, Q. Y., Wang, H. F., Zhang, W., . . . Tan, L. (2014). Genome-wide serum microRNA expression profiling identifies serum biomarkers for Alzheimer's disease. *J Alzheimers Dis, 40*(4), 1017-1027. doi: 10.3233/jad- 132144

Tang, K., Wang, C., Shen, C., Sheng, S., Ravid, R., & Jing, N. (2003). Identification of a novel alternative splicing isoform of human amyloid precursor protein gene, APP639. *Eur J Neurosci, 18*(1), 102-108. doi: 10.1046/j.1460-9568.2003.02731.x

Townsend, M., Shankar, G. M., Mehta, T., Walsh, D. M., & Selkoe, D. J. (2006). Effects ofsecreted oligomers of amyloid beta-protein on hippocampal synaptic plasticity: a potent role for trimers. *J Physiol, 572*(Pt 2), 477-492. doi: 10.1113/jphysiol.2005.103754

Tulving, E., & Markowitsch, H. J. (1998). Episodic and declarative memory: role of the hippocampus. *Hippocampus, 8*(3), 198-204. doi: 10.1002/(sici)1098-1063(1998)8:3<198::aid-hipo2>3.0.co;2-g

Tuppo, E. E., & Arias, H. R. (2005). The role of inflammation in Alzheimer's disease. *Int JBiochem Cell Biol, 37*(2), 289-305. doi: 10.1016/j.biocel.2004.07.009

Turner, N. C., Strauss, S. J., Sarker, D., Gillmore, R., Kirkwood, A., Hackshaw, A., . . . Meyer, T. (2010). Chemotherapy with 5-fluorouracil, cisplatin and streptozocin for neuroendocrine tumours. *Br J Cancer, 102*(7), 1106-1112. doi: 10.1038/sj.bjc.6605618

Uddin, M. S., Kabir, M. T., Al Mamun, A., Abdel-Daim, M. M., Barreto, G. E., & Ashraf, G. M. (2019). APOE and Alzheimer's Disease: Evidence Mounts that Targeting APOE4 may Combat Alzheimer's Pathogenesis. *Mol Neurobiol, 56*(4), 2450-2465.doi: 10.1007/s12035-018-1237-z

Unno, K., Takabayashi, F., Yoshida, H., Choba, D., Fukutomi, R., Kikunaga, N., . . . Hoshino, M. (2007). Daily consumption of green tea catechin delays memory regression in aged mice. *Biogerontology, 8*(2), 89-95. doi: 10.1007/s10522-006-9036-8

Valls-Pedret, C., Molinuevo, J. L., & Rami, L. (2010). [Early diagnosis of Alzheimer's disease: the prodromal and preclinical phase]. *Rev Neurol, 51*(8), 471-480.

van Battum, E. Y., Verhagen, M. G., Vangoor, V. R., Fujita, Y., Derijck, Aaha, O'Duibhir, E., . . . Pasterkamp, R. J. (2018). An Image-Based miRNA Screen Identifies miRNA-135s As Regulators of CNS Axon Growth and Regeneration by Targeting Krüppel-like Factor 4. *J Neurosci, 38*(3), 613-630. doi: 10.1523/jneurosci.0662-17.2017

Verkhratsky, A., Sofroniew, M. V., Messing, A., deLanerolle, N. C., Rempe, D., Rodríguez, J. J., & Nedergaard, M. (2012). Neurological diseases as primary gliopathies: a reassessment of neurocentrism. *ASN Neuro, 4*(3). doi: 10.1042/an20120010

Vetrivel, K. S., Cheng, H., Kim, S. H., Chen, Y., Barnes, N. Y., Parent, A. T., . . . Thinakaran, G. (2005). Spatial segregation of gamma-secretase and substrates in

distinct membrane domains. *J Biol Chem, 280*(27), 25892-25900. doi: 10.1074/jbc.M503570200

Vigneron, N., Meryet-Figuière, M., Guttin, A., Issartel, J. P., Lambert, B., Briand, M., . . . Denoyelle, C. (2016). Towards a new standardized method for circulating miRNAsprofiling in clinical studies: Interest of the exogenous normalization to improve miRNA signature accuracy. *Mol Oncol, 10*(7), 981-992. doi: 10.1016/j.molonc.2016.03.005

von Bergen, M., Friedhoff, P., Biernat, J., Heberle, J., Mandelkow, E. M., & Mandelkow, E. (2000). Assembly of tau protein into Alzheimer paired helical filaments depends on a local sequence motif ((306)VQIVYK(311)) forming beta structure. *Proc Natl Acad Sci U S A, 97*(10), 5129-5134. doi: 10.1073/pnas.97.10.5129

Vuono, R., Winder-Rhodes, S., de Silva, R., Cisbani, G., Drouin-Ouellet, J., Spillantini, M.G., . . . Barker, R. A. (2015). The role of tau in the pathological process and clinicalexpression of Huntington's disease. *Brain, 138*(Pt 7), 1907-1918. doi: 10.1093/brain/awv107

Wang, H., Liu, J., Zong, Y., Xu, Y., Deng, W., Zhu, H., . . . Qin, C. (2010). miR-106b aberrantly expressed in a double transgenic mouse model for Alzheimer's disease targets TGF-β type II receptor. *Brain Res, 1357*, 166-174. doi: 10.1016/j.brainres.2010.08.023

Wang, L. L., Huang, Y., Wang, G., & Chen, S. D. (2012). The potential role of microRNA-146 in Alzheimer's disease: biomarker or therapeutic target? *Med Hypotheses, 78*(3), 398-401. doi: 10.1016/j.mehy.2011.11.019

Wang, L. M., Wu, Q., Kirk, R. A., Horn, K. P., Ebada Salem, A. H., Hoffman, J. M., . . . Morton, K. A. (2018). Lipopolysaccharide endotoxemia induces amyloid-β and p-tau formation in the rat brain. *Am J Nucl Med Mol Imaging, 8*(2), 86-99.

Wang, M., Qin, L., & Tang, B. (2019). MicroRNAs in Alzheimer's Disease. *Front Genet, 10*, 153. doi: 10.3389/fgene.2019.00153

Wang, W. X., Huang, Q., Hu, Y., Stromberg, A. J., & Nelson, P. T. (2011). Patterns of microRNA expression in normal and early Alzheimer's disease human temporal cortex: white matter versus gray matter. *Acta Neuropathol, 121*(2), 193-205. doi: 10.1007/s00401-010-0756-0

Watanabe, H., Iqbal, M., Zheng, J., Wines-Samuelson, M., & Shen, J. (2014). Partial loss of presenilin impairs age-dependent neuronal survival in the cerebral cortex. *J*

Neurosci, 34(48), 15912-15922. doi: 10.1523/jneurosci.3261-14.2014

Weber, J. A., Baxter, D. H., Zhang, S., Huang, D. Y., Huang, K. H., Lee, M. J., . . . Wang, K. (2010). The microRNA spectrum in 12 body fluids. *Clin Chem, 56*(11), 1733-1741. doi: 10.1373/clinchem.2010.147405

Webster, S. J., Bachstetter, A. D., Nelson, P. T., Schmitt, F. A., & Van Eldik, L. J. (2014).Using mice to model Alzheimer's dementia: an overview of the clinical disease andthe preclinical behavioral changes in 10 mouse models. *Front Genet, 5*, 88. doi: 10.3389/fgene.2014.00088

Wei, H., Tang, Q. L., Zhang, K., Sun, J. J., & Ding, R. F. (2018). miR-532-5p is a prognosticmarker and suppresses cells proliferation and invasion by targeting TWIST1 in epithelial ovarian cancer. *Eur Rev Med Pharmacol Sci, 22*(18), 5842-5850. doi: 10.26355/eurrev_201809_15911

Weidemann, A., König, G., Bunke, D., Fischer, P., Salbaum, J. M., Masters, C. L., & Beyreuther, K. (1989). Identification, biogenesis, and localization of precursors of Alzheimer's disease A4 amyloid protein. *Cell, 57*(1), 115-126. doi: 10.1016/0092- 8674(89)90177-3

Weintraub, M. K., Kranjac, D., Eimerbrink, M. J., Pearson, S. J., Vinson, B. T., Patel, J., .. . Chumley, M. J. (2014). Peripheral administration of poly I:C leads to increased hippocampal amyloid-beta and cognitive deficits in a non-transgenic mouse. *Behav Brain Res, 266*, 183-187. doi: 10.1016/j.bbr.2014.03.009

Wenk, G. L. (2004). Assessment of spatial memory using the radial arm maze and Morris water maze. *Curr Protoc Neurosci, Chapter 8*, Unit 8 5A. doi: 10.1002/0471142301.ns0805as26

White, J. A., Manelli, A. M., Holmberg, K. H., Van Eldik, L. J., & Ladu, M. J. (2005). Differential effects of oligomeric and fibrillar amyloid-beta 1-42 on astrocyte-mediated inflammation. *Neurobiol Dis, 18*(3), 459-465. doi: 10.1016/j.nbd.2004.12.013

White, J. D., Eimerbrink, M. J., Hayes, H. B., Hardy, A., Van Enkevort, E. A., Peterman, J. L., . . . Boehm, G. W. (2016). Hippocampal Aβ expression, but not phosphorylatedtau, predicts cognitive deficits following repeated peripheral poly I:C administration. *Behav Brain Res, 313*, 219-225. doi: 10.1016/j.bbr.2016.07.032

Wong, R. S., Cechetto, D. F., & Whitehead, S. N. (2016). Assessing the Effects of Acute Amyloid β Oligomer Exposure in the Rat. *Int J Mol Sci, 17*(9). doi:

10.3390/ijms17091390

Wu, Y., Xu, J., Xu, J., Cheng, J., Jiao, D., Zhou, C., . . . Chen, Q. (2017). Lower Serum Levels of miR-29c-3p and miR-19b-3p as Biomarkers for Alzheimer's Disease. *Tohoku J Exp Med, 242*(2), 129-136. doi: 10.1620/tjem.242.129

Wyss-Coray, T., Loike, J. D., Brionne, T. C., Lu, E., Anankov, R., Yan, F., . . . Husemann J. (2003). Adult mouse astrocytes degrade amyloid-beta in vitro and in situ. *Nat Med, 9*(4), 453-457. doi: 10.1038/nm838

Wyss-Coray, T., & Rogers, J. (2012). Inflammation in Alzheimer disease-a brief review ofthe basic science and clinical literature. *Cold Spring Harb Perspect Med, 2*(1), a006346. doi: 10.1101/cshperspect.a006346

Xiao, Y., & MacRae, I. J. (2019). Toward a Comprehensive View of MicroRNA Biology. *Mol Cell, 75*(4), 666-668. doi: 10.1016/j.molcel.2019.08.001

Xie, X., Pan, J., Han, X., & Chen, W. (2019). Downregulation of microRNA-532-5p promotes the proliferation and invasion of bladder cancer cells through promotion of HMGB3/Wnt/β-catenin signaling. Chem Biol Interact, 300, 73-81. doi: 10.1016/j.cbi.2019.01.015

Xu, D., Sharma, C., & Hemler, M. E. (2009). Tetraspanin12 regulates ADAM10-dependentcleavage of amyloid precursor protein. *FASEB J, 23*(11), 3674-3681. doi: 10.1096/fj.09-133462

Yamada, Y., Arai, T., Kato, M., Kojima, S., Sakamoto, S., Komiya, A., . . . Seki, N. (2019).Role of pre-miR-532 (miR-532-5p and miR-532-3p) in regulation of gene expression and molecular pathogenesis in renal cell carcinoma. *Am J Clin Exp Urol, 7*(1), 11-30.

Yang, G., Song, Y., Zhou, X., Deng, Y., Liu, T., Weng, G., . . . Pan, S. (2015). MicroRNA-29c targets β-site amyloid precursor protein-cleaving enzyme 1 and has a neuroprotective role in vitro and in vivo. *Mol Med Rep, 12*(2), 3081-3088. doi: 10.3892/mmr.2015.3728

Yang, L. B., Lindholm, K., Yan, R., Citron, M., Xia, W., Yang, X. L., . . . Shen, Y. (2003). Elevated beta-secretase expression and enzymatic activity detected in sporadic Alzheimer disease. *Nat Med, 9*(1), 3-4. doi: 10.1038/nm0103-3

Young-Pearse, T. L., Bai, J., Chang, R., Zheng, J. B., LoTurco, J. J., & Selkoe, D. J. (2007). A critical function for beta-amyloid precursor protein in neuronal migrationrevealed by in utero RNA interference. *J Neurosci, 27*(52), 14459-14469. doi: 10.1523/jneurosci.4701-07.2007

Yu, G., Nishimura, M., Arawaka, S., Levitan, D., Zhang, L., Tandon, A., . . . St George-Hyslop, P. (2000). Nicastrin modulates presenilin-mediated notch/glp-1 signal transduction and betaAPP processing. *Nature, 407*(6800), 48-54. doi: 10.1038/35024009

Yu, H., Saura, C. A., Choi, S. Y., Sun, L. D., Yang, X., Handler, M., . . . Shen, J. (2001). APP processing and synaptic plasticity in presenilin-1 conditional knockout mice. *Neuron, 31*(5), 713-726. doi: 10.1016/s0896-6273(01)00417-2

Yuan, A., Kumar, A., Peterhoff, C., Duff, K., & Nixon, R. A. (2008). Axonal transport ratesin vivo are unaffected by tau deletion or overexpression in mice. *J Neurosci, 28*(7),1682-1687. doi: 10.1523/jneurosci.5242-07.2008

Zhan, X., Stamova, B., & Sharp, F. R. (2018). Lipopolysaccharide Associates with AmyloidPlaques, Neurons and Oligodendrocytes in Alzheimer's Disease Brain: A Review.*Front Aging Neurosci, 10*, 42. doi: 10.3389/fnagi.2018.00042

Zhao, X., Kang, J., Svetnik, V., Warden, D., Wilcock, G., David Smith, A., . . . Laterza, O. F. (2020). A Machine Learning Approach to Identify a Circulating Micro RNA Signature for Alzheimer Disease. J Appl Lab Med, 5(1), 15-28. doi: 10.1373/jalm.2019.029595

Zhao, Y., Cong, L., Jaber, V., & Lukiw, W. J. (2017). Microbiome-Derived Lipopolysaccharide Enriched in the Perinuclear Region of Alzheimer's Disease Brain. *Front Immunol, 8*, 1064. doi: 10.3389/fimmu.2017.01064

Zhao, Y., Cui, J. G., & Lukiw, W. J. (2006). Natural secretory products of human neural and microvessel endothelial cells: Implications in pathogenic "spreading" and Alzheimer's disease. *Mol Neurobiol, 34*(3), 181-192. doi: 10.1385/mn:34:3:181

Zheng, K., Hu, F., Zhou, Y., Zhang, J., Zheng, J., Lai, C., . . . Zhu, L. Q. (2021). miR-135a-5p mediates memory and synaptic impairments via the Rock2/Adducin1 signalingpathway in a mouse model of Alzheimer's disease. *Nat Commun, 12*(1), 1903. doi:10.1038/s41467-021-22196-y

Zhou, W., Scott, S. A., Shelton, S. B., & Crutcher, K. A. (2006). Cathepsin D-mediated proteolysis of apolipoprotein E: possible role in Alzheimer's disease. *Neuroscience, 143*(3), 689-701. doi: 10.1016/j.neuroscience.2006.08.019

Zlotorynski, E. (2019). Insights into the kinetics of microRNA biogenesis and turnover. *NatRev Mol Cell Biol, 20*(9), 511. doi: 10.1038/s41580-019-0164-9

Zong, Y., Wang, H., Dong, W., Quan, X., Zhu, H., Xu, Y., . . . Qin, C. (2011). miR-29c regulates BACE1 protein expression. *Brain Res, 1395*, 108-115. doi: 10.1016/j.brainres.2011.04.035

Zong, Y., Yu, P., Cheng, H., Wang, H., Wang, X., Liang, C., . . . Qin, C. (2015). miR-29c regulates NAV3 protein expression in a transgenic mouse model of Alzheimer's disease. *Brain Res, 1624*, 95-102. doi: 10.1016/j.brainres.2015.07.022

Ruth Elizabeth AQUINO ORDINOLA

Analyse de l'expression des microARNs circulants dans un modèle animal de la maladied'Alzheimer

Résumé :

Parmi les maladies neurodégénératives, la maladie d'Alzheimer (MA) est la forme la plus courante de démencesénile caractérisée, dans sa forme typique, par une perte de mémoire immédiate et d'autres capacités cognitives liés au déclin graduel de la viabilité des cellules nerveuses et de l'activité de différentes régions ducerveau. La maladie est également associée à l'accumulation anormale de bêta-amyloïde (βA) et de la protéine Tau dans le cerveau. Le principal problème de la maladie d'Alzheimer est sa détection très tardive qui laisse très peu de place aux stratégies thérapeutiques. Une meilleure compréhension des mécanismes moléculairesde cette pathologie dans des modèles animaux est essentiel pour identifier des biomarqueurs diagnostiques beaucoup plus fiables et pour concevoir des thérapies efficaces. L'analyse des microARNs circulants a ouvertun champ d'exploration pour l'identification de biomarqueurs liés au dérèglement de diverses pathologies. Ici,nous avons évalué l'expression des microARN circulants (miARNs) dans un modèle de pathologie d'Alzheimerinduit par infusion dans les 2 hémisphères d'hippocampe de rats des formes agrégées du peptide βA 1-42. Nos résultats révèlent que la présence de ce peptide est suffisante pour déclencher une perte de l'activité cognitive des rats, une astrogliose et le dérèglement de l'expression de 3 miARNs circulants (miARN-29a, - 29c, et -146a). Nous montrons la cinétique d'expression de ces miARNs et rapportons des différences d'expression notamment du miARN-146a. Nous avons finalement concentré nos études sur ce miARN et avons étudié son rôle biologique dans des cultures primaires astrocytes de rat, utilisé comme modèle in vitro de la maladie d'Alzheimer. Nous avons observé que bien que ce miARN-146a est capable d'interagir avec leurs gènes cibles transcriptomiques tels que IRAK 1/2 et TRAF-6, le traitement des cellules avec le peptide βA 1-42 sous sa forme oligomérique ou fibrillaire ne conduit pas à une réponse inflammatoire. De manière générale,nous rapportons pour la première fois le dérèglement de l'expression de microARNs circulants qui peuvent être directement corrélés à la présence de forme agrégée de βA 1-42, un composant essentiel de l'aggravation chronique de cette pathologie. Nous avons également apporté des données mécanistiques sur le rôle du miARNA-146a dans cette pathologie. Ces résultats prometteurs méritent d'être exploités dans des études à longterme notamment pour évaluer leur potentiel application dans le diagnostic clinique de la maladie Alzheimer.

Mots clés : *miARNs, maladie d'Alzheimer, βA 1-42, biomarqueurs, diagnostique*

Analysis of the expression of circulating microRNAs in an animal model of Alzheimer's disease

Abstract:

Among neurodegenerative diseases, Alzheimer's disease (AD) is the most common form of senile dementia characterized, in its typical form, by immediate memory loss and other cognitive abilities associated with gradual decline in the viability of nerve cells and the activity of different regions of the brain. The disease is also associated with the abnormal accumulation of amyloid-beta (Aβ) and Tau protein in the brain. The mainproblem with Alzheimer's disease is its very late detection, which leaves very little room for therapeutic strategies. A better understanding of the molecular mechanisms of this pathology in animal models is essential to identify much more reliable diagnostic biomarkers and to design effective therapies. The analysis of circulating microRNAs has opened a field of exploration for the identification of biomarkers linked to the deregulation of various pathologies. Here, we evaluated the expression of circulating microRNAs (miRNAs) ina model of Alzheimer's pathology induced by infusion in the 2 hemispheres of the rat hippocampus of the aggregated forms of the Aβ 1-42 peptide. Our results reveal that the presence of this peptide is sufficient to trigger a loss of cognitive activity in rats, astrogliosis and the disruption of the expression of 3 circulating miRNAs (miRNA-29a, -29c, and -146a). We show the kinetics of expression of these miRNAs and report differences in expression of miRNA-146a in particular. Finally, we focused our studies on this miRNA and studied its biological role in primary rat astrocyte cultures, used as an *in vitro* model of Alzheimer's disease. We observed that although this miRNA-146a is able to interact with their transcriptomic target genes such as IRAK1/2 and TRAF-6, the treatment of cells with the Aβ 1-42 peptide in its oligomeric or fibrillar form does not lead an inflammatory response. In general, we report for the first time the deregulation of the expression of circulating microRNAs which can be directly correlated with the presence of aggregated form of Aβ 1-42, an essential component of the chronic worsening of this pathology. We have also provided mechanistic data on the role of miARNA-146 in this pathology. These promising results deserve to be used in long-term studies, inparticular to assess their potential application in the clinical diagnosis of Alzheimer's disease.

Keywords: *miRNAs, Alzheimer's disease, Aβ 1-42, biomarkers, diagnosis*

Centre de Biophysique Moléculaire (CBM, UPR 4301) – Rue Charles Sadron – 45071 Orléans

cells

MDPI

Article

Circulating microRNAs in a rat model of Alzheimer disease produced by intrahippocampal inoculation of Aβ1-42 peptide

Ruth Aquino[1,5], Vidian de Concini[3], Marc Dhenain[4], Suzanne Lam[4], Arnaud Menuet[2,3], Laura Baquedano[5], Manuel G Forero[6], David Gosset[1], Patrick Baril[1,2], Chantal Pichon*[1,2].

1. Center of Molecular Biophysics, UPR 4301 CNRS, Orléans, France
2. Faculty of Science and Techniques, University of Orléans, France
3. Experimental and Molecular Immunology and Neurogenetic, UMR7355 CNRS, Orléans, France
4. Université Paris-Saclay, CEA, CNRS, Laboratoire des Maladies Neurodégénératives, 18 Route du Panorama, F-92265 Fontenay-aux-Roses, France.
5. Faculty of Science and Philosophy, Universidad Peruana Cayetano Heredia, Lima, Peru
6. Semillero Lún, Grupo D+Tec, Faculty of Engineering, Universidad de Ibagué, Ibagué, Tolima, Colombia

* Correspondence: Correspondence: chantal.pichon@cnrs.fr, Tel: +33 238 255 595

Abstract: Circulating microRNAs aroused a lot of interest as reliable diagnostic biomarkers of Alzheimer's disease (AD). This study aims to identify dysregulated serum circulating microRNAs (miRNAs) in a rat model of AD generated by intra-hippocampal inoculation of aggregated Aβ1-42 peptides. In addition to the cognitive impairments and astrogliosis, the presence of aggregated Aβ1-42 peptides led to a downregulation of serum circulating miR-146a-5p, -29a-3p, -29c-3p, -125b-5p and-191-5p. Those miRNAs except miR-146a were as well dysregulated in amyloid-bearing $APP_{swe}/PS1_{dE9}$ transgenic mice. Unlike in the serum, miR-146a was increased in the cerebrospinal-fluid of Aβ1-42–inoculated rats. A functional study performed on primary astrocytes revealed that cell treatment with aggregated forms of Aβ led to miR-146a upregulation *via* NFκB signaling pathway which in turn downregulated the expression of IRAK-1 but was inefficient to downregulate the expression of TRAF-6 key effector. Astonishingly, cell treatment with aggregated forms of Aβ did not modulate IL-1β, IL-6 and TNF-α expression but increased CXCL1 expression. Overall, we show for the first time that the deregulation of specific serum circulating microRNAs can be directly correlated with the presence of aggregated form of Aβ1-42. We provided mechanistic data on the role of miR-146a that support its anti-inflammatory role operating through a negative feedback loop of NFκB pathway. These results give new insights in the early events occurring during Aβ accumulation in the brain.

Keywords: MicroRNAs; miR-146a; Alzheimer's disease; Aβ1-42 peptide; biomarkers; diagnosis

Citation: Lastname, F.; Lastname, F.; Lastname, F. Title. *Cells* **2021**, *10*, x. https://doi.org/10.3390/xxxxx

Academic Editor: Firstname Lastname

Received: date
Accepted: date
Published: date

1. Introduction

Alzheimer's disease (AD) is a complex and multifactorial pathology that affects millions of people around the world [1]. The appearance of amyloid plaques and the formation of neurofibrillary tangles (NFTs) are two representative features of AD, responsible for the gradual deterioration of cognitive functions such as loss of memory, language and thinking ability. Amyloid plaques are deposits of amyloid-beta (Aβ) peptide that accumulate in the extracellular matrix between nerve cells [2]. The Aβ peptides arise from the cleavage of the amyloid precursor protein (APP). Amongst the different Aβ species generated, Aβ1-42 peptides are the most hydrophobic and fibrillogenic, and are the main species deposited in the brain [3]. Neurofibrillary tangles are hyperphosphorylated intraneuronal accumulations of tau protein [4].

One of the main issues of AD is the existence of a long preclinical stage. This pathology begins between 10-20 years before significant neuronal death and before the cognitive symptoms and behaviors are observed [5]. Although much is known about the disease,

the early triggers and pathogenesis of AD are not yet fully understood. It has been postulated that Aβ peptides, especially $A\beta_{1-42}$ peptides, which are more prone to aggregation, initiate a cascade of pathological events that lead to aberrant phosphorylation of Tau, neuronal loss and eventual dementia [3,6]. The aggregation of Aβ peptides can generate oligomers and fibrils forms that can both be toxic.

Today, there is no therapeutic agent capable of curing or preventing AD [7]. There is a real need to predict the development of symptomatic AD, for both mild cognitive impairment (MCI) and dementia in asymptomatic individuals [8]. The current AD diagnosis uses cumbersome and expensive methods such as structural magnetic resonance imaging (MRI) and molecular neuroimaging with positron emission tomography (PET) [7]. Therefore, the search for biomarkers for early diagnosis is still essential and is currently an active field of research.

MicroRNAs (miRNAs) are a subclass of small noncoding RNAs that play important roles in the regulation of post-transcriptional gene expression by binding to complementary sequences of target messenger RNA (mRNA) inducing translation repression and/or mRNA degradation [9,10]. Under different pathological conditions, there is a dysregulation of miRNAs present in most body tissues and fluids including brain tissue, cerebrospinal fluid (CSF), or serum [10]. MicroRNAs present in biofluids are called circulating microRNAs [11]. They are produced and secreted from cells present in tissues and organs and so reflect the composition of the fluid in the extracellular space of the brain for instance. Circulating miRNA are now considered as disease biomarkers [12]. They are stable in different biological fluids, relatively easy to detect using PCR-based methods and have an expression pattern that reflect the disease stages of pathologies as AD [13-15]. All of these characteristics position miRNAs as potential AD biomarkers.

Several animal models have been created for AD research, with transgenic animal models being the most popular [16]. As any animal models, they must mimic all the cognitive, behavioral and neuropathological characteristics of the disease to recapitulate the disease phenotype with high fidelity. Unfortunately, most of AD models currently used are called partial models, as they mimic only some components of AD. Amyloid-bearing transgenic animal models of AD have been created based on the genetic origins of familial AD or early-onset AD (EOAD), detected in patients under 65 years of age that however corresponds only to 5% of AD patients. These models have contributed significantly to better understand the molecular mechanisms involved in the pathology, but they do not represent the majority of AD cases, called late-onset AD (LOAD), representing 95% of cases [17-19]. In addition, the different genetic backgrounds of these models constitute a real issue [20]. Due to these drawbacks, non-transgenic animal models have been developed to study the LOAD form [19]. These represent one or more distinctive features such as AD-like senile plaques, NFT, oxidative stress, and cognitive impairment [20]. Amongst them, one model consists in inoculating Aβ synthetic peptide into the brain of rodents. Previous studies have shown that this procedure causes learning and memory deficits in treated animals due to the formation of amyloid plaques, and the disruption of long-term potentiation and behavior [20-22]. As for the transgenic model, this model is not perfect but it partially gives insights on the early impact of Aβ peptides and of their aggregation.

Different studies have investigated the expression of circulating miRNAs in blood of AD patients and/or in transgenic animal models of AD. Results indicated that the most representative deregulated miRNAs are miR-9a-5p, miR-146a-5p, miR-29a-3p, miR-29c-3p, miR-125b-5p, miR-181c-5p, miR-191-5p, -miR-106b-5p and miR-135a-5p [23-26]. Those miRNAs have been associated with different stages of progression of AD (for a review see [27]).

To our knowledge, no evaluation of circulating miRNA was performed in rodent model generated by intrahippocampal inoculation of aggregated forms of the $A\beta_{1-42}$ peptide. Whilst such study could be interesting as it will permit to trace which miRNAs are firstly dysregulated following the presence of aggregated $A\beta_{1-42}$ peptide inside the hippocampus.

This work performed with a rat model generated by intrahippocampal injection of aggregated $A\beta_{1-42}$ peptide aims to evaluate the relationships between the expression of particular miRNA and the presence of aggregated $A\beta_{1-42}$. Morris Maze Water test was applied to assess the cognitive deficit of the rat model. Then, we quantified the amount of circulating miRNA in serum selected from a short list of the most relevant miRNAs found in the AD literature. The same quantification was performed with the sera of amyloid-bearing $APP_{swe}/PS1_{dE9}$ transgenic mice. We evaluated astroglyosis by GFAP staining of brain tissues. Last, we focused our attention to miR-146a known to be involved in neuroinflammation and conducted a functional *in vitro* study on rat primary astrocytes treated with $A\beta_{1-42}$ peptide. We carried out different experiments to investigate the involvement of NFκB signaling pathway by investigating the impact of miR146a on expression of NFκB regulator genes such *Irak-1*, *Irak-2* and *Traf6* as well as on induction of *IL-1*, *IL-6*, *TNF-α* and *Cxcl1* genes.

2. Materials and Methods

2.1. Animals

Sprague-Dawley rats (aged 8-12 weeks) with a body weight of 200-380 g were obtained from the Bioterium of the Research and Development Laboratory located in the Cayetano Heredia Peruvian University of Peru. Animals were maintained under controlled laboratory temperature (25 ± 2 °C) and humidity (60%) conditions, with a controlled light cycle (12 hours light/12 hours' dark). Water and food were available ad libitum throughout the experiment. Ethics Committee of the Cayetano Heredia Peruvian University (CIEA-102069) approved the animal handling and experimental procedures. The animal care staff monitored the animal behaviors of rats daily to ensure that the animals were safe and healthy. $APP_{swe}/PS1_{dE9}$ transgenic mice and their littermate mice were bred and hosted in the animal facility of Commissariat à l'Energie Atomique, Centre de Fontenay-aux-Roses; European Institutions (Agreement #B92-032-02). These mice express a chimeric mouse/human APP with the Swedish mutation and a human presenilin-1 lacking exon 9. All experimental procedures were conducted in accordance with the European Community Council Directive 2010/63/UE and approved by local ethics committees (CEtEACEA DSV IdF N°44, France) and the French Ministry of Education and Research (APAFIS#21333-2019062611099838v2).

2.2. Preparation of amyloid -β_{1-42} peptide for in vivo infusion

Amyloid-β_{1-42} ($A\beta_{1-42}$) peptides were from Sigma–Aldrich (Sigma–Aldrich, France). The dry powder was solubilized in DMSO, prepared at concentration of 2 mM, to generate a stock solution of $A\beta_{1-42}$ peptides at concentration of 10 μg/μL in PBS. This stock solution was stored at -20 °C until use. For production of aggregated $A\beta_{1-42}$ peptides, the working solutions were diluted in PBS at final concentrations of 0.5, 1 and 2.5 μg/μL and incubated for 1 week at 37 °C [28]. At the end of this incubation period, Aβ solutions were directly inoculated into the hippocampus of the rats as described below.

2.3. Model of Alzheimer disease generated by intracranial infusion of Aβ

The general procedure to infuse the Aβ in the brains of rats derived from [28] with some modifications. Briefly described, anesthetized rats were placed on a stereotaxic frame (KOPF ® 900, David Kopf Instruments, CA, EEUU) to infuse 3 μL of Aβ or PBS solutions into the two hemispheres of the hippocampus using a 10 μL syringe (Hamilton® glass syringe 700 series RN, Hamilton, USA) connected to a 26-G needle (Hamilton®). The precise procedure to inoculate Aβ and PBS solutions consisted in gradual infusion of solutions over a 6 min period followed by an additional 3 min period to ensure optimal dispersion of solutions into the ventricles. The Bregma was used as reference. The coordinates to infuse the solutions were as follows: 2.6 mm lateral, 3.0 mm back, 3.0 mm deep

from the bregma corresponding to the CA1 regions of the hippocampus. After careful removing of the syringe over a final 5 minutes of time, the rats were returned to cages and monitored every day until the time of experimentation.

2.4. Morris Water Maze test

The Morris Water Maze test (MWM) was used to evaluate the spatial memory of animals. The general procedure was from [29] with some modifications. A circular pool was built (126 cm in diameter, 75 cm in high), filled with water at 21-22 °C and loaded with a transparent plastic platform (10 cm in diameter) placed in a constant position. The pool was divided with imaginary lines to delimitate four quadrants: Northeast (NE), Northwest (NW), Southeast (SE), Southwest (SW). Animals were placed in all of quadrants and their swimming trajectories to reach the platform were monitored using a webcam connected to a computer. Videos were processed with a novel RatsTrack plug-in (Under submission), designed for these experiments to accurately record distance, time and velocity of animals in the pool. The MWM was performed 14 days after the infusion of Aβ or PBS solutions and was monitored using an arbitrarily fixed time period of 90 seconds for each trial. A reference memory protocol consisting in familiarization, acquisition and memory sessions was set-up. The familiarization session procedure consisted in placing rats in one quadrant of the pool and to allow the rats to find the platform over 4 trials. The acquisition session was performed the day after the familiarization session and was lasted over four days. The objective of this session was to evaluate the spatial learning of animals by placing rats in all of 4 quadrants of the pool and to evaluate their velocity to reach the platform. A total of 8 trials per rat were recorded. Finally, the memory session was performed on the sixth day. The objective of this trial if to record the reference memory of rats by monitoring the swimming trajectories of rats placed into the pool but without any platform. One trial per rat was used in this specific session.

2.5. Body fluid collection and sampling

2.5.1. Blood collection and serum separation

Blood samples were collected in BD Vacutainer® tubes coated with silica as coagulation activator according to procedures described by [30]. Cardiac punctures was performed to collect enough blood per animal at day 7 (n = 8) , 14 (n = 8) and 21 (n = 8) post-injection of Aβ peptides or PBS solutions by [31]. The samples were left at room temperature for 40 min for the formation of blood clot and then centrifugated at 1 900 x g for 10 min at 4 °C to collect the serum. A second centrifugation at 16 000 x g for 10 min and 4 °C was used to clarify the serum. Hemolyzed samples, inspected visually, were discarded from the study. The clarified sera were stored at - 80 °C until used.

2.5.2. Cerebrospinal fluid collection and preparation

CSF was collected 14 days after the inoculation of Aβ solution from the cisterna magna of the rats according to procedure described by [32]. The procedure to extract the CSF consisted in using an infusion system equipped with a 25-gauge butterfly needle to collect the CSF into the dura mater/atlanto-occipital membrane according to procedure [33]. CSF liquids were loaded in a 0.5 mL eppendorf tube, stand for 1 hour at room temperature before to centrifuge the tubes at 1 000 x g for 5 min at 4 °C to remove cellular debris. A second centrifugation at 16 000 x g for 10 min and 4 °C was used to clarify the sample. The clarified CSF samples were stored at -80 °Cuntil use.

2.6. Analysis of circulating microRNAs expression in animals

2.6.1. Total RNA extraction from body fluids

The NucleoSpin® miRNA Plasma kit from Macherey-Nagel (Hoerdt, France) and the miRNeasy Serum/Plasma Kit (Qiagen, Hilden, Germany) were used to extract respectively total RNAs from sera (300 µL) and CSF (50 µL) samples. In the latter, 5 µg of a

glycogen solution prepared at concentration of 0.1 µg/µL was added to each 50 µL of CSF fraction to optimize the yield of miRNA recovery [34]. Exogenous spike-in miRs (cel-miR 39-3p, -54-3p and cel-miR 238-3p) were added to each sample to normalize the extraction procedure of miRNA according to standardized protocol described by Vigneron et al. [30]. Nucleotide's sequence of spike-in miRs were from miRNA database and were synthesized by Eurogentec (Eurogentec, Liège, Belgium) as SDS-PAGE purified oligonucleotides. These synthetic miR were resuspended in nuclease-free water at a fixed concentration of 200 amol/µL. Then 2.5 µL per each 100 µL of samples was added after the denaturation step of the extraction procedure as recommended by the manufacturer's instructions. Total RNA fractions were quantified using a nanodrop spectrophotometer (Nanodrop 2000, Thermo Scientific). Samples with an RNA integrity number (RIN) superior to 8 were considered for the study.

2.6.2. Reverse transcription reaction (RT)

Total RNAs were reverse transcribed by using the miScript II RT Kit (Qiagen) according to routine procedure described from [35-37]. Fifty ng of total RNAs prepared at concentration of 10 ng/µl were polyadenylated by a poly (A) polymerase and then reverse transcribed to cDNA using oligo-dT primers following recommendations from the manufacturer (Qiagen). The generated cDNAs were then stored at -20 °C until use.

2.6.3. Real time quantitative RT-PCR (qRT-PCR)

qRT-PCR was performed with the miScript SYBR® Green PCR Kit (Qiagen) according to routine procedures described from [35-37]. A volume of 2.5 µL of cDNA corresponding to 50 ng of cDNA were loaded in a final volume of 10 µL containing 5 µL of 2X QuantiTect SYBR Green PCR Master Mix, 1 µL of 10X miScript Universal Primer, 10x miScript Primer Assay and 0.5 µL of RNase-free water. All miR specific forward primers (miScript Primer Assays) were purchased from Qiagen and are listed in the Table 1 (Supplementary data). The quantification of PCR products was collected using the Light Cycler® 480 (Roche Diagnostics Corporation, Indianapolis, IN, USA). The relative miRNAs expression was calculated according to Livak and Schmittgen method [38] and expressed as $2^{-\Delta\Delta Ct}$. The mean of Ct from the 3 spike-in miRNA was used to normalize the data as described by Vigneron et al., and Faraldi et al., [30,39].

2.7. Immunofluorescence staining

Immunostaining was performed following the protocol described in [40] from 5 µm paraffin sections of brain tissues. Sections were saturated (2h at room temperature in TBS containing 0.2% triton, 0.5% FBS and 1% BSA), incubated with primary antibodies; anti-GFAP (Dako, Agilent, Santa Clara, USA, Z0334; 1: 500) at 4 °C overnight, washed and incubated with a secondary anti-rabbit Alexa 488 antibody (Abcam, ab150077, 1: 1000). The slides were stained with DAPI for 10 min, washed with PBS, mounted with Fluoromount-G (SouthernBiotech, Birmingham, England) and inspected visually using a ZEISS AXIOVERT 200 M Apotome microscope (Zeiss, Oberkochen, Germany) connected to a digital camera. Serial sections were analyzed at 20x magnification to reconstruct the whole hippocampus volume of the brain using the ZEN2.1 software (Zeiss). Images were collected as serial Z stack series of from 18 optical slices. GFAP-positive cells were counted manually from cornu ammonis (CA) 1/CA2, CA3 and the dentate gyrus (DG) using Image J -Fiji software [41]. A total of 40 slides were analyzed, corresponding to treated group (n = 5) and control group (n = 5).

2.8. Primary culture, Aβ treatment, qRT-PCR and ELISA

2.8.1. Primary astrocytes preparation and culture

Primary astrocyte cultures were prepared following the protocols described in [42,43]. Six brains of new-born Sprague Dawley rats of 3 days of age were collected aseptically before to isolate manually the cerebral hemispheres. After removing carefully, the meninges, tissues were dissociated mechanically and rinsed with PBS. The cell suspension was centrifuged at 1 000 x g for 5 min at 4 °C. Cell pellets were resuspended in DMEM complete medium and seeded in 24-wells plate at density of 1.5×10^5 cells/cm^2 until they reach 80% of confluency. The medium was changed every 3-4 days. The cells were thereafter maintained in tissue culture for approximatively 15 days.

2.8.2. Preparation of $A\beta_{1-42}$ peptide for cell culture

$A\beta_{1-42}$ stock solution was prepared as described above and then diluted in PBS at the final concentration of 100 μM. The formation of aggregates of $A\beta_{1-42}$ was adapted from procedures described in several publications [44-46]. Briefly, Aβ was generated by incubation of the 100 μM working $A\beta_{1-42}$ solution at 4 °C for 24 hours.

2.8.3. Treatment of primary astrocytes with Aβ, LPS, and BMS-345541

Confluent cells monolayers were washed 2 times with PBS and then incubated with the Aβ at final concentration of 5, 1 and 2 μM for 3 to 7 days at 37 °C. In parallel, cells were also treated with BMS-345541, a NF-κB inhibitor (Sigma-Aldrich, France) used at the final concentration of 5 μM. When specified, the cells were pre-incubated for 1 hour in tissue culture with the BMS-345541 inhibitor before treatment with either the Aβ or LPS solution for 3 days as described in here [47,48].

2.8.4. Cell Viability Assay

Cell viability analysis was performed with the Alamar Blue™ HS reagent according to manufacturer's instructions (Invitrogen, Carlsbad, CA, A50101). Briefly described, a 1/10 dilution of Alamar blue solution was added to each well of 24-wells plate for 2 h at 37 °C. Then 50 μL of cell supernatant were monitored using a fluorescence microplate reader set up at 560 and 605 nm as excitation and emission wavelength respectively.

2.8.5. miRNA and mRNA quantification from primary astrocytes culture

The procedure to quantify the relative miRNA expression from the primary astrocyte culture was the same as described above expect that no miRNA spike-in were added to the samples and that the relative expression of the small nuclear RNA 6 (U6) was used to normalize the data as described before [35]. The procedure to quantify the relative mRNA expression derived also from routine procedures described before [35-37]. Briefly described, total RNA was extracted from cells using the Trizol reagent (Invitrogen, Carlsbad, CA) and reverse transcribed from 100 ng tRNA using the RevertAid RT Reverse Transcription Kit from ThermoFisher (Thermofisher Scientific, MA USA). Commercially available primers (Qiagen) were used to monitor expression of *IRAK1*, *TRAF6* and *IRAK2*. Specific sequence primers to *IL-6*, *IL-1β* were designed in our laboratory. The sequences of primers are listed in the Table 1 (Supplementary data). The relative expression of *GAPDH* was used to normalize expression of mRNA transcripts [38].

2.8.6. Sandwich enzyme-linked immunosorbent assay

A sandwich enzyme-linked immunosorbent assay (ELISA) system was used to quantify concentrations of IL-1β, IL-6, and CXCL1 from the culture medium of astrocytes, using antibodies paired according to routine procedure described in [49].

2.9. Statistical analysis

All data were expressed as the mean ± SEM. Statistical analyzes of the Morris test were performed with the Stata 13.0 software and the non-parametric Kruskal Wallis test was used to evaluate the difference between the groups. To analyze the relative expression

of miRNAs and mRNA, the statistical software XLSTAT by Addinsoft was used and the non-parametric Mann-Whitney U test was used to compare the expression of miRNA between the groups. The t-student test was used to evaluate the difference in the relative expression of mRNA. All graphs were made using GraphPrism 8.0 software. In all cases Statistical significance was set at 95% confidence interval with p values set as * ≤ 0.05, ** ≤ 0.01, *** ≤ 0.001.

3. Results

3.1. Cognitive impairment in rats inoculated with 0.5 and 1 μg/μL of Aβ1-42

The rat model of AD, induced by the intrahippocampal infusion of Aβ1-42 peptide was first challenged using the classic Morris Water Maze test to evaluate the memory and behaviour performance of treated animals [29].

For each rat, we monitored the distance travelled and the latency escape as variables of cognitive performance using a videdo-based system called "RatsTrack" to automatically extract trajectories and time used by of rats to reach the platform on the maze . During the acquisition session, no statistically significant difference was found at day 1 of training session between all groups indicating that animals from both groups have similar motor and visual abilities. In contrast, significant differences in path lengths were found from day 2 to day 5 (Figure 1A). The evaluations of cognitive performance in the NW quadrant showed that the Aβ-treated rats used longer distances to find the platform over these 4 days interval of time compared to PBS-treated rats (Figure S1A). When the rats were placed in NE quadrant, significant differences were only observed at day 4 and day 5 (Figure S1B). For rats placed in the SW quadrant, Aβ-treated rats used longer distances compared to the control group of animals but the differences were not statistically significant (Figure S1C). In the SE quadrant, the path lengths of Aβ treated-group were significantly different to those of the control group from day 2 to day 4 (Figure S1D). The escape latency of each rat was evaluated in 4 quadrants. The groups of animals infused with Aβ1-42 showed a longer escape latency compared to the control group with a significant difference at day 4 and day 5 ($p < 0.05$) (Figure 1B).

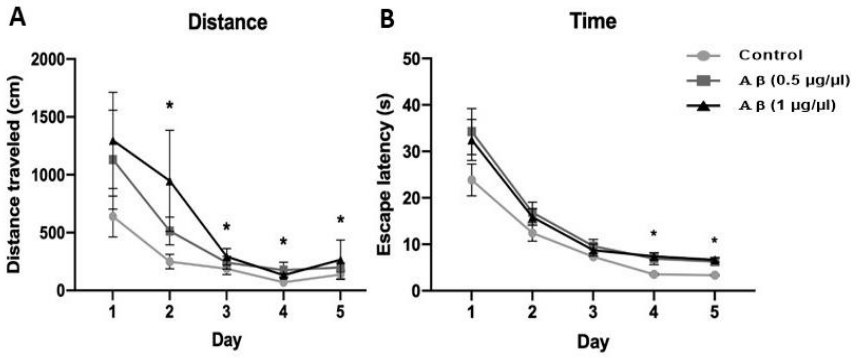

Figure 1. Effects of Aβ1-42 injection on learning and memory, evaluated by the Morris Water Maze test. The distance and the escape latency performed by rats injected with Aβ used at concentration of 0.5 and 1 μg/μL was evaluated at day 14 post-injection. (A) Total distance traveled during the 5 days of training. B) Total escape latency during the 5 days of training. Control group (n = 10); group of animal injected with 0.5 μg/μL Aβ (n = 11); group of animal injected with 1 μg/μL Aβ (n = 13). Data are represented as mean ± SEM. Statistical comparisons were performed using Kruskal-Wallis. *p ≤ 0.05.

3.2. Intrahippocampal injection of Aβ1-42 leads to dysregulation of circulating microRNAs

Our next objective was to evaluate whether the defective cognitive performance of rats infused with Aβ peptides might be correlated with dysregulation of circulating miRNAs detected in serum of these animals collected at day 21, following the last day of the MWM test. We quantified the expression of miR-146a-5p, miR-9a-5p, miR-29a-3p, miR-29c-3p selected from bibliography for their dysregulation in serum samples of animal model of AD and/or AD patients [23-28].

Results from qRT-PCR in Figure 2 indicated that amongst those microRNAs evaluated, only the amount of one miR, miR-146a-5p, was statistically significant different in sera of Aβ-treated animals compared to those from PBS-treated animals ($p < 0.05$). Nevertheless, the amounts of miR-9a-5p, miR-29a-3p and miR-29c-3p tend to be lower in Aβ-treated group compared to control group although the difference was not statistically significant albeit very close to a statistic p value of 0.05 (Figure 2).

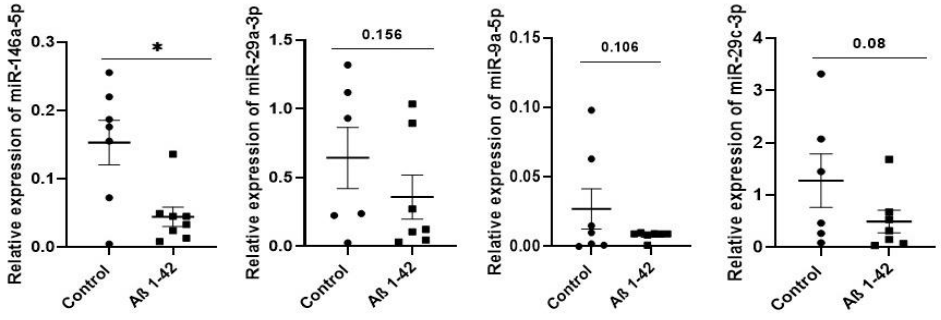

Figure 2. Relative expression of circulating miR-146a-5p, miR-29a-3p, miR-9a-5p, miR-29c-3p in serum samples of rat infused with 1 μg/μL of $A\beta_{1-42}$ peptides. Sera from rats infused with Aβ (treated group) or PBS (Control group) were collected 21 days post-treatment. MiRNA were extracted and quantified by qRT-PCR. Data are represented as mean ± SEM of 7-8 samples evaluated in triplicate. Statistical comparisons between $A\beta_{1-42}$ and PBS groups were performed using the Mann-Whitney test * $p \leq 0.05$.

3.3. Increasing amount of infused $A\beta_{1-42}$ peptide in hippocampus of rats enhanced the relative abundance of circulating miRNA in serum samples.

Then, we followed up our investigation by performing a second cohort of rats infused intrahippocampally with 3 μL of Aβ made with 2.5 μg/μL $A\beta_{1-42}$ peptide. In this cohort, we decided to assess the expression of 4 selected miR described above and, in addition, miR-125b-5p, miR-181c-5p, miR-191-5p, -miR-106b-5p and miR-135a-5p. Data from qRT-PCR analysis made on serum samples collected at day 21 indicated that expression of miR-146a-5p, 29a-3p, miR-29c-3p, miR-125b-5p and miR-191-5p were significantly reduced in the Aβ-treated group of rats compared to the control group. By contrast, the relative abundance of miR-9 and miR-106b-5p did not change despite 2.5 times more amount of injected Aβ (Figure 3 *versus* Figure 2).

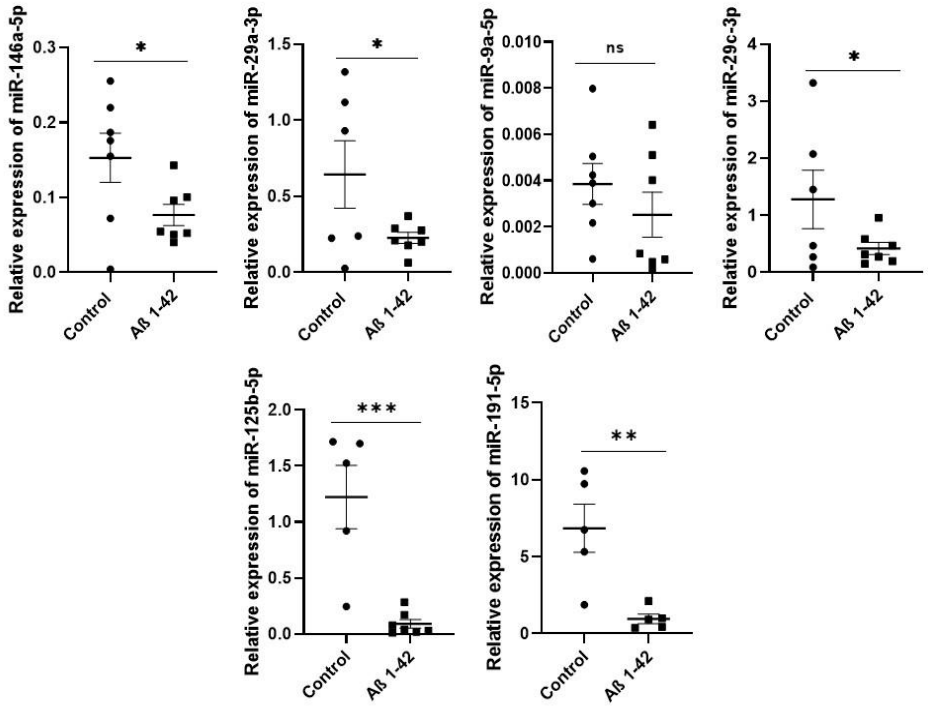

Figure 3. Relative expression of circulating miR-146a-5p, miR-29a-3p, miR-9a-5p, miR-29c-3p, miR-125b, miR-191-5p in serum of rat infused with Aβ at 2.5 μg/μL. Serum samples were collected 21 days post-infusion. MicroRNAs were extracted and quantified by qRT-PCR. Data are represented as mean ± SEM of 7-8 samples evaluated in triplicate. Statistical comparisons between $A\beta_{1-42}$ and PBS groups were performed using the Mann-Whitney test * $p \leq 0.05$, ** $p \leq 0.01$, *** $p \leq 0.001$.

3.4. Kinetics of miRNAs changes in rats after intrahippocampal injection of $A\beta_{1-42}$

Knowing the kinetics of expression of circulating miRNAs could be interesting data to correlate their deregulation in serum samples with deposit and the biological consequence of Aβ peptides in hippocampus of rat overtime. To this purpose, we collected serum samples from rats at several time points after inoculation of Aβ prepared with $A\beta_{1-42}$ at 2.5 μg/μL. We focused our quantification on miR-9-5p, miR-29a-3p, miR-29c-3p and miR-146a-5p as those miRs have been widely investigated in several other animal models of AD [50].

Figure 4 shows the kinetics of microRNAs detected in serum samples. For miR-146, a statistically significant reduction of expression was detected at both, day 14 and day 21 ($p = 0.022$ and $p = 0.027$, respectively, Figure 4A) compared to that from control group. The expression patterns of miR-29a-3p and miR-29c-3p were also found statistically reduced at all evaluation times compared to control group although the most significant difference was found at day 7 ($p < 0.01$; Figure 4B and 4D). The pattern of expression of miR-9-5p tends to be lower as function of time in Aβ-treated group compared to control group but not statistically different (Figure 4C).

Of note, for all kinetics drawn for this analysis, it becomes apparent that, at late time point, *e.g* day 21, the expression all miRNAs investigated tended to return to the baseline expression level detected at day of infusion (day 0). This indicates, as observed in Morris water maze test, that effect of Aβ infused in hippocampus of rats seems reversible.

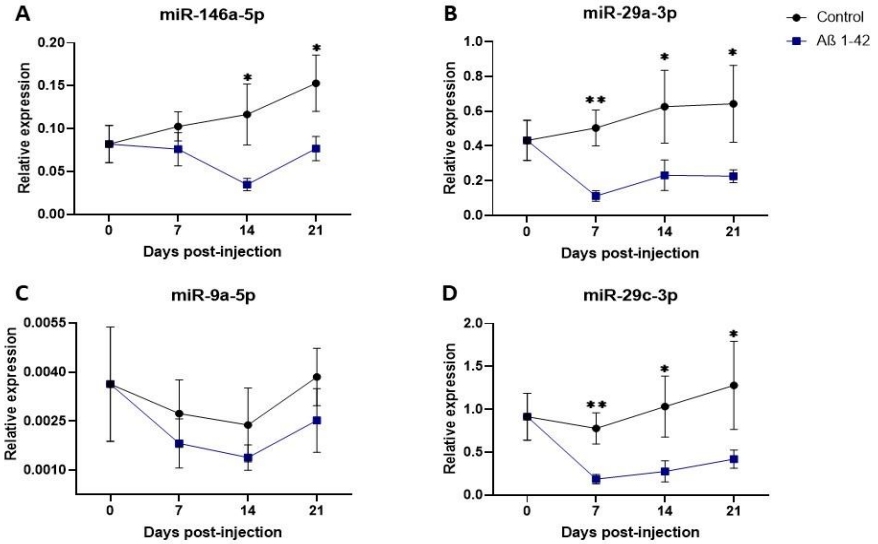

Figure 4. Kinetics of circulating microRNAs detected in the serum. The quantification of miRs in serum was investigated at 0-, 7-, 14- and 21-days post-infusion with Aβ or PBS **(A-D)**. Relative expression profiles of **(A)** miR-146a-5p, **(B)** miR-29a-3p, **(C)** miR-9a-5p**, (D)** miR-29c-3p. The amount of each microRNAs was evaluated by qRT-PCR. Data are expressed as mean ± SEM of result obtained from each serum assessed in triplicate (for each time, n = 8 rats per group). Statistical comparisons between groups at each time were made using the Mann-Whitney test. * $p \leq 0.05$, ** $p \leq 0.01$.

3.5. Common miRNAs deregulated in APP$_{swe}$/PS1$_{dE9}$ transgenic mice and Aβ-brain infused rat models.

Next, we sought to evaluate whether the alteration profile of circulating miRs detected in the rat animal model generated by hippocampal infusion of Aβ could be also observed in the APP$_{swe}$/PS1$_{dE9}$ transgenic mice expressing two constitutive mutant forms of APP and PSEN1. APP$_{swe}$/PS1$_{dE9}$ mice are one of most commonly used transgenic animal model of amyloidosis-β characterized by Aβ deposits by 6-months of age followed by abundant plaques apparition in the hippocampus and cortex by 9 months that continue to increase up to around 12 months of age [51].

We evaluated the expression pattern of 9 miRs mentioned above from serum samples of APP$_{swe}$/PS1$_{dE9}$ mice prepared at 4- and 15-months of age. The results obtained indicated that miRs amount detected in serum sample of 4-month-old mice of APP$_{swe}$/PS1$_{dE9}$ mice were not significantly different to those of control littermate mice (Figure S2). By contrast, in serum samples from 15-months old mice, 4 (miR-125b-5p, miR29a-3p, miR-29c-3p and miR-191-5p) over 9 miRs were found significantly downregulated in the APP$_{swe}$/PS1$_{dE9}$ group of mice (Figure 5). Interestingly, those 4 miRs were also significantly downregulated in high-dose Aβ- injected rats. No statistical significant difference in the expression of miR 146 was detected in the APP$_{swe}$/PS1$_{dE9}$ transgenic mice (not shown).

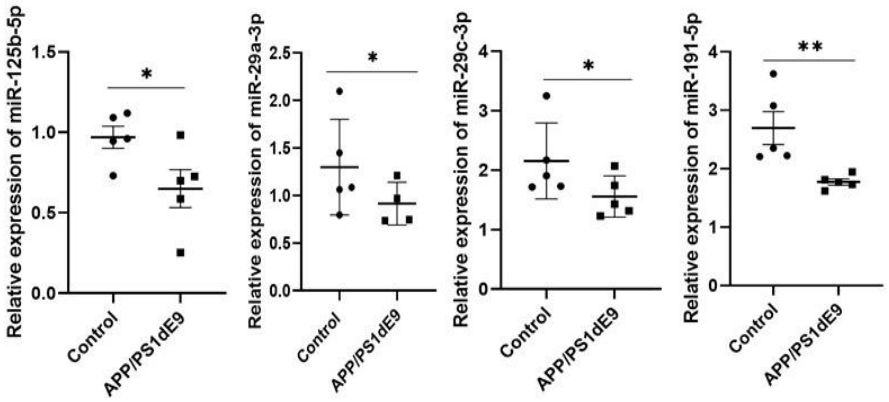

Figure 5. Relative expression of circulating miR-125b-5p, miR-29a, miR-29c and miR-191-5p in serum of $APP_{swe}/PS1_{dE9}$ transgenic animal model of amyloidosis. Serum samples from transgenic animals at 15 months of age were extracted and selected miRNA were quantified by qRT-PCR. Data are represented as mean ± SEM of 5 samples performed in triplicate. Statistical comparisons between the transgenic and control group were performed using the Mann-Whitney test. * $p \leq 0.05$, ** $p \leq 0.01$.

3.6. $A\beta_{1-42}$ infusion leads to an inflammatory response in the hippocampus of rats

Astrogliosis is a universally recognized feature of AD characterized by a cellular hypertrophy and an increase of glial fibrillar acid (GFAP) expression [52]. To confirm the presence of this perturbation in our experimental design performed in the rat model, we performed a GFAP fluorescence immunolabelling of brain tissues of rats harvested at 14 days post-infusion. Representative immunofluorescence images are shown in Figure 6A. As compared to brain sections from control group, a more pronounced fluorescence staining was detected in the whole hippocampal tissues including CA1/CA2, CA3 and DG regions in brain sections from Aβ- treated rats. The quantitative analysis of the whole fluorescence staining indicated that there were 2.1-fold and 1.7-fold more GFAP positive cells in CA1/CA2, CA3 and DG hippocampal regions of Aβ-infused rats compared to control rats.

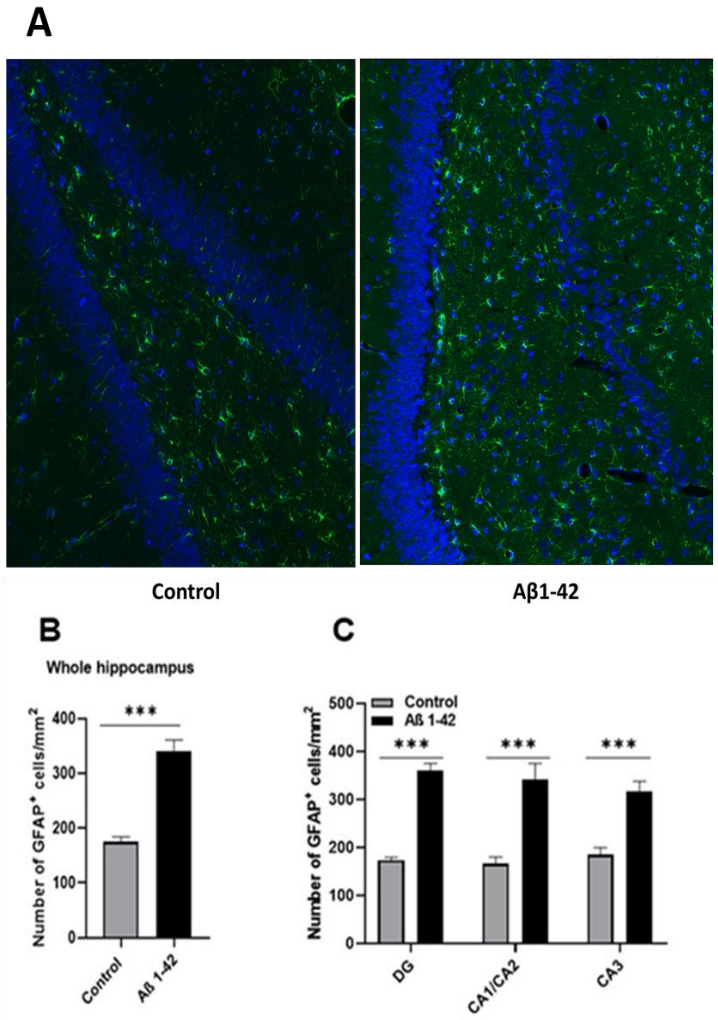

Figure 6. Quantification of astrocytes in the hippocampal areas. Brain sections from rats inoculated with $A\beta_{1\text{-}42}$ or PBS were analyzed 14 days post injection. **(A)** Representative immunohistochemical staining of GFAP expression (in green) in the DG area. The slides were counterstained with DAPI (blue) **(B)** Histograms showing the number of GFAP + cells per mm^2 quantified in the total hippocampus and **(C)** in each area of the hippocampus (CA1/CA2, CA3 and DG). The quantification of GFAP + cells was analyzed in 4-5 sections per animal (n = 5 for each group). Statistical comparisons between both groups were analyzed using the Student's t-test. * $p \leq 0.05$, ** $p \leq 0.01$, *** $p \leq 0.001$.

3.7. Intrahippocampal inoculation of $A\beta_{1\text{-}42}$ leads to an increased expression of miR-146a in CSF

We were intrigued by the fact that the kinetic of miR-146a-5p expression was not significantly altered in serum sample of Aβ-inoculated rats at the early 7 day post-injection time point and also by the observation that the peak of its down regulation was detected at day 14 that is also different to the other miRs (Figure 4). Moreover, this miR was not found deregulated in the $APP_{swe}/PS1_{dE9}$ mice. This, prompt us to focus our following experiments on the biological role of miR-146a in our rat model.

First, we evaluated the expression pattern of miR-146a-5p in CSF sample collected 14 days after infusion of Aβ at 2.5 μg/μL, in rat brains. Our results indicated that in contrast to serum sample in which its expression was found significantly down-regulated (Figure 7; $p = 0.022$), the amount of miR-146a-5p in CSF samples from Aβ-treated group was significantly up-regulated ($p = 0.004$) compared to those obtained from control group. These data highlight the discrepancy between the presence of miR-146a in serum versus CSF samples.

To gain more insight on the role of miR-146a, we completed our work with a mechanistic study performed with primary astrocytes model of AD. Astrocytes are considered to promote the first line of neuroinflammation response [53], by regulating the expression of key mediators of innate and adaptive immune responses in central nervous system.

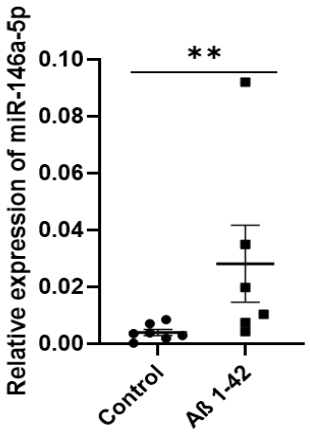

Figure 7. Relative expression of circulating miR-146a-5p in CSF of rats infused with $A\beta_{1-42}$ inside the hippocampus. CSF samples from rats infused with Aβ or PBS solutions were collected at 14 days post-injection. The expression of miR-146-5p was quantified by qRT-PCR. Data are represented as mean ± SEM of n = 7 samples performed in triplicate. Statistical comparisons between Aβ-infused and control group were performed using the Mann-Whitney test. ** $p \leq 0.01$.

3.8. The upregulation of miR-146a is dependent on the state of aggregation and the concentration of $A\beta_{1-42}$ in astrocyte cell culture.

Primary rat astrocytes were treated with $A\beta_{1-42}$ peptides to recapitulate, at least partially, the AD-like environment induced by infusion of Aβ in hippocampal tissues of rats. First, we evaluated the relative toxicity index of induced by several concentrations of $A\beta_{1-42}$ peptides on primary astrocytes viability cultured for 3 days. None of concentrations evaluated in this study were toxic for the cells (Figure S3). Next, we monitored expression of miR-146a-5p in these cells after treatment with $A\beta_{1-42}$ peptides. The qPCR data revealed that treatment of cells with $A\beta_{1-42}$ peptides for 3 days increased the expression of miR-146a at all concentrations evaluated (Figure 8A). An almost of 2 fold of maximum induction of miR-146a expression was detected when 1 μM Aβ was used as compared to control cells.

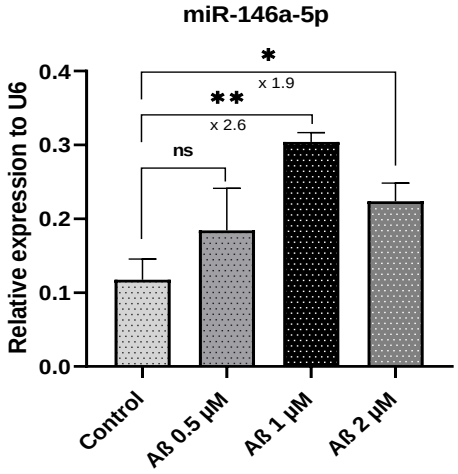

Figure 8. miR-146a-5p is up-regulated in primary astrocytes treated with Aβ1-42 peptides. Cells were treated with Aβ1-42 peptides made at 0.5, 1 and 2 μM for 3 days. (A) Relative expression of miR-146a-5p in primary astrocytes. The expression of miR-146a-5p was evaluated by quantitative real-time qRT-PCR. Small nuclear RNA U6 (RNU6) expression was used for normalization. Data are represented as the mean ± SEM performed in triplicate. Statistical comparisons between Aβ treated cells or DMSO treated cells were made with the Student's t-test. * p≤ 0.05, ** p≤ 0.01, ***p ≤ 0.001.

3.9. Aβ1-42 peptides induce the expression of miR-146a through the NF-κB cell signalling pathway

The expression of miR-146a has been reported to be upregulated in several central nervous cells in response to TNF-α, IL-1β or LPS through the activation of NF-κB cell signalling pathway. In the next step, we evaluated whether Aβ1-42 peptides treatment might induce the expression of miRNA-146a in primary astrocytes using the same cell signaling pathway. For that, cells were treated with Aβ1-42 peptides in presence or absence of the well-known BMS-345541 pharmacological inhibitor of NF-κB pathway for 3 days. As positive control for the activation of NF-κB pathway activation, cells were treated with LPS [54]. Results shown in Figure 9 confirmed that when primary astrocytes was treated with 1 μM Aβ1-42 peptides, the expression of miR-146a-5p was significantly upregulated compared to that of control cells. This expression can be inhibited by pre-treatment of cells with 1 μM of BMS-345541 inhibitor prior to the incubation with Aβ1-42 peptides. The expression level of miR-146a dropped-down significantly and reached the basal expression level detected in non-treated cells. As expected, LPS-treatment of primary astrocytes increased significantly the expression of miRNA-146a that was also significantly reversed by treatment with the BMS-345541 inhibitor. Those results indicate that both, Aβ1-42 peptides increase the basal expression level of miR-146 through the transcriptional regulation of the NF-κB pathway as did pro-inflammatory cytokines [55,56] or here LPS.

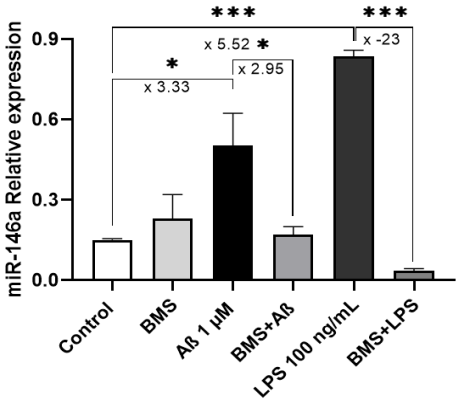

Figure 9. miR-146a is dependent to the NF-κB pathway. The effects of NF-κB inhibition on miR-146a expression were evaluated in Aβ-treated primary astrocytes culture. Primary astrocytes were stimulated with Aβ1-42 peptides at 1μM and LPS 100 ng/μL (Positive Control) with or without pre-incubation with IκB kinase inhibitors (BMS-345541) for 3 days. Data are represented as the mean ± SEM performed in triplicate. Statistical comparisons between Aβ treated cells or DMSO treated cells were made with the Student's t-test. * p≤ 0.05, ** p≤ 0.01, ***p ≤ 0.001.

3.10. Aβ1-42 peptides treatment did not induce any inflammatory cytokines expression

Based on the above results, we checked whether the expression level of pro-inflammatory cytokines produced in primary astrocyte cells could be also induced in response to Aβ1-42 peptides treatment. Surprisingly as shown in Figure 10, none of pro-inflammatory cytokines evaluated as IL-6, IL-1β were transcriptionally induced by treatment of primary cells with Aβ1-42 peptides for 3 days (Figure 10). Same results were obtained when the expression level of these cytokines was evaluated at the protein level by sandwich ELISA (data not shown). As positive control, a significant and high induction level of

those cytokines (IL-6, and IL-1β) were detected in cells upon treatment with LPS for 3 days as expected.

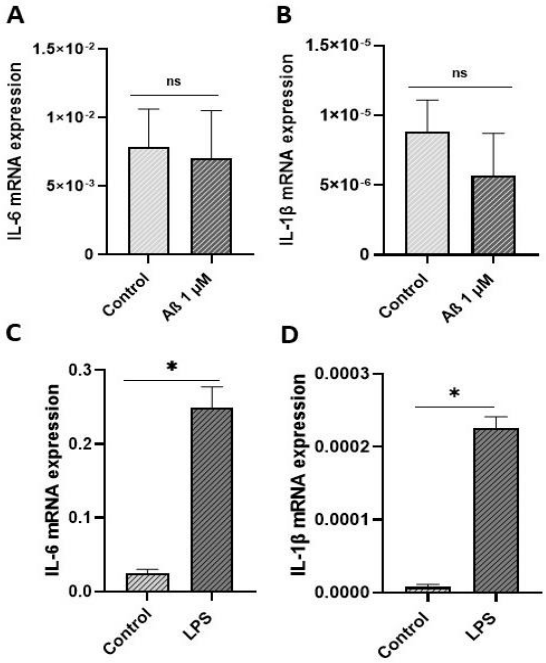

Figure 10. Expression of inflammatory markers mRNAs in cell culture of primary astrocytes stimulated with $A\beta_{1-42}$ peptides. Three days post-stimulation with Aβ peptides (Figure 10A and B), the expression of IL-6 and IL-1β were quantified by RT-qPCR. Astrocytes were also stimulated with LPS at 100 ng/ml as positive control (Fig 10C and D) . Data are represented as mean ± SEM of experiments made in triplicate 3. Statistical comparisons between groups were made using the Student's t-test. * $p \leq 0.05$, ** $p \leq 0.01$, *** $p \leq 0.001$.

3.11. miRNA-146a induction likely counteracts NF-κB signalling pathway in astrocyte through the down-regulation of IRAK-1 and upregulation of IRAK-2 as compensatory mechanism.

To go further in our study, we evaluated the expression of IRAK-1 and TRAF-6, two well known transcriptional targets of miR-146a. Those proteins are part of NF-κB signalling pathway [57] (Figure 11A). As shown in Figure 11B, the relative expression of IRAK-1 was significantly down regulated (1.5-fold) in cells treated with Aβ compared to control cells while the expression of IRAK-2 was upregulated (Figure 11C). Surprisingly, the relative expression of TRAF-6, a direct downstream effector of the IRAK-1/2 complex was unchanged in cells treated with $A\beta_{1-42}$ peptides compared to control cells (Figure 11D).

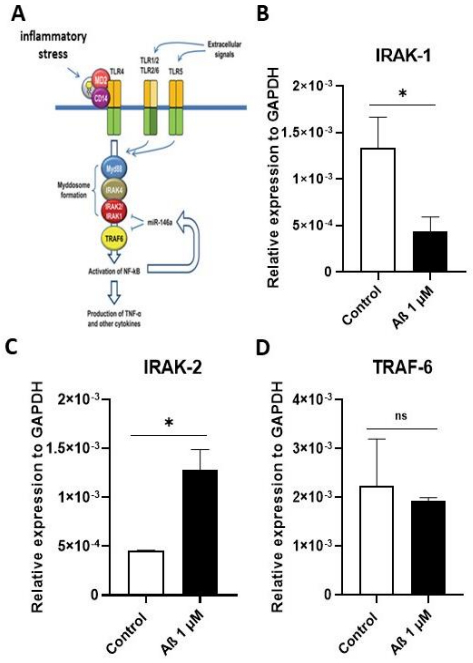

Figure 11. Expression of IRAK-1, IRAK-2 and TRAF-6 targets of the NF-κB cellular pathway in primary cells trated with $A\beta_{1\text{-}42}$ peptides. (A) Schematic representation of NF-κB signalling pathway (B) The relative levels of mRNA of IRAK-1 (C) IRAK-2 (D) TRAF-6 in primary astrocytes incubated with Aβ at 1 μM or cells treated with DMSO for 3 days were detected by qRT-PCR. GAPDH expression was used for normalization. Data are represented as the mean ± SEM of experiments performed in triplicate. Statistical comparisons were made between Aβ-treated cells and DMSO-treated cells with Student's t-test. * $p \leq 0.05$, ** $p \leq 0.01$, *** $p \leq 0.001$. .

3.12. $A\beta_{1\text{-}42}$ peptides treatment stimulates the production of chemokines

Since the treatment of cells with either $A\beta_{1\text{-}42}$ peptides was sufficient to induce the transcriptional changes in IRAK-1 and 2, it prompts us to postulate if other mechanistic events or signalling pathways different than NF-κB signalling might be activated by those treatments. We focused on expression level of chemokine as CXCL1 as potential candidate. In AD, CXCL-1 is amongst chemokines produced by astrocytes activated by Aβ peptides [58]. We evaluated the production of CXCL-1 by primary astrocytes following treatment with $A\beta_{1\text{-}42}$ peptides for 3 days at several concentrations. ELISA data shown in Figure 12, revealed a slight, but significant CXCL-1 production by astrocytes in response to increased concentrations of $A\beta_{1\text{-}42}$ peptides. The maximum level of CXCL-1 production was detected in cells treated with 1 μM of $A\beta_{1\text{-}42}$ peptides that correlated well and again with the maximum induction of miR-146a expression detected at the same concentration.

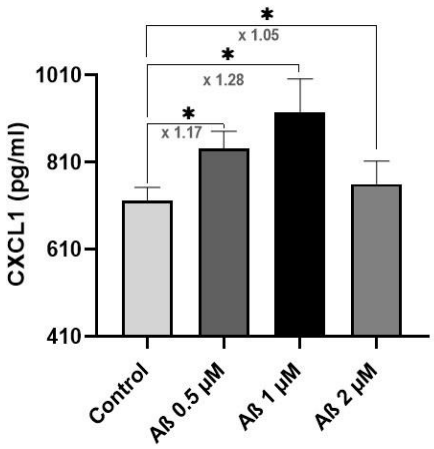

Figure 12. CXCL-1 secretion by Aβ-treated primary astrocytes. CXCL-1 expression was evaluated by ELISA assays on supernatants from primary astrocytes stimulated with $A\beta_{1-42}$ peptides at 0.5, 1 and 2 µM. Data are represented as the mean ± SEM of experiments made in triplicate. Statistical comparisons were made between Aβ-treated cells and DMSO-treated cells with Student's t-test. * $p \leq 0.05$, ** $p \leq 0.01$, *** $p \leq 0.001$.

4. Discussion

It is widely accepted that Aβ peptide plays a central role in the appearance and progression of AD. Bilateral intrahippocampal injections of Aβ peptides did result in a reduction in neuronal density, an increasing expression of of the glial fibrillar acid protein and caused deficiencies in behavioral performance [59]. Borbely et al., demonstrated that intrahippocampal administration of synthetic Aβ peptides simultaneously decreases both the spatial learning capacity in MWM and the density of the dendritic column in the CA1 region of the rat hippocampus [60].

In the present study, we inoculated $A\beta_{1-42}$ peptides into the CA1 region of the hippocampus. MWM tests was conducted to assess the effect of $A\beta_{1-42}$ peptides injection into the hippocampus of rats on spatial learning and working memory, as the memory impairment is one main symptom of AD. Our results showed a deterioration of learning capacity in animals treated with $A\beta_{1-42}$. On day 1 of the test, the absence of significant differences between the injected and control groups with regard to the distance travelled or the latency escape, (Figure 1) indicates that all animals are similar for the start of the learning and memory tasks. MWM test was performed 14 days post- surgery based on reports showing that the deterioration is visibly significant around this time point [22]. A previous study reported an impaired spatial learning memory on day 12 post-injection [3]. When checked at earlier time as 8 days post-injection, no significant differences between the groups were observed [61]. The short period may not have been sufficient to impair spatial learning. Our data are in agreement with previous reports and validate that the injection of $A\beta_{1-42}$ generates learning disorders in treated animals.

It has been shown that abnormal accumulation and shedding of Aβ peptides can lead to localized inflammation involving reactive astrocytes with increased expression of GFAP [52]. This process called gliosis occurs after brain injury and is characteristic of neurodegenerative disorders such as AD [62]. We validated the presence of those reactive astrocytes by immunofluorescence staining analysis of brain sections of animals inoculated with $A\beta_{1-42}$. They had a higher number of astrocytes in all regions of the hippocampus CA1/CA2, CA3 and DG, suggesting an activated state by contrast to animals of the control group having a lower number of astrocytes. Each area contained approximately twice the number of detectable astrocytes than that of control animals (Figure 6). Our data is in line with those of different studies showing an increase in astrocytes in a model of

injection of Aβ in the hippocampus of rat's model of AD [59,63] and, in addition with MWM data, validate our animal model.

To the best of our knowledge, no reports have evaluated the quantification of circulating microRNAs in serum samples in this rat model of amyloidosis induced by infusion of $A\beta_{1-42}$ peptides in hippocampus. It is therefore also interesting to compare the data with those obtained with AD transgenic mice models and even with those obtained from human studies. We selected a short list 9 microRNAs frequently expressed in patients with AD and/or in transgenic animal models. Amongst them, miR-29a, miR-29c, miR-125b, miR-191-5p and miR-146a were found significantly deregulated as compared to control rats (Figures 2 and 3). The degree of dysregulation is proportional to Aβ peptides concentration used for the injection. Since miRNA acts as temporal regulator of different biological processes, we sought to assess the kinetic of the expression of miRs at day 7, 14 and 21 (Figure 4). Kinetic studies were done on miR-9-5p, miR-29a-3p, miR-29c-3p and miR-146a-5p as they were the most deregulated miRs in our animal model but also in other AD model as well as human studies [50,64]. Our data show that there is a clear downregulation tendancy of all microRNAs in Aβ-injected rats compared to controls. MiR-9 is known to regulate BACE1 expression; lowering miR-9 levels resulted in an increase of BACE1 expression, thereby increasing $A\beta_{1-42}$ peptides production [65]. The reduced expression of miR-9 in CNS would promote amyloidogenic processing, leading to a pronounced Aβ aggregation and their deposition into senile plaques [66]. A comparative study of several miRs levels in sera of AD patients with mild cognitive impairment as compared to control patients has shown that the circulating levels of the miR-9 was the lowest [65]. Interestingly, a reduced amount of miR-9 has been also found in the plasma of 3xTg-AD and APP/PS1 transgenic mice models [23,67]. In this work, the passive introduction of Aβ aggregates, in the hippocampal region started to alter the expression of miR-9, the difference between the two groups of rat was very close to statistic significance.

The members of the miR-29 family showed similar trend. There is a strong dysregulation in the Aβ-injected group at 7 days compared to control group. At 14 and 21 days, the dysregulation was maintained but the curve started to rise up very mildly suggesting a reverse phase (Figure 4C and 4D). The down regulation of miR-29a and miR-29c is consistent with many previous reports that have evaluated serum and/or plasma from patients with AD [28,68,69]. Interestingly, miR-29 a/b cluster has been reported to be correlated with BACE1/beta-secretase expression [70]. Combined to miR-9 data, one can suggest that a passive introduction of Aβ aggregates is enough to retrocontrol the level of microRNAs.

Concerning miR-146a expression, it was down-regulated at all times evaluated after treatments. However, the difference was not significant 7 days post-injection by contrast to 14 and 21 days. (Figure 4B). MiR-146a has been shown to be an early and prevalent pathological feature of AD as it is involved in the inflammatory response and neuroinflammation [56]. Our results are consistent with different studies that evaluated the circulating expression profile of miR-146a in transgenic animal models or in humans. Garza-Manero et al., have reported the same profile for miR-146a in 3xTg-AD transgenic model from 14 to 15 months compared to young mice [23] . Studies carried out in humans have shown as well that the circulating profile of miR-146a is decreased in AD [71].

Two other miRNAs, miR-191-5p and miR-125b-5p were also significantly reduced in Aβ-infused rats compared to the control rats. MiR-191-5p has been reported to be down-regulated in the sera of AD patients [14]. MiR-191-5p is involved in the regulation of the level of BACE1 via its binding site targeting BACE1 3'UTR, and its down-regulation resulted in amyloidogenesis. MiR 125b-5p is known to be involved in synaptic plasticity regulation and its level was higher in serum of AD patients [72], compared to healthy controls. This observation is contradictory of ours and it could be explained by the partial recapitulation of the human disorder in this rat model. Interesting to note that the expression profile of the 9 circulating miRNAs from $APP_{swe}/PS1_{dE9}$ transgenic mice model at 15-month old mice were similar to those obtained with the rat model except for miR146a-5p

(Figure 5). These mice recapitulate the early AD phenotype as well, and are characterized by an increased Aβ peptides in the brain [73]. These animals express a human/mouse chimeric APP and a human presenilin-1 and have early synaptic dysfunction and chronic Aβ deposition, neuroinflammation and cognitive impairment from 6 months [74]. Altogether, results concerning the quantification of circulating miRNAs in those two different models and the comparison with data from AD patients highlight the limitations of each model. It worth to note that the down-regulation of circulating miR-29a-3p and miR29c-3p in sera of those models has been consistently observed in serum of AD patients [28,70].

Neuroinflammation is one of the hallmark of AD and miR-146a, is a key mediator of immune response linked to a variety of inflammation processes. To complement our data, we first quantified the amount of miR-146a-5p in CSF obtained from Aβ-injected rats at 14 days post injection. The upregulation of miR-146a in $A\beta_{1-42}$ treated animals compared to the control group (Figure 7) is in line with reports showing high levels of miR-146a expression in CSF human samples of AD patients [75,76]. Due to its direct and intimate relationship with brain tissue, CSF reflects neurophysiological changes in AD [76]. Our data highlight the opposite trend between circulating miR-146a in serum and in CSF of this rat model as also described for other miRs [14]. Reasons for this discrepancy is not clear and may be related to change in extracellular vesicles types secreted by cells of the CNS that might limit their passage across the blood brain barrier [77]. Nevertheless, to understand further the role of the miR-146 in AD development and its relationship with inflammation caused by Aβ peptide aggregation tissues, we conducted functional *in vitro* studies made on primary rat astrocytes. The study was done with astrocytes primary astrocytes because they are the most abundant cell type in the CNS and important modulators of the innate and inflammatory immune response of the brain of patients with AD [78]. Moreover, the severity of glial activation is correlated with the degree of brain atrophy and cognitive impairment. We took as well the opportunity to assess the impact of Aβ aggregates on astrocytes. We observed an upregulation of miR-146a compared to control cells (Figure 8A and 8B). These findings are consistent with previous studies done on human astrocytes that had an upregulation of miR-146a when exposed to Aβ peptides [53,55]. Similarly, Li et al., demonstrated that miR-146a was positively regulated in human neuronal-glial (HNG), human astroglial (HAG) and human microglial (HMG) cells treated with $A\beta_{1-42}$ peptides and TNF-α compared to untreated controls [55]. However, the impact of $A\beta_{1-42}$ peptides alone in expression of miR 146 by these cells was not investigated in those studies. Our data validate that the upregulation of miR-146a expression is under the transcriptional control of NF-κB [56] as it was abolished by BMS-345541, an inhibitor of NF-κB (Figure 9). To go further in the dissection of Aβ peptides impacts on astrocytes, we quantified the expression of *IL-6*, *IL-1β*, and *TNF-α* inflammatory cytokines known to be increased following astrocytes activation and aberrantly expressed in AD brain [79]. We did not observed expression defects of inflammatory cytokines (Figure 10), which are different from those previous findings. Note that in those reports, cells were put under oxidative stress or inflammatory conditions (H_2O_2, LPS, TNF-α) in addition to Aβ treatment. MiR-146a is known to regulate Toll-like (TLR) and interleukin-1 receptors (ILRs) signaling [40,57]. Furthermore, miR-146a causes a direct repression of interleukin-1 receptor associated kinase 1 (IRAK1), and Tumor necrosis factor receptor associated factor 6 (TRAF-6). Different reports made with human astrocytes showed that concurrent to miR-146a upregulation in cells exposed to Aβ peptides, a decrease of IRAK-1 associated with a compensatory increase in the expression of Interleukin-1 receptor-associated kinase-like 2 (IRAK-2) were induced leading to a sustained inflammatory response [57]. The decrease of IRAK-1 gene was also reported when brain cells were stressed by $A\beta_{1-42}$ and TNF-α [55]. Our results are consistent with this observation as we found that in Aβ-treated cells, IRAK1 expression was downregulated whilst IRAK-2 was upregulated. In the majority of studies, cells are concomittantly treated with Aβ peptides and inflammatory molecules as LPS, TNFα or IL-1β amplifying the inflammation state. Here, we found that Aβ

peptides treatment can trigger the induction of miR146a even in a suboptimal inflammatory and non cytotoxic state of primary astrocytes. It is tempting to speculate that the up-regulation of miR-146a by the NF-κB transcription factor activated in response to Aβ peptides might play a negative feedback loop of control of NF-κB signalling pathway by down-regulating IRAK-1 and up-regulating IRAK-2. As a consequence of this retro-control loop of NF-κB pathway, an abrogation of the expression of pro-inflammatory cytokines as IL-6, TNF-α, and IL-1β might occur by keeping constant the expression level of TRAF-6. This, is in line with reports showing that miRNA expression can act as a negative feed-back regulator of the same signalling pathway used for its own induction, thereby preventing an overstimulation of the inflammatory response [80].

5. Conclusion

Data from this study show that circulating miR 146a-5p, 29a-3p, -29c-3p, 191-5p and 125b-5p are downregulated in sera of rats injected with Aβ aggregates. Interestingly, those circulating miRNAs except miR-146a were also deregulated in the widely used amyloid-bearing $APP_{swe}/PS1_{dE9}$ transgenic mice. By contrast, miR146a-5p was upregulated in CSF of those rats which presented astrogliosis in their brain. The mechanistic study done on rat primary astrocytes revealed that their treatment with Aβ aggregates led also to the upregulation of miR-146a *via* NFκB signalling pathway which in turn downregulated the expression of IRAK-1 but without affecting the expression of TRAF-6, key effector of this NFκB signalling pathway. As consequence, no change in the expression of IL-6, IL-1β was detected although a slight but significant expression of CXCL1 was quantified. Based on those data and those reported in the literature, we propose that miR-146a upregulation in astrocyte cells is likely to play an anti-inflammatory role through a negative feedback of the NF-κB pathway. To sum-up, this study contributes to improve our knowledge on the rat model of AD generated by intrahippocampal injection of $A\beta_{1-42}$ peptides and point to of dysregulated miRNAs that could represent early diagnosis markers.

Supplementary Materials: The following are available online at www.mdpi.com/xxx/s1, **Figure S1:** Effects of $A\beta_{1-42}$ injection on memory and learning, evaluated by the Morris Water Maze test**, Figure S2.** Relative expression of circulating miR-9a-5p, miR-29a-3p, miR-146a-5p and miR-29c-3p in serum of $APP_{swe}/PS1_{dE9}$ transgenic animal model of AD, **Figure S3.** Incubation of primary astrocytes cell culture with Aβ at indicated concentration does not lead to any cell toxicity.

Author Contributions: Conceptualization, C.P, P.B, A.M, M.D and R.A; methodology, R.A, V.C, S.L, D.G; plug-in, M.G.F and L.B; validation, C.P, P.B; writing—original draft preparation, R.A; writing—review and editing, C.P, P.B, A.M, M.D; supervision, C.P, P.B, A.M; funding acquisition, C.P. All authors have read and agreed to the published version of the manuscript.

Funding: This research was funded by CNRS and University of Orléans, R.A received a fellowship from the Franco Peruvian School of Life Sciences by Consejo Nacional de Ciencia, Tecnología e Innovación Tecnológica (CONCYTEC), Universidad Peruana Cayetano Heredia and the University of Orléans. **Institutional Review Board Statement:** The study was conducted according to the guidelines of the Declaration of Helsinki, and approved by the Institutional Committee of Ethics in Research - Animals of Cayetano Heredia, Lima, Peru. Code: CIEA-102069 approved on April 5, 2018.

Acknowledgments: We acknowledge all supports from the University of Orléans, **CNRS,** CONCYTEC and Cayetano Heredia Peruvian University**.**

Conflicts of Interest: "The authors declare no conflict of interest."

6. References

1. Prince, M.; Bryce, R.; Albanese, E.; Wimo, A.; Ribeiro, W.; Ferri, C.P. The global prevalence of dementia: a systematic review and metaanalysis. *Alzheimer's & dementia : the journal of the Alzheimer's Association* **2013**, *9*, 63-75 e62, doi:10.1016/j.jalz.2012.11.007.
2. Mullard, A. Alzheimer amyloid hypothesis lives on. *Nature reviews. Drug discovery* **2016**, *16*, 3-5, doi:10.1038/nrd.2016.281.
3. Wong, R.S.; Cechetto, D.F.; Whitehead, S.N. Assessing the Effects of Acute Amyloid β Oligomer Exposure in the Rat. *International journal of molecular sciences* **2016**, *17*, doi:10.3390/ijms17091390.

4. Bekris, L.M.; Yu, C.E.; Bird, T.D.; Tsuang, D.W. Genetics of Alzheimer disease. *Journal of geriatric psychiatry and neurology* **2010**, *23*, 213-227, doi:10.1177/0891988710383571.
5. Bateman, R.J.; Xiong, C.; Benzinger, T.L.; Fagan, A.M.; Goate, A.; Fox, N.C.; Marcus, D.S.; Cairns, N.J.; Xie, X.; Blazey, T.M.; et al. Clinical and biomarker changes in dominantly inherited Alzheimer's disease. *The New England journal of medicine* **2012**, *367*, 795-804, doi:10.1056/NEJMoa1202753.
6. Mantile, F.; Prisco, A. Vaccination against β-Amyloid as a Strategy for the Prevention of Alzheimer's Disease. *Biology* **2020**, *9*, doi:10.3390/biology9120425.
7. Angelucci, F.; Cechova, K.; Valis, M.; Kuca, K.; Zhang, B.; Hort, J. MicroRNAs in Alzheimer's Disease: Diagnostic Markers or Therapeutic Agents? *Frontiers in pharmacology* **2019**, *10*, 665, doi:10.3389/fphar.2019.00665.
8. Shaffer, J.L.; Petrella, J.R.; Sheldon, F.C.; Choudhury, K.R.; Calhoun, V.D.; Coleman, R.E.; Doraiswamy, P.M. Predicting cognitive decline in subjects at risk for Alzheimer disease by using combined cerebrospinal fluid, MR imaging, and PET biomarkers. *Radiology* **2013**, *266*, 583-591, doi:10.1148/radiol.12120010.
9. Bartel, D.P. MicroRNAs: genomics, biogenesis, mechanism, and function. *Cell* **2004**, *116*, 281-297, doi:10.1016/s0092-8674(04)00045-5.
10. Friedman, R.C.; Farh, K.K.; Burge, C.B.; Bartel, D.P. Most mammalian mRNAs are conserved targets of microRNAs. *Genome research* **2009**, *19*, 92-105, doi:10.1101/gr.082701.108.
11. Gilad, S.; Meiri, E.; Yogev, Y.; Benjamin, S.; Lebanony, D.; Yerushalmi, N.; Benjamin, H.; Kushnir, M.; Cholakh, H.; Melamed, N.; et al. Serum microRNAs are promising novel biomarkers. *PloS one* **2008**, *3*, e3148, doi:10.1371/journal.pone.0003148.
12. Edsbagge, M.; Andreasson, U.; Ambarki, K.; Wikkelsø, C.; Eklund, A.; Blennow, K.; Zetterberg, H.; Tullberg, M. Alzheimer's Disease-Associated Cerebrospinal Fluid (CSF) Biomarkers do not Correlate with CSF Volumes or CSF Production Rate. *Journal of Alzheimer's disease : JAD* **2017**, *58*, 821-828, doi:10.3233/jad-161257.
13. Kalogianni, D.P.; Kalligosfyri, P.M.; Kyriakou, I.K.; Christopoulos, T.K. Advances in microRNA analysis. *Analytical and bioanalytical chemistry* **2018**, *410*, 695-713, doi:10.1007/s00216-017-0632-z.
14. Kumar, S.; Reddy, P.H. Are circulating microRNAs peripheral biomarkers for Alzheimer's disease? *Biochimica et biophysica acta* **2016**, *1862*, 1617-1627, doi:10.1016/j.bbadis.2016.06.001.
15. Wang, M.; Qin, L.; Tang, B. MicroRNAs in Alzheimer's Disease. *Frontiers in genetics* **2019**, *10*, 153, doi:10.3389/fgene.2019.00153.
16. Bryan, K.J.; Lee, H.G.; Perry, G.; Smith, M.A.; Casadesus, G. *Transgenic Mouse Models of Alzheimer's Disease: Behavioral Testing and Considerations*

Methods of Behavior Analysis in Neuroscience; © Taylor & Francis Group, LLC.: Boca Raton FL, 2009.
17. Bagyinszky, E.; Youn, Y.C.; An, S.S.; Kim, S. The genetics of Alzheimer's disease. *Clinical interventions in aging* **2014**, *9*, 535-551, doi:10.2147/cia.s51571.
18. Lane-Donovan, C.; Herz, J. ApoE, ApoE Receptors, and the Synapse in Alzheimer's Disease. *Trends in endocrinology and metabolism: TEM* **2017**, *28*, 273-284, doi:10.1016/j.tem.2016.12.001.
19. Lecanu, L.; Papadopoulos, V. Modeling Alzheimer's disease with non-transgenic rat models. *Alzheimer's research & therapy* **2013**, *5*, 17, doi:10.1186/alzrt171.
20. Kaushal, A.; Wani, W.Y.; Anand, R.; Gill, K.D. Spontaneous and induced nontransgenic animal models of AD: modeling AD using combinatorial approach. *American journal of Alzheimer's disease and other dementias* **2013**, *28*, 318-326, doi:10.1177/1533317513488914.
21. Faucher, P.; Mons, N.; Micheau, J.; Louis, C.; Beracochea, D.J. Hippocampal Injections of Oligomeric Amyloid β-peptide (1-42) Induce Selective Working Memory Deficits and Long-lasting Alterations of ERK Signaling Pathway. *Frontiers in aging neuroscience* **2015**, *7*, 245, doi:10.3389/fnagi.2015.00245.
22. Karthick, C.; Nithiyanandan, S.; Essa, M.M.; Guillemin, G.J.; Jayachandran, S.K.; Anusuyadevi, M. Time-dependent effect of oligomeric amyloid-β (1-42)-induced hippocampal neurodegeneration in rat model of Alzheimer's disease. *Neurological research* **2019**, *41*, 139-150, doi:10.1080/01616412.2018.1544745.
23. Garza-Manero, S.; Arias, C.; Bermúdez-Rattoni, F.; Vaca, L.; Zepeda, A. Identification of age- and disease-related alterations in circulating miRNAs in a mouse model of Alzheimer's disease. *Frontiers in cellular neuroscience* **2015**, *9*, 53, doi:10.3389/fncel.2015.00053.
24. Kenny, A.; Jimenez-Mateos, E.M.; Calero, M.; Medina, M.; Engel, T. Detecting Circulating MicroRNAs as Biomarkers in Alzheimer's Disease. *Methods in molecular biology (Clifton, N.J.)* **2018**, *1779*, 471-484, doi:10.1007/978-1-4939-7816-8_29.
25. Kumar, S.; Vijayan, M.; Bhatti, J.S.; Reddy, P.H. MicroRNAs as Peripheral Biomarkers in Aging and Age-Related Diseases. *Progress in molecular biology and translational science* **2017**, *146*, 47-94, doi:10.1016/bs.pmbts.2016.12.013.
26. Wu, H.Z.; Ong, K.L.; Seeher, K.; Armstrong, N.J.; Thalamuthu, A.; Brodaty, H.; Sachdev, P.; Mather, K. Circulating microRNAs as Biomarkers of Alzheimer's Disease: A Systematic Review. *Journal of Alzheimer's disease : JAD* **2016**, *49*, 755-766, doi:10.3233/jad-150619.
27. Zhao, Y.; Zhang, Y.; Zhang, L.; Dong, Y.; Ji, H.; Shen, L. The Potential Markers of Circulating microRNAs and long non-coding RNAs in Alzheimer's Disease. *Aging and disease* **2019**, *10*, 1293-1301, doi:10.14336/ad.2018.1105.
28. Wu, Y.; Xu, J.; Xu, J.; Cheng, J.; Jiao, D.; Zhou, C.; Dai, Y.; Chen, Q. Lower Serum Levels of miR-29c-3p and miR-19b-3p as Biomarkers for Alzheimer's Disease. *The Tohoku journal of experimental medicine* **2017**, *242*, 129-136, doi:10.1620/tjem.242.129.
29. Wenk, G.L. Assessment of spatial memory using the radial arm maze and Morris water maze. *Current protocols in neuroscience* **2004**, *Chapter 8*, Unit 8 5A, doi:10.1002/0471142301.ns0805as26.

30. Vigneron, N.; Meryet-Figuière, M.; Guttin, A.; Issartel, J.P.; Lambert, B.; Briand, M.; Louis, M.H.; Vernon, M.; Lebailly, P.; Lecluse, Y.; et al. Towards a new standardized method for circulating miRNAs profiling in clinical studies: Interest of the exogenous normalization to improve miRNA signature accuracy. *Molecular oncology* **2016**, *10*, 981-992, doi:10.1016/j.molonc.2016.03.005.
31. Beeton, C.; Garcia, A.; Chandy, K.G. Drawing blood from rats through the saphenous vein and by cardiac puncture. *Journal of visualized experiments : JoVE* **2007**, 266, doi:10.3791/266.
32. Blanco, M.E.; Mayo, O.B.; Bandiera, T.; De Pietri Tonelli, D.; Armirotti, A. LC-MS/MS analysis of twelve neurotransmitters and amino acids in mouse cerebrospinal fluid. *Journal of neuroscience methods* **2020**, *341*, 108760, doi:10.1016/j.jneumeth.2020.108760.
33. Liu, L.; Duff, K. A technique for serial collection of cerebrospinal fluid from the cisterna magna in mouse. *Journal of visualized experiments : JoVE* **2008**, doi:10.3791/960.
34. Duy, J.; Koehler, J.W.; Honko, A.N.; Minogue, T.D. Optimized microRNA purification from TRIzol-treated plasma. *BMC genomics* **2015**, *16*, 95, doi:10.1186/s12864-015-1299-5.
35. Ezzine, S.; Vassaux, G.; Pitard, B.; Barteau, B.; Malinge, J.M.; Midoux, P.; Pichon, C.; Baril, P. RILES, a novel method for temporal analysis of the in vivo regulation of miRNA expression. *Nucleic acids research* **2013**, *41*, e192, doi:10.1093/nar/gkt797.
36. Simion, V.; Henriet, E.; Juric, V.; Aquino, R.; Loussouarn, C.; Laurent, Y.; Martin, F.; Midoux, P.; Garcion, E.; Pichon, C.; et al. Intracellular trafficking and functional monitoring of miRNA delivery in glioblastoma using lipopolyplexes and the miRNA-ON RILES reporter system. *Journal of controlled release : official journal of the Controlled Release Society* **2020**, *327*, 429-443, doi:10.1016/j.jconrel.2020.08.028.
37. Simion, V.; Sobilo, J.; Clemoncon, R.; Natkunarajah, S.; Ezzine, S.; Abdallah, F.; Lerondel, S.; Pichon, C.; Baril, P. Positive radionuclide imaging of miRNA expression using RILES and the human sodium iodide symporter as reporter gene is feasible and supports a protective role of miRNA-23a in response to muscular atrophy. *PloS one* **2017**, *12*, e0177492, doi:10.1371/journal.pone.0177492.
38. Livak, K.J.; Schmittgen, T.D. Analysis of relative gene expression data using real-time quantitative PCR and the 2(-Delta Delta C(T)) Method. *Methods (San Diego, Calif.)* **2001**, *25*, 402-408, doi:10.1006/meth.2001.1262.
39. Faraldi, M.; Gomarasca, M.; Sansoni, V.; Perego, S.; Banfi, G.; Lombardi, G. Normalization strategies differently affect circulating miRNA profile associated with the training status. *Scientific reports* **2019**, *9*, 1584, doi:10.1038/s41598-019-38505-x.
40. Reverchon, F.; de Concini, V.; Larrigaldie, V.; Benmerzoug, S.; Briault, S.; Togbé, D.; Ryffel, B.; Quesniaux, V.F.J.; Menuet, A. Hippocampal interleukin-33 mediates neuroinflammation-induced cognitive impairments. *Journal of neuroinflammation* **2020**, *17*, 268, doi:10.1186/s12974-020-01939-6.
41. Schindelin, J.; Arganda-Carreras, I.; Frise, E.; Kaynig, V.; Longair, M.; Pietzsch, T.; Preibisch, S.; Rueden, C.; Saalfeld, S.; Schmid, B.; et al. Fiji: an open-source platform for biological-image analysis. *Nature methods* **2012**, *9*, 676-682, doi:10.1038/nmeth.2019.
42. Galland, F.; Seady, M.; Taday, J.; Smaili, S.S.; Gonçalves, C.A.; Leite, M.C. Astrocyte culture models: Molecular and function characterization of primary culture, immortalized astrocytes and C6 glioma cells. *Neurochemistry international* **2019**, *131*, 104538, doi:10.1016/j.neuint.2019.104538.
43. Gao, Y.J.; Zhang, L.; Samad, O.A.; Suter, M.R.; Yasuhiko, K.; Xu, Z.Z.; Park, J.Y.; Lind, A.L.; Ma, Q.; Ji, R.R. JNK-induced MCP-1 production in spinal cord astrocytes contributes to central sensitization and neuropathic pain. *The Journal of neuroscience : the official journal of the Society for Neuroscience* **2009**, *29*, 4096-4108, doi:10.1523/jneurosci.3623-08.2009.
44. Dahlgren, K.N.; Manelli, A.M.; Stine, W.B., Jr.; Baker, L.K.; Krafft, G.A.; LaDu, M.J. Oligomeric and fibrillar species of amyloid-beta peptides differentially affect neuronal viability. *The Journal of biological chemistry* **2002**, *277*, 32046-32053, doi:10.1074/jbc.M201750200.
45. Heo, C.; Chang, K.A.; Choi, H.S.; Kim, H.S.; Kim, S.; Liew, H.; Kim, J.A.; Yu, E.; Ma, J.; Suh, Y.H. Effects of the monomeric, oligomeric, and fibrillar Abeta42 peptides on the proliferation and differentiation of adult neural stem cells from subventricular zone. *Journal of neurochemistry* **2007**, *102*, 493-500, doi:10.1111/j.1471-4159.2007.04499.x.
46. White, J.A.; Manelli, A.M.; Holmberg, K.H.; Van Eldik, L.J.; Ladu, M.J. Differential effects of oligomeric and fibrillar amyloid-beta 1-42 on astrocyte-mediated inflammation. *Neurobiology of disease* **2005**, *18*, 459-465, doi:10.1016/j.nbd.2004.12.013.
47. Burke, J.R.; Pattoli, M.A.; Gregor, K.R.; Brassil, P.J.; MacMaster, J.F.; McIntyre, K.W.; Yang, X.; Iotzova, V.S.; Clarke, W.; Strnad, J.; et al. BMS-345541 is a highly selective inhibitor of I kappa B kinase that binds at an allosteric site of the enzyme and blocks NF-kappa B-dependent transcription in mice. *The Journal of biological chemistry* **2003**, *278*, 1450-1456, doi:10.1074/jbc.M209677200.
48. Owens, R.; Grabert, K.; Davies, C.L.; Alfieri, A.; Antel, J.P.; Healy, L.M.; McColl, B.W. Corrigendum: Divergent Neuroinflammatory Regulation of Microglial TREM Expression and Involvement of NF-κB. *Frontiers in cellular neuroscience* **2017**, *11*, 256, doi:10.3389/fncel.2017.00256.
49. Reverchon, F.; Mortaud, S.; Sivoyon, M.; Maillet, I.; Laugeray, A.; Palomo, J.; Montécot, C.; Herzine, A.; Meme, S.; Meme, W.; et al. IL-33 receptor ST2 regulates the cognitive impairments associated with experimental cerebral malaria. *PLoS pathogens* **2017**, *13*, e1006322, doi:10.1371/journal.ppat.1006322.
50. Delay, C.; Hébert, S.S. MicroRNAs and Alzheimer's Disease Mouse Models: Current Insights and Future Research Avenues. *International journal of Alzheimer's disease* **2011**, *2011*, 894938, doi:10.4061/2011/894938.
51. Garcia-Alloza, M.; Robbins, E.M.; Zhang-Nunes, S.X.; Purcell, S.M.; Betensky, R.A.; Raju, S.; Prada, C.; Greenberg, S.M.; Bacskai, B.J.; Frosch, M.P. Characterization of amyloid deposition in the APPswe/PS1dE9 mouse model of Alzheimer disease. *Neurobiology of disease* **2006**, *24*, 516-524, doi:10.1016/j.nbd.2006.08.017.

52. Kamphuis, W.; Mamber, C.; Moeton, M.; Kooijman, L.; Sluijs, J.A.; Jansen, A.H.; Verveer, M.; de Groot, L.R.; Smith, V.D.; Rangarajan, S.; et al. GFAP isoforms in adult mouse brain with a focus on neurogenic astrocytes and reactive astrogliosis in mouse models of Alzheimer disease. *PloS one* **2012**, *7*, e42823, doi:10.1371/journal.pone.0042823.
53. Colombo, E.; Farina, C. Astrocytes: Key Regulators of Neuroinflammation. *Trends in immunology* **2016**, *37*, 608-620, doi:10.1016/j.it.2016.06.006.
54. Goshi, N.; Morgan, R.K.; Lein, P.J.; Seker, E. A primary neural cell culture model to study neuron, astrocyte, and microglia interactions in neuroinflammation. *Journal of neuroinflammation* **2020**, *17*, 155, doi:10.1186/s12974-020-01819-z.
55. Li, Y.Y.; Cui, J.G.; Dua, P.; Pogue, A.I.; Bhattacharjee, S.; Lukiw, W.J. Differential expression of miRNA-146a-regulated inflammatory genes in human primary neural, astroglial and microglial cells. *Neuroscience letters* **2011**, *499*, 109-113, doi:10.1016/j.neulet.2011.05.044.
56. Lukiw, W.J.; Zhao, Y.; Cui, J.G. An NF-kappaB-sensitive micro RNA-146a-mediated inflammatory circuit in Alzheimer disease and in stressed human brain cells. *The Journal of biological chemistry* **2008**, *283*, 31315-31322, doi:10.1074/jbc.M805371200.
57. Cui, J.G.; Li, Y.Y.; Zhao, Y.; Bhattacharjee, S.; Lukiw, W.J. Differential regulation of interleukin-1 receptor-associated kinase-1 (IRAK-1) and IRAK-2 by microRNA-146a and NF-kappaB in stressed human astroglial cells and in Alzheimer disease. *The Journal of biological chemistry* **2010**, *285*, 38951-38960, doi:10.1074/jbc.M110.178848.
58. Wyss-Coray, T.; Rogers, J. Inflammation in Alzheimer disease-a brief review of the basic science and clinical literature. *Cold Spring Harbor perspectives in medicine* **2012**, *2*, a006346, doi:10.1101/cshperspect.a006346.
59. He, Y.; Zheng, M.M.; Ma, Y.; Han, X.J.; Ma, X.Q.; Qu, C.Q.; Du, Y.F. Soluble oligomers and fibrillar species of amyloid β-peptide differentially affect cognitive functions and hippocampal inflammatory response. *Biochemical and biophysical research communications* **2012**, *429*, 125-130, doi:10.1016/j.bbrc.2012.10.129.
60. Borbély, E.; Horváth, J.; Furdan, S.; Bozsó, Z.; Penke, B.; Fülöp, L. Simultaneous changes of spatial memory and spine density after intrahippocampal administration of fibrillar aβ1-42 to the rat brain. *BioMed research international* **2014**, *2014*, 345305, doi:10.1155/2014/345305.
61. Nell, H.J.; Whitehead, S.N.; Cechetto, D.F. Age-Dependent Effect of β-Amyloid Toxicity on Basal Forebrain Cholinergic Neurons and Inflammation in the Rat Brain. *Brain pathology (Zurich, Switzerland)* **2015**, *25*, 531-542, doi:10.1111/bpa.12199.
62. Verkhratsky, A.; Sofroniew, M.V.; Messing, A.; deLanerolle, N.C.; Rempe, D.; Rodríguez, J.J.; Nedergaard, M. Neurological diseases as primary gliopathies: a reassessment of neurocentrism. *ASN neuro* **2012**, *4*, doi:10.1042/an20120010.
63. Chacón, M.A.; Barría, M.I.; Soto, C.; Inestrosa, N.C. Beta-sheet breaker peptide prevents Abeta-induced spatial memory impairments with partial reduction of amyloid deposits. *Molecular psychiatry* **2004**, *9*, 953-961, doi:10.1038/sj.mp.4001516.
64. Delay, C.; Mandemakers, W.; Hébert, S.S. MicroRNAs in Alzheimer's disease. *Neurobiology of disease* **2012**, *46*, 285-290, doi:10.1016/j.nbd.2012.01.003.
65. Souza, V.C.; Morais, G.S., Jr.; Henriques, A.D.; Machado-Silva, W.; Perez, D.I.V.; Brito, C.J.; Camargos, E.F.; Moraes, C.F.; Nóbrega, O.T. Whole-Blood Levels of MicroRNA-9 Are Decreased in Patients With Late-Onset Alzheimer Disease. *American journal of Alzheimer's disease and other dementias* **2020**, *35*, 1533317520911573, doi:10.1177/1533317520911573.
66. Miya Shaik, M.; Tamargo, I.A.; Abubakar, M.B.; Kamal, M.A.; Greig, N.H.; Gan, S.H. The Role of microRNAs in Alzheimer's Disease and Their Therapeutic Potentials. *Genes* **2018**, *9*, doi:10.3390/genes9040174.
67. Hong, H.; Li, Y.; Su, B. Identification of Circulating miR-125b as a Potential Biomarker of Alzheimer's Disease in APP/PS1 Transgenic Mouse. *Journal of Alzheimer's disease : JAD* **2017**, *59*, 1449-1458, doi:10.3233/jad-170156.
68. Geekiyanage, H.; Jicha, G.A.; Nelson, P.T.; Chan, C. Blood serum miRNA: non-invasive biomarkers for Alzheimer's disease. *Experimental neurology* **2012**, *235*, 491-496, doi:10.1016/j.expneurol.2011.11.026.
69. Kumar, P.; Dezso, Z.; MacKenzie, C.; Oestreicher, J.; Agoulnik, S.; Byrne, M.; Bernier, F.; Yanagimachi, M.; Aoshima, K.; Oda, Y. Circulating miRNA biomarkers for Alzheimer's disease. *PloS one* **2013**, *8*, e69807, doi:10.1371/journal.pone.0069807.
70. Hébert, S.S.; Horré, K.; Nicolaï, L.; Papadopoulou, A.S.; Mandemakers, W.; Silahtaroglu, A.N.; Kauppinen, S.; Delacourte, A.; De Strooper, B. Loss of microRNA cluster miR-29a/b-1 in sporadic Alzheimer's disease correlates with increased BACE1/beta-secretase expression. *Proceedings of the National Academy of Sciences of the United States of America* **2008**, *105*, 6415-6420, doi:10.1073/pnas.0710263105.
71. Kiko, T.; Nakagawa, K.; Tsuduki, T.; Furukawa, K.; Arai, H.; Miyazawa, T. MicroRNAs in plasma and cerebrospinal fluid as potential markers for Alzheimer's disease. *Journal of Alzheimer's disease : JAD* **2014**, *39*, 253-259, doi:10.3233/jad-130932.
72. Barbagallo, C.; Mostile, G.; Baglieri, G.; Giunta, F.; Luca, A.; Raciti, L.; Zappia, M.; Purrello, M.; Ragusa, M.; Nicoletti, A. Specific Signatures of Serum miRNAs as Potential Biomarkers to Discriminate Clinically Similar Neurodegenerative and Vascular-Related Diseases. *Cellular and molecular neurobiology* **2020**, *40*, 531-546, doi:10.1007/s10571-019-00751-y.
73. Ryan, M.M.; Guévremont, D.; Mockett, B.G.; Abraham, W.C.; Williams, J.M. Circulating Plasma microRNAs are Altered with Amyloidosis in a Mouse Model of Alzheimer's Disease. *Journal of Alzheimer's disease : JAD* **2018**, *66*, 835-852, doi:10.3233/jad-180385.
74. Savonenko, A.; Xu, G.M.; Melnikova, T.; Morton, J.L.; Gonzales, V.; Wong, M.P.; Price, D.L.; Tang, F.; Markowska, A.L.; Borchelt, D.R. Episodic-like memory deficits in the APPswe/PS1dE9 mouse model of Alzheimer's disease: relationships to beta-amyloid deposition and neurotransmitter abnormalities. *Neurobiology of disease* **2005**, *18*, 602-617, doi:10.1016/j.nbd.2004.10.022.
75. Alexandrov, P.N.; Dua, P.; Hill, J.M.; Bhattacharjee, S.; Zhao, Y.; Lukiw, W.J. microRNA (miRNA) speciation in Alzheimer's disease (AD) cerebrospinal fluid (CSF) and extracellular fluid (ECF). *International journal of biochemistry and molecular biology* **2012**, *3*, 365-373.

76. Denk, J.; Boelmans, K.; Siegismund, C.; Lassner, D.; Arlt, S.; Jahn, H. MicroRNA Profiling of CSF Reveals Potential Biomarkers to Detect Alzheimer`s Disease. *PloS one* **2015**, *10*, e0126423, doi:10.1371/journal.pone.0126423.
77. Banks, W.A.; Sharma, P.; Bullock, K.M.; Hansen, K.M.; Ludwig, N.; Whiteside, T.L. Transport of Extracellular Vesicles across the Blood-Brain Barrier: Brain Pharmacokinetics and Effects of Inflammation. *International journal of molecular sciences* **2020**, *21*, doi:10.3390/ijms21124407.
78. Bai, Y.; Su, X.; Piao, L.; Jin, Z.; Jin, R. Involvement of Astrocytes and microRNA Dysregulation in Neurodegenerative Diseases: From Pathogenesis to Therapeutic Potential. *Frontiers in molecular neuroscience* **2021**, *14*, 556215, doi:10.3389/fnmol.2021.556215.
79. Garwood, C.J.; Pooler, A.M.; Atherton, J.; Hanger, D.P.; Noble, W. Astrocytes are important mediators of Aβ-induced neurotoxicity and tau phosphorylation in primary culture. *Cell death & disease* **2011**, *2*, e167, doi:10.1038/cddis.2011.50.
80. Mattsson, N.; Rosén, E.; Hansson, O.; Andreasen, N.; Parnetti, L.; Jonsson, M.; Herukka, S.K.; van der Flier, W.M.; Blankenstein, M.A.; Ewers, M.; et al. Age and diagnostic performance of Alzheimer disease CSF biomarkers. *Neurology* **2012**, *78*, 468-476, doi:10.1212/WNL.0b013e3182477eed.